

Distribution Agreement:

In presenting this thesis or dissertation as a partial fulfillment of the requirements for an advanced degree from Emory University, I hereby grant to Emory University and its agents the non-exclusive license to archive, make accessible, and display my thesis or dissertation in whole or in part in all forms of media, now or hereafter known, including display on the world wide web. I understand that I may select some access restrictions as part of the online submissions of this thesis or dissertation. I retain all ownership rights to the copyright of the thesis or dissertation. I also retain the right to use in future works (such as articles or books) all or part of this thesis or dissertation.

Signature

Clayton P. Owens

Date

Design, Synthesis, and Utilization of Iridium(III) Bis(oxazoliny)phenyl and Iridium(III)
Bis(imidazoliny)phenyl Complexes for Catalytic Enantioselective Atom Transfer
C-H Functionalization.

By
Clayton P. Owens
Doctor of Philosophy

Chemistry

Simon B. Blakey, Ph.D.
Advisor

Frank E. McDonald, Ph.D.
Committee Member

Huw M. L. Davies, Ph.D.
Committee Member

Accepted:

Lisa A. Tedesco, Ph.D.
Dean of the James T. Laney School of Graduate Studies

Date

Design, Synthesis, and Utilization of Iridium(III) Bis(oxazoliny)phenyl and Iridium(III)
Bis(imidazoliny)phenyl Complexes for Catalytic Enantioselective Atom Transfer
C-H Functionalization.

By

Clayton P. Owens

B.S., Kennesaw State University, 2007

Advisor: Simon B. Blakey, Ph.D.

An abstract of

A dissertation submitted to the Faculty of the
James T. Laney School of Graduate Studies of Emory University

in partial fulfillment of the requirements for the degree of

Doctor of Philosophy

in Chemistry

2014

Abstract

Design, Synthesis, and Utilization of Iridium(III) Bis(oxazoliny)phenyl and Iridium(III) Bis(imidazoliny)phenyl Complexes for Catalytic Enantioselective Atom Transfer C-H Functionalization.

By

Clayton P. Owens

The science of organic chemistry has experienced significant advances in recent years due to the increase in efficient methodologies for the synthesis of complex molecules. Traditional synthetic methods have relied on functional groups for selective reactions to be achieved, but these functional groups often require independent preparation and may not be present in the target molecule. Thus, the consideration of carbon-hydrogen (C-H) bonds as functional groups represents a direct approach for overcoming this inherent limitation. C-H bonds were once perceived as being inert, but recent progression of technologies for their functionalization has allowed chemists to incorporate them in synthetic strategies. One such technology involves the design of transition metal complexes that generate a reactive metallocarbene or metallonitrene, which then selectively engages the desired C-H bond to be functionalized and forges a new C-C or C-N bond, respectively. Dirhodium(II) complexes have emerged as state of the art catalysts in metallocarbene and metallonitrene chemistry, but recent reports have revealed that iridium complexes offer reactivity which is unattainable under dirhodium catalysis. Our laboratory discovered that iridium(III) bis(oxazoliny)phenyl complexes perform catalytic and highly chemo-, regio-, and enantioselective C-H insertion into cyclic dienes using donor/acceptor metallocarbenes. Further catalyst design has led to new iridium(III) bis(imidazoliny)phenyl complexes which catalyze chemo- and enantioselective C-H functionalization of cyclic ethers using acceptor-only metallocarbenes. Computational analysis of the reactive intermediates has provided substantial insight into the controlling factors for the observed selectivity. Detailed analyses of our efforts to advance the technologies for C-H functionalization through catalyst design are described in this dissertation.

Design, Synthesis, and Utilization of Iridium(III) Bis(oxazoliny)phenyl and Iridium(III)
Bis(imidazoliny)phenyl Complexes for Catalytic Enantioselective Atom Transfer
C-H Functionalization.

By

Clayton P. Owens

B.S., Kennesaw State University, 2007

Advisor: Simon B. Blakey, Ph.D.

A dissertation submitted to the Faculty of the
James T. Laney School of Graduate Studies of Emory University
in partial fulfillment of the requirements for the degree of
Doctor of Philosophy
in Chemistry
2014

*Dedicated to each member of my family that has passed since
I began my undergraduate and graduate studies.*

Acknowledgments

Graduate school is something that did not come easy to me, and I am very thankful to those who have helped me persevere and complete my studies at Emory. First and foremost thank you Simon. You have always made a teaching moment out of any situation you possibly could, and I've learned a lot since becoming a member of your research group. You have taught me a lot of chemistry and most importantly how to become an independent scientist. There were many times that I did not like what you had to say, but I realize that your comments and criticisms regarding my research have made me a better chemist and person. Thanks for your support so I could pursue various avenues outside of my PhD research. My internship broadened my skill set and helped me decide the career path I should take. Thanks also for taking time to develop my professional skills, especially sitting through many of my painful practice talks. I ask that you invest as much time to mentor your future graduate and undergraduate students as you have with me, the group will strongly benefit from your continued support.

Thank you Dr. Davies and Dr. McDonald for working with me the last 5 years as part of my committee. You both always pushed me to become a better scientist and I am grateful for your many comments and suggestions regarding my research. Huw, I have enjoyed our collaboration over the last three years and I cannot emphasize enough how valuable it's been for me to be a part of the center; I wish you and your group the best from here on out. Dr. McDonald, thanks for having me as your TA during organic I lecture a few years back. Your course reminded me of some of the basics I'd forgotten, and you were an excellent example of a thorough and effective teacher.

Thank you Jamal, Shentan, Adrian, and Slava for all your hard work performing the calculations for all of my iridium complexes and reactions. Our collaboration over the last 3 years has been very fruitful and I hope many exciting discoveries continue to be revealed.

Thank you Ann for making everything less complicated during graduate school, I'm pretty sure you've registered for me every semester! Patti and Steve, I've enjoyed our interactions and shenanigans over the past five years. You're both incredibly helpful people and I'll miss stopping by the stockroom every day. Steve, I'm glad that someone in the department likes as good of music as I do!

To my lab mates – the fact that you've put up with my tomfoolery is remarkable. I'll miss being able to make inappropriate remarks at any chance I get and not being hesitant to say what I think. Although this might haunt me in the future it was totally worth it! Ricardo –working/sitting next to you in lab was ridiculous and fun, but I'm glad you left so I could be more productive. Veronique – your hard work, especially towards the end of your PhD, was very motivating and you deserve everything you've earned. Aaron, you were the only person in the entire chemistry department I could talk sports with, and when you left it was pretty depressing. I'm glad we keep in touch, but just remember I will always be the lab septa ball champion. Annnnd...veggie tables. Jen, I've enjoyed sharing lab and lunchtime with you, and I truly appreciate your sense of sarcasm. Aidi, you are the hardest working person in the chemistry department. How you've balanced having George, not having Wenyong, and being the most productive member of the lab I'll never know...you've been an inspiration to me. Nina, I hope iridium treats you well. Eric, your chemistry knowledge is great and I've enjoyed sharing

the lab with you. Pablo, thanks for reminding me that there is life outside of chemistry. Playing basketball and talking music with you were great ways to relieve stress. Danny - I didn't like you at first. You stole and broke my glassware and didn't tell me...but I knew. Eventually however we became good friends, I've learned a lot of chemistry from you, and I've enjoyed our many bouts of uncontrollable laughter over the years. I've also learned how good you are at botching up sayings... it's actually kind of impressive. It has been great to get to know you and Juliya, as well as to be around for Sofie's first few years. You've become like a brother to me and I'm glad we still keep in touch.

Dr. Tapu – thank you for having me in your lab at KSU. You taught me all the fundamentals of working in the lab and had the patience of a saint... even though you called me a chicken the first time I tried to break open a vial in the glove box. Mr. Coffey - you were the teacher to spark my interest in science. You made learning science fun, and your passion for mentoring young students was and continues to be unmatched. So many others feel the same way I do, and I only wish that more people could have had the chance to know you before you passed. Thank you.

To all my friends and family, especially Dad and Cathy, Mom and Larry, Bud and Deana, Memaw and Pops, and Greg and Tori, your support means the world to me. You are all daily reminders of how lucky I am to have so many people that care about me. To y'all and everyone I haven't listed here...I love you and thank you.

To my Holly – I cannot even begin to describe how much your support has meant to me during this time in graduate school. You've listened to me talk about chemistry, you've listened to me complain, you've been here for me through the low points and the

high points. Your patience is indescribable, and every time I said I'd be home in 30 minutes and it wound up being 3 hours you completely understood and did not complain. There is no way I would have made it through graduate school without you, your love, and all of the home cooked meals waiting for me when I got home. If I had a bad day in the lab it all seemed to disappear the moment I got home to you and our little boy Bosco. I am looking forward to our lives after graduate school, and I hope I can be every bit as supportive of you as you have been for me...I love you.

Table of Contents

1 Chapter One: C-H Functionalization by Metallocarbenes and Metallonitrenes:	
Background and Significance	1
1.1 Introduction.....	1
1.2 Metallocarbenes.....	4
1.2.1 Generation and Classification.....	4
1.2.2 C-H Insertion with donor/acceptor metallocarbenes	6
1.2.3 C-H Insertion with acceptor-only metallocarbenes.....	7
1.2.4 Conclusions and challenges.....	13
1.3 Metallonitrenes.....	14
1.3.1 Introduction.....	14
1.3.2 Generation of metallonitrenes.....	14
1.3.3 Intramolecular C-H amination	16
1.3.4 Intermolecular C-H amination	16
1.3.5 Conclusions and challenges	28
1.4 Conclusions.....	29
2 Chapter Two: Iridium Catalyzed Metallocarbene and Metallonitrene Atom-	
Transfer Reactions.....	30
2.1 Introduction.....	30
2.2 Iridium(III) Salen Metallocarbene Atom-Transfer.....	30
2.2.1 Iridium(III) salen synthesis.....	30

2.2.2	Iridium(III) salen catalyzed cyclopropanation.....	32
2.2.3	Iridium(III) salen catalyzed cyclopropanation.....	35
2.2.4	Iridium(III) salen catalyzed C-H functionalization.....	37
2.2.5	Iridium(III) salen catalyzed Si-H insertion.....	41
2.3	Iridium(III) Porphyrin Metallocarbene Atom-Transfer.....	42
2.3.1	Iridium(III) porphyrin synthesis.....	42
2.3.2	Iridium(III) porphyrin catalyzed cyclopropanation.....	43
2.3.3	Iridium(III) porphyrin catalyzed C-H functionalization.....	46
2.3.4	Asymmetric intermolecular C-H functionalization by iridium(III) complexes of chiral Halterman porphyrin ligands.....	48
2.3.5	Intramolecular C-H functionalization by iridium(III) porphyrin complexes.....	54
2.4	Iridium(I) Catalyzed Metallocarbene Atom-Transfer.....	56
2.5	Iridium (III) Catalyzed Metallonitrene Atom-Transfer.....	57
2.5.1	Iridium(III) salen catalyzed intramolecular C-H amination of sulfonyl azides.....	57
2.5.2	Intermolecular C-H amidation using acyl azides.....	59
2.6	Iridium (I) Catalyzed Metallonitrene Atom-Transfer.....	60
2.7	Conclusions.....	62
3	Chapter Three: Development of Iridium NCN Pincer Catalysts for Enantioselective Metallocarbene C-H Functionalization.....	63
3.1	Bis(oxazoliny)phenyl (phebox) complexes.....	65

3.1.1	Palladium(II) phebox complexes developed by Denmark.....	65
3.1.2	Rhodium(III) phebox complexes.....	66
3.1.3	Stoichiometric Reactions at the Rhodium(III) Phebox Metal Center.....	68
3.1.4	Rhodium(III) phebox complexes in asymmetric catalysis.....	70
3.1.5	Phebox complexes with metals other than rhodium.....	72
3.2	Iridium(III) Phebox Complexes.....	73
3.2.1	Synthesis of iridium phebox complexes.....	73
3.2.2	Stoichiometric and catalytic C-H functionalization using iridium(III) phebox complexes	75
3.3	Design and Synthesis of New Iridium(III) Phebox Complexes.....	79
3.3.1	Synthesis of iridium(III) phebox complex 174	79
3.3.2	Proof of principle for iridium(III) phebox catalyzed atom transfer using a donor/acceptor metallocarbene.....	81
3.3.3	Design concept and synthesis of new iridium(III) phebox complexes.....	83
3.3.4	X-ray structure analysis of [(<i>R,R</i>)- ^{<i>t</i>} BuPhebox-Bn]IrCl ₂ (OH ₂) 216	85
3.4	Iridium(III) Phebox Catalyzed C-H Insertion of Donor/Acceptor Diazoesters... ..	86
3.4.1	Initial optimization of catalyst and reaction conditions.....	86
3.4.2	Scope of aryl diazoesters for C-H insertion into cyclic 1,4 dienes.....	92
3.4.3	Confirmation of the absolute stereochemistry for iridium(III) phebox catalyzed C-H insertion of methyl phenyldiazoacetate into 1,4-cyclohexadiene.. ..	95
3.4.4	C-H functionalization of substituted cyclic 1,4-dienes.....	97
3.4.5	Iridium(III) phebox catalyzed C-H insertion into 1,3,5-cycloheptatriene ..	102

3.4.6	Iridium(III) phebox catalyzed C-H insertion into tetrahydrofuran.	103
3.4.7	Reactions of iridium(III) phebox complexes with alpha-alkyl diazoesters.	104
3.4.8	Evaluation of non-ester donor/acceptor carbene precursors for iridium(III) phebox catalyzed C-H functionalization of 1,4-cyclohexadiene.	105
3.5	Computational Studies for Iridium(III) Phebox Catalyzed ... Donor/Acceptor C-H Insertion into 1,4-cyclohexadiene.	109
3.5.1	DFT Analysis of the reactive carbene intermediate.	110
3.5.2	Attempts to experimentally validate the computation.	118
3.6	Structural Studies Performed by the Berry Group.	120
3.6.1	Introduction.	120
3.6.2	Variable temperature ¹³ C NMR studies.	121
3.6.3	UV-Vis studies on the reaction of iridium(III) phebox 213 mediated decomposition of methyl <i>p</i> -methoxyphenyldiazoacetate 264	124
3.7	Conclusions.	125
4	Chapter Four: Iridium(III) Phebox and Iridium(III) Phebim Catalyzed Acceptor-only Metallocarbene C-H Functionalization	127
4.1	Introduction.	127
4.2	Iridium(III) Phebox Catalyzed Acceptor-only Atom Transfer.	128
4.2.1	Insertion of ethyl diazoacetate into 1,4-cyclohexadiene.	128
4.2.2	Insertion of ethyl diazoacetate into tetrahydrofuran.	130
4.2.3	Evaluation of other acceptor-only metallocarbene precursors for C-H insertion into THF.	134

4.2.4	Iridium(III) phebox catalyzed enantioselective C-H functionalization of phthalan.....	137
4.2.5	Iridium(III) phebox catalyzed enantioselective C-H functionalization of tetrahydrofuran and 2,5-dihydrofuran.....	141
4.2.6	Kinetic isotope effect for the C-H insertion of ethyl diazoacetate into tetrahydrofuran.....	143
4.2.7	Attempts to perform C-H functionalization into other cyclic ethers	145
4.2.8	Attempts to perform acceptor-only C-H functionalization into acyclic ethers.....	147
4.2.9	Conclusions.....	149
4.3	Computational Studies for Iridium(III) Phebox Catalyzed Acceptor-only C-H Insertion into THF and Phthalan.....	150
4.3.1	DFT analysis of the geometry of the reactive acceptor-only carbene intermediate derived from ethyl diazoacetate.....	150
4.3.2	Calculated transition state and intrinsic reaction coordinate for iridium(III) phebox catalyzed C-H insertion of ethyl diazoacetate into THF	152
4.3.3	Factors controlling the enantioselectivity for C-H insertion of ethyl diazoacetate into THF <i>via</i> TSHT-<i>eq</i>	154
4.3.4	Factors controlling the enantioselectivity for C-H insertion of ethyl diazoacetate into phthalan.....	156
4.4	Bis(imidazoliny)phenyl (phebim) Iridium(III) Complexes.....	158
4.4.1	Introduction.....	158
4.4.2	Synthesis of phebim ligands and rhodium(III) complexes thereof.....	159

4.4.3	Synthesis of phehim ligand 295 and its iridium(III) phehim complex 296 .	162
4.4.4	Enantioselective intermolecular C-H insertion of ethyl diazoacetate into phthalan catalyzed by iridium(III) phehim complex 296 .	164
4.4.5	Synthesis of electronically varied iridium(III) phehim ligands 295, 297-300 and their iridium(III) phehim complexes 296, 301-304 .	165
4.4.6	Catalytic activity of electronically varied iridium(III) phehim complexes 301-304 for C-H insertion of ethyl diazoacetate into phthalan.	166
4.4.7	Synthesis of iridium(III) bromo phebox complexes 305 and 306 and their reactivity towards C-H insertion of ethyl diazoacetate into phthalan.	168
4.4.8	Synthesis of <i>sec</i> -butyl, cyclohexyl, <i>iso</i> -butyl, and CH ₂ -cyclohexyl iridium(III) chloro phebox complexes 311 - 314 .	169
4.4.9	Catalytic activity of <i>sec</i> -butyl, cyclohexyl, <i>iso</i> -butyl, and CH ₂ -cyclohexyl iridium(III) chloro phebox complexes 315-318 .	173
4.4.10	C-H insertion of ethyl diazoacetate into 2,5-dihydrofuran and THF.	174
4.4.11	Iridium(III) phehim catalyzed C-H insertion of ethyl diazoacetate into isochroman.	177
4.5	Conclusions.	180
5	Chapter Five: Iridium(III) Phebox Catalyzed C-H Amination.	182
5.1	Iridium(III) Phebox Catalyzed C-H Amination.	182
5.1.1	Iridium(III) phebox catalyzed intramolecular C-H amination using aryl azides.	183
5.1.2	Iridium(III) phebox catalyzed intramolecular C-H amination using sulfamate esters.	185

5.2	Conclusions.....	187
6	Experimentals.....	188
6.1	General Informaation.....	188
6.2	Chapter 3 Procedures and Characterization.....	190
6.2.1	Synthesis of 4,6-dimethylisophthaloyl dichloride 196	190
6.2.2	Synthesis of phebox ligands and iridium(III) phebox complexes.....	192
6.2.3	Synthesis of triphenylphosphine iridium(III) phebox complexes 262 and 263 and their NMR spectra.....	211
6.2.4	Procedures and characterization data for C-H insertion reactions using donor/acceptor carbenes.....	215
6.2.5	X-ray Crystallographic Data for [(<i>R,R</i>)- ^t BuPhebox-Bn]IrCl ₂ (H ₂ O) 216	248
6.3	Chapter 4 Procedures and Characterization.....	253
6.3.1	Iridium(III) phebox catalyzed enantioselective C-H insertion of acceptor-only metallocarbenes.....	253
6.3.2	Synthesis of amides 274, 307-310	262
6.3.3	Synthesis of phebim ligands 295, 297-300, 311-314	267
6.3.4	Synthesis of iridium(III) phebim complexes 296, 301-306, 299, 315-317, <i>trans</i>-318, <i>cis</i>-318	276
6.4	Chapter 5 Procedures and Characterization.....	288
7	Appendix –List of Synthesized Compounds.....	291
	References.....	299

List of Schemes

Scheme 1.1 Metallocarbene and metallonitrene C-H functionalization.....	1
Scheme 1.2 Selectivity studies on the Rh ₂ (oct) ₄ catalyzed intramolecular C-H amination of sulamate esters.....	2
Scheme 1.3 Rh ₂ (S-DOSP) ₄ catalyzed enantioselective intermolecular C-H functionalization alpha to nitrogen.....	3
Scheme 1.4. Du Bois' synthesis of (-)-tetrodotoxin via metallocarbene and metallonitrene C-H insertion.....	4
Scheme 1.5 Donor/acceptor enantioselective intermolecular C-H insertion towards the synthesis of dihydrobenzofurans.....	7
Scheme 1.6 Intermolecular acceptor-only C-H insertion versus dimerization.....	9
Scheme 1.7 C-H insertion versus cyclopropanation for Rh ₂ (OAc) ₄ catalyzed reactions with acceptor-only and donor/acceptor metallocarbenes.....	9
Scheme 1.8 Copper catalyzed acceptor-only intermolecular C-H insertion into cyclic ethers and cyclic alkanes.....	10
Scheme 1.9 Dirhodium(II) tetracarboxamidate catalyzed acceptor-only intramolecular C-H insertion.....	11
Scheme 1.10. Synthesis of baclofen <i>via</i> acceptor-only intramolecular insertion.....	12
Scheme 1.11. Synthesis of baclofen <i>via</i> acceptor-only intramolecular C-H insertion using ethyl diazoacetate.....	12

Scheme 1.12. Rh ₂ (esp) ₂ catalyzed intramolecular C-H amination reactions.	17
Scheme 1.13. Cobalt(II) tetraphenylporphyrin (28) catalyzed C-H amination of sulfonyl azides.....	18
Scheme 1.14. Select examples of Rh ₂ (esp) ₂ catalyzed aliphatic C-H amination using aryl azides.....	19
Scheme 1.15. Iron catalyzed C-H amination using aliphatic azides.	20
Scheme 1.16. Protodemetalation and β-hydride elimination of an alkyl-substituted metallonitrene.	20
Scheme 1.17. Manganese porphyrin catalyzed intermolecular C-H amination.	23
Scheme 1.18. Rh ₂ (esp) ₂ catalyzed intermolecular C-H amination with Tces-NH ₂	23
Scheme 1.19. Selectivity studies on Rh ₂ (esp) ₂ catalyzed intermolecular C-H amination.	24
Scheme 1.20. Rh ₂ (<i>S</i> -nta) ₄ catalyzed diastereoselective C-H amination using chiral sulfonimidamide auxiliary 48	25
Scheme 1.21. Co(TPP) 28 catalyzed benzylic C-H amination using Troc-N ₃	26
Scheme 1.22. Substrate scope for Ru ^{II} (salen) catalyzed C-H amination.	28
Scheme 2.1. Synthesis of salen ligand 62	31
Scheme 2.2. Synthesis of salen complexes 69-71	32
Scheme 2.3. Iridium(III) salen catalyst evaluation for cyclopropanation of styrene with <i>tert</i> -butyldiazoacetate.....	33

Scheme 2.4 Iridium(III) salen catalyzed cyclopropanation of terminal olefins with vinyl diazylactone 72	35
Scheme 2.5 Iridium(III) salen catalyzed cyclopropanation using aryl diazoesters, aryl diazophosphonates, and trifluoromethyl phenyldiazomethane.....	37
Scheme 2.6 Iridium(III) salen catalyzed cyclopropanation of phenylacetylene with α -cyano- α -diazacetamide 77	37
Scheme 2.7 Iridium(III) salen catalyzed donor/acceptor C-H insertion into tetrahydrofuran.....	38
Scheme 2.8 Iridium(III) salen catalyzed donor/acceptor C-H insertion into 1,4-cyclohexadiene.	39
Scheme 2.9 β -hydride elimination in metallocarbenes derived from α -alkyl diazoesters.....	40
Scheme 2.10 Iridium(III) salen catalyzed alkyl diazoester Si-H insertion.....	41
Scheme 2.11 General porphyrin ligand synthesis.	42
Scheme 2.12. Synthesis of [Ir(TTP)CH ₃] 83	43
Scheme 2.13 [Ir(TTP)CH ₃] 83 catalyzed cyclopropanation of olefins with ethyl diazoacetate.....	44
Scheme 2.14 [Ir(TTP)CH ₃] 83 catalyzed cyclopropanation of styrene with methyl phenyldiazoacetate.....	44
Scheme 2.15 [Ir(TTP)CH ₃] 83 catalyzed C-H insertion with methyl phenyldiazoacetate.....	46

Scheme 2.16 [Rh(TTPPP)CH ₃] 86 catalyzed C-H insertion with methyl phenyldiazoacetate.....	49
Scheme 2.17 [Rh(<i>D</i> ₄ -por*)(CH ₃)] 90 catalyzed enantioselective C-H insertion with methyl phenyldiazoacetate.....	50
Scheme 2.18 Synthesis of the chiral iridium(III) Halterman porphyrin complex 96	51
Scheme 2.19 [Ir(<i>D</i> ₄ -por*)(CH ₃)] 96 catalyzed C-H insertion into 1,4-cyclohexadiene...	52
Scheme 2.20 [Ir(<i>D</i> ₄ -por*)(CH ₃)] 96 catalyzed C-H insertion into tetrahydrofuran.....	53
Scheme 2.21 <i>Cis</i> - and enantioselective [Ir(<i>D</i> ₄ -por*)(CH ₃)] 96 catalyzed intramolecular C-H insertion of aryldiazoesters.	56
Scheme 2.22 [Ir(cod)Cl] ₂ catalyzed X-H insertion.	57
Scheme 2.23 Synthesis of MK-7655 <i>via</i> iridium(I) catalyzed N-H insertion.	57
Scheme 2.24 Iridium(III) salen catalyzed enantioselective synthesis of benzosultams from aryl sulfonyl azides.	58
Scheme 2.25 [IrCp*Cl ₂] ₂ catalyzed intermolecular C-H amidation using acyl azides as nitrene precursor.	60
Scheme 2.26 [Ir(cod)(OMe)] ₂ catalyzed intramolecular benzylic C-H amination using simple aryl azides.....	61
Scheme 3.1 Similarities between pybox and phebox frameworks.	64
Scheme 3.2 General synthesis of phebox metal complexes.	64
Scheme 3.3. Denmark's palladium(II) phebox synthesis.	66

Scheme 3.4 Palladium phebox catalyzed cyclopropanation.....	66
Scheme 3.5 Nishiyama's one-pot phebox ligand synthesis.....	67
Scheme 3.6 Rhodium(III) phebox complex synthesis by transmetallation (method A) and cyclometallation (method B).....	67
Scheme 3.7 Chloride ligand substitution reactions.	68
Scheme 3.8 Chloride ligand substitution reactions of chloro complex 158	68
Scheme 3.9 C-H activation reactions of rhodium(III) phebox acetate complex 160	69
Scheme 3.10 Formation of rhodium(III) Fischer carbene complex 168	69
Scheme 3.11 Rhodium(III) phebox catalyzed enantioselective allylation of aldehydes..	70
Scheme 3.12 Ruthenium(II) phebox catalyzed asymmetric cyclopropanation.	72
Scheme 3.13 Cyclopalladation into the 4(6) position of phebox ligand 170	73
Scheme 3.14 Effect of 4,6-dimethyl substitution on rhodium phebox metallation.....	74
Scheme 3.15 Synthesis of iridium(III) phebox complexes 174 and 175	74
Scheme 3.16 Asymmetric conjugate reduction of esters and asymmetric reductive aldol reactions using rhodium(III) and iridium(III) phebox complexes 176 and 175	75
Scheme 3.17 C-H activation reactions of iridium(III) phebox acetate complex 180 with substituted arenes	76
Scheme 3.18 Proposed mechanism for iridium(III) phebox acetate-assisted C-H insertion.....	77
Scheme 3.19 Iridium(III) phebox 180 catalyzed C-H borylation.....	77

Scheme 3.20 Iridium(III) phebox 180 mediated 1° aliphatic C-H functionalization.	78
Scheme 3.21 Iridium(III) phebox dehydrogenation of <i>n</i> -octane.	79
Scheme 3.22 Synthesis of 4,6-dimethylisophtalooyl dichloride 196	80
Scheme 3.23 Synthesis of (diMePhebox) ligand 172 and its corresponding iridium(III) complex [(<i>S,S</i>)-diMePhebox- ^{<i>i</i>} Pr]IrCl ₂ (OH ₂) 174	81
Scheme 3.24 Initial insertion reaction of methyl phenyldiazoacetate into 1,4-cyclohexadiene.	82
Scheme 3.25 Synthesis of (diMePhebox) ligands 172, 198-200 and their iridium(III) complexes 174, 201-203	83
Scheme 3.26 Connell's synthesis of <i>tert</i> -butyl containing nickel(II) phebox complexes.	84
Scheme 3.27 Synthesis of (^{<i>t</i>} BuPhebox) ligands 209-212 and their iridium(III) complexes 213-216	85
Scheme 3.28 Synthesis of [(<i>R,R</i>)- ^{<i>t</i>} BuPhebox-Bn]IrCl ₂ (OAc) ₂ 217	89
Scheme 3.29 Synthesis of [(<i>S,S</i>)- ^{<i>t</i>} BuPhebox- ^{<i>i</i>} Pr]IrBr ₂ (OH ₂) 218	90
Scheme 3.30 C-H insertion of methyl phenyldiazoacetate into 1,4-cyclohexadiene using [(<i>S,S</i>)- ^{<i>t</i>} BuPhebox- ^{<i>i</i>} Pr]IrBr ₂ (OH ₂) 218	90
Scheme 3.31 Iridium(III) phebox 216 catalyzed C-H insertion and C-H/Cope reaction of methyl 2-benzofuranyldiazoacetate 230 with 1,4-cyclohexadiene.	95
Scheme 3.32 <i>S-cis</i> transition state 233 for the C-H functionalization / Cope rearrangement reaction.	95

Scheme 3.33 Absolute stereochemistry determination of (<i>R</i>)-cyclohexylphenylacetic acid 237 by Camps.	96
Scheme 3.34 Iridium(III) phebox 209 catalyzed C-H insertion to form enantioenriched diene 197	97
Scheme 3.35 Determination of the absolute configuration obtained in iridium(III) phebox catalyzed C-H insertion by conversion of enantioenriched diene 197 to (<i>S</i>)-cyclohexylphenylacetic acid ent-237	97
Scheme 3.36 Iridium(III) phebox 216 catalyzed C-H insertion of methyl phenyldiazoacetate into 1-methyl-1,4-cyclohexadiene.....	98
Scheme 3.37 DDQ oxidation of 239	98
Scheme 3.38 LiAlH ₄ reduction of ester 240 to alcohol 241 for determination of enantiomeric excess.	99
Scheme 3.39 Enantioselective C-H insertion of aryl diazoacetates into 1-substituted 1,4-cyclic dienes.	100
Scheme 3.40 Iridium(III) phebox catalyzed enantioselective C-H insertion of methyl phenyldiazoacetate into cycloheptatriene..	103
Scheme 3.41 Iridium(III) phebox 216 catalyzed C-H insertion of methyl phenyldiazoacetate into tetrahydrofuran.....	104
Scheme 3.42 Attempted iridium phebox catalyzed C-H insertion using methyl <i>tert</i> -butyldiazoacetate.....	105

Scheme 3.43 Iridium phebox catalyzed C-H insertion of trifluoromethyl phenyldiazomethane into 1,4-cyclohexadiene.....	108
Scheme 3.44 Calculated transition state for copper bisoxazoline catalyzed C-H insertion of methyl phenyldiazoacetate into tetrahydrofuran.....	114
Scheme 3.45 Synthesis of the equatorial and axial triphenylphosphine complexes 262 and 263	118
Scheme 3.46 Reaction used by the Berry group to conduct structural studies on the iridium carbene.....	121
Scheme 4.1 Synthesis of U-101387 270	130
Scheme 4.2 C-H functionalization approach to enantioenriched ester <i>S</i> - 267	131
Scheme 4.3 Iridium(III) phebox catalyzed acceptor-only C-H into tetrahydrofuran.....	131
Scheme 4.4 Enantioselective intermolecular C-H insertion into THF using ethyl diazoacetate.....	132
Scheme 4.5 Enantioselective intermolecular C-H insertion into THF using <i>tert</i> -butyl diazoacetate.....	135
Scheme 4.6 Enantioselective intermolecular C-H insertion into THF using phenyl diazoacetate catalyzed by 213	136
Scheme 4.7 Enantioselective intermolecular C-H insertion into THF using phenyl diazoacetate catalyzed by 216	136
Scheme 4.8 Synthesis of chiral/racemic iridium(III) phebox complex rac 213	138

Scheme 4.9 Iridium(III) chloro phebox 213 catalyzed enantioselective intermolecular C-H insertion into phthalan.....	138
Scheme 4.10 Iridium(III) bromo phebox 218 catalyzed enantioselective intermolecular C-H insertion into phthalan.....	138
Scheme 4.11 Iridium(III) phebox 213 catalyzed acceptor-only enantioselective C-H insertion using 4 equivalents THF.	141
Scheme 4.12 Iridium phebox 213 catalyzed chemo- and enantioselective C-H insertion of ethyl diazoacetate into 2,5-dihydrofuran	142
Scheme 4.13 Attempted C-H insertion into tetrahydropyra.....	146
Scheme 4.14 Attempted C-H insertion into 2,2-dimethyl dioxolane and dihydrobenzofuran	147
Scheme 4.15 Attempted C-H insertion into TBS protected allyl alcohol 280	148
Scheme 4.16 Attempted C-H insertion into TBS protected allylic alcohol 282	148
Scheme 4.17 Generalized synthesis of phehim metal complexes	159
Scheme 4.18 Song's synthesis of rhodium(III) phehim complexes 291 and 292	161
Scheme 4.19 Rhodium(III) phehim 291 catalyzed asymmetric allylation of benzaldehydes.....	161
Scheme 4.20 Chloride ligand exchange in rhodium(III) phehim complex 292	162
Scheme 4.21 Rhodium(III) phehim 293 catalyzed asymmetric alkynylation of trifluoropyruvates.....	162

Scheme 4.22 Synthesis of phehim ligand 295 and its iridium(III) phehim complex 296	163
Scheme 4.23 Iridium(III) phehim 296 catalyzed enantioselective acceptor-only C-H insertion of ethyl diazoacetate into phthalan	164
Scheme 4.24 Synthesis of iridium(III) bromo phehim complexes 305 and 306	169
Scheme 4.25 Synthesis of iridium(III) phehim complexes 299, 315-317	171
Scheme 4.26 Synthesis of the <i>trans</i> and <i>cis</i> CH ₂ -cyclohexyl iridium phehim complexes <i>trans</i> - 318 and <i>cis</i> - 318	172
Scheme 4.27 Iridium(III) phehim 317 catalyzed C-H insertion of ethyl diazoacetate into isochroman	178
Scheme 4.28 Reduction of esters 267 and 319 using LiAlH ₄	180
Scheme 5.1 Reaction of iridium(III) phebox complex 216 with aryl azide 321 at room temperature.	183

List of Figures

Figure 1.1. Mechanism for metallocarbene formation and C-H functionalization using diazo compounds.	5
Figure 1.2. Classes of metallocarbenes.....	6
Figure 1.3 Mechanism for metallonitrene formation and C-H functionalization.	15
Figure 1.4 Ruthenium porphyrin 38 , ruthenium pybox 39 , and dirhodium(II) tetracarboxamidate 40 catalyzed asymmetric intramolecular C-H amination.....	21
Figure 2.1 Select examples of iridium(III) salen catalyzed olefin cyclopropanation using <i>tert</i> -butyldiazoacetate.....	34
Figure 2.2 Catalyst evaluation for iridium(III) salen catalyzed cyclopropanation of terminal alkynes.....	36
Figure 2.3 Iridium(III) salen catalyzed insertion of α -alkyl diazoacetates into THF and 1,4-cyclohexadiene.	40
Figure 2.4 Potential rate-determining pathways in the [Ir(TTP)CH ₃] 83 catalyzed cyclopropanation of styrene with ethyl diazoacetate	45
Figure 2.5 Iridium(III) salen catalyzed enantioselective synthesis of benzosultams.....	59
Figure 3.1 Proposed transition state for the allylation reaction.	70
Figure 3.2 Examples of rhodium phebox catalyzed enantioselective reactions.	71
Figure 3.3 Proposed transition state model for Ru(II) phebox cyclopropanation.....	72
Figure 3.4 X-ray structure of [(<i>R,R</i>)- <i>t</i> BuPhebox-Bn]IrCl ₂ (OH ₂) complex 216	86

Figure 3.5 Confirmation of predicted facial selectivity for insertion into 1-methoxy-1,4-cyclohexadiene.....	101
Figure 3.6 C-H insertion into 1,4-dihydronaphthalene.....	102
Figure 3.7 Free energy profile for the formation of the axial and equatorial carbenes.	111
Figure 3.8 Predictive model for ruthenium pybox catalyzed cyclopropanation.....	114
Figure 3.9 Calculated transition state for copper bisoxazoline catalyzed C-H insertion into THF.....	115
Figure 3.10 Relative stabilities of the axial and equatorial carbene intermediates as explained by the <i>trans</i> effect of the phenyl anion.....	116
Figure 3.11 Conformational analysis of the potential isomers of the axial carbene. The $\Delta E(\Delta H)[\Delta G]$ values are in kcal mol ⁻¹ and are relative to 19-ax . The two sets of values under each conformer were obtained by rotation around the C _{carbene} -CO ₂ Me bond.....	117
Figure 3.12 The predictive model for stereinduction for the iridium phebox catalyzed C-H insertion reaction of methyl phenyldiazoacetate into 1,4-cyclohexadiene.....	117
Figure 3.13 ¹³ C NMR spectrum of the reaction between iridium(III) phebox complex 213 and ¹³ C labeled methyl <i>p</i> -methoxyphenyl diazoacetate 264 at 14.5 °C in CDCl ₃	122
Figure 3.14 Variable temperature ¹³ C NMR spectra for the reaction of iridium(III) complex 213 with ¹³ C-labeled methyl <i>p</i> -methoxyphenyldiazoacetate 264	123
Figure 3.15 UV-Vis spectrum of the iridium(III) phebox 213 mediated decomposition of ¹³ C-labeled methyl <i>p</i> -methoxyphenyldiazoacetate 264	125

Figure 4.1 Crude ¹ H NMR spectrum for the chemoselective C-H insertion of ethyl diazoacetate into 2,5-dihydrofuran.	143
Figure 4.2 Determination of the kinetic isotope effect by +ESI mass spectrometry for the iridium(III) phebox catalyzed insertion of ethyl diazoacetate into tetrahydrofuran.	144
Figure 4.3 Free energy profile for axial and equatorial acceptor-only iridium carbene formation. All energy values ΔG(ΔH) are given in kcal·mol ⁻¹ . EDA = ethyl diazoacetate.....	152
Figure 4.4 Lowest free energy profile for iridium phebox catalyzed acceptor-only C-H insertion into tetrahydrofuran <i>via</i> TSHT-eq	153
Figure 4.5 Intrinsic reaction coordinate for C-H insertion into THF <i>via</i> TSHT-eq	154
Figure 4.6 Comparison of the transition states leading to the <i>S</i> (TSHT-eq) and <i>R</i> (TSCH-R) enantiomers of THF insertion product 271	155
Figure 4.7 Comparison of the transition states leading to the <i>R</i> (TSCHP-R) and <i>S</i> (TSCHP-S) enantiomers of phthalan insertion product 275	157
Figure 4.8 Structural differences between phebox and phevim ligands.	159
Figure 4.9 Synthesis of amides 274 , 307-310 and <i>N</i> - <i>para</i> -trifluoromethylphenyl phevim ligands 299 , 311-314	170
Figure 4.10 Stacked ¹ H NMR spectra of the <i>trans</i> iridium(III) complex <i>trans</i> - 318 (blue) and the <i>cis</i> iridium(III) phevim complex <i>cis</i> - 318 (black)..	172
Figure 4.11 ¹ H NMR spectrum of the combined insertion products 267 and 319	179

Figure 4.12 HPLC chromatograms for the determination of enantiopurity of alcohols **269**
and **320**..... 180

List of Tables

Table 1.1 Evaluation of Ru ^{II} (salen) complexes 51-54 for asymmetric C-H amination using SES-N ₃	27
Table 2.1 [Ir(TTP)(CH ₃)] 83 catalyzed intramolecular C-H insertion of aryl diazoacetates.	54
Table 2.2 [Ir(TTP)(CH ₃)] 83 catalyzed intramolecular C-H insertion of phenyldiazoacetates	55
Table 3.1 Catalyst optimization for the insertion of methyl phenyldiazoacetate into 1,4-cyclohexadiene	87
Table 3.2 The effect of solvent and 1,4-cyclohexadiene equivalents on the iridium(III) phebox catalyzed donor/acceptor C-H insertion reaction using methyl phenyldiazoacetate	92
Table 3.3 Scope of aryl diazoesters for C-H insertion into 1,4-cyclohexadiene.....	93
Table 3.4 Rh ₂ (<i>S</i> -DOSP) ₄ and Rh ₂ (<i>S</i> -PTAD) ₄ catalyzed cyclopropanation using phenyl diazoacetone.....	106
Table 3.5 Iridium(III) phebox 216 catalyzed C-H insertion of diazoketones into 1,4-cyclohexadiene.	107
Table 3.6 Synthesis of ruthenium(II) pybox carbenes 259-261 by Nishiyama.....	113
Table 3.7 Cyclopropanation of styrene with ruthenium pybox carbenes 259-261	113
Table 3.8 C-H insertion of methyl phenyldiazoacetate into 1,4-cyclohexadiene using triphenylphosphine complexes 262 and 263	120

Table 4.1 Iridium(III) phebox catalyzed acceptor only C-H insertion into 1,4-cyclohexadiene.	129
Table 4.2 Iridium(III) phebox catalyst evaluation for the enantioselective C-H functionalization of tetrahydrofuran using ethyl diazoacetate.....	134
Table 4.3 Lowering the equivalents of phthalan for the iridium catalyzed intermolecular C-H insertion into phthalan using ethyl diazoacetate.	140
Table 4.4 Solvent evaluation for iridium phebox catalyzed C-H insertion of ethyl diazoacetate into phthalan.....	140
Table 4.5 Synthesis of electronically varied <i>N</i> -aryl isopropyl phevim ligands 295, 297-300	165
Table 4.6 Synthesis of iridium(III) phevim complexes 296, 301-304	166
Table 4.7 Evaluation of electronic effects imparted by iridium(III) phevim chloro complexes 296, 301-304 on the enantioselective C-H insertion of ethyl diazoacetate into phthalan.....	167
Table 4.8 C-H insertion of ethyl diazoacetate into phthalan using iridium(III) bromo phevim complexes 305 and 306	168
Table 4.9 Evaluation of iridium(III) phevim complexes 299, 315-318 for the enantioselective C-H insertion of ethyl diazoacetate into phthalan.....	174
Table 4.10 Performance of iridium(III) phevim complexes 317 and <i>trans</i> - 318 for the enantioselective C-H insertion of ethyl diazoacetate into 2,5-dihydrofuran.	175

Table 4.11 Performance of iridium(III) phebim complexes 317 and <i>trans</i> - 318 for the enantioselective C-H insertion of ethyl diazoacetate into tetrahydrofuran.....	176
Table 5.1 Iridium(III) phebox catalyzed asymmetric intramolecular benzylic C-H amination using aryl azides.....	185
Table 5.2 Iridium(III) phebox catalyzed asymmetric intramolecular benzylic C-H amination using sulfamate esters.	186

Abbreviations

Ac	acetyl
AcOH	acetic acid
9-BBN	9-borabicyclo[3.3.1]nonene
Boc	<i>tert</i> -butoxycarbonyl
Bn	benzyl
br	broad
<i>n</i> -BuLi	<i>n</i> -butyllithium
<i>t</i> -BuOOH	<i>tert</i> -butylhydroperoxide
Cbz	benzyloxycarbonyl
d	doublet
dba	dibenzylideneacetone
DCE	1, 2-dichloroethane
DCM	dichloromethane
DIBAL-H	diisobutylaluminum hydride
DMAP	<i>N, N</i> -dimethylaminopyridine
DME	1, 2-dimethoxyethane
DMF	<i>N, N</i> -dimethylformamide
DMP	Dess-Martin periodinane
DMPU	<i>N, N'</i> -dimethyl- <i>N, N'</i> -propylene urea
DMS	dimethylsulfide
DMSO	dimethylsulfoxide

EDCI	1-ethyl-3-(3-dimethylaminopropylcarbodiimide)
equiv.	equivalent
ESI	electrospray ionization
EtOAc	ethyl acetate
HMPA	hexamethylphosphoric triamide
HOBt	1-hydroxybenzotriazole
HRMS	high resolution mass spectroscopy
IBX	2-iodoxybenzoic acid
KHMDS	potassium <i>bis</i> (trimethylsilyl)amide
LA	Lewis acid
LAH	lithium aluminum hydride
LDA	lithium diisopropylamide
LiHMDS	lithium <i>bis</i> (trimethylsilyl)amide
LiTMP	lithium 2,2,6,6-tetramethylpiperidide
m	multiplet
mmol	millimole
NaHMDS	sodium <i>bis</i> (trimethylsilyl)amide
Naph	naphtyl
NIS	<i>N</i> -iodosuccinimide
NMO	<i>N</i> -methylmorpholine <i>N</i> -oxide
NMR	nuclear magnetic resonance
Ns	4-nitrobenzenesulfonyl
PIDA	phenyliododiacetate

Ph	phenyl
phebim	bis(imidazoliny)phenyl
phebox	bis(oxazoliny)phenyl
PMP	<i>para</i> -methoxyphenyl
ppm	parts per million
PTSA	<i>para</i> -toluenesulfonic acid
q	quartet
quint	quintet
rt	room temperature
s	singlet
t	triplet
TBAHS	tetrabutylammonium hydrogen sulfate
TBME	<i>tert</i> -butyl methyl ether
TBDMS	<i>tert</i> -butyldimethylsilyl
TBDPS	<i>tert</i> -butyldiphenylsilyl
TCBoc	2,2,2-trichloro- <i>tert</i> -butyloxycarbonyl
Tf	trifluoromethanesulfonyl
TFA	trifluoroacetic acid
TFAA	trifluoroacetic anhydride
TFP	tris(2-furyl)phosphine
THF	tetrahydrofuran
THP	tetrahydropyran
TMS	trimethylsilyl

TPAP	tetrapropylammonium perruthenate
Ts	<i>para</i> -toluenesulfonyl
w	wea

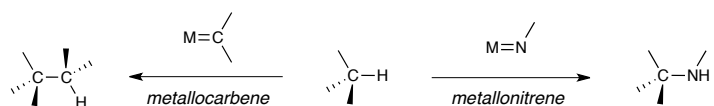
Chapter 1

C-H Functionalization by Metallocarbenes and Metallonitrenes: Background and Significance

1.1 Introduction

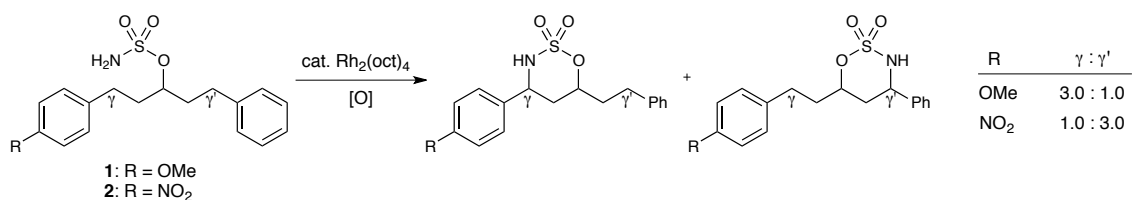
The field of carbon-hydrogen (C-H) bond functionalization has experienced tremendous growth over the past 20 years. The ability for one to selectively convert a C-H bond, which was traditionally considered inert, into a value-added functional group represents a powerful methodology in modern organic synthesis. This approach increases reaction efficiency and redox economy within a synthesis. Achieving predictable reactivity and selectivity in C-H functionalization reactions remains a global research focus.¹

There are many challenges associated with performing selective atom transfer C-H functionalization reactions, the most obvious being that there are often multiple C-H bonds within the substrate. Significant advances have been made to achieve selective functionalization, and transition metal catalysis represents the most efficient tactic for C-H functionalization in complex molecule synthesis. In particular, transition metal catalyzed C-H insertion reactions by metallocarbenes and metallonitrenes are powerful methods for the formation of C-C and C-N bonds, respectively (Scheme 1.1).²⁻⁶



Scheme 1.1. Metallocarbene and metallonitrene C-H functionalization.

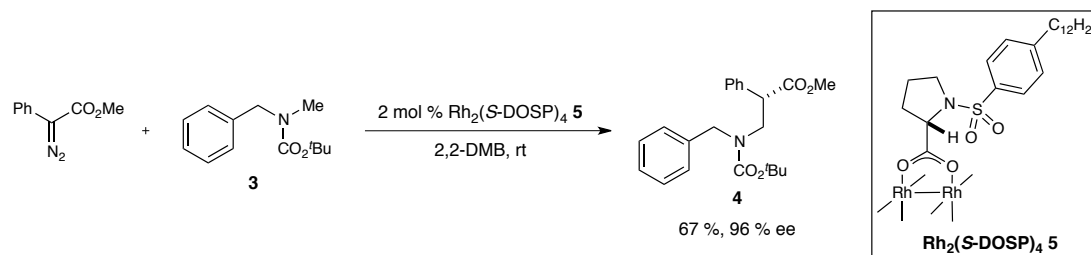
The selectivity can be substantially affected by the inherent electronic and the steric environment around the targeted C-H bond. For dirhodium(II) catalyzed C-H functionalization, the insertion reaction occurs at the site best able to stabilize partial positive charge buildup during the transition state ($3^\circ > 2^\circ > 1^\circ$).⁷⁻⁹ An example of this phenomenon is demonstrated in the $\text{Rh}_2(\text{oct})_4$ catalyzed intramolecular C-H amination reaction of sulfamate esters, where two benzylic sites (γ and γ') are available to undergo functionalization (Scheme 1.2).¹⁰ When *para*-methoxy substituted sulfamate ester **1** is used as the substrate C-H insertion occurs with a 3.0:1.0 preference for the more electron rich γ position. When the *para*-nitro substituted sulfamate ester **2** is employed a reversal in selectivity is observed, and the now electron poor γ site is disfavored in a 1.0:3.0 ratio.



Scheme 1.2. Selectivity studies on the $\text{Rh}_2(\text{oct})_4$ catalyzed intramolecular C-H amination of sulfamate esters.

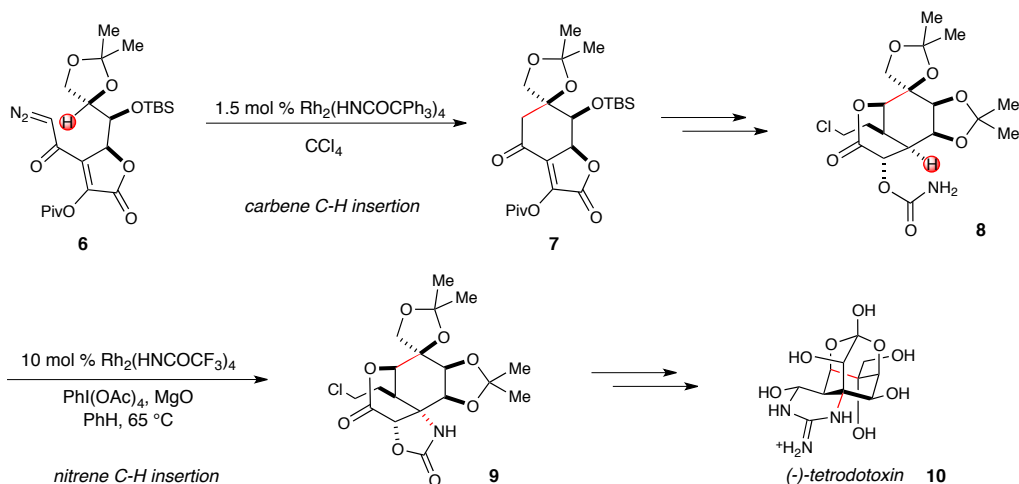
The steric environment around the C-H bond can sometimes supersede electronic control such that the selectivity is reversed ($1^\circ > 2^\circ > 3^\circ$). An example of this effect is shown for the $\text{Rh}_2(S\text{-DOSP})_4$ (**5**) catalyzed reaction of the metallocarbene generated from methyl phenyldiazoacetate with *N*-Boc protected amine **3** (Scheme 1.3).¹¹ In this reaction, the more electronically favored 2° benzylic C-H bonds are not functionalized. Instead, the C-H functionalization occurs exclusively at the methyl group alpha to nitrogen to

provide enantioenriched amine **4**. Steric effects imparted by the catalyst also play a significant role in C-H functionalization selectivity.



Scheme 1.3. $\text{Rh}_2(\text{S-DOSP})_4$ catalyzed enantioselective intermolecular C-H functionalization alpha to nitrogen.

Perhaps one of the most elegant examples of metallocarbene and metallocarbene C-H functionalization in complex molecule synthesis arose from Du Bois' synthesis of tetrodotoxin, one of nature's most potent neurotoxins (Scheme 1.4).¹² Treatment of diazoketone **6** with dirhodium(II) catalyst $\text{Rh}_2(\text{HNCOCPh}_3)_4$ formed a metallocarbene intermediate that underwent stereospecific C-H insertion to generate cyclohexanone **7** in > 80 % yield. A series of manipulations furnished compound **8**, which upon treatment with 10 mol % $\text{Rh}_2(\text{HNCOCF}_3)_4$, $\text{PhI}(\text{OAc})_4$, and MgO in benzene at 65 °C formed a metallonitrene intermediate from the corresponding carbamate. This rhodium nitrene then performed an intramolecular C-H amination reaction to form **9** in 77 % yield. This adduct was elaborated to furnish (-)-tetrodotoxin **10**, and its enantioselective synthesis represents the most efficient to date, highlighting the power of metallocarbene and metallonitrene reactive intermediates for complex molecule construction.



Scheme 1.4. Du Bois' synthesis of (-)-tetrodotoxin via metallocarbene and metallonitrene C-H insertion.

1.2 Metallocarbenes

1.2.1 Generation and classification

Electrophilic metallocarbenes can be generated from a wide variety of transition metals and carbene precursors.¹³ These intermediates have a diverse reactivity profile and are known to undergo C-H insertion, cyclopropanation, cyclopropanation, ylide formation, cycloaddition, metathesis and olefination reactions.¹⁴⁻¹⁶ Diazo compounds are the most common metallocarbene precursors used in C-H functionalization chemistry due to their ease of synthesis and that environmentally benign dinitrogen gas is the sole byproduct after carbene formation.^{13,17-20} The mechanism of metallocarbene formation from diazo compounds and the catalytic cycle for C-H functionalization is illustrated in Figure 1.1.

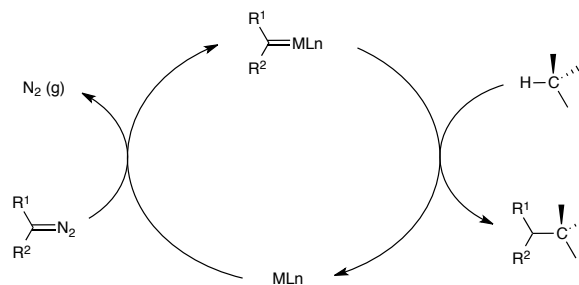


Figure 1.1. Mechanism for metallocarbene formation and C-H functionalization using diazo compounds.

Carbene structure can greatly affect both reactivity and selectivity. Hence, there are three main classifications of metallocarbenes: donor/acceptor, acceptor, and acceptor/acceptor (Figure 1.2).^{2,5,21} Donor/acceptor metallocarbenes feature both an electron-withdrawing group (e.g. ester, ketone) and an electron-donating group, most commonly in the form of a substituted aryl, heteroaryl, or vinyl moiety. Acceptor-only metallocarbenes are monosubstituted with an electron-withdrawing functional group, e.g. an ester, ketone, amide, sulfonate, nitro, or phosphonate *etc.* Acceptor/acceptor metallocarbenes consist of two electron-withdrawing functionalities. These groupings exist because each class has its own distinct reactivity and selectivity in metallocarbene atom-transfer reactions. The acceptor functionality serves to render the carbene very electrophilic and increase its reactivity. As a consequence, intermolecular C-H insertion reactions using acceptor-only carbenes are typically less regio- and stereoselective due to their exceptional electrophilicity. Thus, aryl and vinyl donor substituents are introduced in donor/acceptor carbenes to decrease electrophilicity and enhance reaction selectivity.

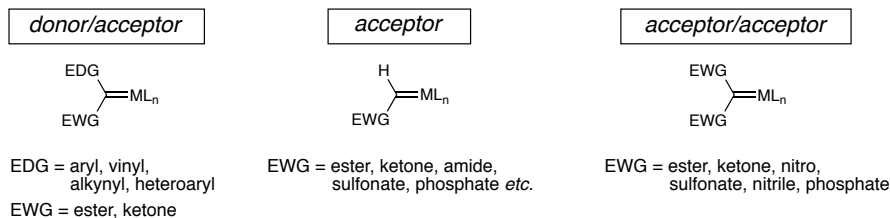


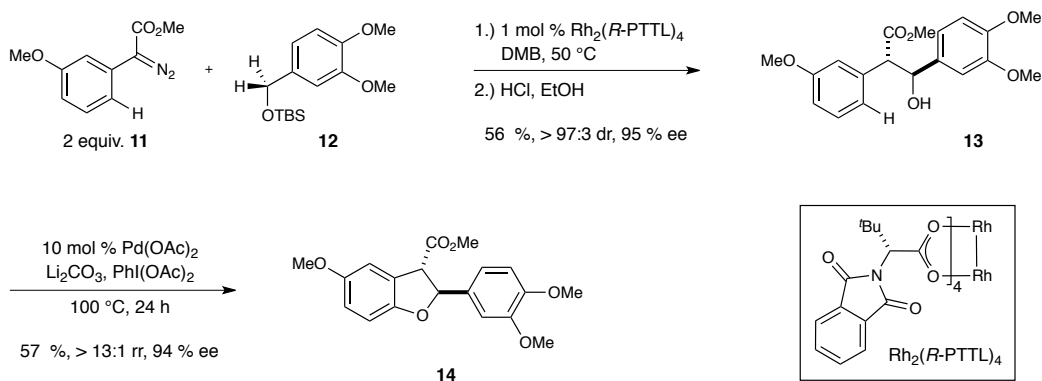
Figure 1.2. Classes of metallocarbenes.

The design of transition metal catalysts (ML_n) has allowed for further modulation of the electrophilicity, and chiral catalysts have been introduced to effect asymmetric C-H insertion reactions. The subtle interplay between the substituents on the carbene and the ligands surrounding the metal center offers many avenues for the design of efficient and selective C-H functionalization methodology. Intra- and intermolecular C-H insertion reactions using donor/acceptor and acceptor-only metallocarbenes are the most established and are further discussed below.

1.2.2 C-H Insertion with donor/acceptor metallocarbenes

Donor/acceptor metallocarbenes exhibit the highest selectivity profile amongst the other metallocarbene classes for intermolecular C-H functionalization.⁵ Dirhodium(II) tetracarboxylate and tetracarboxamidate complexes are the most widely developed and successful in donor/acceptor metallocarbene C-H functionalization and high enantioselectivity can be achieved.^{2,5,7,21-24} Work from the Davies lab has shown that the dirhodium(II) tetracarboxylate complexes perform insertion into a variety of unactivated (alkyl, cycloalkyl) and activated (allylic, benzylic, α to heteroatom) C-H bonds.^{2,5,7,25} For example, the reaction of donor/acceptor diazoester **11** with TBS-protected benzyl alcohol

12 in the presence of 1 mol % $\text{Rh}_2(\text{R-PTTL})_4$ in dimethylbutane at 50 °C furnishes C-H insertion product **13** in 56 % yield with 97 : 3 dr and 95 % ee after TBS deprotection (Scheme 1.5).²⁵ Further elaboration of **13** using a palladium catalyzed C-H etherification reaction developed by Yu afforded highly-substituted dihydrobenzofuran **14** in 75 % yield with a 13:1 regioisomeric ratio and 94 % ee. This sequential C-H functionalization approach was used for the synthesis of a variety of enantioenriched dihydrobenzofurans and the core of the lithospermic acid family of natural products, which exhibit potent yet non-toxic anti-HIV activity.²⁶



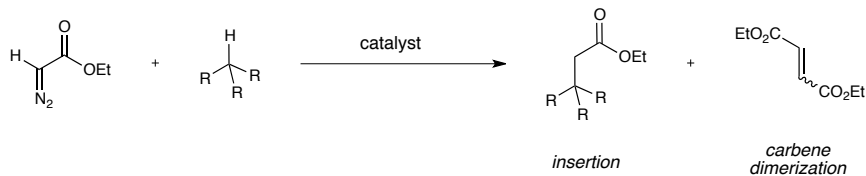
Scheme 1.5. Donor/acceptor enantioselective intermolecular C-H insertion towards the synthesis of dihydrobenzofurans.

1.2.3 C-H Insertion with acceptor-only metallocarbenes

As mentioned in Section 1.2.1, acceptor-only metallocarbenes are highly electrophilic and developing selective C-H insertion reactions with these reagents is difficult. Davies and Austchbach computationally studied the reactivity differences between dirhodium metallocarbenes derived from methyl phenyldiazoacetate (donor/acceptor) and methyl diazoacetate (acceptor-only) for C-H insertion reactions.⁷

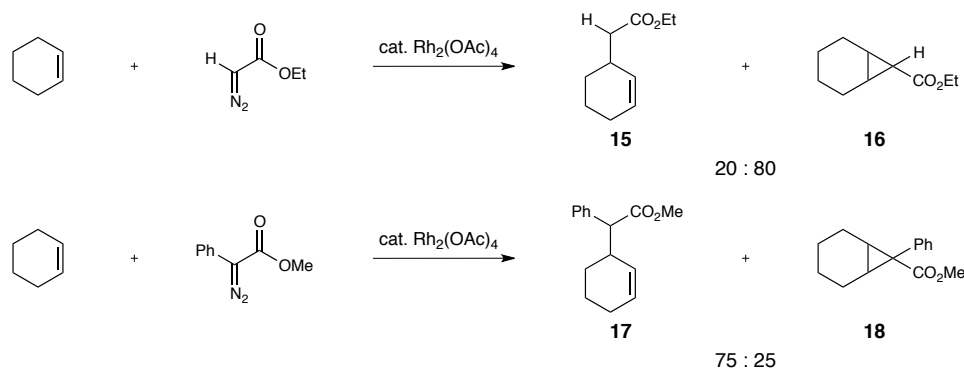
For the donor/acceptor rhodium carbene, it was calculated that the potential energy barrier for the C-H insertion into cyclopentane is $17.4 \text{ kcal}\cdot\text{mol}^{-1}$. A much lower energy barrier for the acceptor-only rhodium carbene was found at $3.5 \text{ kcal}\cdot\text{mol}^{-1}$. It was also found that there is more positive charge buildup in the transition state for the donor/acceptor carbene, which indicates a later transition state during the C-H insertion. The calculations were also carried out on 1,4-cyclohexadiene, which possesses a doubly allylic methylene system. For the acceptor-only carbene, the transition state for the insertion was essentially barrierless at $1.2 \text{ kcal}\cdot\text{mol}^{-1}$, and for the donor/acceptor carbene this energy was $6.2 \text{ kcal}\cdot\text{mol}^{-1}$. These computational data indicate that the transition state for C-H insertion is much earlier for acceptor-only carbenes compared to the donor/acceptor system. This helps to explain why the donor/acceptor carbenes are typically more selective in comparison.

Intermolecular reactions with these reactive metallocarbenes present exceptional challenges. For example, the acceptor metallocarbene generated from ethyl diazoacetate is highly prone to dimerization to form the maleate and fumarate esters before the C-H insertion event can occur (Scheme 1.6).²⁷ Slow addition of the diazo compound to the reaction mixture and/or a large excess of the substrate are absolutely necessary to suppress this side reaction. Furthermore, the very electrophilic carbene is unable to discriminate between C-H bonds with similar bond dissociation energies, and selectivity is difficult to control unless electronically or sterically biased substrates are employed.



Scheme 1.6. Intermolecular acceptor-only C-H insertion versus dimerization.

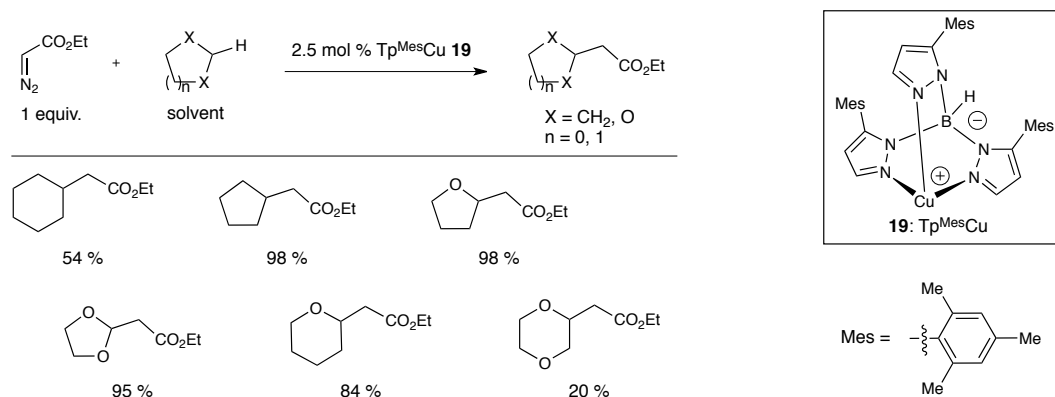
Chemoselectivity between C-H insertion and cyclopropanation using acceptor-only carbenes is also challenging in that the olefin is more likely than the C-H bond to engage the metallocarbene. The Müller group found that reacting cyclohexene with ethyl diazoacetate and catalytic $\text{Rh}_2(\text{OAc})_4$ results in a 20 : 80 mixture of allylic C-H insertion product **15** to cyclopropane **16** (Scheme 1.7).²⁸ Decreasing the electrophilicity of the carbene by using the donor/acceptor carbene precursor methyl phenyldiazoacetate reversed the selectivity and provided a 75 : 25 mixture of C-H insertion (**17**) to cyclopropane **18**.



Scheme 1.7. C-H functionalization versus cyclopropanation for $\text{Rh}_2(\text{OAc})_4$ catalyzed reactions with acceptor-only and donor/acceptor metallocarbenes.

Effective intermolecular C-H insertion reactions into cyclic and acyclic hydrocarbons using acceptor-only metallocarbenes have been established using copper,²⁹⁻

³² silver,^{33,34} and gold³¹ complexes that employ very sterically demanding ligands.^{27,35} In 2002, the copper homoscorpionate tris-(3-mesityl)-pyrazolylborate (Tp^{Mes}Cu) complex **19** was shown to catalyze the C-H insertion of ethyl diazoacetate into cyclic alkanes and cyclic ethers in moderate to excellent yields (Scheme 1.8). In this chemistry, slow addition of ethyl diazoacetate over 2-20 hours was required and the substrate is used as solvent. Another drawback is that the homoscorpionate ligand is not easily prepared.^{36,37} Moreover, chiral copper, silver, or gold homoscorpionate complexes have not been reported in the literature.^{38,39,40} To the best of our knowledge, C-H insertion into substrates which also possess an olefin has not been disclosed. Although the intermolecular metallocarbene C-H insertion using ethyl diazoacetate is a significant achievement, these limitations have precluded the extension to its enantioselective variant.

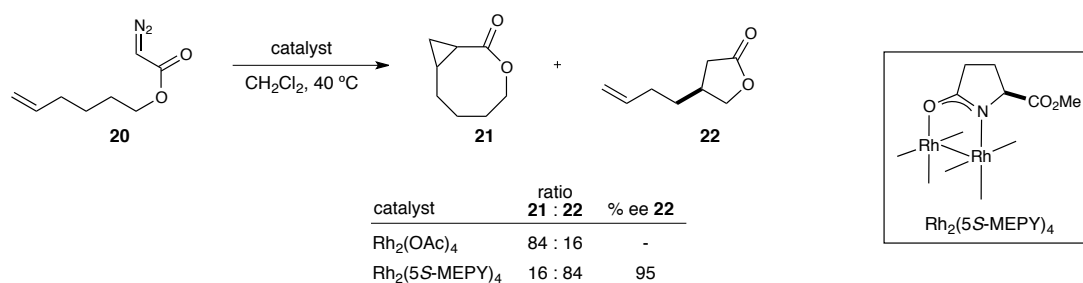


Scheme 1.8. Copper catalyzed acceptor-only intermolecular C-H insertion into cyclic ethers and cyclic alkanes.

Given these limitations of the state-of-the-art intermolecular acceptor-only C-H insertion reactions, the major advances using these metallocarbenes have arisen *via*

intramolecular reactions. Tethering the acceptor-only carbene precursor onto the substrate to be functionalized inhibits the dimerization side reaction by placing the carbene and C-H bond into proximity with each other, and the preference for 5 membered ring over 6 membered ring formation dominates.³ In this chemistry however, complete chemoselectivity for C-H insertion over cyclopropanation is difficult to achieve due to the highly electrophilic nature of the carbene intermediate.

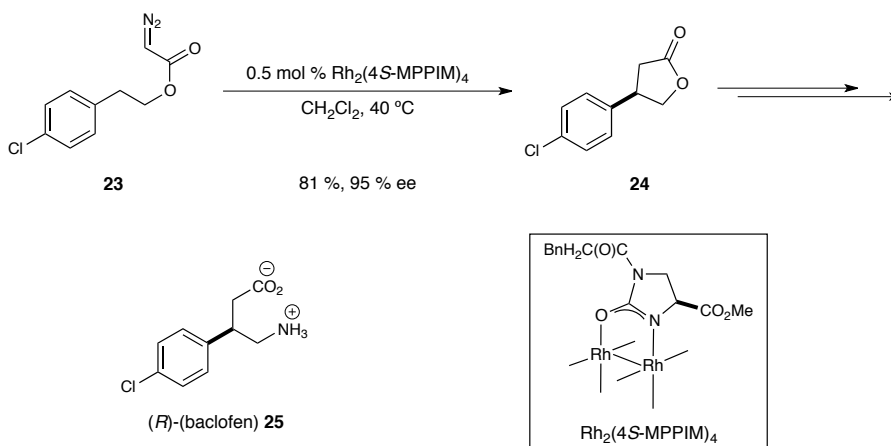
The more electron-rich dirhodium(II) tetracarboxamidate complexes (compared to dirhodium(II) tetracarboxylate complexes) developed by Doyle have been very successful with respect to chemoselective asymmetric C-H functionalization. Competition studies revealed that in the reaction of the pendant alkenyl diazoacetate **20** with $\text{Rh}_2(\text{OAc})_4$, cyclopropanation to give **21** occurs with an 86 : 14 preference over C-H insertion (Scheme 1.9).⁴¹ When the dirhodium(II) tetracarboxamidate complex $\text{Rh}_2(5S\text{-MEPY})_4$ was used, an exact reversal of chemoselectivity was observed and butyrolactone **22** was formed with 95 % enantiomeric excess.



Scheme 1.9. Dirhodium(II) tetracarboxamidate catalyzed acceptor-only intramolecular C-H insertion.

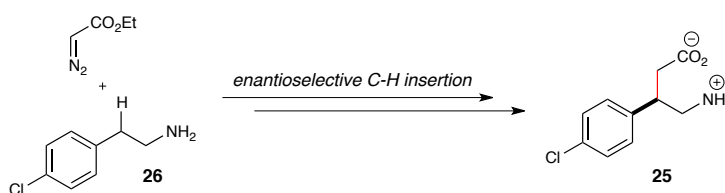
To highlight the utility of acceptor-only intramolecular C-H insertion reactions, Doyle showed that acceptor-only diazoacetate **23** could undergo highly enantioselective

C-H insertion using $\text{Rh}_2(4S\text{-MPPIM})_4$ to form lactone **24** in 81 % yield and 95 % ee (Scheme 1.10).⁴² This lactone was further elaborated in four steps to the GABA_B receptor agonist (*R*)-(-)-baclofen (**25**).



Scheme 1.10. Synthesis of baclofen *via* acceptor-only intramolecular C-H insertion.

As showcased in the synthesis of (*R*)-(-)-baclofen, our understanding of acceptor-only intramolecular C-H insertion has enabled efficient syntheses of enantiopure complex molecules. However, current methods may not always enable the most efficient route to a molecule. For example, a more obvious disconnection towards the synthesis of baclofen would entail the enantioselective intermolecular benzylic C-H insertion using ethyl diazoacetate and 4-chloro-phenethylamine **26**, both of which are commercially available (Scheme 1.11). This overall transformation is not achievable by current methodologies, but nevertheless highlights the need for new catalyst development.



Scheme 1.11. Synthesis of baclofen *via* acceptor-only intramolecular C-H insertion using ethyl diazoacetate.

1.2.4 Conclusions and challenges

There are many factors governing the development of efficient and selective C-H functionalization reactions. The substituents on the metallocarbene precursors have been shown to significantly influence the selectivity of the reaction. The enhanced stability of donor/acceptor metallocarbenes has enabled the advancement of chemo- and enantioselective intermolecular C-H functionalization, and these reactive intermediates have proven broadly effective in complex molecule synthesis. On the other hand, acceptor-only metallocarbenes are very reactive because of their increased electrophilicity. This property has impeded the development of chemo- and enantioselective intermolecular C-H insertion using these reagents, and the best acceptor-only reactions are those that are performed intramolecularly.

Furthermore, catalyst design has played an important role in the expansion of methods for enantioselective C-H insertion methodologies. A general catalyst that is effective for all classes of metallocarbenes described above has not yet been developed. Davies' dirhodium(II) tetracarboxylate catalysts are most successful for intermolecular carbene C-H insertion, while Doyle's more electron-rich dirhodium(II) carboxamidate catalysts are best for acceptor intramolecular C-H insertion. Bulky coinage metal catalysts have been showed to effect intermolecular acceptor-only C-H insertion, however enantioselective methodologies do not currently exist due to limited variability of the ligands necessary to prevent side reactions.

1.3 Metallonitrenes

1.3.1 Introduction

Due to the prevalence of nitrogen in biologically active molecules, the development of efficient carbon-nitrogen bond forming reactions represents a central theme in current synthetic chemistry research.^{2,4,6,35,43-46} Methods for this transformation have increased significantly in recent years and oxidative amination via metallonitrene intermediates have contributed significantly towards this growth. However, reactions of metallonitrenes are far less developed than their metallocarbene counterparts, with aziridination and C-H insertion dominating the literature.⁴⁷ Only within the last five years have these intermediates been used in other reaction manifolds, namely ones in which non-alkenyl π systems are engaged in the oxidative amination process.⁴⁸⁻⁵⁴ This growth highlights the potential of such intermediates for the synthesis of nitrogen containing molecules.

1.3.2 Generation of metallonitrenes

Metallonitrenes are by far the most utilized intermediates for C-H amination reactions. The recognition that the *N*-tosylimino-phenyliodinane (PhI=NTs) could act as an electrophilic nitrogen atom transfer reagent laid the foundation upon which oxidative C-H amination has been built.^{55,56} Breslow and Gellman demonstrated the utility of aryl sulfonyliminoiodinanes for intramolecular C-H amination using manganese and iron

porphyrins, iron salts, and dirhodium(II) tetraacetate.⁵⁷ The Müller group further established the efficacy of $\text{Rh}_2(\text{OAc})_4$ for aziridination and insertion reactions via metallonitrenes.^{58,59} The technology has become significantly more practical since the discovery of convenient procedures that allow for the *in situ* generation of the reactive imido species, which upon reacting with a transition metal forms the metallonitrene intermediate after extrusion of a leaving group. The mechanism for metallonitrene formation is outlined in Figure 1.3.

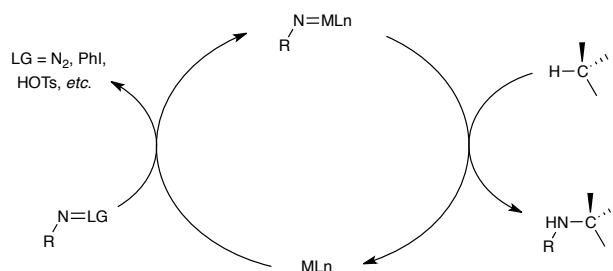
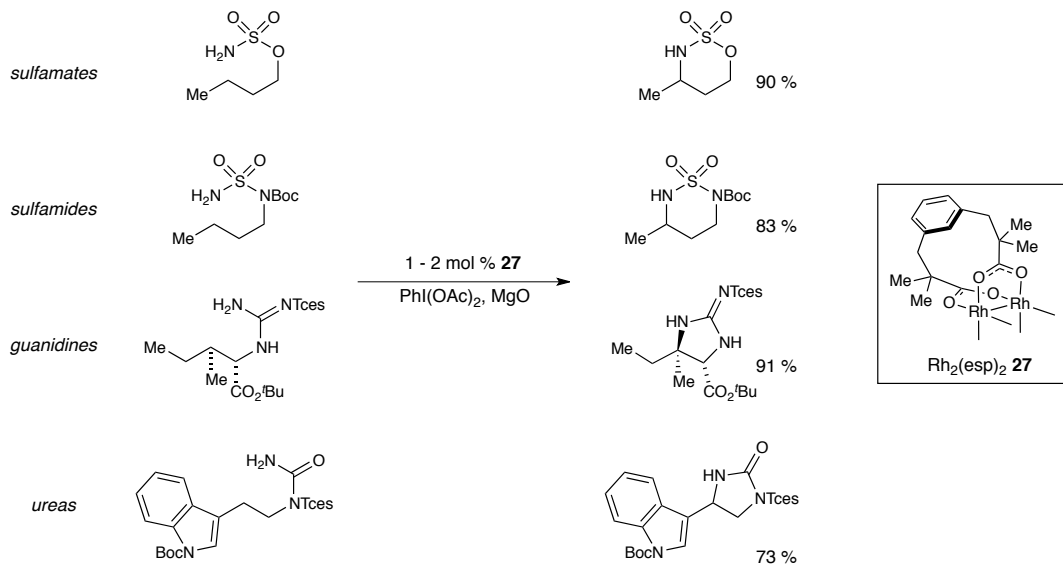


Figure 1.3. Mechanism for metallonitrene formation and C-H functionalization.

Building upon the seminal work by Breslow and Müller, the groups of Che and Du Bois found that the iminoiodinane metallonitrene precursor could be generated *in situ* by mixing a suitable amine source with bis-acetoxyiodobenzene $[\text{PhI}(\text{OAc})_2]$. Since this discovery, significant and rapid advances in C-H amination have been achieved and numerous applications to the synthesis of complex molecular architectures have been realized.^{45,60,61}

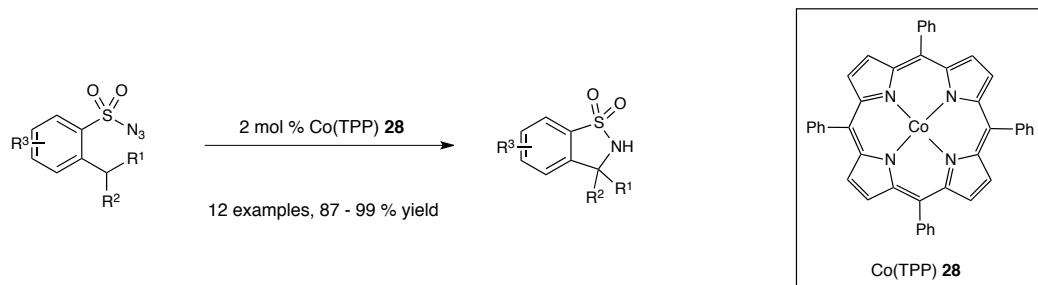
1.3.3 Intramolecular C-H amination

Initially Che developed achiral ruthenium and manganese porphyrin complexes⁶²⁻⁶⁴ for C-H amination that used sulfamates with the *in situ* iminoiodinane formation protocol for the formation of six and five membered sulfamidate heterocycles.⁶⁵ Du Bois has also utilized dirhodium(II) tetracarboxylates and tetracarboxamidates for efficient C-H amination using sulfamate and carbamate substrates,^{4,66} and further catalyst design has improved the scope of intramolecular amination reactions. The standard dirhodium(II) tetracarboxylate catalysts, such as $\text{Rh}_2(\text{OAc})_4$, were found to undergo rapid ligand exchange and degradation in the presence of the hypervalent iodine oxidant. The bridged carboxylate complex $\text{Rh}_2(\text{esp})_2$ **27** (Scheme 1.12) was subsequently designed on the grounds that ligand exchange would occur less and that the stability of the catalyst would increase. In fact, this catalyst has permitted the use of sulfamide, guanidine, and urea derivatives as nitrene precursors for efficient C-H amination.⁶⁷ The design of $\text{Rh}_2(\text{esp})_2$ highlights the importance of catalyst design for the invention of new synthetic technologies.



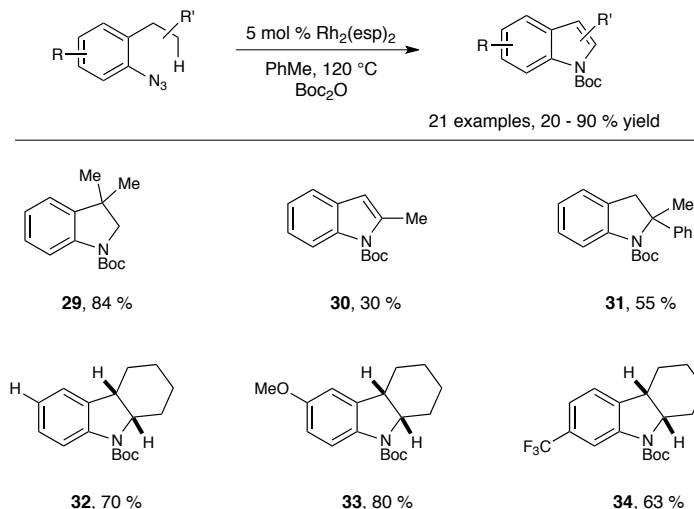
Scheme 1.12. $\text{Rh}_2(\text{esp})_2$ catalyzed intramolecular C-H amination reactions.

Further progress has been made regarding intramolecular amination reactions that exclude the need for an external oxidant. Lebel and coworkers have used preoxidized tosyloxycarbamates to generate the metallonitrene in the presence of K_2CO_3 and a dirhodium(II) catalyst.⁶⁸ A strong argument can be made that azides are the most atom-economical and environmentally friendly sources of metallonitrenes. Additives are not needed to generate the metallonitrene and dinitrogen gas is the only byproduct of the reaction [see Figure 1.3, $\text{LG} = \text{N}_2(\text{g})$].⁶⁹ An ideal situation would entail using an azide that is prefunctionalized to contain the desired substitution on the resultant amine. The Zhang group has reported that cobalt(II) porphyrin complex **28** is a competent catalyst for intramolecular C-H amination using the electron deficient aryl-phosphoryl and aryl-sulfonyl azides (Scheme 1.13).^{70,71}



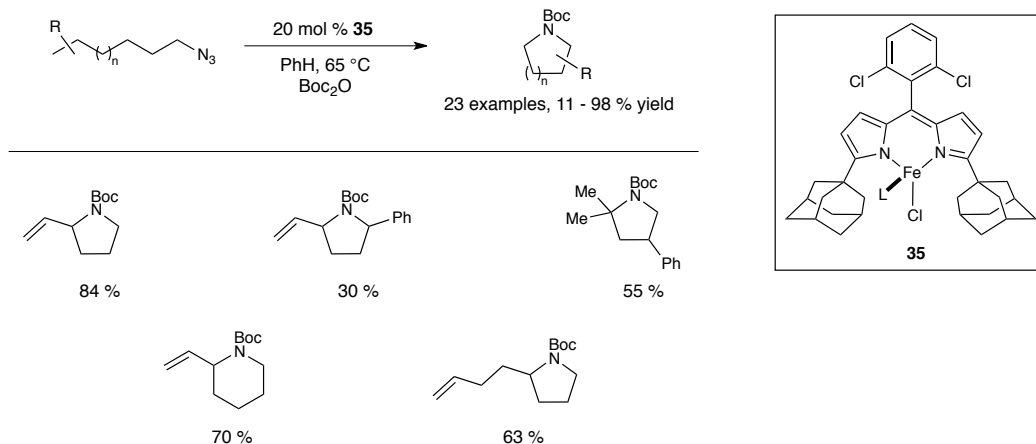
Scheme 1.13. Cobalt(II) tetraphenylporphyrin (**28**) catalyzed C-H amination of sulfonyl azides.

All of the metallonitrenes described above rely on the use of an electron-withdrawing group on the nitrogen to make the nitrene electrophilic enough to engage the C-H bond. To alleviate this limitation, the Driver group has made substantial advances in which simple aryl and vinyl azides undergo intramolecular sp^2 and sp^3 C-H amination under transition metal catalysis to form substituted indolines, indoles, and pyrroles.^{48-50,72-74} One report showed that azide-derived rhodium(II) nitrenes can successfully aminate 1°, 2°, and 3° aliphatic C-H bonds in good yields (Scheme 1.14).⁷³ Notably, the electron-rich azide precursor to **33** efficiently performed the amination in 80 % yield. However, asymmetric C-H amination has not been achieved in the cases where indoline products are formed.

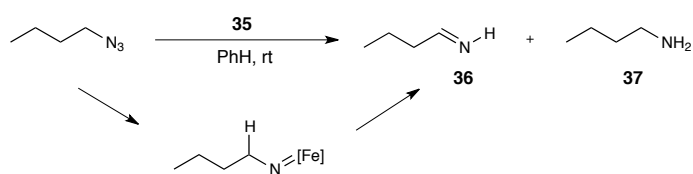


Scheme 1.14. Select examples of $\text{Rh}_2(\text{esp})_2$ catalyzed aliphatic C-H amination using aryl azides.

Betley and coworkers recently reported another impressive example of iron catalyzed intramolecular 2° and 3° C-H amination using simple aliphatic azides as the *N*-atom source.⁷⁵ Iron complex **35** furnished a variety of functionalized azetidine, pyrrolidine, and piperidine heterocycles in moderate to high yields, a few of which are shown in Scheme 1.15. The foremost significance of this report is that alkyl azides are viable substrates for this reaction. For example, when catalyst **35** was treated with 1-azidobutane the only products observed were those derived from β -hydride elimination (**36**) and protodemetalation (**37**) of the iron nitrene (Scheme 1.16). Thus, primary C-H bonds are too unreactive to undergo insertion with this catalyst system.



Scheme 1.15. Iron catalyzed C-H amination using aliphatic azides.



Scheme 1.16. Protodemetalation and β -hydride elimination of an alkyl-substituted metallonitrene.

Asymmetric intramolecular C-H amination has built upon the use of external oxidants to generate the metallonitrene, and catalyst design has made the most impact on developing efficient amination protocols. Che set the precedent for enantioselective C-H amination with the discovery that chiral ruthenium porphyrin catalyst **38** could achieve asymmetric induction in the amination of sulfamate esters (48 %, 84 % ee, entry 1, Figure 1.4).^{76,77} This was a significant achievement, but further development of these catalysts was impeded by the lengthy, inefficient, and expensive synthesis of the chiral porphyrin complex. The Blakey group recognized this setback and designed the ruthenium(II) pybox complex **39**.⁷⁸ An advantage to using this system is that the asymmetric environment is readily prepared from chiral amino alcohols, many of which are

commercially available. Although the enantioselectivity for the amination of sulfamate **41** was lower (entry 2, Figure 1.4) than the ruthenium porphyrin catalyzed reaction, pybox catalyst **39** exhibited consistently high reaction yields and enantioselectivities across a wider range of sulfamates. *Trans*-olefins were particularly amenable to allylic C-H insertion and aziridination was not observed. Du Bois also reported that the chiral dirhodium(II) tetracarboxamidate $\text{Rh}_2(\text{S-nap})_4$ (**40**) provided excellent enantioselectivities across a similar range of sulfamates (entry 3, Figure 1.4).⁷⁹ The enantioselectivities for all systems were comparable, with the dirhodium(II) system being more successful in allylic C-H amination of *cis*-olefins.

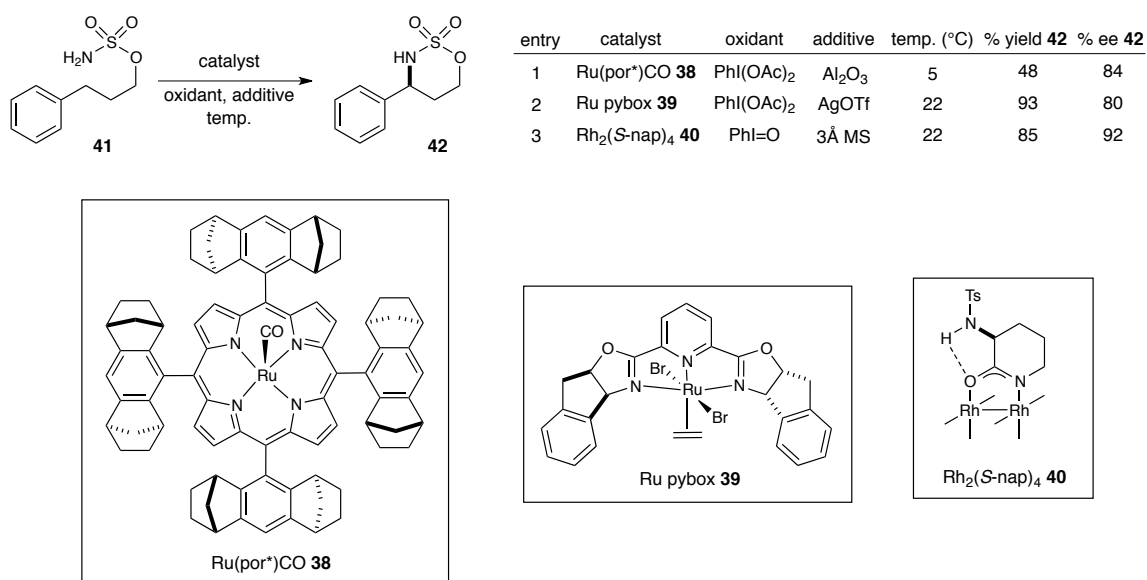
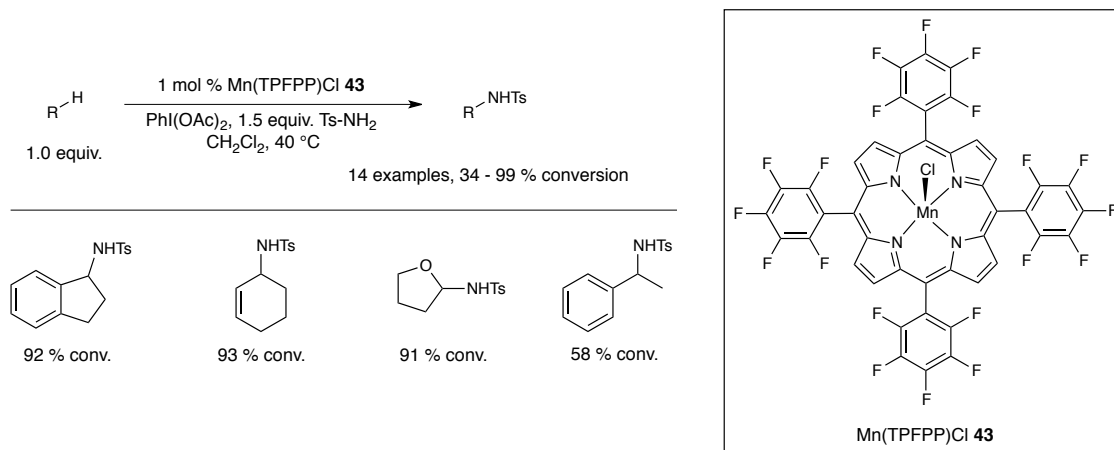


Figure 1.4. Ruthenium porphyrin **38**, ruthenium pybox **39**, and dirhodium(II) tetracarboxamidate **40** catalyzed asymmetric intramolecular C-H amination.

1.3.4 Intermolecular C-H amination

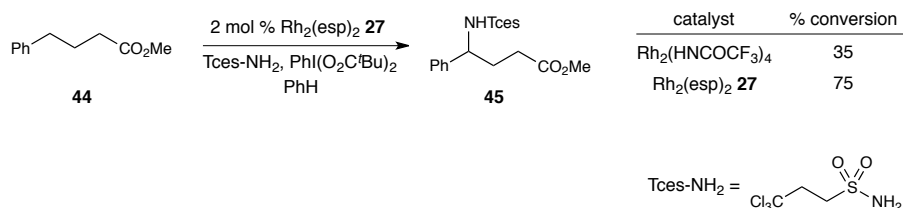
Similar to the analogous metallocarbene chemistry, the development of intermolecular C-H amination comes with many challenges not encountered in the intramolecular manifold. The reactive metallonitrene is not in proximity to the C-H bond to be functionalized but must still discriminate amongst multiple C-H bonds in a molecule. In addition, modification of the nitrene precursor is not as readily achieved as with the metallocarbene precursor diazo compounds. Electronic modification on the *N*-atom source is limited to an electron-withdrawing group, which is necessary to make the metallonitrene reactive enough to engage the C-H bond. Thus, the catalyst itself imparts the only further electronic and steric modifications, and intermolecular C-H amination reactions typically require a catalyst that is tailored for a specific nitrene source.

Che pioneered this field when he discovered that manganese porphyrin catalyst **43** is effective for the intermolecular benzylic, allylic, 3°, and ethereal C-H amination of alkanes using 1.25 equivalents $\text{PhI}=\text{NTs}$, which was generated *in situ* from 1.5 equivalents Ts-NH_2 and $\text{PhI}(\text{OAc})_2$ (Scheme 1.17).⁶⁵ A key feature in this reaction is that the alkane is used as the limiting reagent. Cobalt and ruthenium porphyrin complexes have also been described as effective C-H amination catalysts.⁸⁰

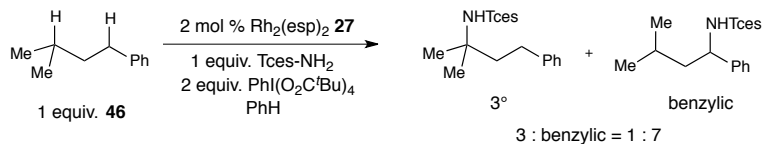


Scheme 1.17. Manganese porphyrin catalyzed intermolecular C-H amination.

Copper and silver complexes are also known to perform intermolecular C-H amination, but selectivity between 1°, 2°, and 3° C-H bonds is low. Another significant challenge lies in the need for a large excess of the substrate.^{27,35,45} The broad utility of Rh₂(esp)₂ was again displayed by Du Bois when they found that one equivalent of sulfamate Tces-NH₂ could generate a metallonitrene capable of intermolecular C-H amination (Scheme 1.18). This catalyst was far superior over the other dirhodium catalysts investigated.⁸¹ In contrast to intramolecular sulfamate C-H amination with Rh₂(esp)₂, benzylic insertion is preferred over 3° C-H functionalization (Scheme 1.19).

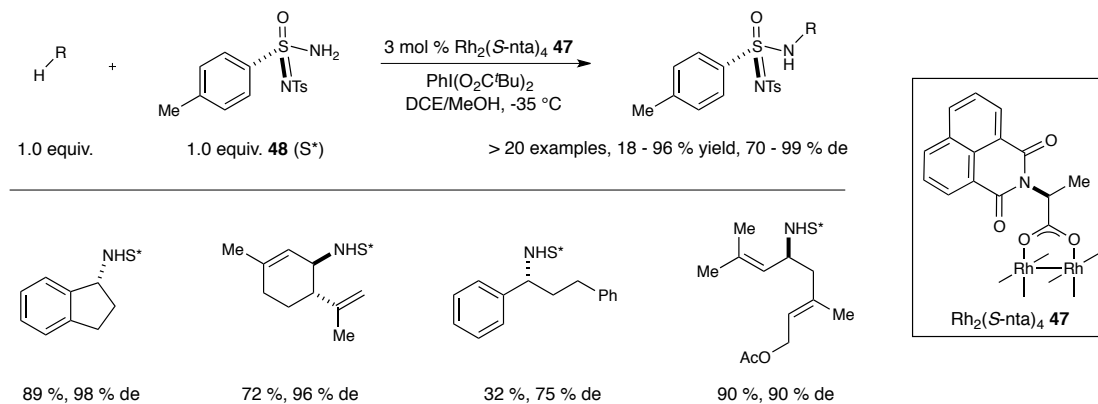


Scheme 1.18. Rh₂(esp)₂ catalyzed intermolecular C-H amination with Tces-NH₂.



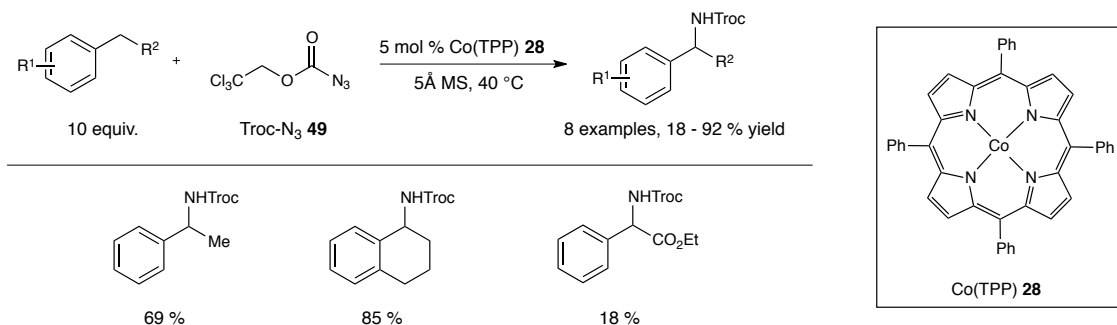
Scheme 1.19. Selectivity studies on $\text{Rh}_2(\text{esp})_2$ catalyzed intermolecular C-H amination.

Progress has also been made in asymmetric intermolecular C-H amination via the development of chiral dirhodium catalysts. Hashimoto⁸² and Davies⁸³ have made significant contributions in this area and high enantioselectivities can be achieved using iminoiodinanes as the nitrene sources. Limitations of these methods include the need for a large excess of substrate to achieve acceptable reaction yields and enantioselectivities. Dauben et. al. took a different approach by employing a chiral sulfonimidamide nitrene source alongside the chiral dirhodium(II) tetracarboxylate $\text{Rh}_2(S\text{-nta})_4$ **47**.⁴⁵ In fact highly diastereoselective C-H amination of 3°, 2°, allylic, and benzylic C-H bonds in cyclic as well as acyclic substrates was achieved using this catalyst/reagent combination (Scheme 1.20). One equivalent of the sulfonimidamide **48** (abbreviated S^*) with respect to the substrate was employed, and chemoselectivity in this system for C-H insertion over aziridination was superb. While the sulfonimidamide can be readily cleaved by sodium naphthalenide while maintaining enantiopurity, the use of a chiral auxiliary in addition to a chiral catalyst is not atom-economical.



Scheme 1.20. Rh₂(S-nta)₄ catalyzed diastereoselective C-H amination using chiral sulfonimidamide auxiliary **48**.

To address the issue of atom economy, azides have been investigated as the *N*-atom source for intermolecular C-H amination. Substantial advances have been made using azides for aziridination reactions, but C-H insertion using these nitrene precursors is far less established. Cobalt porphyrins are prolific in achieving insertion reactions using sulfonyl and aryl azides, but many of these protocols require impractical functional groups on nitrogen to achieve satisfactory yields.⁶⁹ Zhang and coworkers reported the Co(TPP) **28** catalyzed racemic benzylic C-H amination using Troc-N₃ **49** as the nitrogen source (Scheme 1.21, Troc = trichloroethoxycarbonyl).⁸⁴ This protocol has an advantage over other methodologies in that the Troc protecting group can be easily removed, however the insertion substrate must be used in large excess and the substrate scope is limited.



Scheme 1.21. Co(TPP) **28** catalyzed benzylic C-H amination using Troc-N₃.

In 2010 the Katsuki group discovered that ruthenium salen complexes were capable of enantioselective intermolecular aziridination using SES-N₃ **50** (SES = 2-(trimethylsilyl)ethanesulfonyl).⁸⁵ They built upon this finding by extending these complexes' capabilities in atom-transfer chemistry by performing allylic and benzylic C-H amination using the substrate as the limiting reagent.⁸⁶ Eight ruthenium(II) salen complexes (**51-54**) were initially examined for the C-H insertion into the benzylic position of indane, and the results from four of the complexes are given in Table 1.1. It is imperative to mention that very subtle changes on the aryl group of the salen ligand can have a strong effect on yield and selectivity. When Ar = phenyl, the reaction yield is undesirable at 4 % while the enantioselectivity is good at 85 % (entry 1). Placing chloride substituents on the 3- and 5- positions of the aryl ring provides a dramatic increase in yield to 44 % with 83 % enantioselectivity (entry 2). Simply replacing chloride with fluoride in the 3- and 5- positions substantially increases the enantioselectivity to 92 % (entry 3). Changing the position of the two fluorine substituents gives a further increase in yield and enantioselectivity to 51 % and 95 %, respectively (entry 4). This catalyst screen demonstrates that very small changes on the catalyst can dramatically influence

the reaction outcome. Unfortunately the synthesis of this ligand framework is not divergent and rapid modifications cannot be made. For example, the salen ligand precursors to catalysts **51-54** require a nine-step synthesis from commercially available materials and the aryl substituent is introduced at the sixth step of the synthesis. As a consequence, it is difficult to evaluate a broad ligand set for a particular transformation.

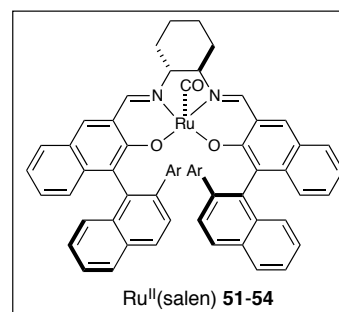
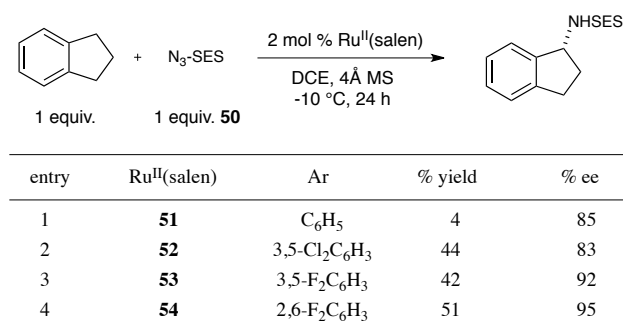
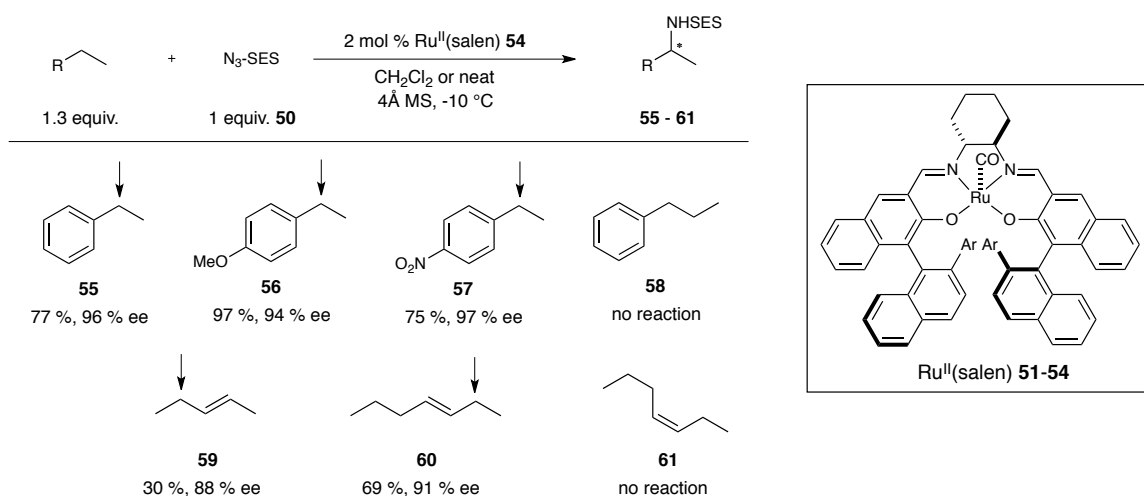


Table 1.1. Evaluation of Ru^{II}(salen) complexes **51-54** for asymmetric C-H amination using SES-N₃.

After catalyst **54** was determined to perform the best in the amination reaction the substrate scope was investigated. Examples of the selectivity profile for ruthenium(II) salen catalyst **54** are shown in Scheme 1.22. Electron-neutral (**55**), electron-rich (**56**), and electron-deficient (**57**) ethylbenzene derivatives were aminated in high yield and enantioselectivity. Propylbenzene **58** did not undergo the amination reaction, and it was presumed that the increased steric interactions with the catalyst were responsible. Secondary allylic C-H insertion was preferred for **59**, and the catalyst was regioselective for the external methylene position in (*E*)-3-heptene substrate **60**. This suggests that the catalyst is very susceptible to steric effects since the internal methylene site was not

functionalized. No reaction occurred with (*Z*)-3-heptene **61**, and competition experiments revealed that this substrate inhibited insertion into previously amenable substrates. This result implies that the *cis*-olefin inhibits the amination reactivity by strongly binding to the catalyst.



Scheme 1.22. Substrate scope for Ru^{II}(salen) catalyzed C-H amination.

1.3.5 Conclusion and challenges

Many nitrogen-atom transfer technologies have been made available through careful reagent selection and the design of new transition metal catalysts. The Rh₂(esp)₂ complex developed by Du Bois is currently the most broadly applicable catalyst for both intra- and intermolecular racemic C-H amination. Further catalyst developments have led to aliphatic azides being effective nitrene sources in asymmetric reactions, allowing for increased atom-economy in the synthesis of enantioenriched nitrogen containing molecules. Even with these advances, each of the above-described methodologies has their limitations. The majority of the existing catalysts are tailored to accommodate

specific metallonitrene precursors. Intermolecular reactions are often plagued by the necessity for the substrate to be in large excess relative to the nitrogen source, and inducing asymmetry for intermolecular amination has proved challenging.

1.4 Conclusions

Clearly, catalyst design has been largely responsible for the accessibility of new substrates and reagents available for high yielding and selective C-H insertion reactions. The ideal catalyst should be readily accessible, predictably selective across a wide range of substrates, and accommodating to a variety of carbene and nitrene precursors. Considering the impact that catalyst design has had in both metallocarbene and metallonitrene C-H functionalization, the development of a catalyst family that possesses all of these characteristics is a research goal worth pursuing towards developing new technologies for C-H functionalization.

Chapter 2

Iridium Catalyzed Metallocarbene and Metallonitrene Atom Transfer Reactions

2.1 Introduction

Iridium has played a crucial role in our understanding of many processes in organometallic chemistry. For instance, Bergman reported the first intermolecular oxidative addition reaction into saturated hydrocarbons by the photochemical generation of Cp*Ir(PMe)₃, which provided a solid foundation for further understanding of this fundamental organometallic process.⁸⁷⁻⁹⁰ Numerous stoichiometric and catalytic C-H functionalization reactions have since been well-established, such as alkane dehydrogenation, alkane metathesis, borylation, and hydroalkylation, to name a few.⁹¹ In contrast to the above-mentioned reactions, the use of iridium complexes in metallocarbene and metallonitrene atom-transfer is in its infancy.

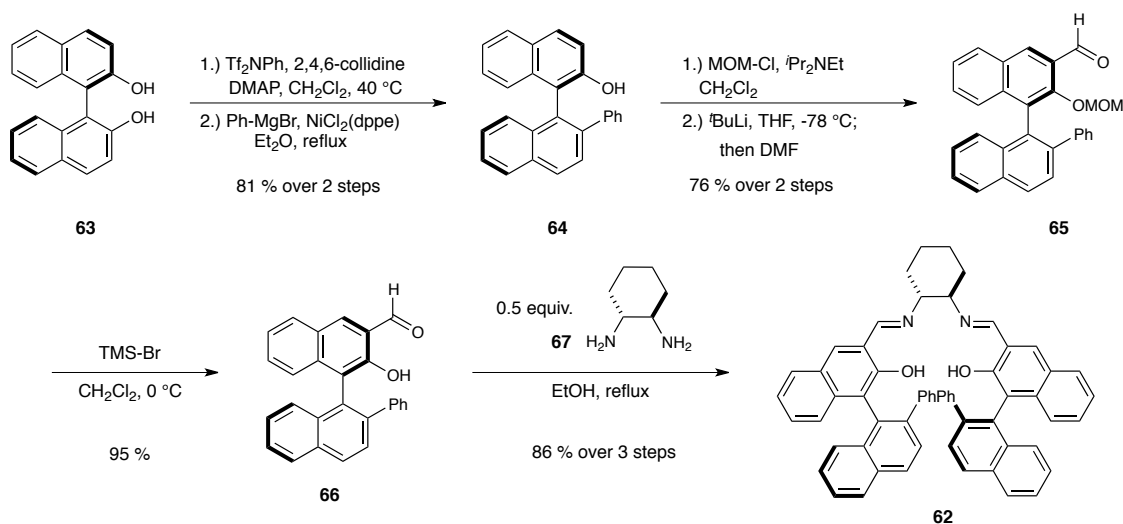
2.2 Iridium(III) Salen Metallocarbene Atom-Transfer

2.2.1 Iridium(III) salen synthesis

As described in Chapter 1, dirhodium(II) complexes are the most widely investigated carbene transfer catalysts of the group nine transition metals. Katsuki discovered that cobalt salen complexes are effective catalysts for *cis*- and enantioselective cyclopropanation of styrenes using *tert*-butyl diazoacetate as the

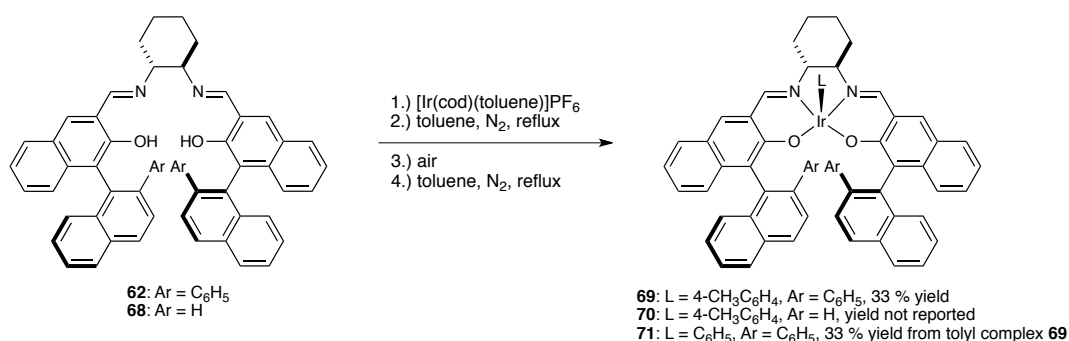
acceptor carbene precursor, but substrate scope was limited to styrene derivatives.⁹² In an effort to improve the substrate scope and knowing that the salen ligand framework was capable for inducing enantioinduction in *cis*-selective cyclopropanation, they thought that iridium could accommodate the salen ligand framework and potentially facilitate enantioselective carbene transfer.

Synthesis of salen ligand **62** is shown in Scheme 2.1. Optically active binaphthol **63** was first mono-triflated with Tf₂NPh in the presence of DMAP and 2,4,6-collidine. Kumada coupling using NiCl₂(dppe) and PhMgBr afforded arylated intermediate **64** in 81 % yield over two steps. Alcohol **64** was protected as the methoxymethyl ether, which underwent *ortho*-lithiation and formylation when treated with ^tBuLi and DMF, giving rise to aldehyde **65** in 76 % yield over two steps. MOM deprotection and condensation of the resultant aldehyde **66** with chiral non-racemic diamine **67** furnished salen ligand **62** in 86 % yield over three steps.⁹³



Scheme 2.1. Synthesis of salen ligand **62**.

The iridium(III) salen ligands were then metallated *via* a four step protocol (Scheme 2.2). First, $[\text{Ir}(\text{cod})(\text{toluene})]\text{PF}_6$ was synthesized in 99 % yield by reacting $[\text{Ir}(\text{cod})\text{Cl}]_2$ with AgPF_6 in toluene. The ligand **62** or **68** was introduced, and the reaction was refluxed in toluene under nitrogen. The mixture was filtered then the filtrate was exposed to air and concentrated. The resulting material was then refluxed in toluene (the source of the apical tolyl anion) under nitrogen and the resultant complexes were purified by silica gel column chromatography, providing salen complexes **69** (33 % yield) and **70** (yield not reported). Salen complex **71** was subsequently synthesized in 33 % yield by refluxing tolyl complex **69** in benzene.

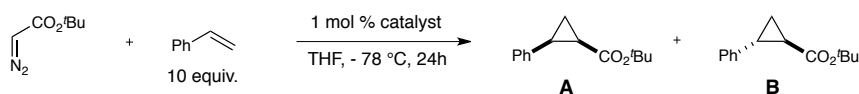


Scheme 2.2. Synthesis of salen complexes **69-71**.

2.2.2 Iridium(III) salen catalyzed cyclopropanation

Initial catalyst evaluation revealed that iridium complexes **69** and **71** were excellent catalysts for *cis*- and enantioselective acceptor-only cyclopropanation using *tert*-butyl diazoacetate and 10 equivalents styrene in THF, providing *cis*-**A** with near perfect yield (99 %) and selectivity (> 98 % ee) (entry 1 and entry 3, Scheme 2.3).^{93,94} Having a phenyl substituent on the binaphthyl moiety (Ar = Ph) was indispensable as

evidenced by the poor yield, diastereo-, and enantioselectivity imparted by catalyst **70** (Ar = H)(entry 2, Scheme 2.3). This result emphasizes the importance of the substituent on the binaphthyl ring, and unfortunately this functional group is installed during the second step of the catalyst synthesis. Of note is that insertion into the THF solvent was not observed, a reaction that is known in copper catalyzed intermolecular C-H functionalization (*cf.* Chapter 1). These reactions provided proof of principle that iridium is proficient in atom-transfer catalysis, and that enantioselectivity can be achieved by careful ligand design. In fact, this was the first reported example of iridium in asymmetric carbene-transfer catalysis.



entry	catalyst	% yield	A : B	% ee A	% ee B
1	69	99	> 99:1	>99	-
2	70	44	41:59	63	60
3	71	99	> 99:1	98	-

Scheme 2.3. Iridium(III) salen catalyst evaluation for cyclopropanation of styrene with *tert*-butyldiazoacetate.

Slow addition of the diazoester was unnecessary, but temperatures greater than - 40 °C were damaging to reaction yield, diastereo-, and enantioselectivity. Ethyl diazoacetate was also examined, but *tert*-butyldiazoacetate generally provided better yields and selectivities. In addition, the experimental section stated, “Olefins and *tert*-butyl or ethyl diazoacetates were also distilled before use. The use of a non-freshly distilled olefin or α -diazoacetate may be detrimental to the stereoselectivity of the

reaction.”⁹⁴ It is not clear as to what extent the selectivity suffered, but it indicates that the iridium(III) salen catalyst is sensitive even to minor impurities.

Substrate scope for this reaction was subsequently examined, and a wide variety of activated (aryl, heteroaryl), conjugated (diene and enyne), and unactivated (alkyl, terminal) olefins were amenable to the transformation. Representative examples are given in Figure 2.1. For alkyl-substituted terminal alkenes slow addition of the diazoester was needed to increase yield and suppress carbene dimerization. The development of these catalysts has led to a new and state-of-the-art method for the construction of highly enantioenriched *cis*-cyclopropanes.

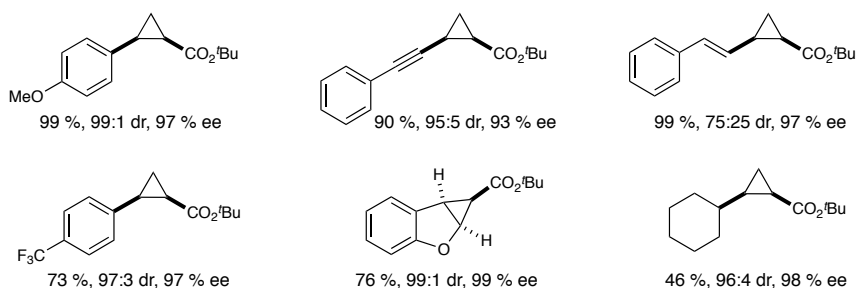
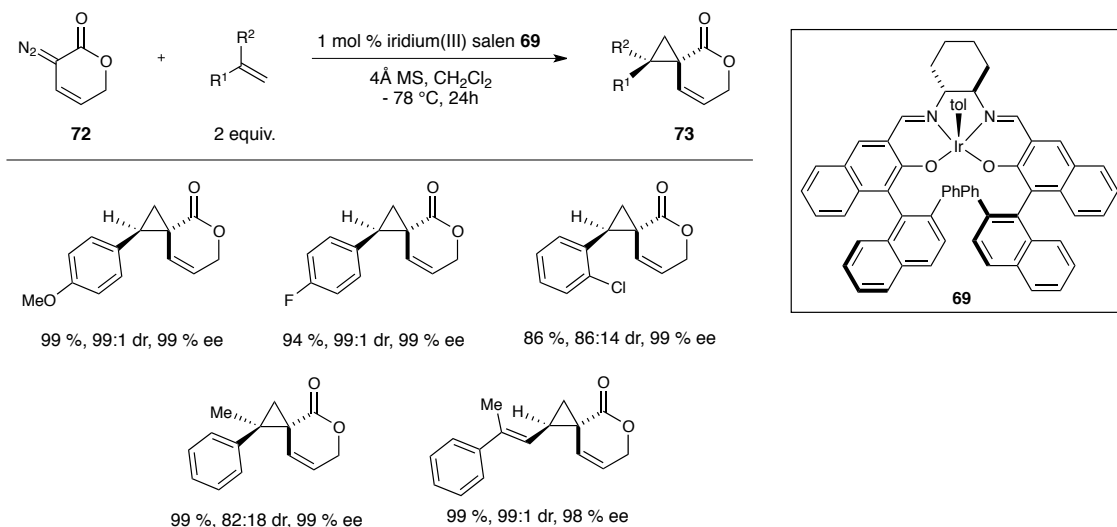


Figure 2.1. Select examples of iridium(III) salen catalyzed olefin cyclopropanation using *tert*-butyldiazoacetate.

These complexes were also effective catalysts in cyclopropanation of terminal styryl and conjugated olefins using metallocarbenes generated from vinyl diazolactone **72**, generating the corresponding spirocyclopropyl lactones with the highest enantioselectivity reported to date (Scheme 2.4).^{95,96}



Scheme 2.4. Iridium(III) salen catalyzed cyclopropanation of terminal olefins with vinyldiazolactone **72**.

2.2.3 Iridium(III) salen catalyzed cyclopropanation

The atom transfer chemistry of these iridium(III) salen complexes was extended to cyclopropanation of terminal alkynes with donor/acceptor metallocarbenes (Figure 2.2).⁹⁷ Catalyst **69**, in which the configuration at the cyclohexane chiral centers is (*R*), provided the cyclopropene in only -52 % ee. When the configuration was changed to (*S*) (catalyst **75**) the enantioselectivity substantially increased to 91 % ee. The selectivity is therefore highly dependent on both the binaphthyl and cyclohexane configurations. The steric bulk on the binaphthyl portion on the catalyst was increased by replacing the phenyl aryl substituent in catalyst **75** with 4-(*tert*-butyldiphenylsilyl)phenyl to form complex **76**. This substitution was beneficial and increased the enantioselectivity to 94 % ee. While this study revealed that minor changes are impactful on the enantioselectivity, a

drawback is that altering the aryl substituent on the binaphthyl ring is performed at the second step of the ligand synthesis (*cf.* Scheme 2.1).

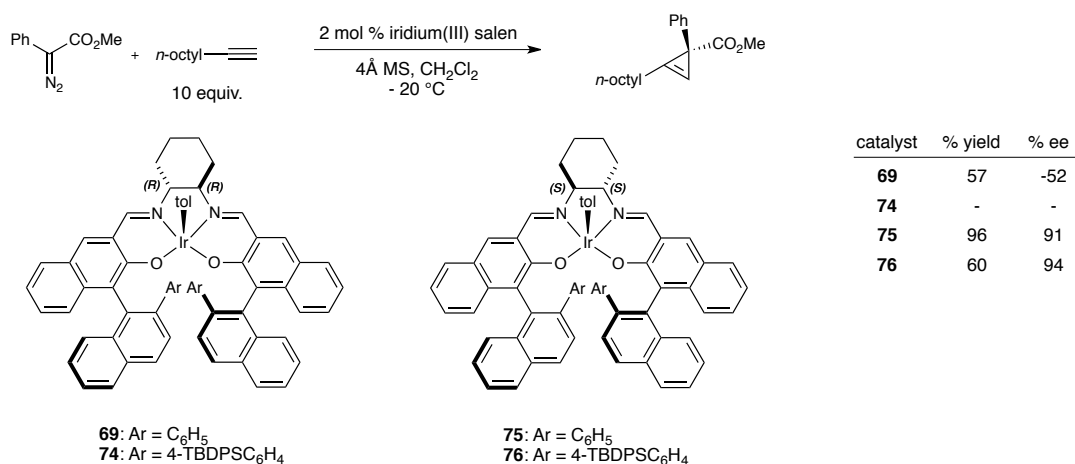
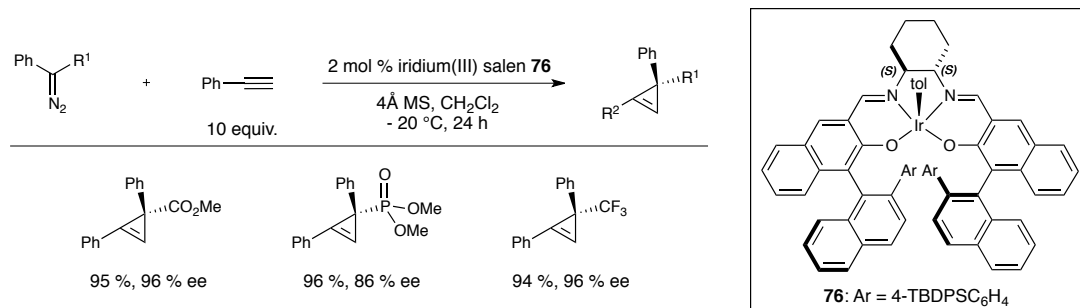
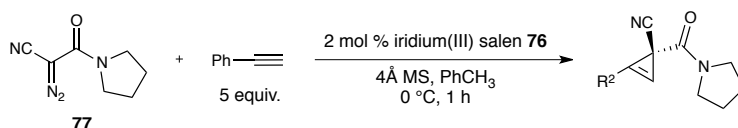


Figure 2.2. Catalyst evaluation for iridium(III) salen catalyzed cyclopropenation of terminal alkynes.

Substrate scope was good when donor/acceptor diazoesters were used, but perhaps the most significant advance was that phosphonate and trifluoromethyl acceptor groups also provided the cyclopropanes in high yields and enantioselectivities (Scheme 2.5). Another improvement upon existing methodologies was that the acceptor-acceptor carbene generated from α -cyano- α -diazoacetamide **77** was a viable substrate for cyclopropenation using iridium salen catalyst **76** (Scheme 2.6).⁹⁸ The ability to use acceptor/acceptor carbenes with the iridium(III) salen catalysts provides an advantage over rhodium tetracarboxylate catalyzed reactions since they are not strictly limited to the donor/acceptor class of carbenes.^{99,100} Unfortunately the iridium catalysts were ineffective for the cyclopropenation of internal alkynes.¹⁰¹



Scheme 2.5. Iridium(III) salen catalyzed cyclopropenation using aryl diazoesters, aryl diazophosphonates, and trifluoromethyl phenyldiazomethane.

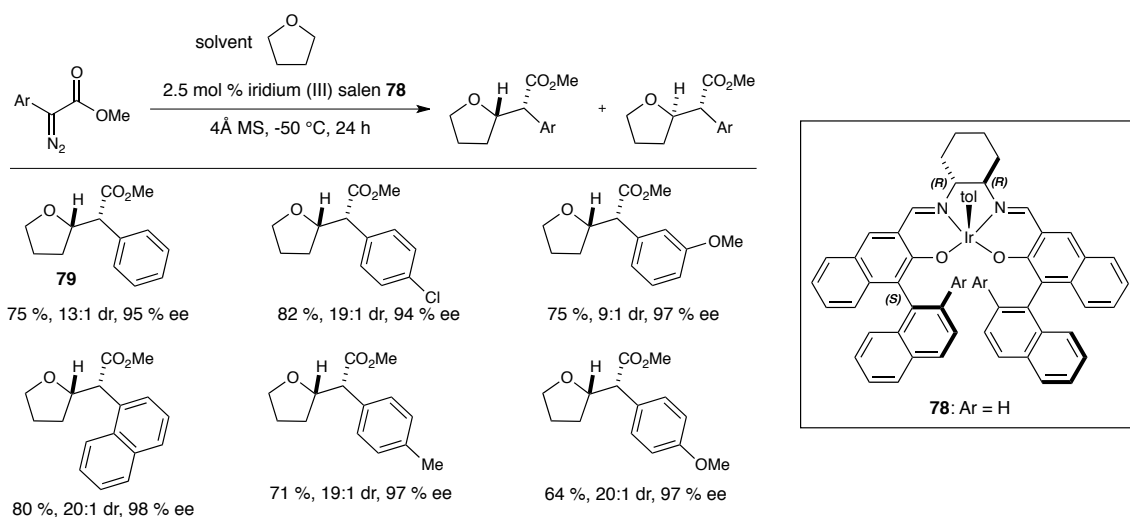


Scheme 2.6. Iridium(III) salen catalyzed cyclopropenation of phenylacetylene with α -cyano- α -diazoacetamide **77**.

2.2.4 Iridium(III) salen catalyzed C-H functionalization

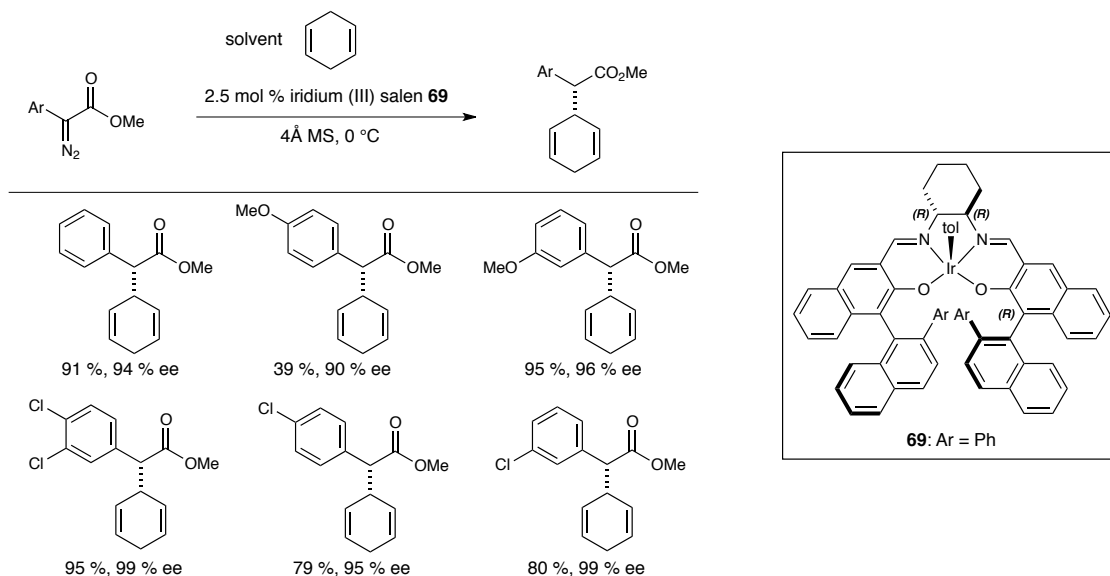
Katsuki broadened the utility of the iridium(III) salen complexes in 2009 to include diastereo- and enantioselective C-H functionalization.¹⁰² They found that iridium(III) salen catalyst **78** ($\text{Ar} = \text{H}$) was effective in performing selective C-H insertion into the ethereal C-H bond α to oxygen in tetrahydrofuran using donor/acceptor diazoesters. Initially they examined the insertion of methyl phenyldiazoacetate into THF at room temperature, but the fumarate/maleate esters, which arose from carbene dimerization, were the major products. However, decreasing the reaction temperature to $-50\text{ }^\circ\text{C}$ provided the functionalized product **79** in 75 % yield as a 13:1 diastereomeric

mixture with 95 % ee (Scheme 2.7). Nearly all diazoesters underwent the insertion reaction in high yield and selectivities. An advantage of using the iridium(III) salen catalyst is that diastereoselectivity for the insertion into THF is much higher (up to 20:1) than when dirhodium(II) tetracarboxylate catalysts are used (up to 4.0:1).⁸



Scheme 2.7. Iridium(III) salen catalyzed donor/acceptor C-H insertion into tetrahydrofuran.

C-H insertion also proceeded well into the bis-allylic methylene site of 1,4-cyclohexadiene at 0 °C with catalyst **69**, furnishing the insertion products with high enantiopurity (Scheme 2.8). Notably, competing cyclopropanation of the olefin was not observed in the reaction, and dimerization was suppressed by conducting the reaction at 0 °C.



Scheme 2.8. Iridium(III) salen catalyzed donor/acceptor C-H insertion into 1,4-cyclohexadiene.

The most important discovery that came out of this report for us was that α -alkyl diazoacetates were viable carbene precursors for the C-H insertion reaction into both THF and cyclohexadiene (Figure 2.3). Performing the insertion into THF with *tert*-butyl diazopropionate and catalyst **78** at -60 °C furnished **80** in 70 % yield, 13:1 dr, and 90 % ee (Figure 2.3a). Enantioselectivity for insertion into 1,4-cyclohexadiene was dependent on the size of the ester and the catalyst. The metallocarbene generated from catalyst **78** and ethyl diazopropionate gave **81** in 68 % yield and 83 % ee (Figure 2.3a, entry 1). Using *tert*-butyl diazopropionate and catalyst **69** generated the insertion product **82** in higher yield and enantioselectivity at 84 % and 99 %, respectively (Figure 2.3b, entry 2).

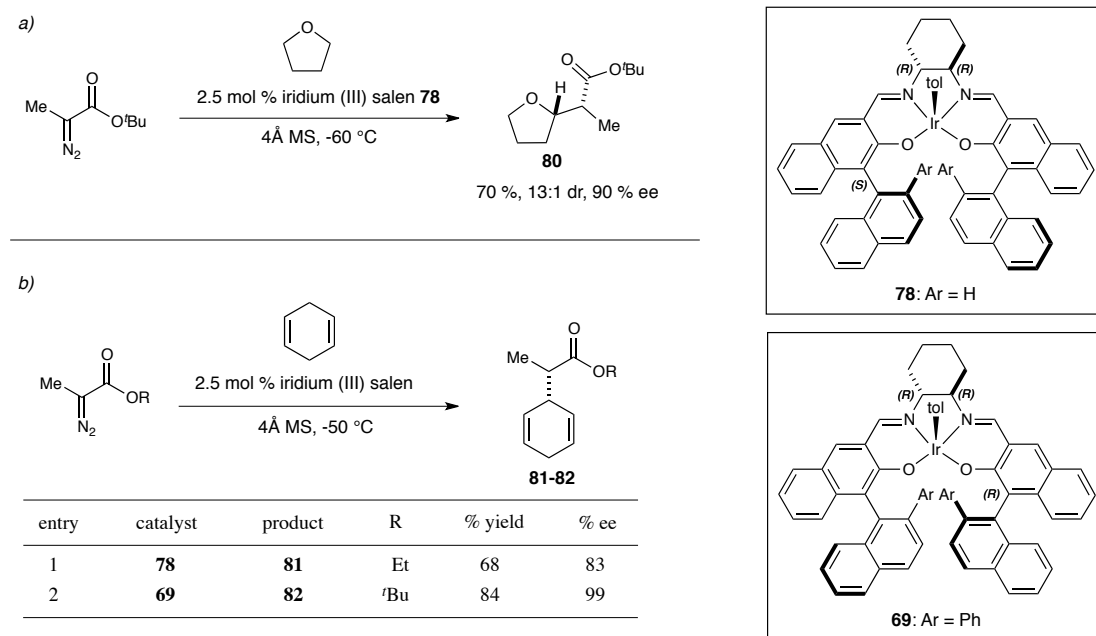
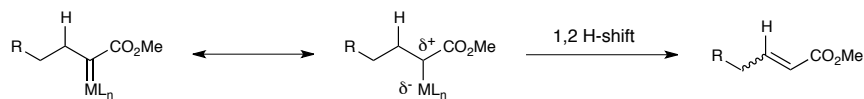


Figure 2.3. Iridium(III) salen catalyzed insertion of α -alkyl diazoacetates into THF and 1,4-cyclohexadiene.

The reason these results were exceptionally significant is that β -hydride elimination is a competing and often-favored pathway when using α -alkyl metallocarbenes in an intermolecular manifold (Scheme 2.9).



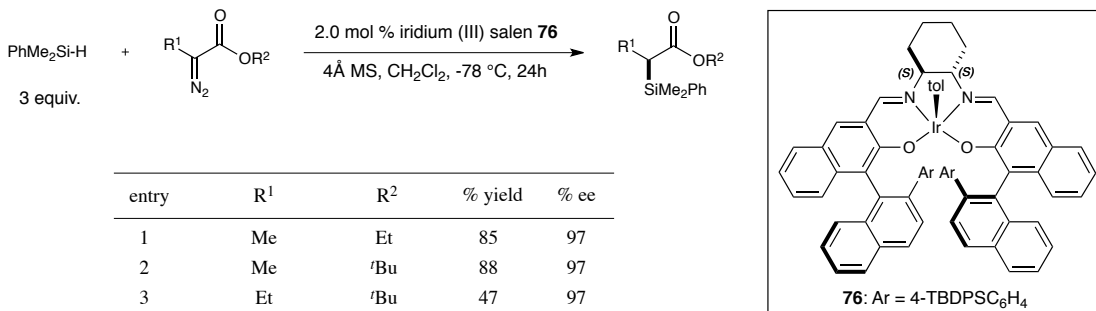
Scheme 2.9. β -hydride elimination in metallocarbenes derived from α -alkyl diazoesters.

In recent years the Fox group has developed intra- and intermolecular reactions with α -alkyl substituted metallocarbenes in dirhodium(II) tetracarboxylate catalyzed cyclopropanation,¹⁰³⁻¹⁰⁷ cyclopropenation,^{103,104,108} ylide cycloaddition,^{104,109,110} and C_{sp^2} -H functionalization of indoles at C3.^{103,111,112} The key to these reactions lies in the

use of very sterically demanding dirhodium(II) complexes to prevent the undesired elimination, presumably by preventing the β -hydrogen from aligning itself antiperiplanar to the metallocarbene.^{103,104} In the case of Fox's indole C-H functionalization, the insertion was proposed to occur *via* a [3+2] cycloaddition/elimination rather than a direct C-H insertion pathway.¹¹¹ Both Katsuki and Fox pose the same argument for the successful use of α -alkyl diazoesters in atom transfer reactions, although neither group has obtained experimental nor theoretical evidence to support their claims.

2.2.5 Iridium(III) salen catalyzed Si-H insertion

The Katsuki group then exploited the effectiveness of alkyl and aryl diazoesters in asymmetric intermolecular carbene transfer and performed enantioselective Si-H insertion into di- and triorganosilanes.¹¹³ These reactions occurred with high enantioselectivity in nearly all cases using the 4-TBDPS-phenyl substituted iridium(III) salen complex **76**, and select examples of the alkyl diazoester Si-H insertions are shown in Scheme 2.10. The lower yield for α -ethyl-*tert*-butyldiazoacetate (entry 3) was attributed to increased formation of the carbene dimer.



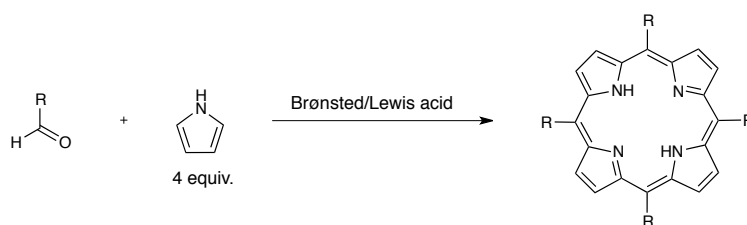
Scheme 2.10. Iridium(III) salen catalyzed alkyl diazoester Si-H insertion.

The fact that iridium complexes catalyzed the first intermolecular asymmetric C-H insertion reaction using α -alkyl diazoacetates was a breakthrough in enantioselective catalysis and provided the first example in the literature that iridium atom transfer catalysis may in certain cases provide reactivity not attainable under dirhodium(II) catalysis.

2.3 Iridium(III) Porphyrin Metallocarbene Atom-Transfer

2.3.1 Iridium(III) porphyrin synthesis

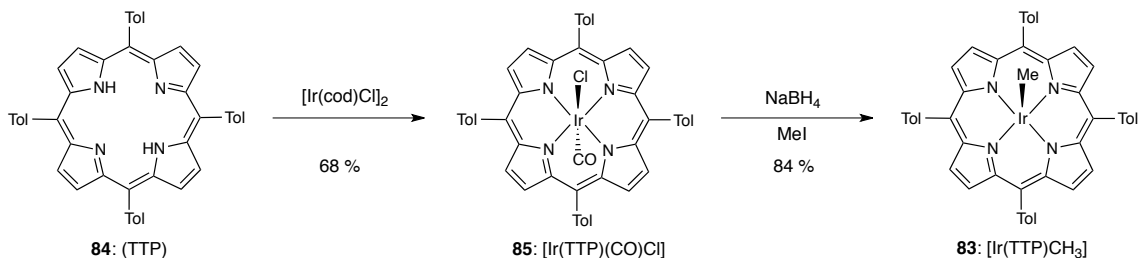
Katsuki's pioneering work in iridium catalyzed atom transfer reactions encouraged several research groups to investigate other iridium(III) complexes in efforts to better understand their performance in metallocarbene transfer. Porphyrins constitute a readily available ligand set and are generally prepared by condensing an aldehyde with pyrrole in the presence of a Brønsted or Lewis acid (Scheme 2.11).¹¹⁴



Scheme 2.11. General porphyrin ligand synthesis.

In 2012, the Woo group recognized that porphyrin complexes of cobalt and ruthenium were effective carbene and nitrene transfer reagents and subsequently explored porphyrin-ligated iridium(III) complexes in this context. They synthesized previously

reported iridium(III) tetratolylporphyrinato methyl $[\text{Ir}(\text{TTP})\text{CH}_3]$ complex **83** to begin their studies.¹¹⁵ Ligand **84** (TTP) was synthesized according to Scheme 2.11 and subsequently metallated with $[\text{Ir}^{\text{I}}(\text{cod})\text{Cl}]_2$ in air to form $[\text{Ir}^{\text{III}}(\text{TTP})(\text{CO})\text{Cl}]$ **85** in 68 % yield (Scheme 2.12). Reductive methylation with NaBH_4 and MeI furnished $[\text{Ir}(\text{TTP})\text{CH}_3]$ **83** in 84 % yield.

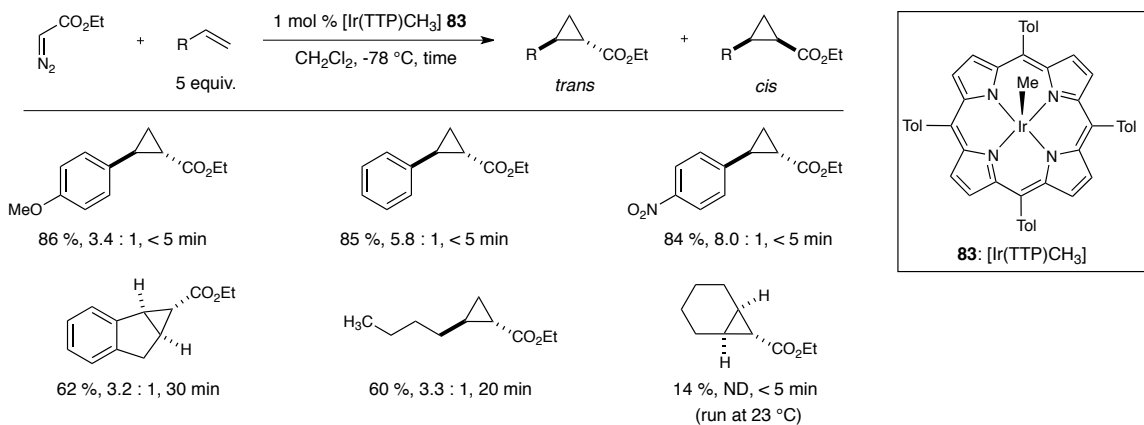


Scheme 2.12. Synthesis of $[\text{Ir}(\text{TTP})\text{CH}_3]$ **83**.

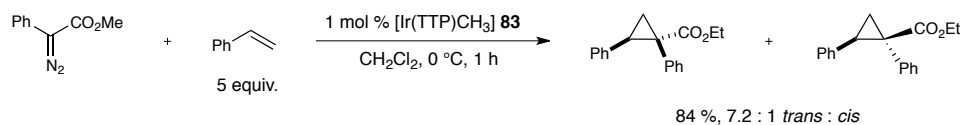
2.3.2 Iridium(III) porphyrin catalyzed cyclopropanation

They first investigated the carbene transfer reactivity of $[\text{Ir}(\text{TTP})\text{CH}_3]$ **83** in the cyclopropanation of olefins using the acceptor-only carbene precursor ethyl diazoacetate (Scheme 2.13). Styryl derivatives underwent cyclopropanation with **83** in good yields at $-78\text{ }^\circ\text{C}$ within five minutes after the dropwise addition of ethyl diazoacetate over 30 seconds, but the reaction showed only modest preference for the *trans* cyclopropanes. The remainder of the reaction mixture consisted of the maleate and fumarate esters derived from carbene dimerization. Cyclopropanation was also possible using the donor/acceptor carbene precursor methyl phenyldiazoacetate, furnishing the cyclopropanes in 84 % yield as a 7.2 : 1 mixture of *trans* : *cis* isomers (Scheme 2.14). The reaction using the donor/acceptor system proceeded at higher temperature ($0\text{ }^\circ\text{C}$) and

longer reaction time (1 hour). There are currently no hypotheses as to why the iridium(III) porphyrin and iridium(III) salen catalysts provide the opposite *cis/trans* selectivities for cyclopropanation.



Scheme 2.13. [Ir(TTP)CH₃] **83** catalyzed cyclopropanation of olefins with ethyl diazoacetate.



Scheme 2.14. [Ir(TTP)CH₃] **83** catalyzed cyclopropanation of styrene with methyl phenyldiazoacetate.

NMR experiments were conducted in attempts to elucidate the rate-determining step in the cyclopropanation reactions. Three steps in the reaction are potentially rate-determining and are shown in Figure 2.4. For the analogous Rh(TPP)I complexes it has been shown that carbene formation is rate limiting, i.e. $k_1, k_{-1} > k_2$.¹¹⁶ However, experiments revealed that addition of 1-hexene to Ir(TPP)CH₃ **83** and methyl diazoacetate accelerated cyclopropane formation and decreased the dimer formation. This data

suggests that k_2 cannot be the rate-determining step and that carbene transfer, likely in the form of cyclopropanation (k_3), controls the reaction rate.

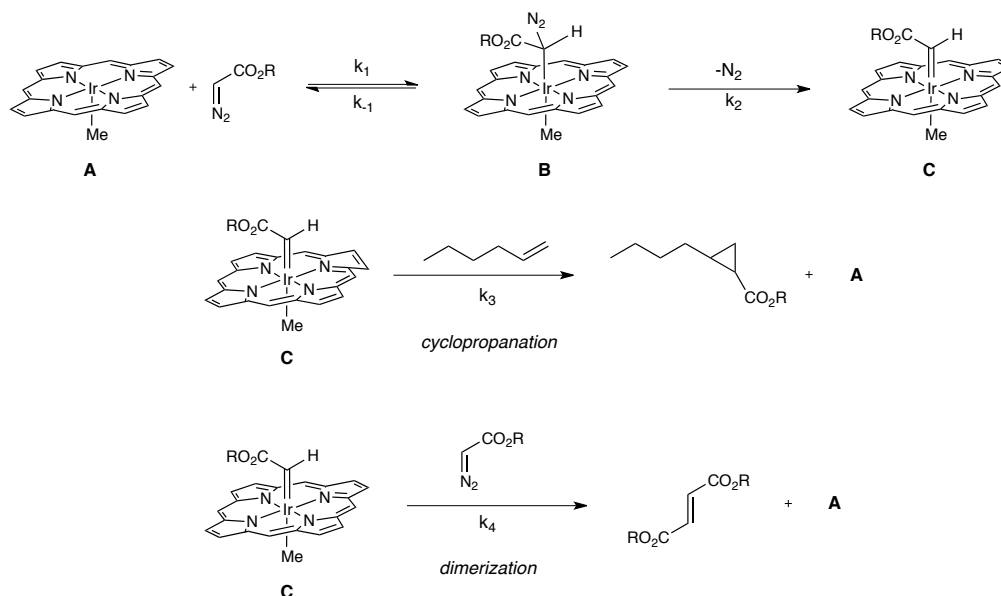


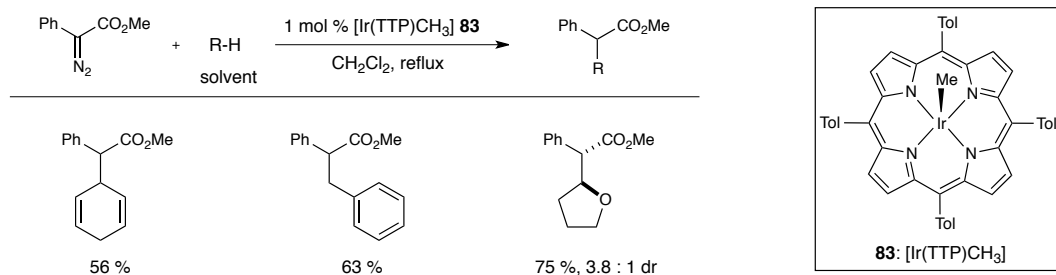
Figure 2.3. Potential rate-determining pathways in the $[\text{Ir}(\text{TTP})\text{CH}_3]$ **83** catalyzed cyclopropanation of styrene with ethyl diazoacetate.

Another informative observation was made during competition experiments for the $\text{Ir}(\text{TTP})\text{CH}_3$ **83** catalyzed cyclopropanation of styrene and d_8 styrene with ethyl diazoacetate. The catalyst **83** displayed an inverse isotope effect of 0.86 ± 0.03 , which indicates that olefin rehybridization occurs before the carbene transfer transition state. This value is lower than the inverse isotope effect observed for the analogous $\text{Rh}(\text{TMP})\text{CH}_3$ complex, which lies at unity ($\text{IIE} = 1.0 \pm 0.07$) ($\text{TMP} = \text{tetramethylporphyrin}$).¹¹⁷ The data obtained by Woo is in agreement with a transition state that is later and more product-like compared rhodium(III) porphyrins, which implies that the iridium carbene is less electrophilic and bound more tightly. Thus, the higher diastereoselectivity that was experimentally observed for *para*-electron withdrawing

styrene substrates is in agreement with this inference, which is in contrast to the lack of *trans:cis* preference for electronically differentiated alkenes in the rhodium(III) porphyrin cyclopropanations.

2.3.3 Iridium(III) porphyrin catalyzed C-H functionalization

Racemic C-H insertion was reported by Woo shortly after the cyclopropanation studies.¹¹⁸ Ethyl diazoacetate was first reacted with cyclohexane and Ir(TTP)CH₃ complex **83** at 0 °C. Unfortunately, the maleate and fumarate esters were the sole products of the reaction. Reacting the donor/acceptor carbene precursor methyl phenyldiazoacetate with Ir(TTP)CH₃ **83** in cyclohexane at 80 °C formed the insertion product in 94 % yield. In this reaction, slow addition of the diazoester over 2 hours was necessary to suppress carbene dimerization. The iridium(III) porphyrin catalyst **83** showed modest yields for insertion into other substrates in refluxing dichloromethane (Scheme 2.15). Most notably, insertion into the primary and benzylic C-H bond of toluene was successful, which is a difficult reaction to achieve under dirhodium catalysis due to competing cyclopropanation of the aromatic ring.¹¹⁹



Scheme 2.15. [Ir(TTP)CH₃] **83** catalyzed C-H insertion with methyl phenyldiazoacetate.

The authors note that the reaction exhibits a color change from orange to green-brown upon the addition of methyl phenyldiazoacetate and presumed that the intermediate carbene could be observed. UV/Vis absorption studies revealed that complex Ir(TTP)CH₃ **83** gave an absorbance at 404 nm. Upon addition of methyl phenyldiazoacetate, the peak at 404 nm disappeared and formed three new peaks at 375, 417, and 443 nm. These bands disappeared after five minutes and the diazoester was consumed, at which time the peak at 404 nm was regenerated. The absorbance at 417 nm persisted after adding a large excess of the diazoester, and it was concluded that this absorbance was a product of catalyst decomposition since none of the excess diazoester was further consumed. They presumed that the peaks at either 375 or 443 nm indicated a putative carbene intermediate responsible for the C-H insertion, but no further evidence for this was obtained by UV-Vis studies.

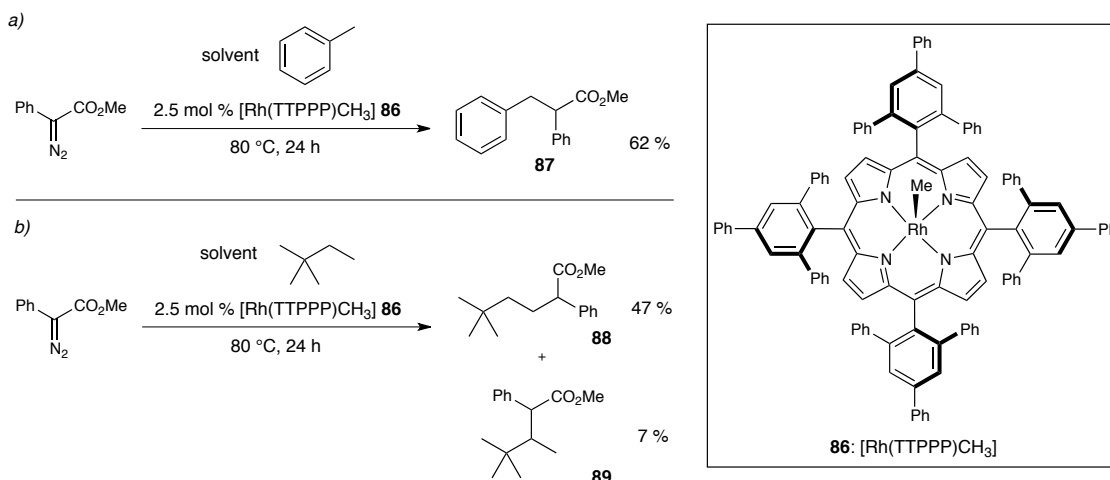
Time-dependent density functional theory (TD-DFT) was then used to computationally estimate the absorption spectra of the reactive intermediate.¹²⁰ In fact, the calculated spectrum was in good agreement with the experimentally obtained one, predicting the absorbances of the carbene with values of 357 nm and 427 nm. The calculated structure showed a calculated Ir-C_{carbene} bond length of 2.047 Å, which is longer than that observed by group 8 metalloporphyrins.¹²¹ The authors state that this is reasonable, given the high carbene transfer reactivity of the iridium porphyrin complex. Additionally, these absorbances were representative of π to π^* transitions that are believed to be responsible for the color change in the reaction.¹²² Results of kinetic studies of the C-H insertion reaction using the donor/acceptor methyl phenyldiazoacetate

and Ir(TTP)CH₃ **83** were similar to those obtained during the acceptor-only cyclopropanation studies and indicated that carbene transfer is rate limiting.

Woo has also reported the use of Ir(TTP)CH₃ **83** for N-H insertion reactions of acceptor and donor/acceptor 1° and 2° amines and anilines *via* a metal-ylide intermediate.¹²³

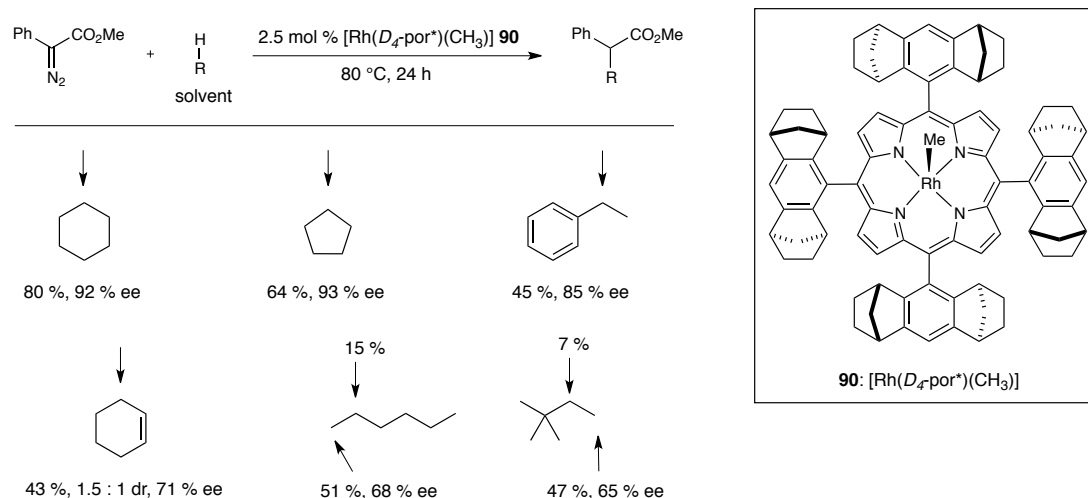
2.3.4 Asymmetric intermolecular C-H functionalization by iridium(III) complexes of chiral Halterman porphyrin ligands

Che reported in 2008 that the sterically demanding rhodium(III) porphyrin [Rh(TTPPP)CH₃] (TTPPP = tetrakis(2,4,6-triphenylphenyl)porphyrin) complex **86** was an effective catalyst for intermolecular C-H insertion of donor/acceptor metallocarbenes into alkanes (Scheme 2.16a).¹²⁴ Insertion into the methyl group of toluene provided **87** in 62 % yield. In Rh₂[(*S*)-DOSP]₄ catalyzed intermolecular C-H insertion with methyl *p*-bromophenyldiazoacetate only 6 % of the insertion product was generated, with the major products resulting from cyclopropanation of the aromatic ring.¹¹⁹ Additionally, the catalyst exerted a 6.7:1 preference for 1° C-H insertion (**88**) over 2° C-H insertion (**89**) into 2,2-dimethylbutane (2,2-DMB) (Scheme 2.16b). This result is unique in comparison to Rh₂[(*S*)-DOSP]₄ catalyzed insertion into this substrate wherein minimal reactivity is observed. This argument is based on the grounds that the usually more reactive 2° site is very sterically hindered, and that the 1° C-H bonds are simply too unreactive with the dirhodium(II) catalysts. In fact, 2,2-DMB is often used as solvent for Rh₂[(*S*)-DOSP]₄ catalyzed reactions.



Scheme 2.16. [Rh(TTPPP)CH₃] **86** catalyzed C-H insertion with methyl phenyldiazoacetate.

Che also described the synthesis and use of chiral rhodium(III) porphyrin complexes for asymmetric C-H insertion reactions in the same report. Bulky rhodium(III) Halterman porphyrin complex **90** was an effective catalyst for asymmetric 1° and 2° C-H insertion into alkanes, providing enantioselectivities up to 93 % (Scheme 2.17). Notably, this catalyst also displayed a 6.7 : 1 preference for 1° over 2° C-H bond insertion in the reaction with 2,2-DMB.

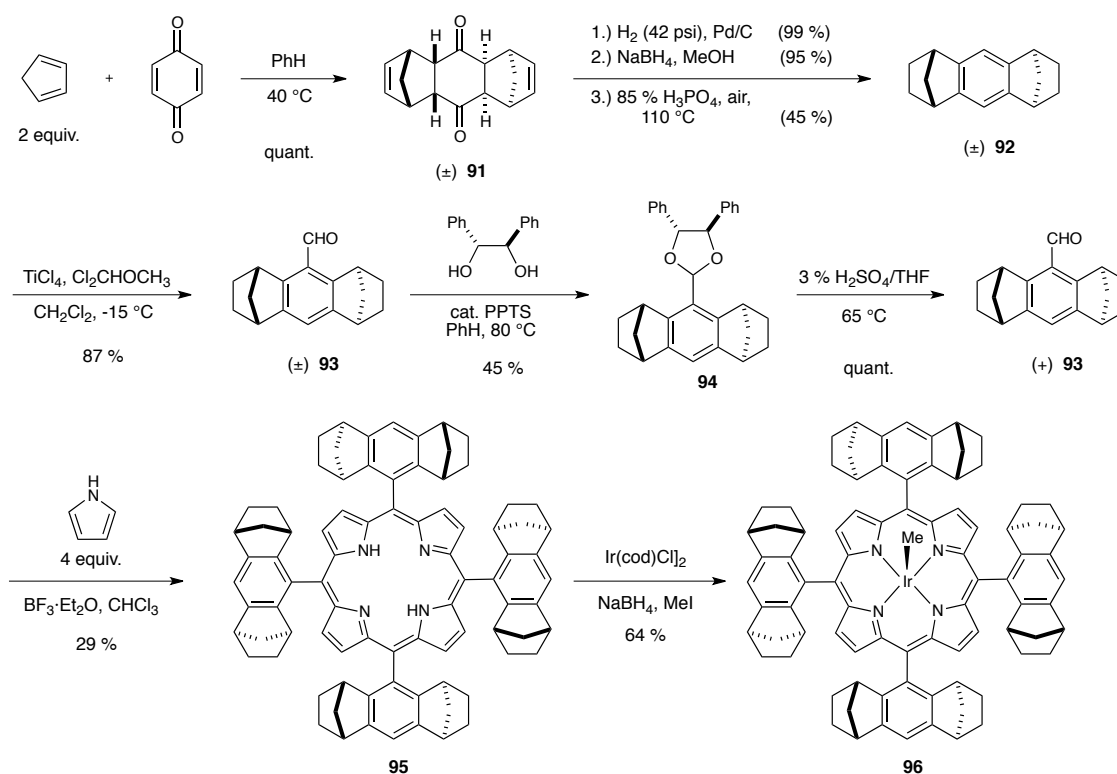


Scheme 2.17. $[\text{Rh}(\text{D}_4\text{-por}^*)(\text{CH}_3)]$ **90** catalyzed enantioselective C-H insertion with methyl phenyldiazoacetate.

Guided by Katsuki's work in iridium(III) salen catalyzed carbene transfer reactions, the Che group recognized that synthesizing iridium(III) complexes bearing a chiral porphyrin framework could provide rapid access to new iridium catalysts for asymmetric carbene transfer reactions.¹²¹ They were drawn to the Halterman porphyrin ligand since it was previously shown that ruthenium (Figure 1.4),^{76,77} rhodium¹²⁴ (Scheme 2.17), and manganese¹²⁵ complexes thereof were capable of performing asymmetric nitrene, carbene, and oxene transfer reactions, respectively.

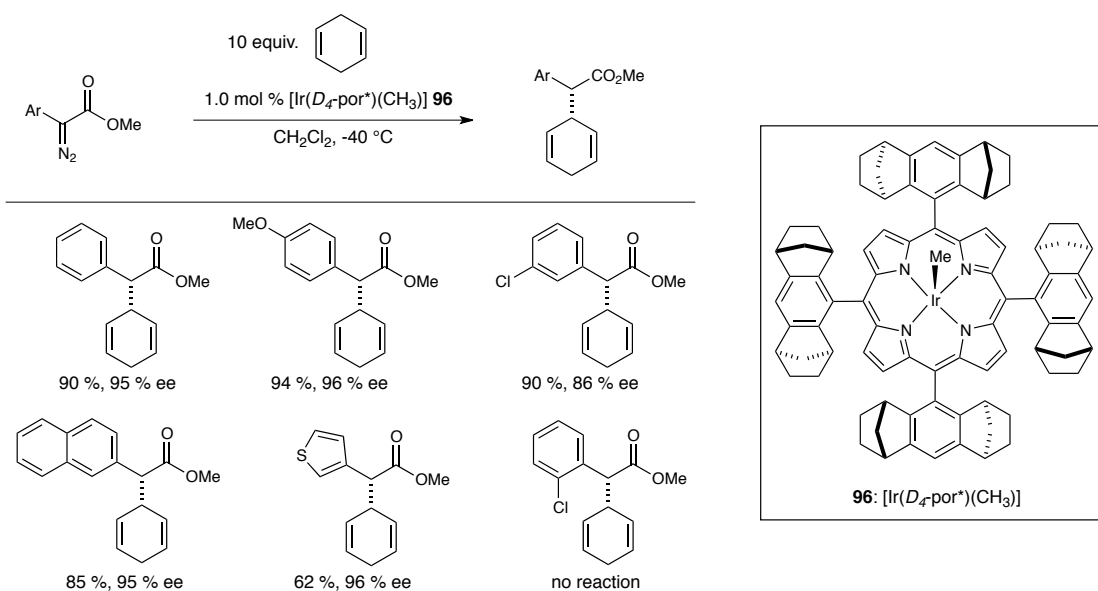
The porphyrin ligands were prepared by the original method reported by Halterman (Scheme 2.18).¹²⁵ The reaction between cyclopentadiene and quinone furnished racemic Diels Alder adduct (\pm) **91** in quantitative yield. A hydrogenation/reduction/dehydration/oxidation sequence followed to provide arene **92** in 42 % over three steps. Friedel-Crafts formylation of arene **92** was achieved in 87 % yield by the reaction with $\text{Cl}_2\text{CHOCH}_3$ in the presence of titanium tetrachloride. At this stage,

the two enantiomers were resolved by forming the diastereomeric ketals derived from (*R,R*)-hydrobenzoin, and the crystalline diastereomer (+) **94** was isolated in 45 % yield. Hydrolysis of ketal **94** with 3 % sulfuric acid in THF furnished the enantiopure aldehyde (+) **93** in quantitative yield. Completion of the porphyrin synthesis was achieved by reacting 4 equivalents pyrrole in the presence of $\text{BF}_3 \cdot \text{OEt}_2$, yielding **95** in 29 % yield. This synthesis is accomplished in 4.8 % overall yield from cyclopentadiene and benzoquinone. Formation of the iridium(III) porphyrin complex **96** was then achieved by treating **95** with $[\text{Ir}(\text{cod})\text{Cl}]_2$, followed by reductive methylation using sodium borohydride and methyl iodide.



Scheme 2.18. Synthesis of the chiral iridium(III) Halterman porphyrin complex **96**.

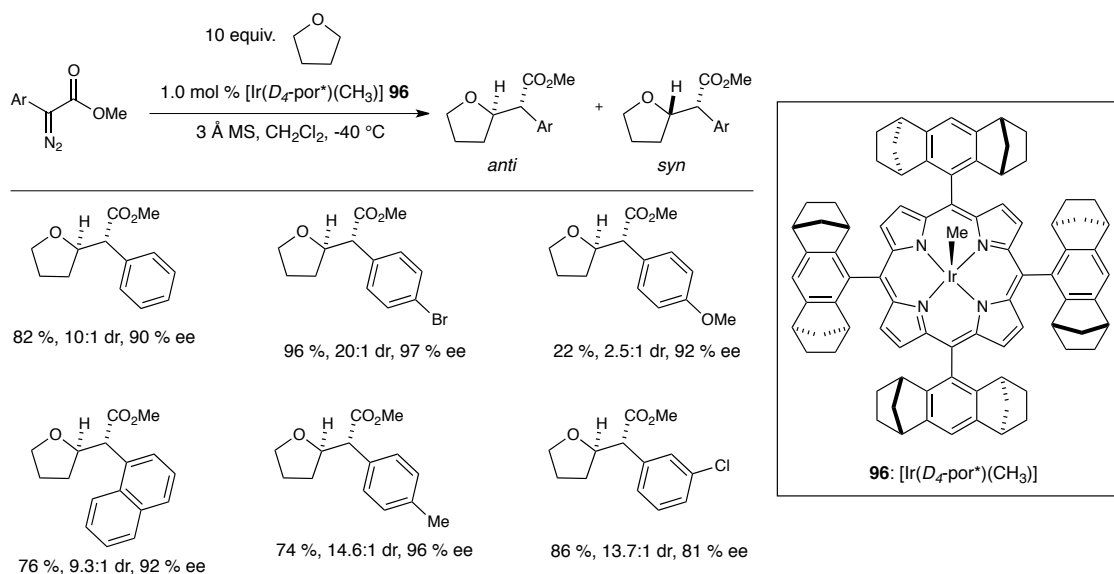
This new chiral iridium(III) porphyrin complex **96** was found to be an effective catalyst for enantioselective C-H functionalization into 1,4-cyclohexadiene (10 equivalents), furnishing insertion products in up to 94 % yield and 98 % ee (Scheme 2.19). No reaction occurred with methyl *o*-chlorophenyldiazoacetate presumably due to prohibitive steric interactions with the catalyst. Reactions with this catalyst did not require slow addition of the diazoester. Furthermore, neither cyclopropanation of the olefin nor dimerization of the metallocarbene was observed.



Scheme 2.19. $[\text{Ir}(\text{D}_4\text{-por}^*)(\text{CH}_3)]$ **96** catalyzed C-H insertion into 1,4-cyclohexadiene.

Insertion into THF was also efficient and afforded the functionalized tetrahydrofurans in good yields with enantioselectivities up to 97 % (Scheme 2.20). In contrast to Katsuki's iridium(III) salen catalysts and the dirhodium(II) tetracarboxylate catalysts, the *anti* isomer of the product is preferentially formed in up to 20:1 diastereoselectivity. The catalyst was also effective in the enantioselective insertion into

Si-H bonds, and seven substrates were reported to undergo insertion in up to 94 % yield and 91 % ee.



Scheme 2.20. $[\text{Ir}(\text{D}_4\text{-por}^*)(\text{CH}_3)]$ **96** catalyzed C-H insertion into tetrahydrofuran.

UV-Vis studies were performed on the iridium(III) Halterman porphyrin catalyzed C-H insertion. The absorbance observed for the catalyst lied at 407 nm, and upon addition of methyl phenyldiazoacetate the band shifted to 419 nm. When 1,4-cyclohexadiene was added the band reverted to 407 nm. These values are nearly identical with those obtained by Woo in the achiral C-H insertion reactions using $\text{Ir}(\text{TTP})(\text{CH}_3)$ **83** (405 nm and 417 nm).¹¹⁸ Unfortunately, the elucidation of the reactive intermediates has not been achieved.

2.3.5 Intramolecular C-H functionalization by iridium(III) porphyrin complexes

In 2013, Che continued his studies in catalytic carbene transfer reactions with both chiral and achiral iridium(III) porphyrin complexes. The methodology was extended to include *cis*- and enantioselective intramolecular C-H insertion of donor/acceptor metallocarbenes to form *cis*- β -lactones.^{126,127}

Their investigation began by attempting C-H insertion into the 3° C-H bond using substituted isopropyl aryldiazoacetates with the achiral [Ir(TTP)(CH₃)] complex **83** (Table 2.1). The *p*-bromophenyl arene furnished the highest yield of the β -lactone **98** at 86 % (entry 2), while only 53 % yield was obtained with the *p*-methylphenyl arene (entry 4).

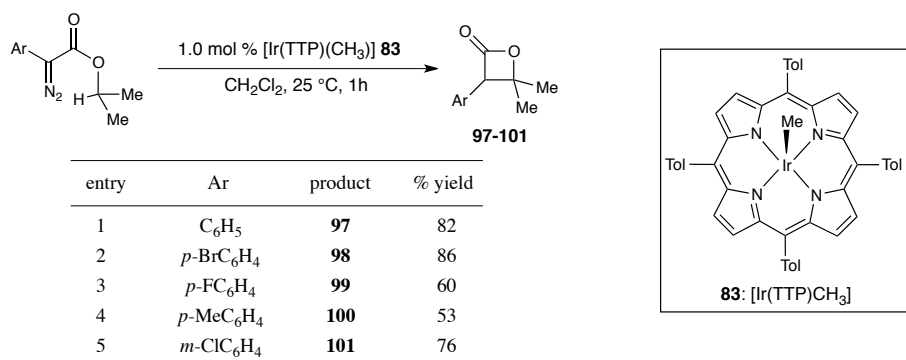


Table 2.1. [Ir(TTP)(CH₃)] **83** catalyzed intramolecular C-H insertion of aryl diazoacetates.

Changing the substitution on the ester portion of the substrate was also investigated (Table 2.2). Tetrahydropyran derivative **102** underwent intramolecular 3° C-H insertion to form spiro β -lactone **106** in 53 % yield. Insertion into the benzylic C-H bond of substrate **103** proceeded well in 68 % yield. Tetrahydrofuran derivatives **104** and

105 were also examined, and C-H insertion proceeded exclusively α to oxygen to form γ -lactones **108** and **109** in 81 % and 74 % yield, respectively.

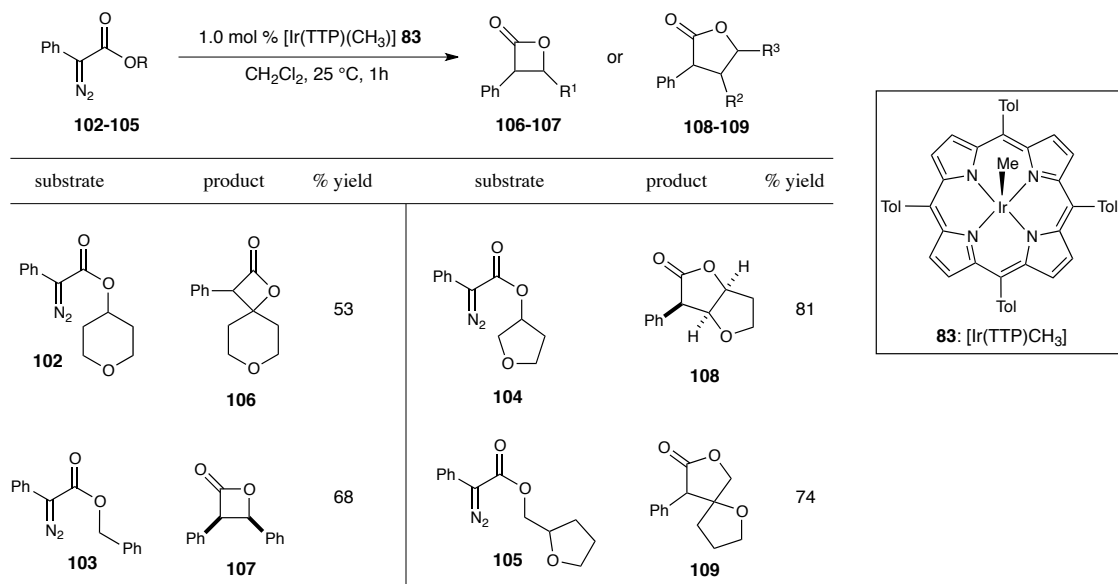
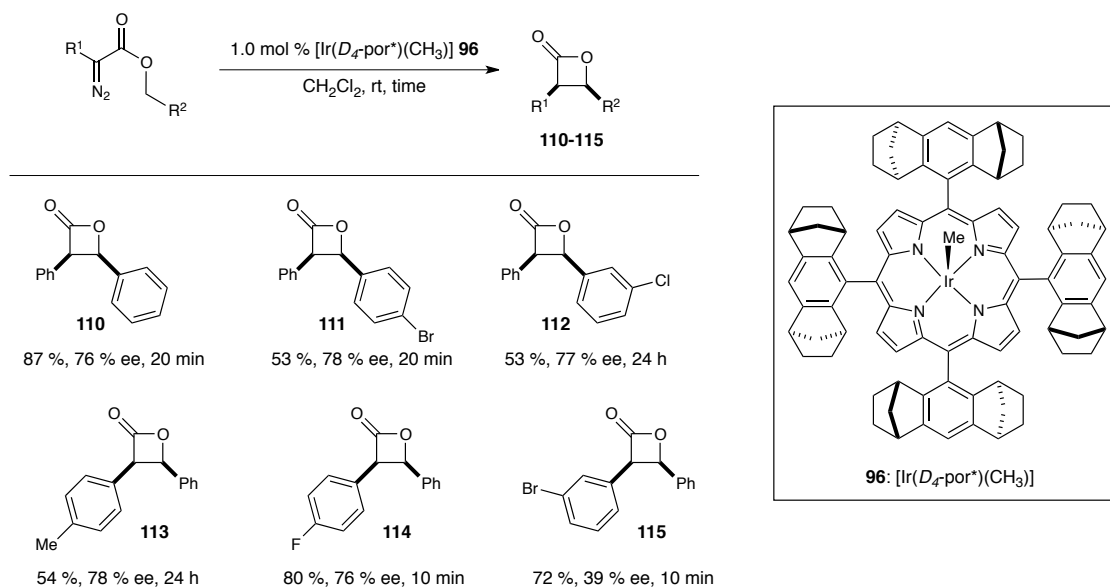


Table 2.2. [Ir(TTP)(CH₃)] **83** catalyzed intramolecular C-H insertion of phenyldiazoacetates.

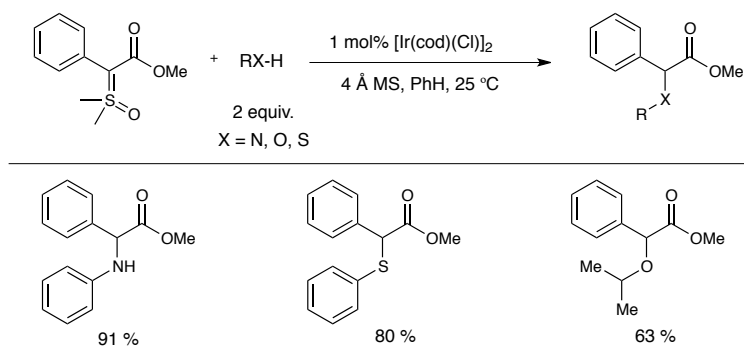
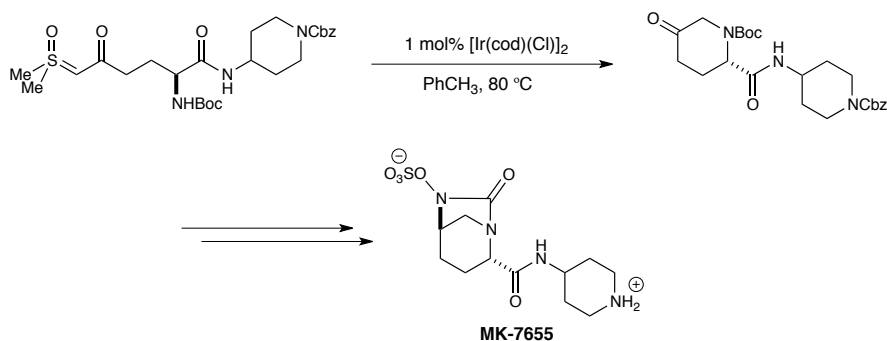
This chemistry was further expanded towards the *cis*- and enantioselective synthesis of β -lactones using the chiral [Ir(*D*₄-por*)(CH₃)] complex **96** via benzylic C H functionalization, and select examples are displayed in Scheme 2.21. Substitution on the ester aromatic ring did not have a significant effect on the reaction enantioselectivity, although the reaction time increased as a result of *m*-chloro substitution (**112**). *Para*-methyl substitution on the arene donor group resulted in a sluggish reaction time (**113**, 24 h) relative to the more electron-deficient *p*-fluoro arene substrate (**114**, 10 min). Enantioselectivities and yields for these products were nearly identical, however *m*-bromophenyl substituted lactone **115** was produced in only 39 % ee.



Scheme 2.21. *Cis*- and enantioselective [Ir(*D*₄-por*)(CH₃)] **96** catalyzed intramolecular C-H insertion of aryldiazoesters.

2.4 Iridium(I) Catalyzed Metallocarbene Atom-Transfer

The earliest example of an iridium(I) metallocarbene atom transfer reaction was reported by the Merck Process group in which iridium metallocarbenes were generated by the reaction of [Ir(cod)Cl]₂ with sulfoxonium ylides.¹²⁸ Upon extrusion of DMSO, the resultant carbenes performed inter- and intramolecular N-H, S-H, and O-H insertion reactions in good to excellent yields (Scheme 2.22). This methodology was ultimately used to synthesize MK-7655, a potent β -lactamase inhibitor that helps restore the activity of β -lactam antibiotics (Scheme 2.23).¹²⁹

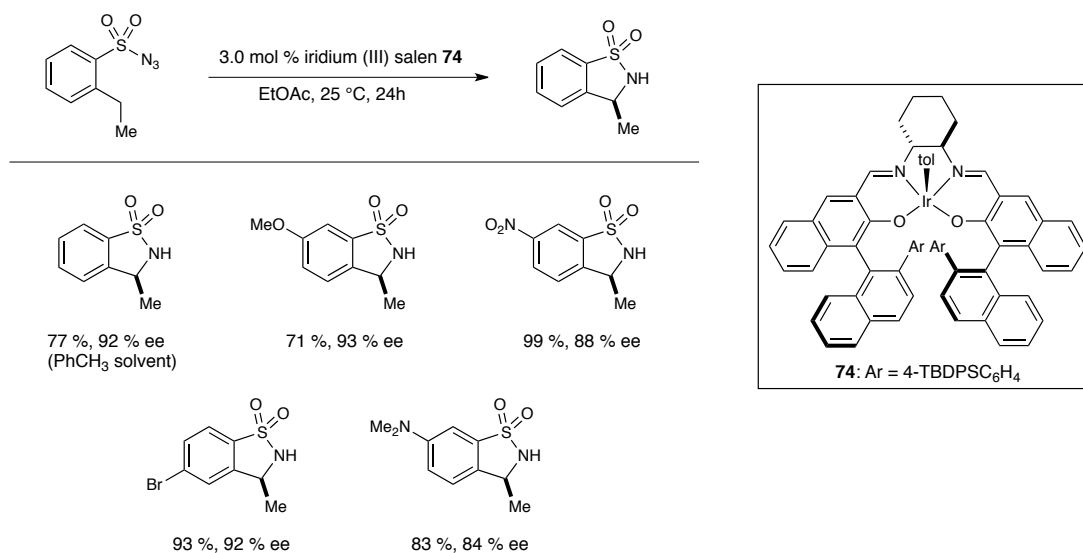
Scheme 2.22. $[\text{Ir}(\text{cod})\text{Cl}]_2$ catalyzed X-H insertion.Scheme 2.23. Synthesis of MK-7655 *via* iridium(I) catalyzed N-H insertion.

2.5 Iridium (III) Catalyzed Metallonitrene Atom-Transfer

2.5.1 Iridium(III) salen catalyzed intramolecular C-H amination of sulfonyl azides

As described in Section 2.2, Katsuki developed a family of chiral iridium(III) salen catalysts that were shown to perform highly enantio- and diastereoselective C-H¹⁰² and Si-H¹¹³ insertion reactions *via* metallocarbene atom transfer. It was only logical that the catalysts' capabilities were investigated in metallonitrene atom transfer, and in 2011

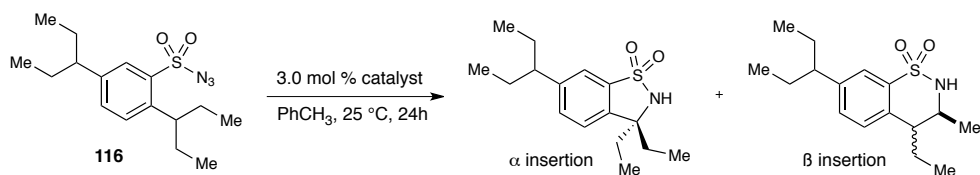
they reported the intramolecular C-H amination of aryl sulfonyl azides with catalyst **74** for the synthesis of optically active benzosultams (Scheme 2.24).¹³⁰



Scheme 2.24. Iridium(III) salen catalyzed enantioselective synthesis of benzosultams from aryl sulfonyl azides.

The resultant regio-, diastereo-, and enantioselectivities of the insertion reactions were determined to be very catalyst and substrate dependent. For example, the reaction of sulfonyl azide **116** with iridium(III) salen catalyst **74** (Ar = 4-TBDPSC₆H₄) furnishes the α -insertion product with a 2 : 1 preference over β -insertion (entry 1, Figure 2.5). The reaction produces a 1 : 3 *cis/trans* mixture, with the *trans* isomer being formed in 97 % ee. If catalyst **69** is used (Ar = C₆H₅) then a switch in selectivity is observed and the *cis* β -insertion isomer is formed exclusively in 98 % ee. It appears that factors other than sterics and bond energies are affecting the regio- and diastereoselectivity of the reaction, and the reason for these drastic changes in selectivity is not well understood. Katsuki also trialed the iridium(III) salen catalysts for intermolecular C-H amination with SES-N₃, but

the insertion into indane occurred in only 28 % ee. In this case, the ruthenium(II) salen complexes were far superior (see section 1.3.4).¹³¹



entry	catalyst	yield	α : β	cis/trans	% ee β (cis)	% ee β (trans)
1	74	86	2 : 1	1 : 3	53	97
2	69	90	1 : 1	20 : 1	98	-

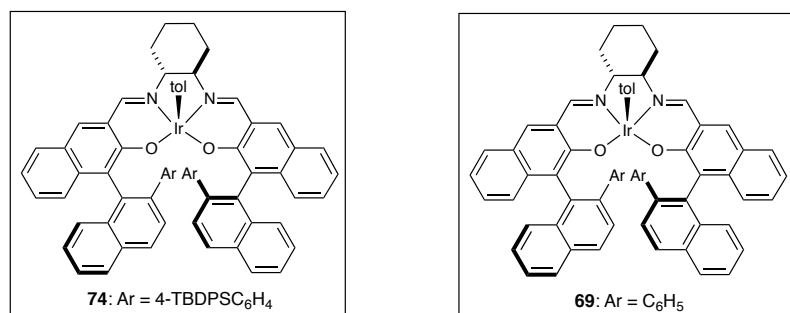
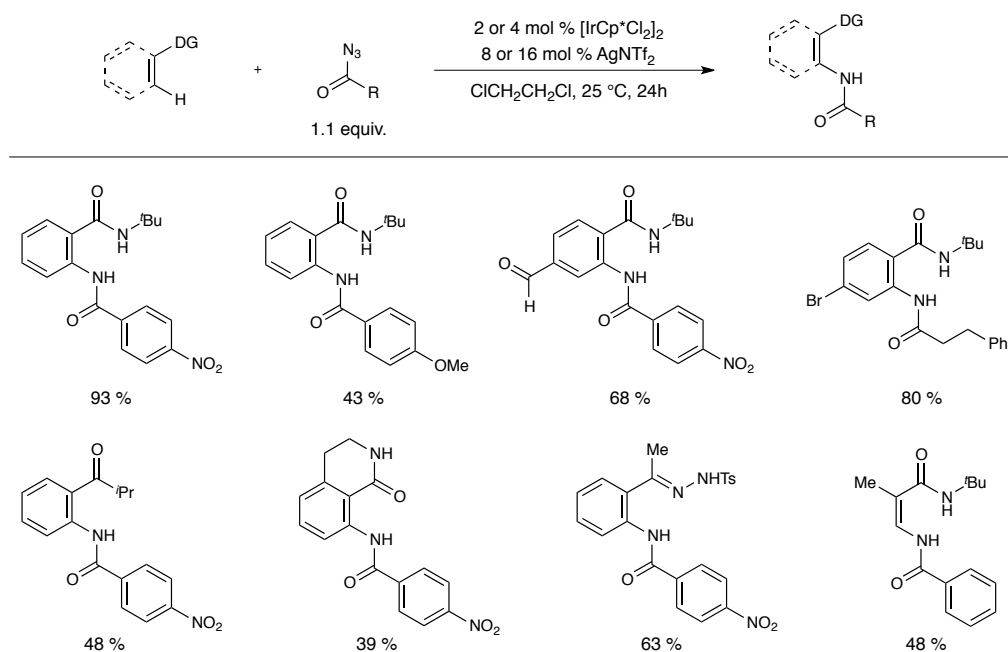


Figure 2.5. Iridium(III) salen catalyzed enantioselective synthesis of benzosultams.

2.5.2 Intermolecular C-H amidation using acyl azides

In 2013, the Chang group reported a breakthrough in intermolecular C-H amination with the discovery that the iridium(III) complex $[\text{IrCp}^*\text{Cl}_2]_2$ could catalyze directed *sp*² C-H amidation using acyl azides as the nitrene precursor (Scheme 2.25).¹³² The importance of this reaction lies in that acyl azides are typically not viable nitrene precursors for C-H insertion due to their propensity to undergo Curtius rearrangement.¹³³ The amidation reaction was tolerant to numerous functional groups, and amides, ketones, lactams, lactones, carbamates, ketoximes, heteroaryls, and

hydrazones could be amidated at 4 mol % catalyst loading. The chemistry was further extended to include sulfonyl and aryl azides in a subsequent report.¹³⁴

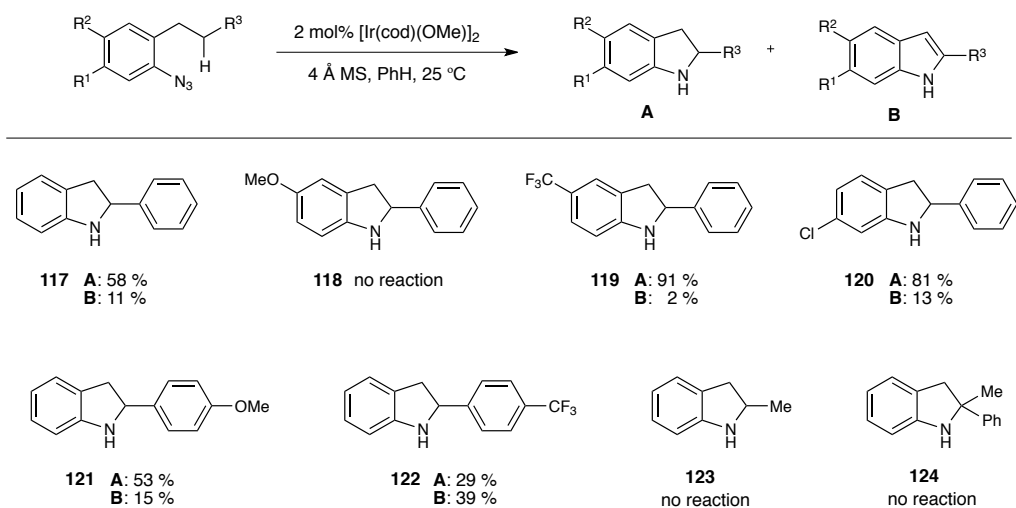


Scheme 2.25. $[\text{IrCp}^*\text{Cl}_2]_2$ catalyzed intermolecular C-H amidation using acyl azides as nitrene precursor.

2.6 Iridium (I) Catalyzed Metallonitrene Atom-Transfer

In 2009 the Driver group disclosed the first example^{135,136} of iridium(I) catalyzed metallonitrene C-H amination.¹³⁷ This report was significant in that simple aryl azides, ones that do not contain an electron withdrawing functionality, were capable of supporting a metallonitrene intermediate that performed C-H functionalization. After screening nearly 200 different transition metal salts and complexes, the iridium(I) dimer $[\text{Ir}(\text{cod})(\text{OMe})]_2$ catalyzed the intramolecular amination into 2° benzylic C-H bonds to generate substituted indolines (Scheme 2.26). While electron neutral and deficient

substituents on the aryl ring were efficient substrates (**117**, **119**, **120**), the *p*-methoxyphenyl azide did not react (**118**). Electron rich β -aryl substitution was tolerated in the reaction, giving product **121** in 53 % yield. Insertion into 2° alkyl and 3° benzylic positions did not occur and azide was recovered quantitatively. In nearly all reactions, the formation of the indole (**B**) was a significant side reaction, and the ratio of indole to indoline would increase upon purification by column chromatography. All yields shown were determined by ¹H NMR analysis of the crude reaction mixture. Notably, all dirhodium(II) salts that were investigated did not form any of the C-H amination products, which is intriguing since dirhodium(II) was found to catalyze aliphatic 1°, 2°, and 3° C-H insertion (see section 1.3.3).⁷³



Scheme 2.26. [Ir(cod)(OMe)]₂ catalyzed intramolecular benzylic C-H amination using simple aryl azides.

2.7 Conclusions

The field of iridium catalyzed atom-transfer reactions has experienced tremendous growth over the last four years. Namely, Katsuki's iridium(III) salen catalysts have can perform highly diastereo- and enantioselective intermolecular C-H and Si-H insertion. The development of these catalysts has expanded our capabilities for enantioselective intermolecular X-H functionalization in that alkyl-substituted diazoesters are now accessible metallocarbene precursors. These catalysts also perform asymmetric cyclopropanation, cyclopropenation, and intramolecular benzylic C-H amination using aryl sulfonyl azides. Che's chiral Halterman porphyrin iridium(III) complexes are also excellent catalysts for enantioselective inter- and intramolecular C-H insertion. The drawbacks in each of these systems are that the chiral ligands needed to induce asymmetry are lengthy to prepare and very expensive. There are many examples for the iridium(III) salen catalysts where the selectivity of the reaction is greatly dependent on the nature of the aryl substituent on the binaphthyl ring. Unfortunately, this important controlling element is installed very early in the ligand synthesis.

It is evident that iridium catalyzed metallocarbene and metallonitrene atom transfer reactions have provided reactivity that is advantageous in certain cases relative to more established systems, but the fundamental differences for this complimentary reactivity are still not well-understood. With these limitations identified, we began a research program dedicated to generating new iridium complexes with the goal of expanding the classes of catalysts available for enantioselective C-H functionalization.

Chapter 3

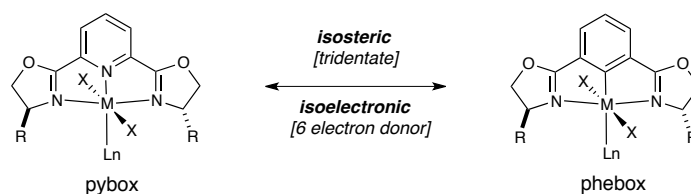
Development of Iridium NCN Pincer Catalysts for Enantioselective Metallo-carbene C-H Functionalization

Exciting progress has been made in the field of enantioselective atom transfer reactions by the development of new iridium catalysts but the field remains in its infancy. Having identified some limitations in current iridium catalyzed atom transfer technology, we began a research program dedicated to generating new iridium complexes with the goal of expanding the classes of catalysts available for enantioselective C-H functionalization.

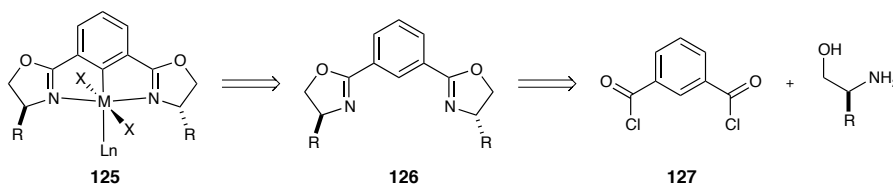
We hypothesized that a potential reason for iridium's unique reactivity is due to the stronger shielding effect experienced by iridium compared to rhodium.¹³⁸ This increased shielding could in principle increase the backbonding ability of iridium to the carbene, decrease carbene electrophilicity, and allow for selective C-H functionalization reactions to occur with typically more reactive acceptor-only carbenes. The shielding effect may also in part help explain the iridium(III) salen complexes' ability to prevent β -elimination of alkyl-substituted metallo-carbene and allow for C-H functionalization to take place. Katsuki postulated that the bulky salen ligand framework prevented the β -hydrogen from aligning *syn*-coplanar with the iridium metal such that elimination could not occur, but no experimental evidence was obtained to support this argument.¹¹³

We sought to develop a modular iridium catalyst platform in order to quickly assess its ability to perform enantioselective atom-transfer reactions using acceptor-only carbenes, with the most obvious precursor being ethyldiazoacetate. Chiral C₂-symmetric

ruthenium(II) pybox catalysts are widely used in atom-transfer reactions,¹³⁹ most frequently in asymmetric cyclopropanation of olefins using ethyl diazoacetate.¹⁴⁰ Our research group has also discovered that ruthenium pybox complexes are effective catalysts for enantioselective intramolecular C-H amination via metallonitrenes.⁷⁸ Knowing that ligand frameworks of this type are capable of performing enantioselective atom-transfer reactions, we were attracted to the isosteric and isoelectronic bis(oxazolonyl)phenyl (phebox) family of NCN pincer metal complexes, which feature a covalent metal-ligand bond (Scheme 3.1). This family of complexes is readily available after the metallation of the phebox ligand **126**, which is obtainable from the corresponding isophthaloyl dichloride **127** and a chiral amino alcohol (Scheme 3.2).^{141,142} The following chapter of this dissertation will provide a historical background on the synthesis and utility of transition metal phebox complexes. Furthermore, our contributions in the design, synthesis, and catalytic activity in atom-transfer reactions with new iridium(III) phebox complexes will be described.



Scheme 3.1. Similarities between pybox and phebox frameworks.

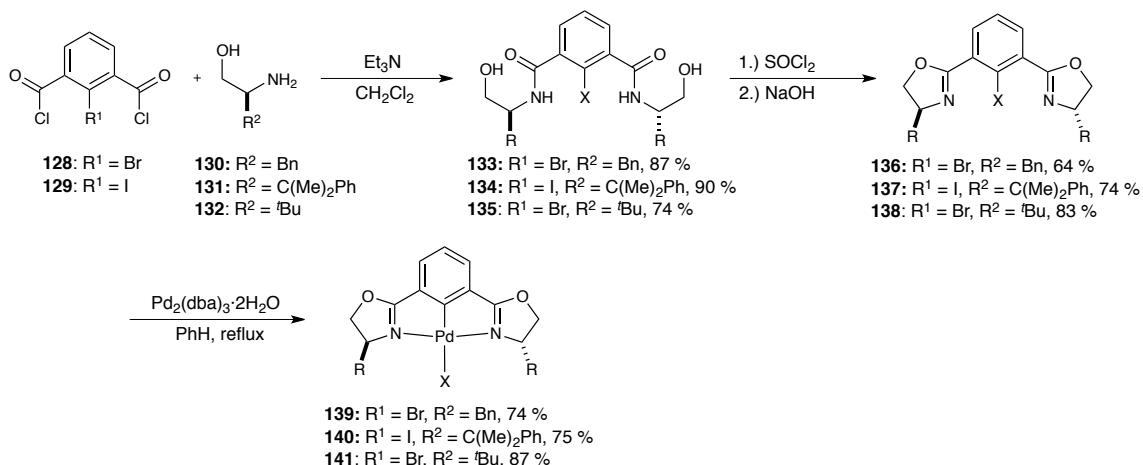


Scheme 3.2. General synthesis of phebox metal complexes.

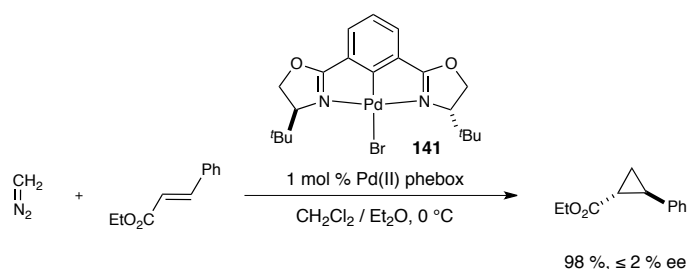
3.1 Bis(oxazolinyl)phenyl (phebox) complexes

3.1.1 Palladium(II) phebox complexes developed by Denmark

Phebox ligands were pioneered by Denmark, who initially examined their palladium(II) complexes as catalysts in cyclopropanation reactions using diazomethane.¹⁴³ Synthesis of the palladium phebox complexes began from chiral amino alcohols (**130-132**) and 2-haloisophthaloyl dichlorides (**128-129**) to form amides **133-135** (Scheme 3.3). Cyclization of the amides occurred upon treatment with thionyl chloride and sodium hydroxide to give the 2-halo-substituted phebox ligands **136-138**. The metallation to furnish the palladium phebox complexes **139-141** was accomplished by the oxidative addition of $\text{Pd}_2(\text{dba})_3 \cdot 2\text{H}_2\text{O}$ into haloarenes **136-138** in refluxing benzene.¹⁴⁴ These complexes were tested in the cyclopropanation of ethyl-(*E*)-cinnamate using a palladium carbene derived from diazomethane (Scheme 3.4). Unfortunately, asymmetric induction was not achieved even though the cyclopropanation was *cis*-selective and high yielding.



Scheme 3.3. Denmark's palladium(II) phebox synthesis.

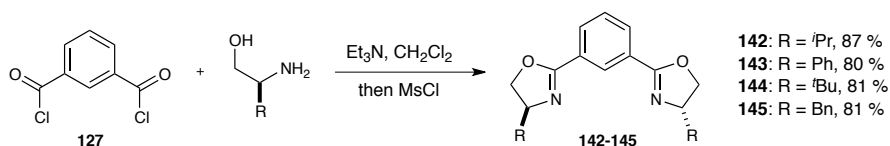


Scheme 3.4. Palladium phebox catalyzed cyclopropanation.

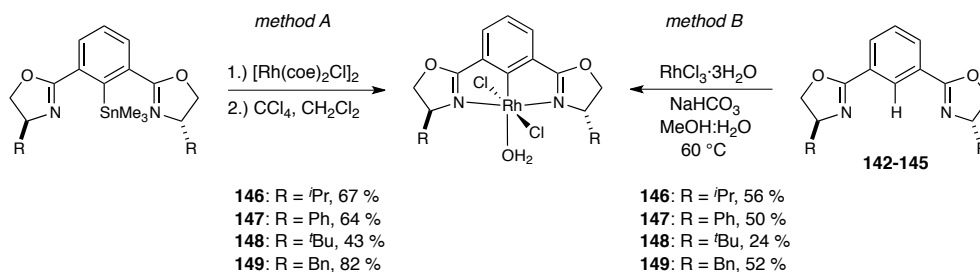
3.1.2 Rhodium(III) phebox complexes

Nishiyama has most extensively developed and studied a variety of chiral phebox complexes, especially those bearing a rhodium(III) metal center.^{141,145} The ligands are usually prepared in a one-pot fashion by condensation of an isophthaloyl dichloride **127** with a chiral amino alcohol, followed by mesylation with methanesulfonyl chloride and cyclization to furnish the phebox ligands **142-145** in good yields (Scheme 3.5). The initial strategy to synthesize the rhodium(III) aqua complexes **146-149** involved transmetalation of the corresponding stannylated phebox ligands with [Rh(coe)₂Cl]₂

followed by treatment with CCl_4 (Scheme 3.6, method A).¹⁴⁶ A more atom-economical and straightforward approach was developed soon after, and directed cyclometallation of the phebox ligands **142-145** with rhodium trichloride afforded the air and moisture stable rhodium phebox aqua complexes **146-149** in comparable yields (Scheme 3.6 method B).¹⁴⁷ To summarize, the chiral rhodium(III) phebox complexes are available in only two steps from commercial materials.



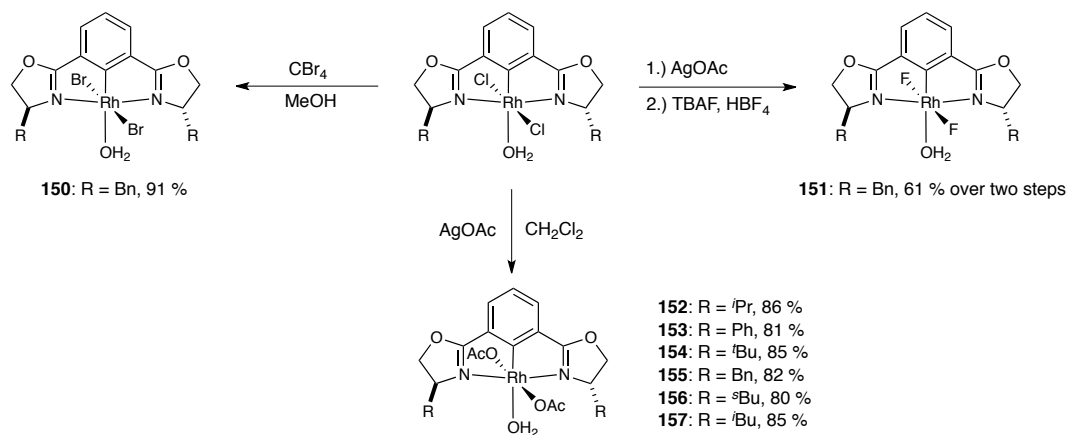
Scheme 3.5. Nishiyama's one-pot phebox ligand synthesis.



Scheme 3.6. Rhodium(III) phebox complex synthesis by transmetalation (method A) and cyclometallation (method B).

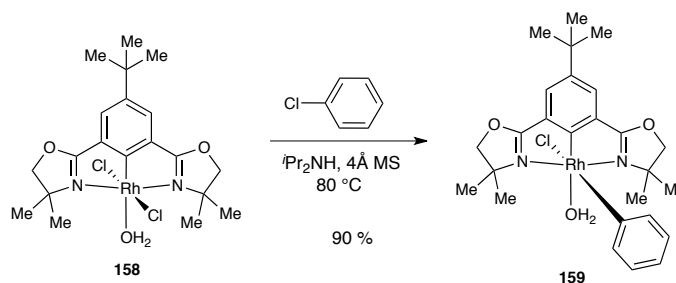
3.1.3 Stoichiometric Reactions at the Rhodium(III) Phebox Metal Center

The rhodium(III) phebox complexes are very versatile and undergo a wide variety of stoichiometric reactions at the metal center. The corresponding bromide (**150**),¹⁴⁸ acetate (**152-157**),¹⁴⁷ and fluoride (**151**)¹⁴⁸ complexes containing an assortment of chiral environments are all readily obtained under straightforward conditions (Scheme 3.7).



Scheme 3.7. Chloride ligand substitution reactions.

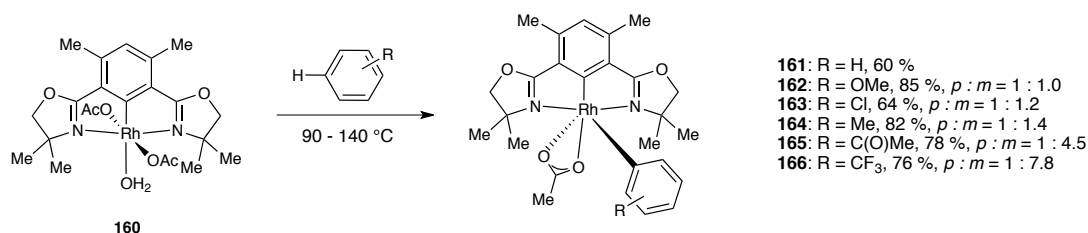
Other ligand substitution reactions are also achievable with these complexes. For example, achiral rhodium(III) phebox chloride complex **158** was shown to oxidatively add into aryl chloride bonds to afford phenyl complex **159** in 90 % yield (Scheme 3.8).¹⁴⁹ Diisopropylamine is postulated to reduce the rhodium(III) metal to a rhodium(I) species, which then inserts into the carbon-chlorine bond.



Scheme 3.8. Chloride ligand substitution reactions of chloro complex **158**.

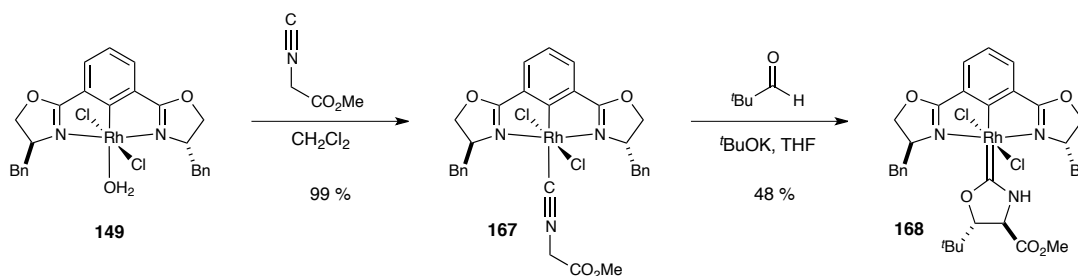
A switch in reactivity can be achieved when the chloride ligands are substituted for acetate ligands. The acetate complex **160** can perform a C-H activation reaction into substituted arenes (Scheme 3.9).¹⁵⁰ For the arene complexes **161-166**, the ratio of *meta* to *para* product distribution increased in a fashion consistent with selectivity in electrophilic

aromatic substitution reactions. The acetate ligand presumably serves as an internal base to facilitate cleavage of the C-H bond. Notably, oxidative addition into the aryl-chloride bond was not observed.



Scheme 3.9. C-H activation reactions of rhodium(III) phebox acetate complex **160**.

Further stoichiometric reactions of chiral rhodium(III) phebox complexes include resolution of racemic BINOL ligands,¹⁵¹ formation of rhodium phebox acetylides,¹⁵² and the formation of unique azarhodacycles.¹⁵³ Additionally, rhodium(III) phebox Fischer carbene complexes are also known.¹⁵⁴ Treatment of **149** with methyl isocynoacetate provided the isocyanide complex **167** in excellent yield (Scheme 3.10). Deprotonation of **167** with ^tBuOK and subsequent condensation with pivaldehyde generated the chiral rhodium(III) Fischer carbene complex **168** in 48 % yield. Clearly, each of the stoichiometric reactions outlined above are indicative of the diverse coordination chemistry and flexible nature of rhodium(III) phebox complexes.

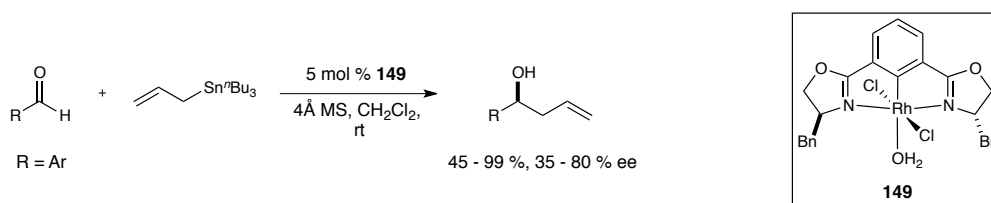


Scheme 3.10. Formation of rhodium(III) Fischer carbene complex **168**.

3.1.4 Rhodium(III) phebox complexes in asymmetric catalysis

The ability to alter the chiral environment around the oxazolines as well as modify the coordination environment around the metal center makes the phebox ligand framework highly modular and tunable. Therefore, it is not surprising that these complexes have found diverse application in asymmetric catalysis.

It was presumed that the water ligand bound to rhodium could readily dissociate to form a coordinatively unsaturated complex in which rhodium could act as a chiral Lewis acid. In fact, the first example of rhodium(III) phebox complexes in catalysis was in asymmetric allylation reactions of substituted benzaldehydes with allyl tributylstannanes.¹⁴⁶ Enantioenriched homoallylic alcohols were formed in the presence of 5 mol % catalyst **149** in up to 99 % yield and 80 % ee (Scheme 3.11). The transition state proposed by Nishiyama for this transformation invokes binding of the Lewis basic aldehyde carbonyl to rhodium and is shown in Figure 3.1.



Scheme 3.11. Rhodium(III) phebox catalyzed enantioselective allylation of aldehydes.

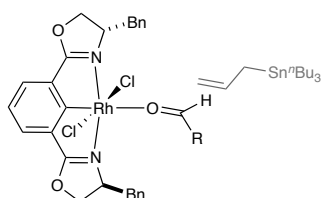


Figure 3.1. Proposed transition state for the allylation reaction.

Other examples of chiral C_2 -symmetric rhodium phebox catalyzed reactions include hetero-Diels-Alder reactions,¹⁴⁸ Michael addition,¹⁵⁵ hydrosilylation,¹⁵⁶ conjugate reduction,^{147,157-159} reductive aldol,^{157,160-166} reductive Mannich¹⁶⁷, direct aldol,^{165,166} borylation¹⁶⁸, diboration¹⁶⁹, and alkynylation¹⁵² reactions. Examples of diastereo- and enantioselective transformations are shown in Figure 3.2. The extensive development of chiral rhodium phebox catalysts has greatly enhanced our capabilities of achieving highly selective reactions of these types.

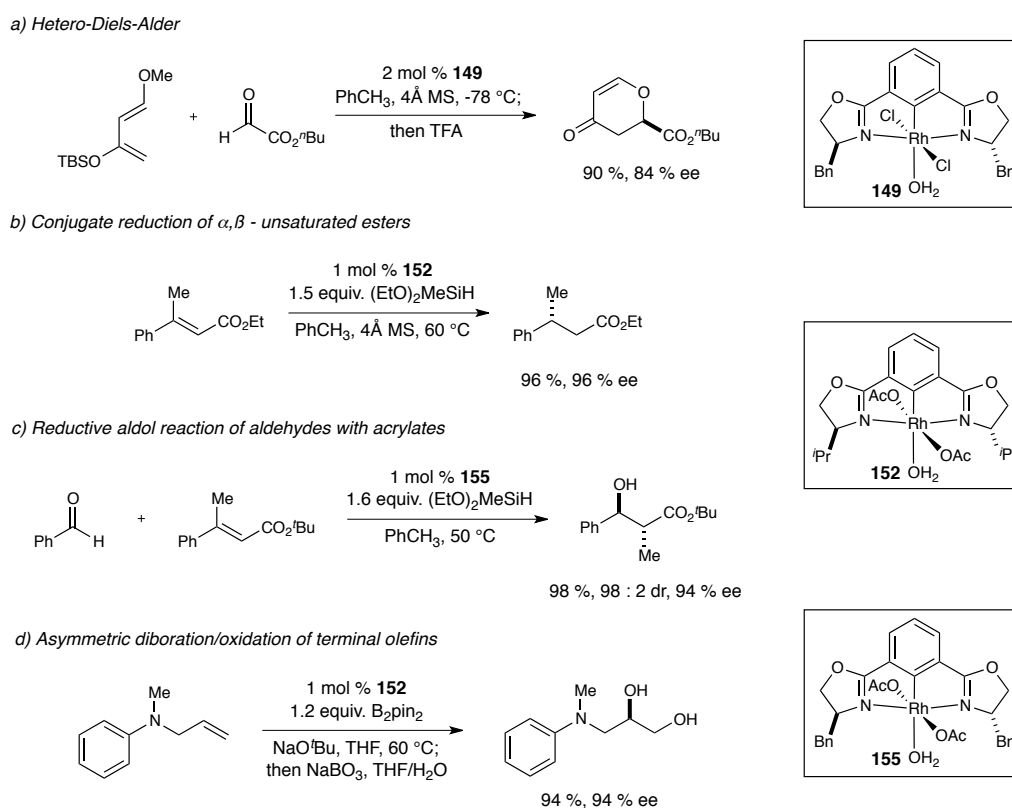
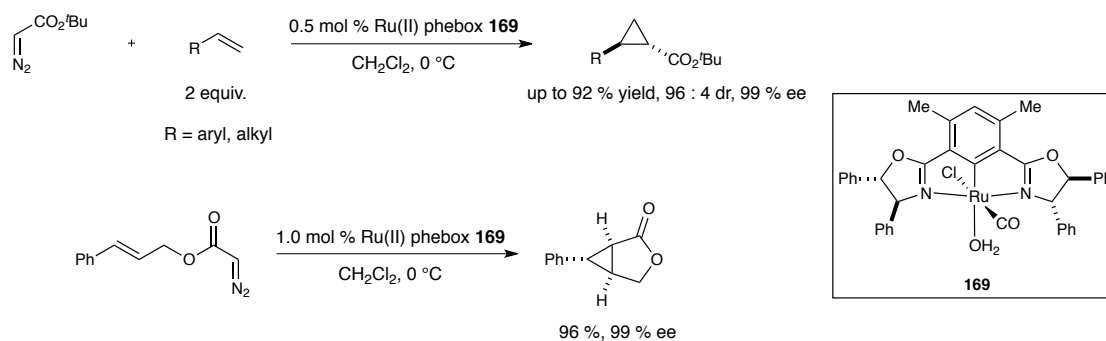


Figure 3.2. Examples of rhodium phebox catalyzed enantioselective reactions.

3.1.5 Phebox complexes with metals other than rhodium

The literature is populated with many other examples of phebox complexes, including those bearing iron, cobalt, ruthenium, nickel, palladium, iridium, and platinum transition metals.^{145,170} There was a particularly interesting report by Nishiyama on the use of *pseudo*-C₂-symmetric ruthenium(II) phebox complex **169** for asymmetric inter- and intramolecular cyclopropanation reactions of alkenes with acceptor-only diazoesters (Scheme 3.12).¹⁷¹ In fact, this was the first example of an asymmetric carbene atom-transfer reaction catalyzed by a discrete transition metal phebox complex. The origin of enantioselectivity and *trans* diastereoselectivity for the cyclopropanation was proposed to arise from equatorial coordination of the carbene intermediate followed by *Re*-facial approach of the alkene (Figure 3.3).



Scheme 3.12. Ruthenium(II) phebox catalyzed asymmetric cyclopropanation.

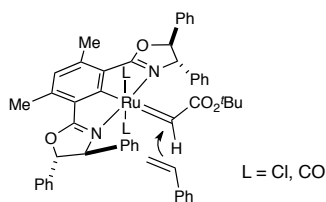
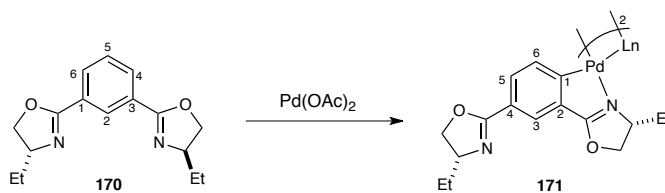


Figure 3.3. Proposed transition state model for Ru(II) phebox cyclopropanation.

3.2 Iridium(III) Phebox Complexes

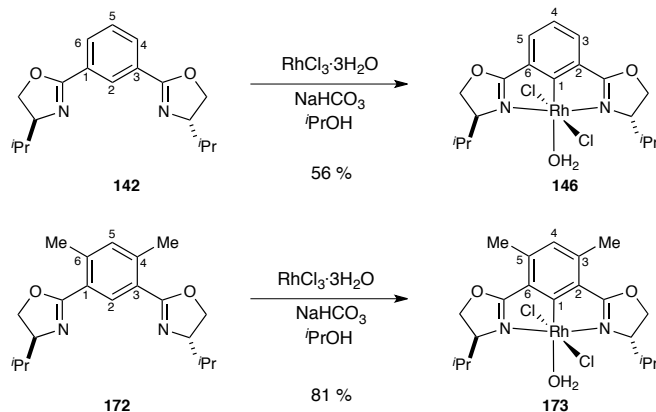
3.2.1 Synthesis of iridium phebox complexes

While investigating rhodium(III) phebox catalyzed conjugate reduction and reductive aldol reactions, Nishiyama reported another strategy for the synthesis of phebox complexes. The cyclometallation route that was previously reported for rhodium generally gave yields around 50 % despite many efforts towards optimizing the reaction.¹⁵⁷ They hypothesized that the low yields could be attributed to undesired cyclometallation at the 4 or 6 position. In fact, it is known that metallation of phebox ligands with palladium is problematic due to the preference of palladium to metallate the 4(6) position (Scheme 3.13).^{172,173} This type of reactivity destroys the C₂-symmetry of the resultant complexes, and the design of chiral complexes for use in asymmetric catalysis becomes substantially more challenging.



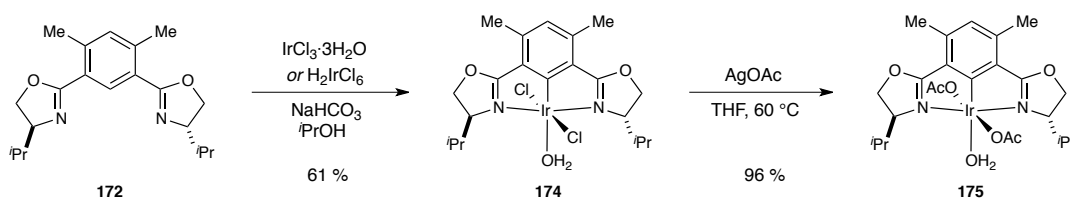
Scheme 3.13. Cyclopalladation into the 4(6) position of phebox ligand **170**.

With this in mind, they found that methyl substitution at the 4 and 6 positions of ligand **172** provided a considerable increase in yield from 56 % for rhodium phebox complex **146**¹⁴⁷ to 81 % for dimethyl substituted complex **173** (Scheme 3.14).¹⁵⁷



Scheme 3.14. Effect of 4,6-dimethyl substitution on rhodium pbeox metallation.

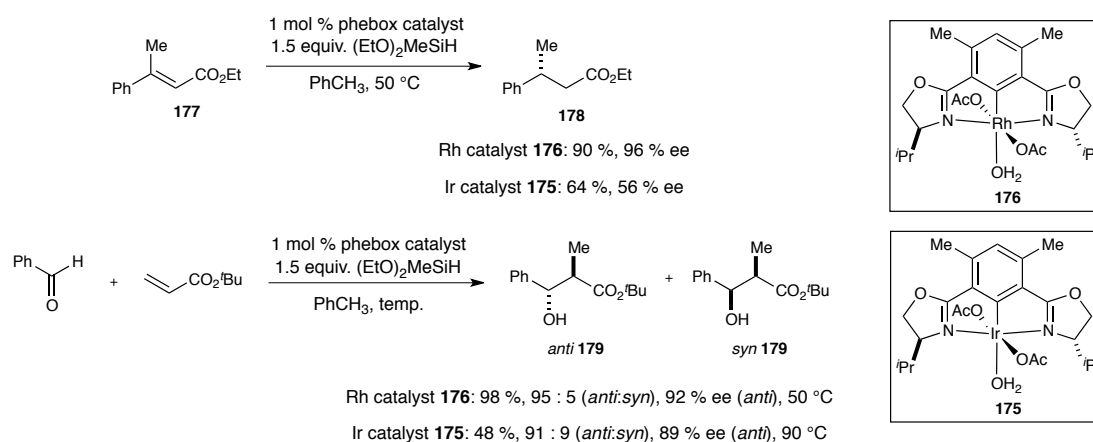
The most exciting result for us was that this strategy was successful for synthesizing the iridium(III) pbeox chloride complex **174**. Without the dimethyl substitution the iridium pbeox complexes were previously inaccessible. The complex was synthesized in 61% yield by reacting the dimethyl-substituted ligand with either IrCl_3 or H_2IrCl_6 in the presence of sodium bicarbonate in refluxing isopropanol (Scheme 3.15). Ligand exchange reactions could also be performed, and the chloride ligands could be traded for acetate in high yield by treating complex **174** with AgOAc (**175**).



Scheme 3.15. Synthesis of iridium(III) pbeox complexes **174** and **175**.

The rhodium(III) and iridium(III) complexes **176** and **175** were then investigated for their efficiency in asymmetric conjugate reduction of esters and in the asymmetric reductive aldol reaction (Scheme 3.16). In the conjugate reduction of

(*E*)-ethyl 3-phenyl-2-butenate **177** with 1.5 equivalents (EtO)₂MeSiH, rhodium phebox acetate catalyst **176** furnished ester **178** in 90 % yield and 96 % ee at 50 °C in 30 minutes. The corresponding iridium phebox acetate catalyst **175** provided the ester in 64 % yield and only 56 % ee and required a longer reaction time of 6 hours. Additionally, the iridium catalyst **175** exhibited inferior performance compared to rhodium in the reductive aldol reaction of benzaldehyde and *tert*-butyl acrylate, providing lower yield, diastereoselectivity, and enantioselectivity for adducts *anti*-**179** and *syn*-**179** at much higher temperature.

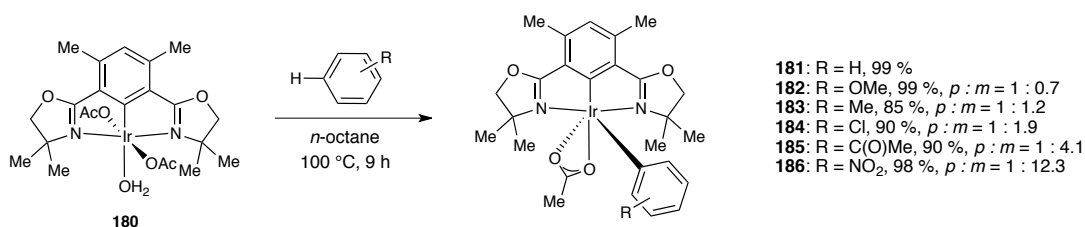


Scheme 3.16. Asymmetric conjugate reduction of esters and asymmetric reductive aldol reactions using rhodium(III) and iridium(III) phebox complexes **176** and **175**.

3.2.2 Stoichiometric and catalytic C-H functionalization using iridium(III) phebox complexes

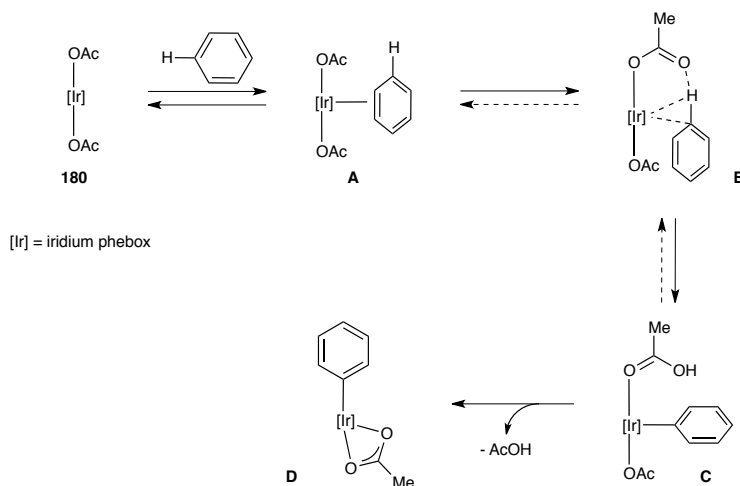
These iridium(III) phebox complexes have not been reported for atom-transfer catalysis, but there are recent reports of their use in stoichiometric and catalytic C-H functionalization reactions. As described in Section 3.1.3, Nishiyama has reported the

synthesis of aryl-substituted rhodium(III) phebox complexes via C-H functionalization of arenes using the acetate series of complexes (*cf.* Scheme 3.9). Recently they observed that the iridium(III) phebox series of catalysts exhibit similar reactivity.¹⁷⁴ They found that reacting achiral iridium phebox **180** with 500 equivalents of a substituted arene affords the iridium(III) phebox aryl complexes **181-186** in excellent yields but as mixtures of *para* and *meta* regioisomers (Scheme 3.17). In general the yields were higher than with rhodium phebox complexes and the distribution of products followed the same trend consistent with electrophilic aromatic substitution reactions.



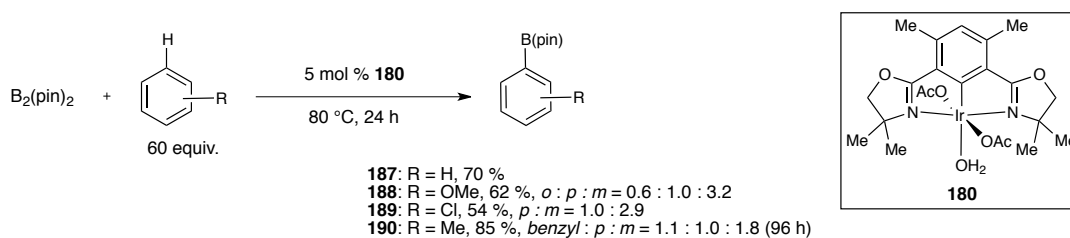
Scheme 3.17. C-H activation reactions of iridium(III) phebox acetate complex **180** with substituted arenes.

The proposed mechanism for C-H activation is outlined in Scheme 3.18. First, reversible dissociation of the water ligand from complex **180** can lead to η^2 -arene coordinated complex **A**. Acetate-assisted bond cleavage can occur *via* 3-centered transition state **B** to form C-H insertion adduct **C**, and dissociation of acetic acid forms the observed iridium phebox arene complex **D**. In line with this proposal, employing the analogous iridium(III) phebox chloride complex resulted in no product formation, suggesting that the C-H bond cleavage is indeed assisted by the acetate ligand.



Scheme 3.18. Proposed mechanism for iridium(III) phebox acetate-assisted C-H insertion.

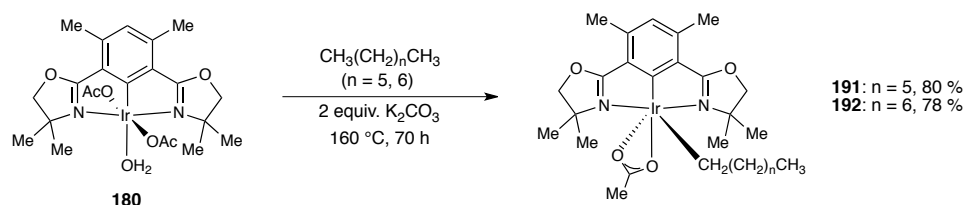
Iridium-catalyzed borylation by direct C-H functionalization is a powerful method for the transformation of arenes and alkanes.^{175,176} In the same report, Nishiyama described the stoichiometric and catalytic C-H borylation of arenes using the iridium phebox complex **180** (Scheme 3.19).¹⁷⁴ The selectivity of the reaction was quite poor amongst the substrates that were investigated, although insertion into a 1° benzylic C-H bond was observed.



Scheme 3.19. Iridium(III) phebox **180** catalyzed C-H borylation.

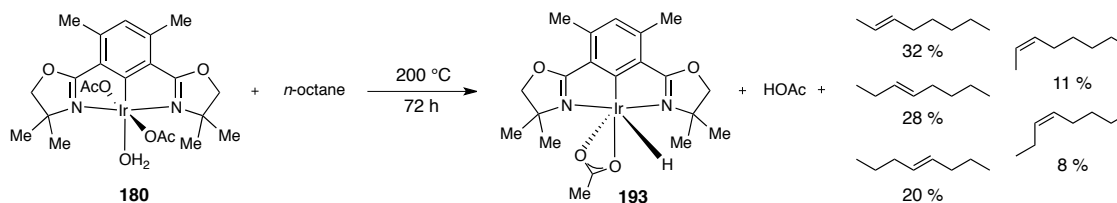
Further demonstration of the versatility of these complexes for stoichiometric C-H functionalization was also provided. Nishiyama found that even the 1° aliphatic C-H

bonds of *n*-heptane and *n*-octane could be selectively functionalized in good yields (80 %, and 78 %, respectively) in the presence of potassium carbonate and iridium phebox complex **180** at 160 °C (Scheme 3.20). The role of base in the reaction is presumed to drive the equilibrium towards C-H functionalization/iridium-alkyl formation. The resulting iridium(III) alkyls **191** and **192** were stable to air and moisture and purified by silica gel chromatography.



Scheme 3.20. Iridium(III) phebox **180** mediated 1° aliphatic C-H functionalization.

Goldberg and coworkers have also applied these iridium phebox complexes to the dehydrogenation of *n*-octane via initial C-H functionalization.¹⁷⁷ In the absence of base, iridium phebox complex **180** quantitatively converts to the iridium hydride complex **193** while producing a mixture of octene isomers (Scheme 3.21). The metal alkyl complex can be thermally driven to undergo β-hydride elimination after its formation, and the regioisomers observed in the reaction outcome were all derived from 1-octene. This indicates that the initial dehydrogenation is completely stereoselective for 1-octene at earlier reaction times, albeit in low conversion (ca. 30 %). It was additionally found that the iridium(III) phebox C-H activation reaction was not inhibited by alkenes, nitrogen, or water; all of which are significant problems with systems that activate C-H bonds by oxidative addition to iridium(I).^{178,179}



Scheme 3.21. Iridium(III) phebox dehydrogenation of *n*-octane.

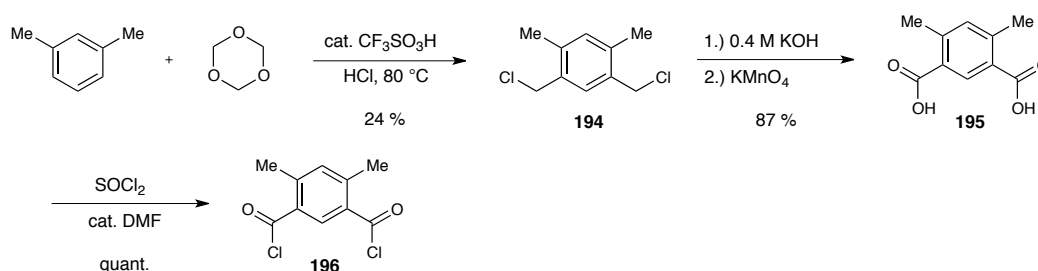
It is clear that transition metal phebox complexes exhibit a wide array of intriguing and synthetically useful transformations. Their attractiveness for their use in catalysis lies in the modularity and tunability of the ligand framework, as well as the ability to integrate them with numerous transition metals. In particular, the recent development of iridium(III) phebox complexes has revealed their diverse reactivity and potential for C-H bond functionalization reactions. This reactivity, combined with their rapid accessibility, has encouraged us to pursue this catalyst family for the expansion of iridium atom-transfer C-H functionalization methodologies.

3.3 Design and Synthesis of New Iridium(III) Phebox Complexes

3.3.1 Synthesis of iridium(III) phebox complex 174

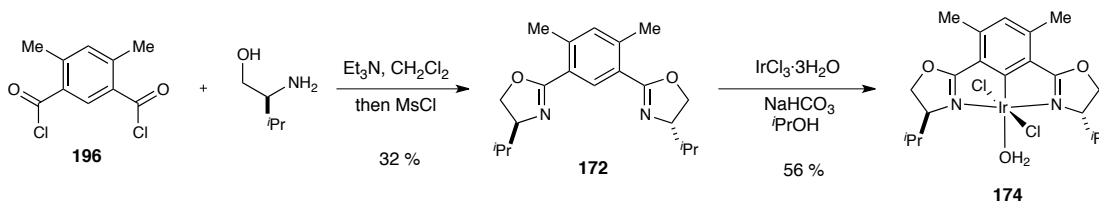
We began our investigations by synthesizing the known 4,6-dimethyl substituted iridium(III) phebox (diMe-Phebox) complex **174**.¹⁸⁰ The synthesis commenced by making 4,6-dimethylisophthaloyl dichloride **196**. Treatment of *m*-xylene with trioxane in the presence of hydrochloric acid and catalytic triflic acid at 80 °C furnished 1,3-bis(chloromethyl)-4,6-dimethylbenzene **194** in 14-24 % yield (Scheme 3.22).¹⁸¹ The

yield of this reaction was variable, and mixtures of mono- and dichloromethylated products as well as products resulting from chlorination of the xylene methyl groups were obtained. Fortunately, these could be removed by trituration with hexanes and the desired dichloromethylated product **194** could be isolated as a single isomer. Hydrolysis of the dichloride followed by KMnO_4 oxidation gave the dimethylisophthalic acid **195** in 87 % yield over two steps.¹⁸² The corresponding 4,6-dimethylisophthaloyl dichloride **196** was produced in quantitative yield by refluxing the diacid **195** in thionyl chloride and catalytic DMF.



Scheme 3.22. Synthesis of 4,6-dimethylisophthaloyl dichloride **196**.

First, the isopropyl-substituted diMePhebox ligand **172** was obtained in 32 % yield by the one-pot amide formation/cyclization protocol (Scheme 3.23). We were then successful in synthesizing the known iridium(III) phebox catalyst **174** in 56 % yield by metallation with iridium trichloride. The yield of our metallation was similar to Nishiyama's previously reported 61 % yield for the same complex.¹⁵⁷

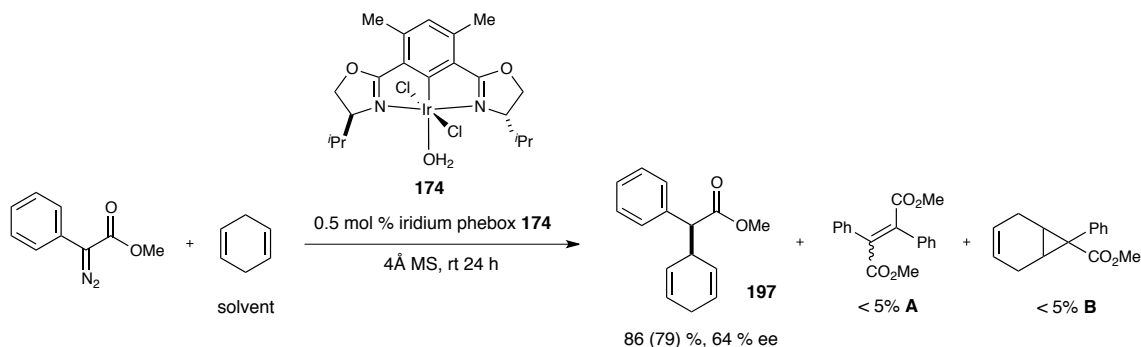


Scheme 3.23. Synthesis of (diMePhebox) ligand **172** and its corresponding iridium(III) complex [(*S,S*)-diMePhebox-*i*Pr]IrCl₂(OH₂) **174**.

3.3.2 Proof of principle for iridium(III) phebox catalyzed atom transfer using a donor/acceptor metallocarbene

Although our ultimate goal was to use the iridium phebox complexes for enantioselective intermolecular C-H insertion reactions using acceptor-only metallocarbenes, we sought to obtain proof of principle that these catalysts were capable of generating carbenes that perform enantioselective atom transfer C-H insertion. To this end, we started with the better-studied donor/acceptor carbene system and used 1,4-cyclohexadiene as the C-H insertion substrate. In fact, enantioselective C-H insertion was achieved by adding 0.5 mol % [(*S,S*)-diMePhebox-*i*Pr]IrCl₂(OH₂) complex **174** to a mixture of methyl phenyldiazoacetate, 4Å molecular sieves, and 1,4-cyclohexadiene at room temperature, giving the insertion product **197** in 86 % yield by ¹H NMR, 79 % isolated yield, and 64 % ee (Scheme 3.24). The absolute configuration was initially assigned by analogy to the literature value.¹⁸³ It is notable that the color of the mixture before catalyst addition was the color of the diazoester (red/orange), and upon addition of the catalyst the reaction mixture immediately turned dark green. Once the diazo had been completely consumed the color of the reaction reverted to the orange color of the starting

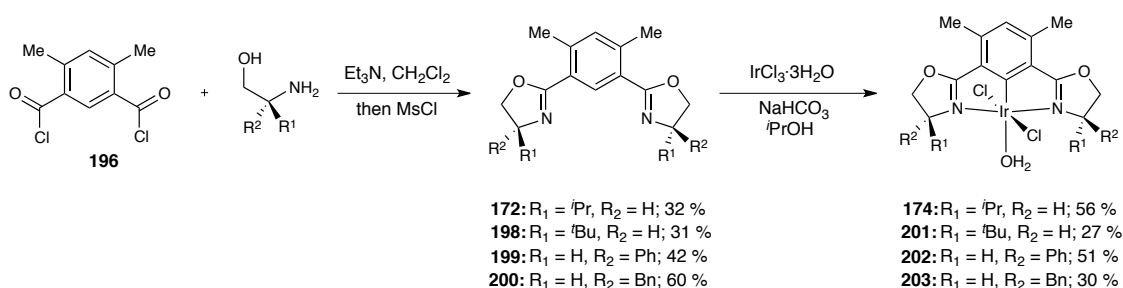
catalyst. This phenomenon is consistent with previous observations by Woo and indicates a charge transfer event from iridium to the carbenic carbon.¹¹⁸



Scheme 3.24. Initial insertion reaction of methyl phenyldiazoacetate into 1,4-cyclohexadiene.

There are potentially two competing reaction pathways in this reaction. First, dimerization of the carbene to form **A** is very problematic for highly reactive rhodium and iridium carbenes (Scheme 3.24). Katsuki observed in the iridium(III) salen catalyzed donor/acceptor C-H insertion reactions that lower temperature was required to suppress dimerization.¹⁰² Additionally, slow addition of the diazoester via syringe pump is typically used in dirhodium-catalyzed reactions to prevent this side reaction. Furthermore, Woo reported that slow addition of the diazoester was necessary in the iridium(III) porphyrin catalyzed C-H insertion of donor/acceptor diazoesters.¹¹⁸ Second, cyclopropanation of the olefin becomes problematic especially in the case of acceptor-only carbenes (**B**, Scheme 3.24).²⁸ The iridium phebox catalyst system is remarkable in that, at room temperature, the products arising from dimerization of the carbene (**A**) and cyclopropanation of the olefin (**B**) were present in < 5 % of the crude reaction mixture as detected by ¹H NMR analysis.

In order to increase the enantioselectivity of the insertion, we desired a range of chiral environments on the oxazoline ring. To this end, the analogous *tert*-butyl (**198**), phenyl (**199**), and benzyl (**200**) substituted diMePhebox ligands were made from the corresponding commercially available chiral amino alcohols in 31 %, 42 %, and 60 % yields, respectively (Scheme 3.25). The series of ligands was successfully metallated under Nishiyama's conditions to afford diMePhebox iridium complexes **174**, **201-203** in 27 - 56 % yields as orange solids after purification by silica gel column chromatography.

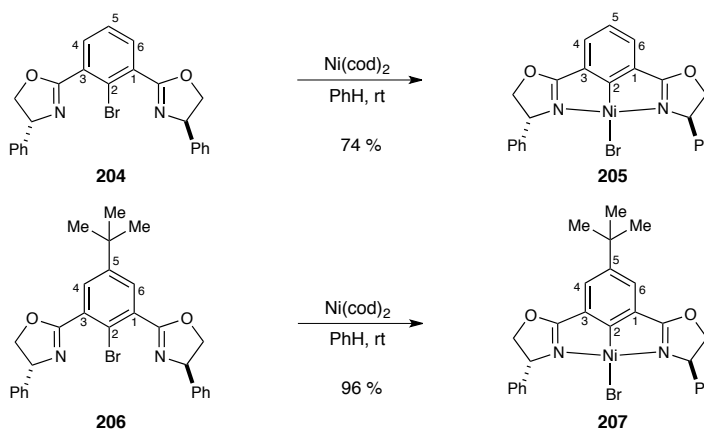


Scheme 3.25. Synthesis of (diMePhebox) ligands **172**, **198-200** and their iridium(III) complexes **174**, **201-203**.

3.3.3 Design concept and synthesis of new iridium(III) phebox complexes.

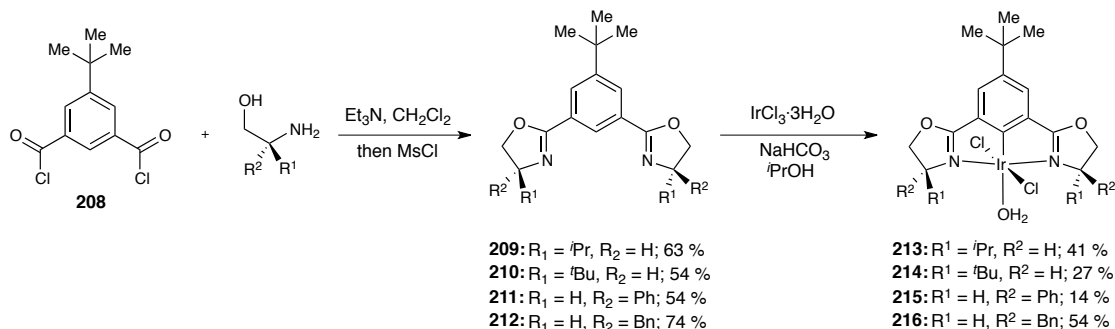
After getting variable results for the synthesis of the dimethyl isophthaloyl dichloride, we wanted access to a commercially available isophthalic acid that would serve the same purpose of blocking the undesired metallation into the 4(6) positions. We found that 5-*tert*-butyl isophthalic acid was commercially available and the corresponding 5-*tert*-butyl isophthaloyl dichloride **208** could be accessed quantitatively using the SOCl₂ mediated chlorination procedure (Scheme 3.27). We hypothesized that the large steric environment imposed by the *tert*-butyl functionality would serve to

minimize the unwanted 4(6) position insertion during metallation. Connell *et. al.* observed an effect on yield during investigations on the synthesis of palladium(II) and nickel(II) phebox complexes (Scheme 3.26).¹⁸⁴ The synthesis of nickel(II) *tert*-butyl phebox complex **207** was higher yielding than that of the unsubstituted phebox complex **205**. Although this metallation was achieved using an oxidative addition route, it is likely that the *tert*-butyl functionality played a significant role in the reaction outcome.



Scheme 3.26. Connell's synthesis of *tert*-butyl containing nickel(II) phebox complexes.

Second, we rationalized that the *tert*-butyl substitution would increase solubility of the iridium complex compared to its dimethyl analog and perhaps increase its catalytic performance. To this end, a second series of chiral 5-*tert*-butyl substituted phebox ligands (*t*BuPhebox) **209-212** were synthesized in 54-74 % yields and subsequently metallated with IrCl_3 to provide **213-216** in 14-54 % yields (Scheme 3.27). It is worth noting that all of our iridium(III) phebox complexes were purified by silica gel column chromatography and stable to air and moisture.



Scheme 3.27. Synthesis of (^tBuPhebox) ligands **209-212** and their iridium(III) complexes **213-216**.

3.3.4 X-ray structure analysis of [(*R,R*)-^tBuPhebox-Bn]IrCl₂(OH₂) **216**

A single crystal of [(*R,R*)-^tBuPhebox-Bn]IrCl₂(OH₂) complex **216** suitable for X-ray diffraction was obtained by slow diffusion of hexanes into a 5 mg saturated solution of **216** in CH₂Cl₂ (Figure 3.4). The complex exhibits C₂-symmetry and the water ligand is coordinated in the equatorial position of the Phebox plane. A distorted octahedral geometry was indicated by the N(1)-Ir(1)-N(2) bond angle of 157.8°. This angle is smaller than that observed by Nishiyama for the related (diMePhebox-diMe)IrCl₂(OH₂) (158.5°).¹⁵⁷ Additionally, the Ir(1)-C(13) bond distance is 1.924 Å, which is slightly shorter than the bond length observed by Nishiyama for (diMePhebox-diMe)IrCl₂(OH₂) (1.930 Å).

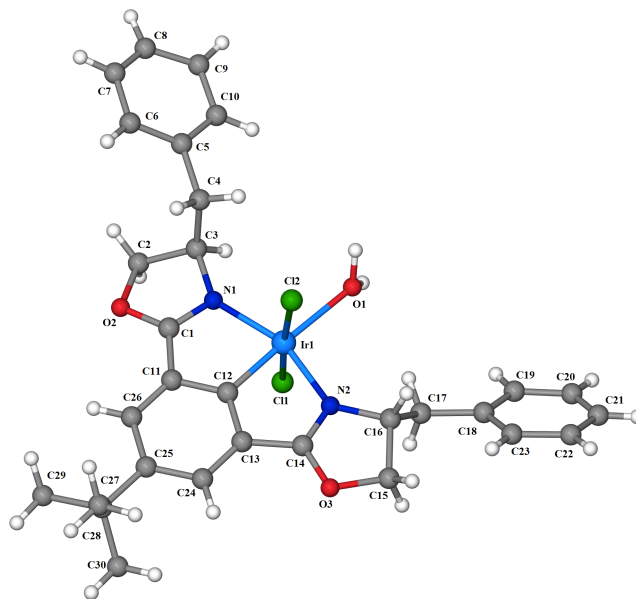


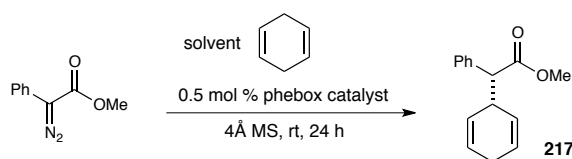
Figure 3.4. X-ray structure of [(*R,R*)-*t*BuPhebox-Bn]IrCl₂(OH₂) complex **216**.

3.4 Iridium(III) Phebox Catalyzed C-H Insertion of Donor/Acceptor Diazoesters

3.4.1. Initial optimization of catalyst and reaction conditions

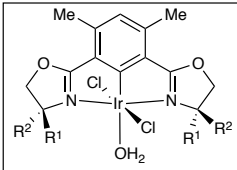
After establishing that the iridium(III) phebox complexes were competent metallocarbene atom transfer catalysts, we investigated the impact of catalyst structure on yield and enantioselectivity for the C-H functionalization of 1,4-cyclohexadiene. All racemic insertion products were synthesized by the slow addition of methyl phenyldiazoacetate to Rh₂(OAc)₄ over 12 hours. When the reaction was conducted with [(*S,S*)-diMePhebox-*t*Bu]IrCl₂(OH₂) **201**, decomposition of the diazoester was not observed, as the crude ¹H NMR indicated only diazoester in the reaction mixture (Table

3.1, entry 2). Presumably, steric hindrance imparted by the *tert*-butyl substituent on the catalyst prohibited the approach of the diazoester and subsequent carbene formation. The phenyl-substituted catalyst **202** gave a substantial drop in yield to 43 %, although the enantioselectivity of the reaction was substantially improved to 94 % (entry 3). Reaction of the benzyl-substituted diMePhebox catalyst **203** further increased the yield of **217** to 83 %, and the enantioselectivity was outstanding at 98 %.

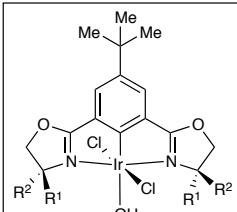


entry ^a	catalyst	% yield 217 ^b	% ee 217 ^c
1	174	86 (79)	-64 ^d
2	201	≤ 5	-
3	202	52 (43)	94
4	203	84 (83)	98
5	213	≥ 95 (97)	-94 ^d
6	214	≤ 5	-
7	215	85 (80)	98
8	216	≥ 95 (94)	97

^a Catalyst added in a single portion to a mixture of diazo (40 mg, 0.23 mmol), cyclohexadiene (0.5 mL), and 4Å MS (46 mg). ^b Yield determined by ¹H NMR using 1, 3, 5-trimethoxybenzene as the internal standard. ^c Value in parentheses denotes isolated yield. ^d Determined by chiral HPLC. ^e The negative sign denotes that the product obtained is the enantiomer of the one shown.



174: R¹ = *i*Pr, R² = H
201: R¹ = *t*Bu, R² = H
202: R¹ = H, R² = Ph
203: R¹ = H, R² = Bn



213: R¹ = *i*Pr, R² = H
214: R¹ = *t*Bu, R² = H
215: R¹ = H, R² = Ph
216: R¹ = H, R² = Bn

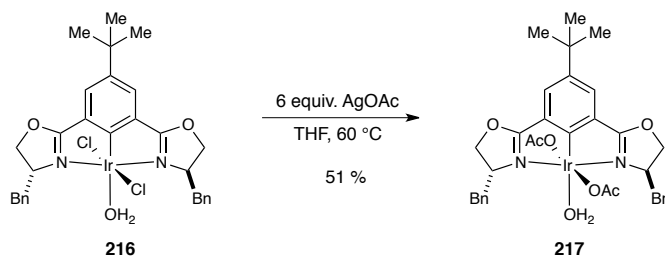
Table 3.1. Catalyst optimization for the insertion of methyl phenyldiazoacetate into 1,4-cyclohexadiene.

The reactions with the *t*BuPhebox iridium catalysts **213-216** are shown in entries 5-8. Intriguingly, simply employing the 4-*tert*-butyl phebox catalyst **213**, which contains isopropyl substitution on the oxazoline, gave the insertion product in nearly quantitative yield and 94 % ee. This enantioselectivity is in stark contrast when compared with its 4,6-dimethyl counterpart **174** (64 % ee, entry 1), and it is not currently understood as to

why there is such a drastic difference in enantioselectivity between these two catalysts. We think that the dimethyl substitution might twist the plane of the *NCN* the ligand *via* steric interactions with the oxazoline, but there is no experimental evidence for this hypothesis. As observed for the dimethyl phebox catalyst family, *tert*-butyl substitution on the oxazoline is detrimental to carbenoid formation (entry 6). The phenyl substituted *t*BuPhebox iridium catalyst **215** furnished **217** in higher yield and enantioselectivity than the corresponding dimethyl catalyst **202** (entry 7). The best combination of yield and enantioselectivity was achieved by using the 4-*tert*-butyl benzyl catalyst **216** at 94 % and 97 %, respectively. Gratifyingly, the 4-*tert*-butyl iridium phebox aqua catalysts **213-216** generally exhibited superior yields and enantioselectivities and than the 3,5-dimethyl substituted catalysts **174, 201-203**. Our strategy of employing the *tert*-butyl substituent in the 4 position of the aryl backbone of the catalysts was highly effective in allowing us to quickly synthesize this family of complexes. Additionally, the requisite carboxylic acid needed for the ligand synthesis is commercially available. This approach provided a more rapid access to iridium phebox catalysts when compared to the related family of dimethyl substituted iridium complexes. To our delight, our design resulted in an overall better catalyst performance with respect to donor/acceptor C-H insertion into 1,4-cyclohexadiene.

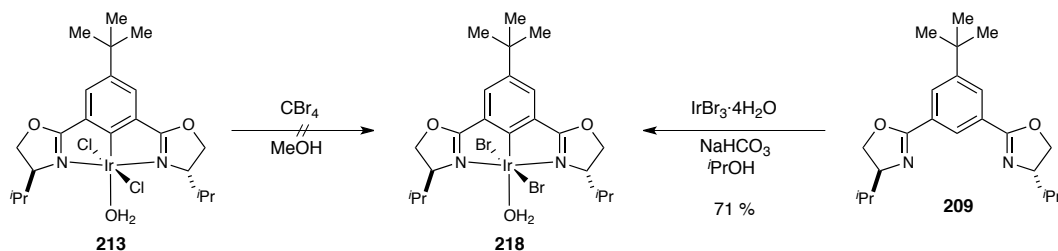
We were also interested in evaluating the effects of chloride ligand exchange on the yield and enantioselectivity for the C-H insertion. Our first ligand exchange attempt entailed reacting the chloro iridium(III) phebox complex **216** with 6 equivalents silver acetate in THF at 60 °C according to Nishiyama's protocol (Scheme 3.28).¹⁵⁷ This furnished the acetate complex **217** in 51 % yield as a light orange solid. Unfortunately,

this complex was completely unreactive towards decomposition of the diazoester at room temperature after three days.



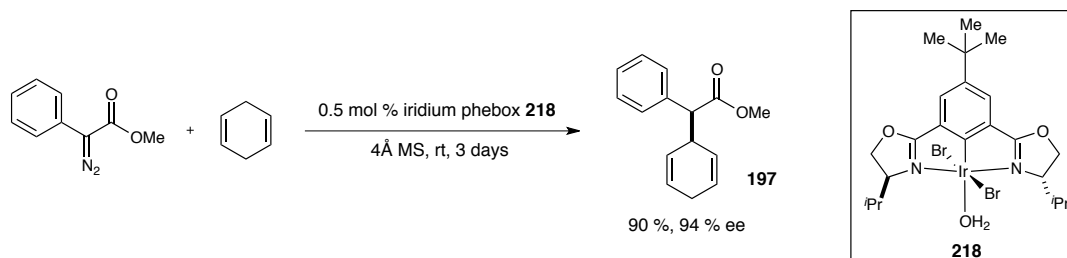
Scheme 3.28. Synthesis of $[(R,R)\text{-}^t\text{BuPhebox-Bn}]\text{IrCl}_2(\text{OAc})_2$ **217**.

We were then curious to investigate the effect of chloride to bromide exchange on the catalytic performance for the C-H insertion reaction. To this end, we reacted the *tert*-butyl isopropyl phebox complex **213** with carbon tetrabromide in methanol according to Nishiyama's protocol (Scheme 3.29).¹⁴⁸ Unfortunately, the desired bromo iridium complex **218** could not be obtained by this method. Crude ¹H NMR revealed that small amount of a new species was formed but that starting complex **213** was the main component of the reaction mixture. In addition, no new spots were observed by thin layer chromatography. We then hypothesized that the metallation could be achieved by reacting ligand **209** with iridium tribromide tetrahydrate. Indeed, this method furnished the bromo iridium(III) phebox **218** complex as a brown/orange solid in 71 % yield. The ¹H NMR and ¹³C NMR spectra were nearly identical with the corresponding chloride complex **213** and exhibited C₂-symmetry, but HRMS analysis confirmed the incorporation of bromine.



Scheme 3.29. Synthesis of $[(S,S)\text{-}^t\text{BuPhebox-}^i\text{Pr}]\text{IrBr}_2(\text{OH}_2)$ **218**.

This complex was tested in the C-H insertion reaction of methyl phenyldiazoacetate with 1,4-cyclohexadiene and the product **197** was obtained in 90 % yield with 94 % ee (Scheme 3.30). The enantioselectivity was identical to that obtained with the analogous chloro complex **213** (Table 3.1, entry 5), but the reaction required three days for complete consumption of the starting diazoacetate. Therefore, we continued our studies using catalyst **216**.



Scheme 3.30. C-H insertion of methyl phenyldiazoacetate into 1,4-cyclohexadiene using $[(S,S)\text{-}^t\text{BuPhebox-}^i\text{Pr}]\text{IrBr}_2(\text{OH}_2)$ **218**.

During the catalyst optimization studies, each reaction was run neat in 1,4-cyclohexadiene. Even though 1,4-cyclohexadiene is a relatively cheap substrate we realized that this was not practical from a synthetic standpoint. To this end, PhH , CH_2Cl_2 , and PhCF_3 were evaluated as solvents for the insertion reaction using catalyst **216**,

methyl phenyldiazoacetate and 10 equivalents 1,4-cyclohexadiene (Table 3.2). When the reaction was conducted in benzene, disappearance of methyl phenyldiazoacetate was not complete even after five days reaction time by TLC (entry 1). The major product of the reaction arose from dimerization of the carbene as observed in the crude ^1H NMR spectrum. One possibility for the lack of diazo decomposition could be from displacement of the water ligand by η^2 coordination of benzene to the iridium(III) metal center, a process which has been deemed feasible by computational analysis for similar 16 electron iridium(III) complexes.¹⁸⁵ This type of interaction was also proposed by Nishiyama in the arene C-H activation reaction described in Scheme 3.18.¹⁷⁴ This seems unlikely in our case since Nishiyama has shown that arene C-H functionalization by iridium(III) phebox complexes occurs only at elevated temperatures,^{174,177} and it remains unclear as to why benzene inhibited our reaction. Conducting the reaction in dichloromethane resulted in a 79 % yield and 91 % ee (entry 2), both of which are lower than the reaction run in neat cyclohexadiene (Table 3.1, entry 8). We found that running the reaction in trifluorotoluene preserved the enantioselectivity, furnishing **217** in 97 % ee (Table 3.2, entry 3). Decreasing the equivalents of cyclohexadiene to 2.5 and 1.1 resulted in decreased yields but the enantioselectivity remained high at 96 % and 95 %, respectively (entry 4 and entry 5). Adding an excess of the aryl diazoester could potentially increase the reaction yield, but this was not explored. For the purpose of our investigations, we examined substrate scope using the original conditions with 1,4-cyclohexadiene as solvent.

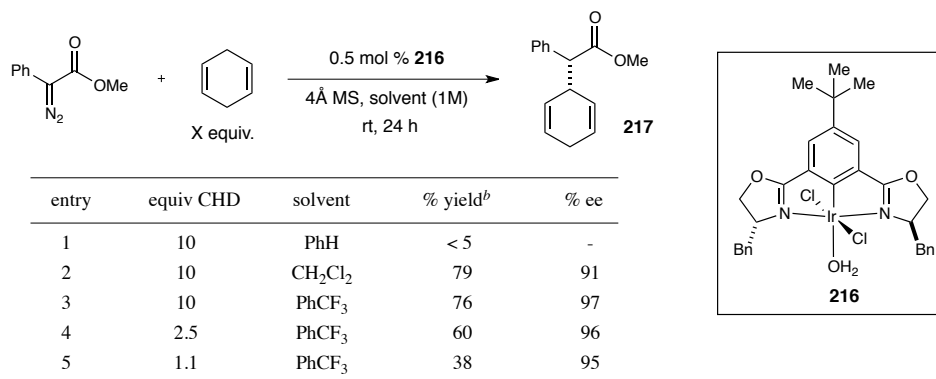
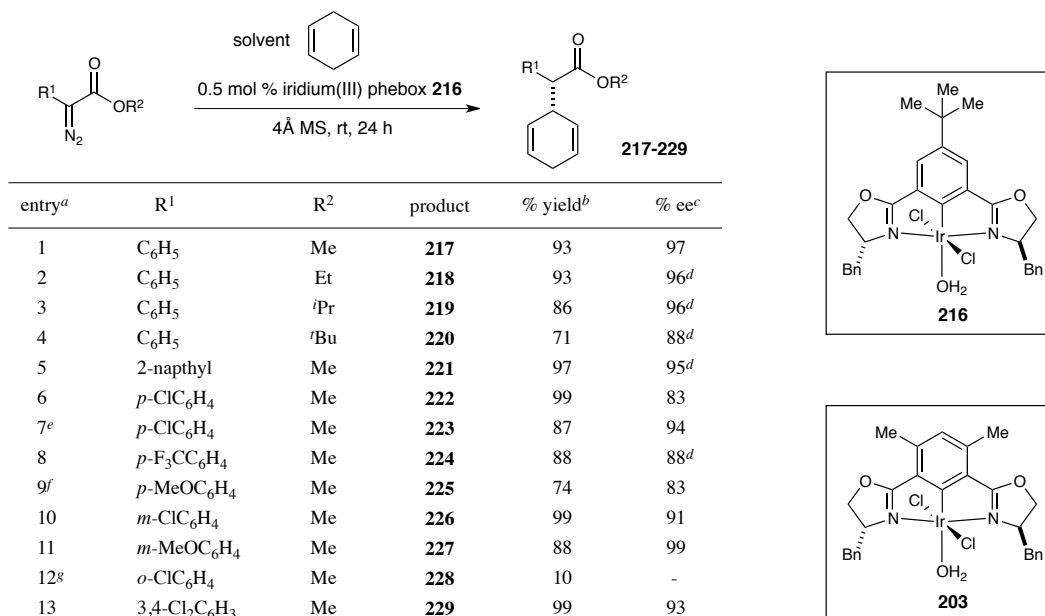


Table 3.2. The effect of solvent and 1,4-cyclohexadiene equivalents on the iridium(III) pbeox catalyzed donor/acceptor C-H insertion reaction using methyl phenyldiazoacetate.

3.4.2. Scope of aryl diazoesters for C-H insertion into cyclic 1,4 dienes.

We then examined the size of the ester on the reaction yield and enantioselectivity. Increasing the ester size on the donor/acceptor diazoester had minimal impact on the enantioselectivity of the reaction (Table 3.3, entries 1-4), which is contrast to previous observations made by Davies in Rh₂(S-DOSP)₄ catalyzed intermolecular donor/acceptor C-H insertion reactions.⁸ However, the increasing size of the ester did cause a slight drop in reaction yield. Extending the π -system on the aryl portion of the diazoester was tolerated and provided the insertion product **221** in 97 % yield and 95 % ee (entry 5). An interesting observation was made in the reactions of methyl *para*-chlorophenyldiazoacetate with catalysts **216** and **203**. With catalyst **216** (entry 6) the product was formed in nearly quantitative yield but with 83 % ee. A simple change to the analogous benzyl-substituted 4,6-dimethyl catalyst **203** dramatically improved the enantioselectivity to 94 % (entry 7). This result highlights the advantage of utilizing the

phebox ligand framework, which is readily accessible and adjustable for tailoring catalytic performance.



^a Reactions carried out on a 0.82 mmol scale. ^b Isolated yield. ^c Determined by chiral HPLC.

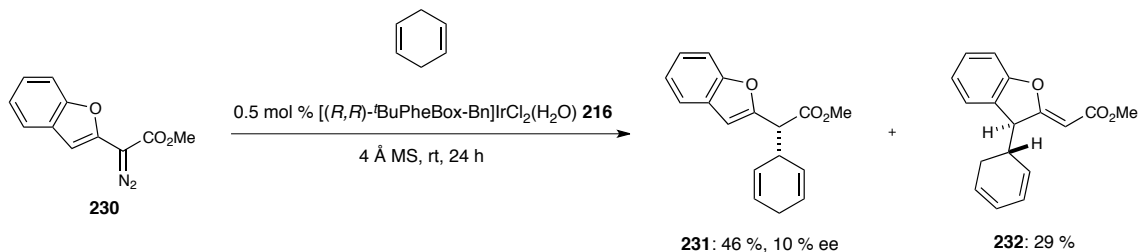
^d The absolute configuration was assigned by analogy. ^e Reaction carried out using 0.5 mol % catalyst **203**. ^f Reaction stirred for 4 days. ^g Reaction stirred for 6 days.

Table 3.3. Scope of aryl diazoesters for C-H insertion into 1,4-cyclohexadiene.

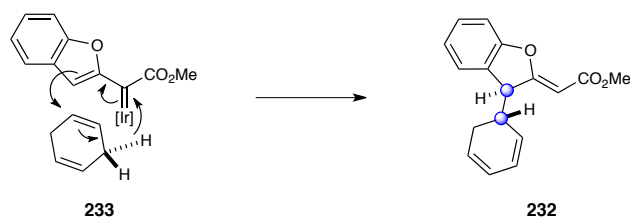
More strongly electron-withdrawing functionality is also well tolerated (entry 8), but moving to the electron-rich diazoester methyl *p*-methoxyphenyldiazoacetate slowed down the reaction tremendously, taking approximately four days for complete consumption of the diazoester (entry 9). The reaction yield and enantioselectivity remained good at 74 % and 83 % ee. The electron rich nature of the diazoester appears to generate a more stabilized metallocarbene intermediate that slows down the insertion event. This feature is currently being exploited in attempt to structurally characterize the reactive carbene intermediate and collaboration is ongoing with John Berry at the University of Wisconsin.¹⁸⁶ *Meta*-substituted aryldiazoesters also perform insertion with

high yield and enantioselectivity (entries 10 and 11), but *ortho*-substitution is detrimental to the reaction outcome as methyl *o*-chlorophenyldiazoacetate furnished only 10 % of the insertion product after six days, with the remainder of the reaction mixture consisting of unreacted diazo. Additionally, the disubstituted methyl 3,4-dichlorophenyldiazoacetate reacted to give **229** in 99 % yield and 93 % enantioselectivity (entry 13).

We were intrigued by the possibility of using heteroaryl diazoacetates for the C-H insertion reaction, as it would provide access to enantioenriched heterocyclic products. The reaction of methyl 2-benzofuranyldiazoacetate **230** with 1,4-cyclohexadiene provided the C-H insertion product **231** in 46 % yield but in only 10 % ee (Scheme 3.31). It is not clear as to why the enantioselectivity substantially suffers for this particular diazoester. The product arising from a combined C-H activation / Cope rearrangement was also obtained in 29 % yield (**232**).^{23,24} This process is well established for dirhodium-catalyzed reactions using vinyl diazoacetates, and the benzofuranyl diazoester **230** used in our chemistry strongly resembles a substrate of this type. The absolute stereochemistry at C3 of the benzofuran was not determined, but the relative stereochemistry at the chiral centers highlighted in blue is presumed to be *trans* by invoking an *s-cis*/chair-like transition state proposed by Davies for the C-H / Cope reaction of styryl diazoacetate with 1,4-cyclohexadiene (Scheme 3.32).²⁴ Unfortunately the enantiomeric excess of the C-H/Cope product **232** was unable to be determined.



Scheme 3.31. Iridium(III) phebox **216** catalyzed C-H insertion and C-H/Cope reaction of methyl 2-benzofuranyldiazoacetate **230** with 1,4-cyclohexadiene.



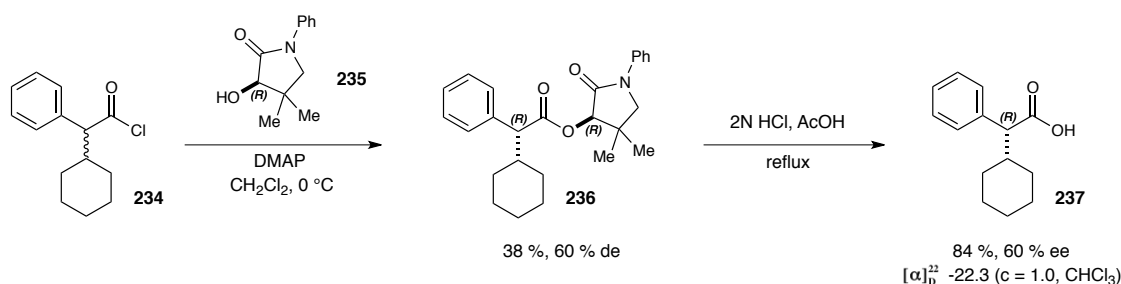
Scheme 3.32. *S-cis* transition state **233** for the C-H functionalization / Cope rearrangement reaction.

3.4.3. Confirmation of the absolute stereochemistry for iridium(III) phebox catalyzed C-H insertion of methyl phenyldiazoacetate into 1,4-cyclohexadiene.

Up to this point the absolute configuration of the insertion products obtained with catalyst **216** was assigned to be (*R*) based on the assignment made by Davies et. al.¹⁸³ Upon closer inspection however, the compound that was used to verify the configuration was not the same as the compound of known absolute configuration that was referenced. Furthermore, the optical rotation of the C-H insertion product was not included in the

report. Thus, we wanted to ensure the stereochemical configuration was correct by synthesizing the exact same derivative of which the configuration is known.

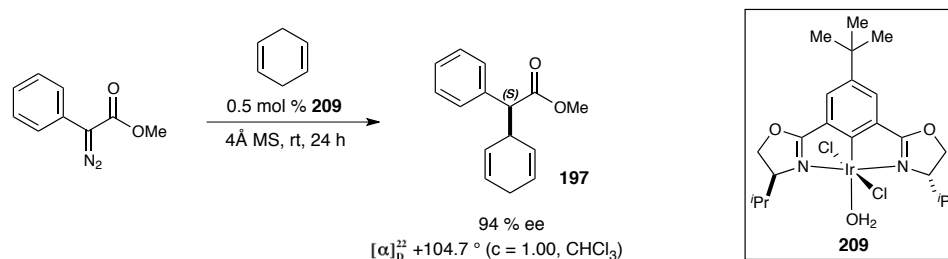
Chiral auxiliary **235**, whose absolute configuration was unambiguously determined by X-ray crystallography, was used by Camps and coworkers to resolve the racemic acyl chloride **234** (Scheme 3.33).^{187,188} The diastereomerically enriched ester **236** was then hydrolyzed to give (*R*)-cyclohexylphenylacetic acid **237** in 60 % ee, whose specific rotation was observed to be -22.3° .¹⁸⁷ In a separate report by Barlow, the stereochemistry of (*R*)-cyclohexylphenylacetic acid **237** was determined by resolution with quinine and had an enantiomeric excess of 99 % and a specific rotation of -38.8° .¹⁸⁹



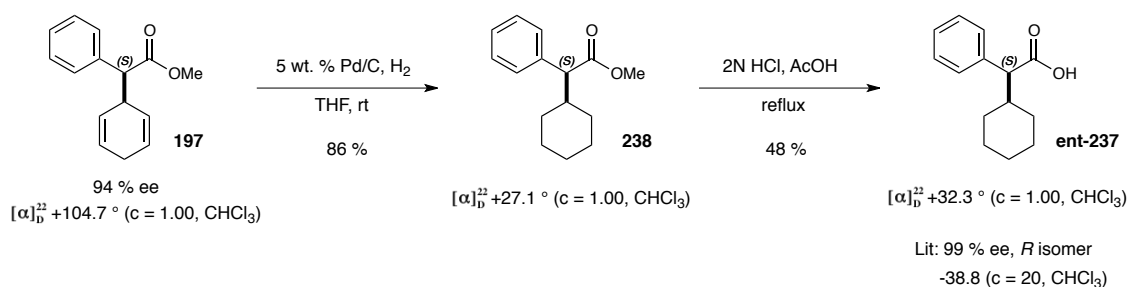
Scheme 3.33. Absolute stereochemistry determination of (*R*)-cyclohexylphenylacetic acid **237** by Camps.

In order to verify the configuration of our insertion products, enantioenriched diene **197** (obtained using iridium(III) phebox complex **209**, Scheme 3.34) was first hydrogenated using H_2 and Pd/C in THF to give cyclohexyl ester **238** in 86 % yield (Scheme 3.35). The ester was hydrolyzed using 2N HCl in refluxing acetic acid to give (*S*)-cyclohexylphenylacetic acid **ent-237** in 48 % yield. The specific rotation was determined to be $+32.3^\circ$, and its configuration was assigned to be *S* since the sign of the rotation is opposite of that obtained by Camps and Barlow. Thus, the absolute

configuration obtained in our iridium(III) phebox catalyzed C-H insertion reactions is consistent with the literature assignments.



Scheme 3.34. Iridium(III) phebox **209** catalyzed C-H insertion to form enantioenriched diene **197**.

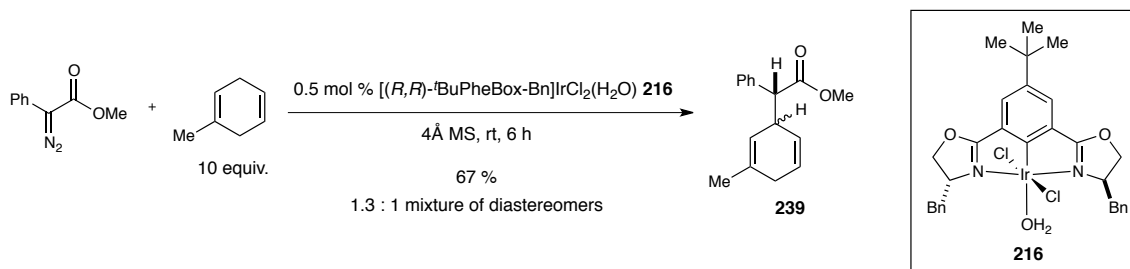


Scheme 3.35. Determination of the absolute configuration obtained in iridium(III) phebox catalyzed C-H insertion by conversion of enantioenriched diene **197** to (*S*)-cyclohexylphenylacetic acid **ent-237**.

3.4.4. C-H functionalization of substituted cyclic 1,4-dienes

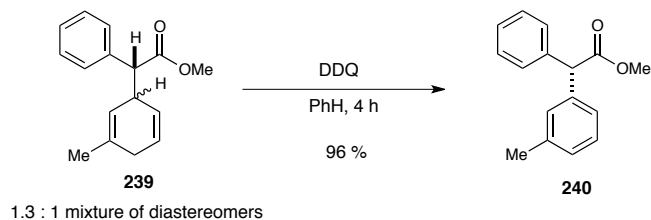
Substituted cyclic dienes were also surveyed for their reactivity in the C-H insertion reaction with catalyst **216**. The reaction of methyl phenyldiazoacetate with 1-methyl-1,4-cyclohexadiene in trifluorotoluene at room temperature went to completion in 6 hours, and a 1.3:1.0 inseparable mixture of diastereomers was obtained upon

isolation of **239** in 67 % yield (Scheme 3.36). This indicates that the catalyst imparts very little influence on the facial approach of the diene substrate. Similar to the insertion with 1,4-cyclohexadiene, neither the cyclopropane nor dimer was detected. Additionally, the insertion was completely regioselective for insertion into the bis-allylic C-3 methylene position.



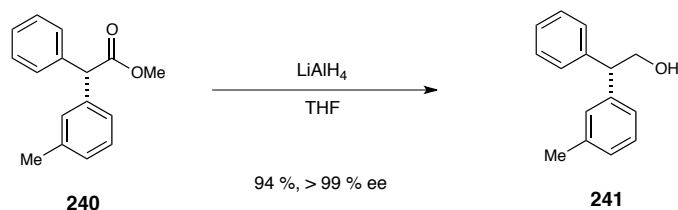
Scheme 3.36. Iridium(III) phebox **216** catalyzed C-H insertion of methyl phenyldiazoacetate into 1-methyl-1,4-cyclohexadiene.

The enantiopurity for each diastereomer in the mixture was unable to be assessed by HPLC, and in an effort to eliminate the complication imparted by the diastereomeric mixture the compound was subjected to DDQ oxidation. The oxidation proceeded in 96 % yield from diene **239** to provide the α, α' -biaryl acetate **240** in 64 % yield over the two step sequence (Scheme 3.37). This protocol is highly efficient for the preparation of enantioenriched biaryl esters, which are difficult to synthesize by state of the art procedures.^{190,191}



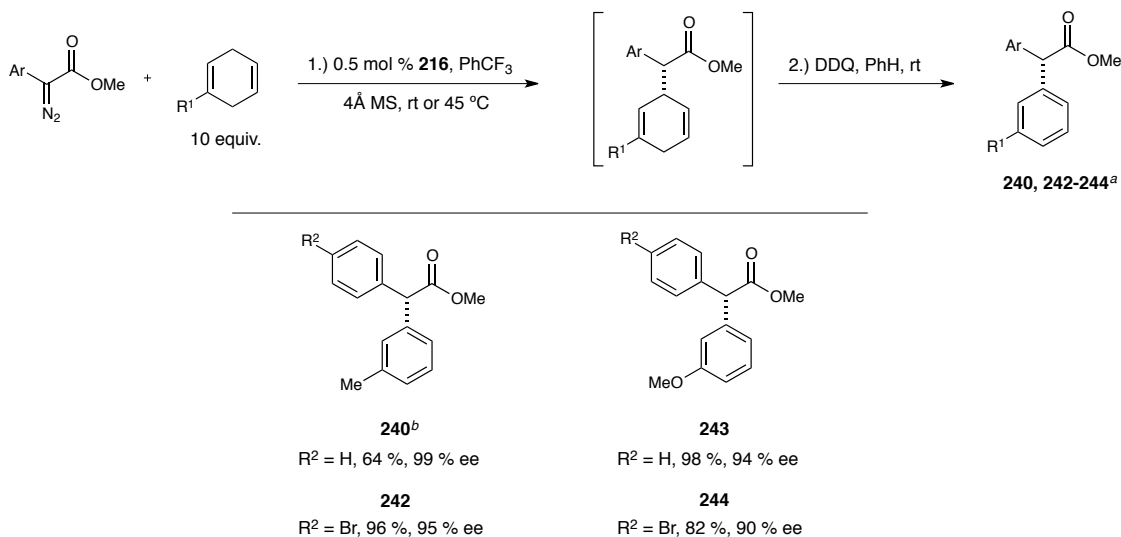
Scheme 3.37. DDQ oxidation of **239**.

The enantiomeric excess of **240** still could not be determined, therefore compound **240** was reduced to the corresponding alcohol **241** in 94 % yield using lithium aluminum hydride (Scheme 3.38). Analysis by HPLC was then successful and indicated an enantiomeric excess of > 99 % for **241**.



Scheme 3.38. LiAlH₄ reduction of ester **240** to alcohol **241** for determination of enantiomeric excess.

The scope of diazoesters and other substituted 1,4-cyclic dienes was further investigated (Scheme 3.39). C-H insertion of methyl *p*-bromophenyldiazoacetate into 1-methyl-1,4-cyclohexadiene followed by DDQ oxidation provided **242** in 96 % yield and 95 % enantioselectivity over the two step protocol. The C-H insertion reaction using this particular diazoester and diene required 17 hours for completion and also resulted in an inseparable 1.3:1.0 diastereomeric mixture as determined by crude ¹H NMR. The C-H insertion reactions into freshly prepared 1-methoxy-1,4-cyclohexadiene¹⁹² proceeded quickly in only 2 hours for each diazoester, presumably due to the increased electron-rich nature at the C-3 methylene site. Additionally, the reactions were completely chemoselective for C-H insertion even in the presence of the highly electron rich olefin. After oxidation the biaryl acetates were obtained in high yields and enantioselectivities (**243** = 98 %, 94 % ee; **244** = 82 %, 90 % ee).



^a Percent yields and enantioselectivities shown are of the isolated products after DDQ oxidation. ^b The enantiopurity was determined after reduction of the ester intermediate **239** to the corresponding alcohol.

Scheme 3.39. Enantioselective C-H insertion of aryl diazoacetates into 1-substituted 1,4-cyclic dienes (the dr of the crude insertion products of **243** and **244** was 1.1:1 and 4.3:1, respectively).

We further confirmed the facial selectivity of the insertion/oxidation reaction to form ent-**243** by oxidizing enantioenriched product **227** (Table 3.3, entry 11) with DDQ. If the selectivity was consistent then the opposite configuration was expected. Indeed, the product obtained after oxidation was formed in 96 % ee with an optical rotation of -12.9° (ent-**243**, Figure 3.5). The product obtained for the insertion into the substituted cyclohexadiene and oxidation gave an optical rotation of $+10.4^\circ$ at 94 % ee. This result is consistent with the observed selectivity and was further confirmed by HPLC analysis.

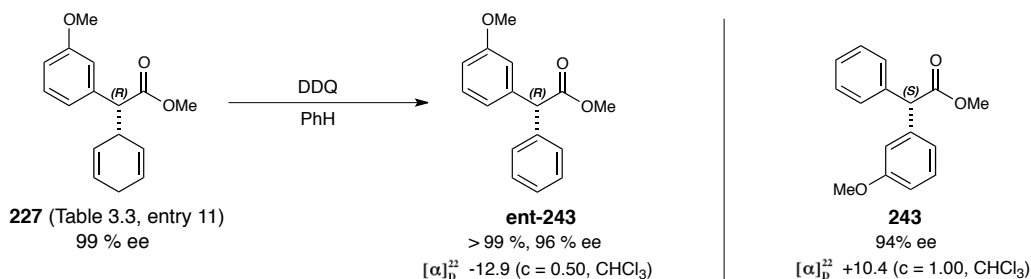


Figure 3.5. Confirmation of predicted facial selectivity for insertion into 1-methoxy-1,4-cyclohexadiene.

The insertion reactions into the slightly less activated allylic/benzylic methylene C-H bonds of 1,4-dihydronaphthalene required some optimization. When the reaction was run at room temperature with slow addition (42 h) of methyl *p*-bromophenyldiazoacetate, consumption of the diazoester was not complete even after 5 days (condition A, Figure 3.6). The crude insertion product was nonetheless isolated (dr not determined), and after DDQ oxidation the biaryl ester **245** was obtained in 27 % yield and 96 % ee. When the temperature was raised to 45 °C, the diazoester was completely consumed after 2 days, and after oxidation provided an increased yield of **245** in 52 % yield albeit with a drop in enantioselectivity to 88 % (condition B, Figure 3.6). Dimerization of the carbene was a major byproduct of the reaction in each case and efforts to further increase the yield and/or enantioselectivity for this substrate were not pursued. Condition B was then used for the insertion of methyl phenyldiazoacetate into 1,4-dihydronaphthalene, and compound **246** was obtained in 53 % yield with 95 % enantiomeric excess (8:1 crude dr). These benchmarking reactions using donor/acceptor diazoester provided proof of principle that these iridium phebox catalysts are capable of performing highly enantioselective atom transfer reactions.

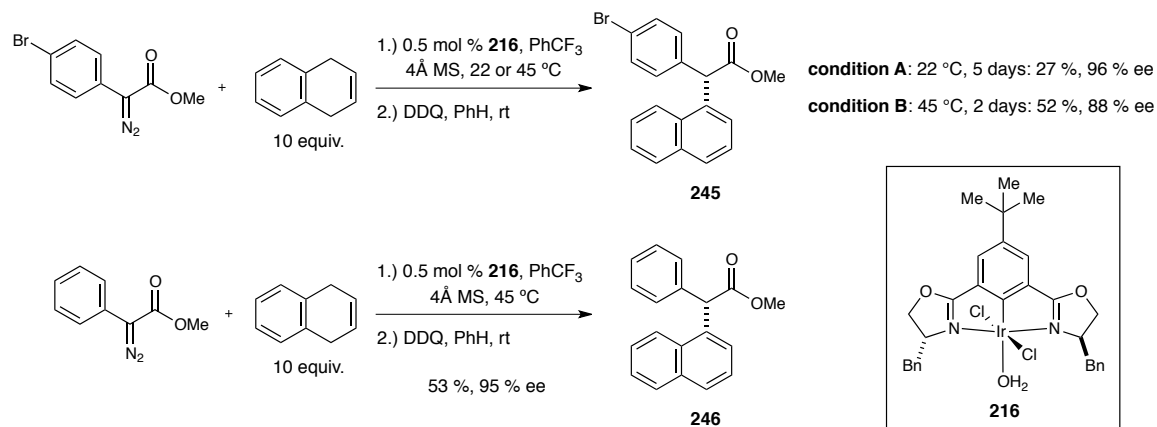
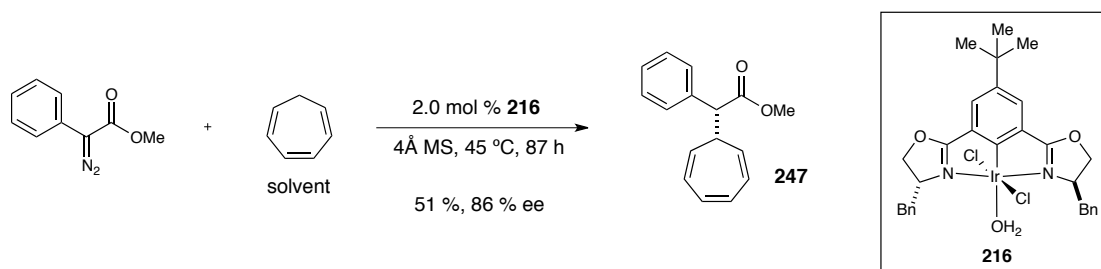


Figure 3.6. C-H insertion into 1,4-dihydronaphthalene.

3.4.4. Iridium(III) phebox catalyzed C-H insertion into 1,3,5-cycloheptatriene

We then wanted to further test the reactivity of the iridium(III) catalyzed donor/acceptor C-H insertion by examining the substrate scope past cyclohexadienes. 1,3,5-cycloheptatriene was expected to be an exceptionally reactive substrate towards C-H insertion since the buildup of partial positive charge at the methylene site would be stabilized by homoaromaticity. In fact, enantioselective C-H functionalization of cycloheptatriene has been accomplished using dirhodium(II) tetracarboxylate catalysts at -50 °C in up to 95 % ee.¹⁹³ Reacting 0.5 mol % iridium(III) phebox complex **216** with 10 equivalents cycloheptatriene and methyl phenyl diazoacetate in PhCF₃ at room temperature resulted in minimal decomposition of the diazoester even after 1 week. After some optimization of the reaction conditions, it was found that slow addition of methyl phenyl diazoacetate as a solution in cycloheptatriene over the course of 72 hours to a 45 °C mixture of 2.0 mol % iridium phebox complex **216** and 4Å MS led to a 51 % yield of the cycloheptatriene insertion product **247** with 86 % enantioselectivity (Scheme 3.40).

Lower reaction temperatures led to poor reaction yields (< 25 %), and running the reaction without slow addition of the diazoester led to significant carbene dimerization.

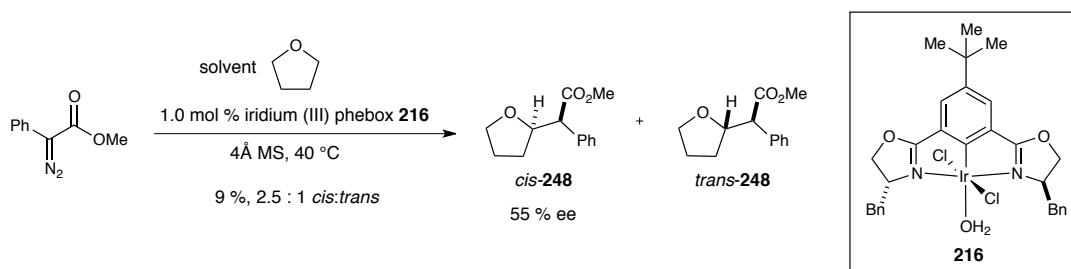


Scheme 3.40. Iridium(III) phebox catalyzed enantioselective C-H insertion of methyl phenyldiazoacetate into cycloheptatriene.

3.4.5. Iridium(III) phebox catalyzed C-H insertion into tetrahydrofuran

As discussed in Chapter 2, Katsuki showed that iridium(III) salen complexes are efficient catalysts for highly diastereo- and enantioselective C-H insertion of aryl and alkyl diazoesters into tetrahydrofuran.¹⁰² Specifically, the C-H insertion of methyl phenyl diazoacetate into THF proceeded in 75 % yield, 13 : 1 dr, and 95 % ee (cf. Chapter 2, Scheme 2.7). To evaluate our catalysts for C-H insertion into substrates other than cyclic dienes, we added 1 mol % iridium phebox complex **216** to a mixture of methyl phenyldiazoacetate and 4 Å MS in THF at room temperature. The diazoester was consumed within three hours, but carbene dimerization was the sole product of the reaction. In an attempt to circumvent this problem we added a solution of methyl phenyldiazoacetate in THF over six hours to a 40 °C mixture of 1 mol % iridium(III) phebox complex **216** and 4 Å MS in THF (Scheme 3.41). Crude ¹H NMR analysis revealed a 2.5 : 1 mixture of *cis*-**248** and *trans*-**248**, and dimerization of the carbene was a

significant side product. The major isomer *cis*-**248** was isolated in only 9 % yield and 55 % enantiomeric excess.¹⁹⁴ This result suggests that the iridium phebox donor/acceptor carbene is less reactive towards substrates containing C-H bonds that are not as activated towards insertion as cyclic 1,4 dienes.

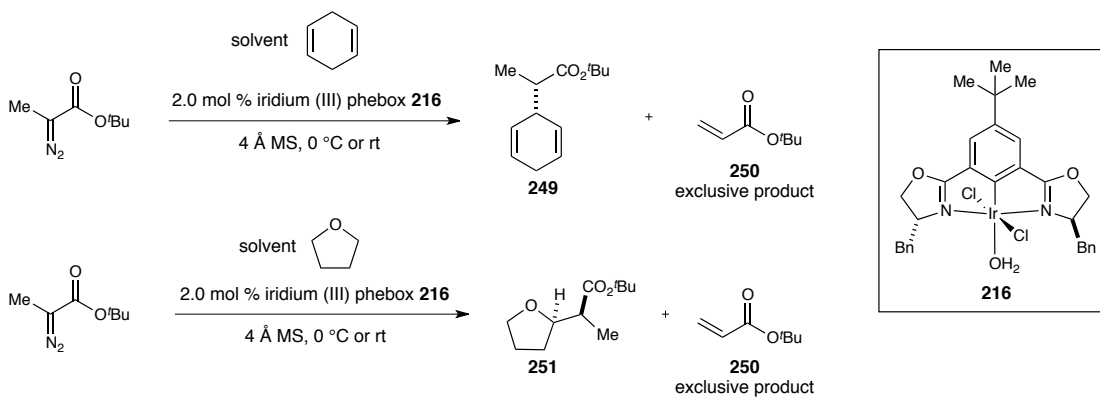


Scheme 3.41. Iridium(III) phebox **216** catalyzed C-H insertion of methyl phenyldiazoacetate into tetrahydrofuran

3.4.6. Reactions of iridium(III) phebox complexes with alpha-alkyl diazoesters

The ultimate goal for our research was to expand the catalysts and reagents available for enantioselective atom transfer reactions. The development of iridium(III) salen catalysts by Katsuki led to a major advance in that alpha alkyl diazoesters became viable carbene precursors for enantioselective intermolecular C-H functionalization.¹⁰² They hypothesized that it was the sterically encumbered nature of the salen framework that prevented the undesired β -elimination side reaction from occurring. However, there were no mechanistic studies conducted to support or refute their theory. To probe the effectiveness of our iridium(III) complexes for C-H insertion using alkyl diazoesters, both 1,4-cyclohexadiene and THF were chosen as substrates for the reaction of methyl *tert*-butyldiazoacetate with iridium(III) phebox complex **216**. A solution of the diazoester

in either 1,4-cyclohexadiene or THF substrate was added over 1 hour to a stirring mixture of iridium complex **216** and 4 Å MS in the corresponding substrate as solvent. In all cases, the diazoester was consumed immediately upon addition, but C-H insertion was never observed and β -elimination product **250** was formed exclusively (Scheme 3.42).



Scheme 3.42. Attempted iridium phebox catalyzed C-H insertion using methyl *tert*-butyldiazoacetate.

3.4.7. Evaluation of non-ester donor/acceptor carbene precursors for iridium(III) phebox catalyzed C-H functionalization of 1,4-cyclohexadiene.

The ester functional group is by far the most widely used acceptor group in metallocarbene atom transfer chemistry.^{3,5} As described in Chapter 2, Rh₂(DOSP)₄ is an exceptionally effective catalyst for these carbene precursors. However, acceptor groups other than methyl esters are not suitable substrates for this catalyst. When phenyl diazoacetone was investigated for its reactivity in cyclopropanation of styrenes using 2 mol % Rh₂(*S*-DOSP)₄ **5**, good yield (93 %) and excellent diastereoselectivity (> 95:5) were obtained for cyclopropane **252** in refluxing DMB, but enantioselectivity was

negligible (< 5 %) (Table 3.4, entry 1). In contrast, using 2 mol % $\text{Rh}_2(\text{S-PTAD})_4$ **253** as catalyst resulted in highly diastereo- and enantioselective cyclopropanation and furnished cyclopropane **252** in 92 % yield, > 95:5 dr, and 85 % ee (entry 2). Davies and coworkers also showed that $\text{Rh}_2(\text{S-PTAD})_4$ is an effective intermolecular cyclopropanation catalyst using phosphonate,¹⁹⁵ nitrile,¹⁹⁶ and trifluoromethyl¹⁹⁷ acceptor groups.

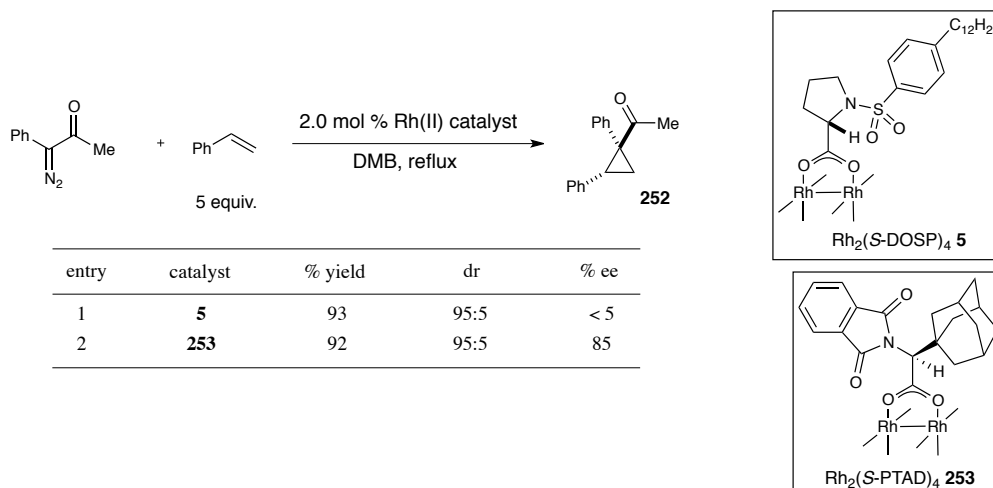


Table 3.4. $\text{Rh}_2(\text{S-DOSP})_4$ and $\text{Rh}_2(\text{S-PTAD})_4$ catalyzed cyclopropanation using phenyl diazoacetone.

It would be advantageous if the same catalyst could be used in enantioselective intermolecular C-H insertion for a range of acceptor groups on the donor/acceptor carbene. To this end, we investigated the performance of iridium(III) phebox complex **216** in asymmetric C-H insertion of diazoketones into 1,4-cyclohexadiene. One mol % iridium(III) phebox complex **216** was added in a single portion to a stirring mixture of 4 Å MS and phenyl diazoacetophenone in 1,4-cyclohexadiene at room temperature. After stirring 44 hours the mixture was filtered and analyzed by ^1H NMR, which revealed a 2.5:1 mixture of C-H insertion product **254A** to cyclopropane **255A**. Purification by

column chromatography furnished **254A** in 32 % yield but only 6 % ee (Table 3.5, entry 1). When the phenyl substituent on the ketone was replaced with a propyl group trace amounts of the cyclopropane **255B** were observed by crude ^1H NMR analysis. In this case, the insertion product **254B** was formed in only 17 % yield and 22 % ee (entry 2). These experiments indicate that the iridium(III) phebox complex **216** is not as effective when aryl diazoketones are used compared to using aryl diazoesters.

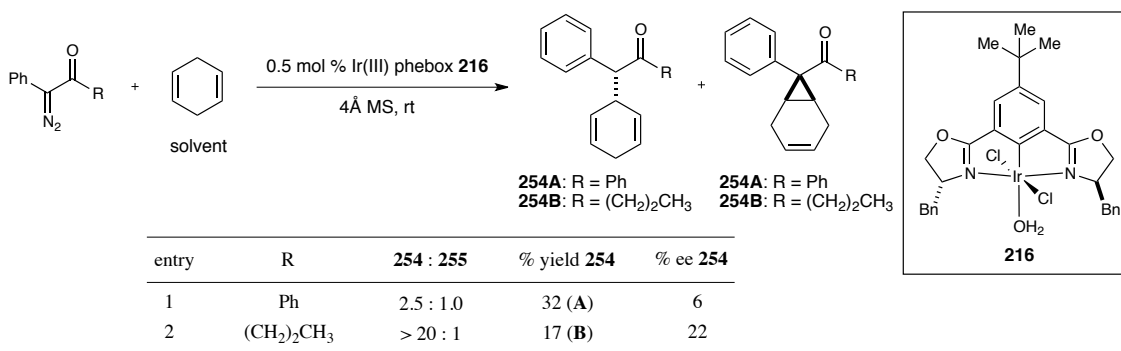
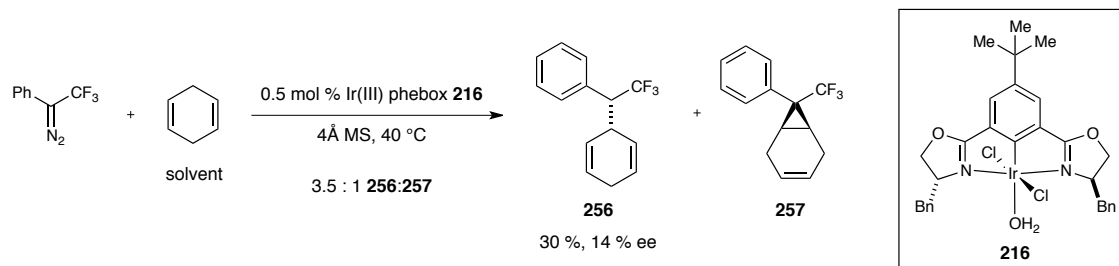


Table 3.5. Iridium(III) phebox **216** catalyzed C-H insertion of diazoketones into 1,4-cyclohexadiene.

We also investigated the reaction of trifluoromethyl phenyldiazomethane and 1,4-cyclohexadiene with iridium phebox complex **216** at 40 °C, but unfortunately the reaction furnished a 3.5:1 mixture of C-H insertion adduct **256** with cyclopropane **257**. The C-H insertion product **256** was obtained in 30 % yield with only 14 % enantiomeric excess (Scheme 3.43).



Scheme 3.43. Iridium phebox catalyzed C-H insertion of trifluoromethyl phenyldiazomethane into 1,4-cyclohexadiene.

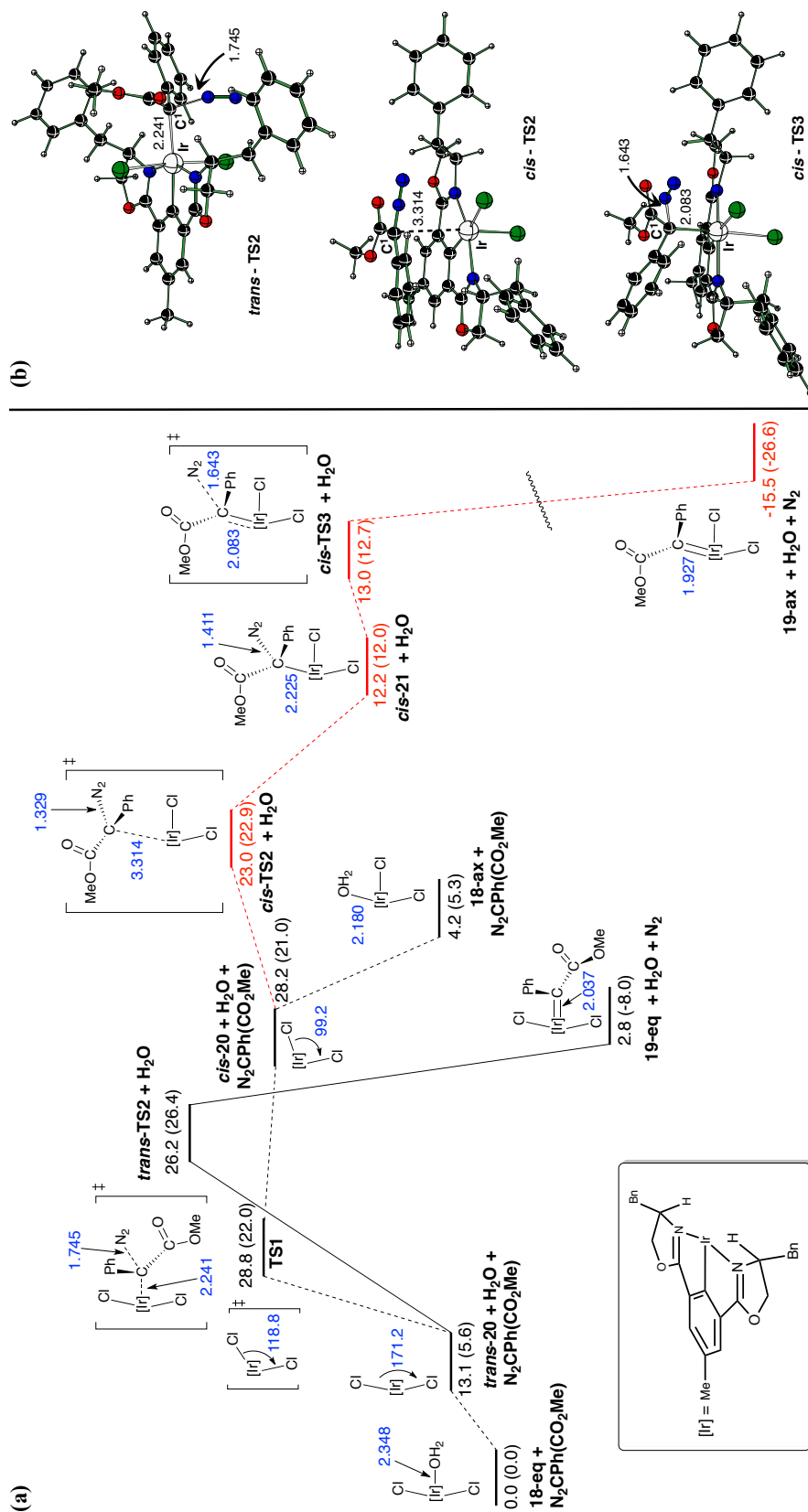
3.5 Computational Studies for Iridium(III) Phebox Catalyzed Donor/Acceptor C-H Insertion into 1,4-cyclohexadiene.

It became apparent that the donor/acceptor carbenes generated by our iridium phebox catalysts were less general in terms of substrate scope for C-H functionalization compared with the dirhodium(II) tetracarboxylate, iridium(III) salen, and iridium(III) porphyrin catalyst systems. Our insertion reactions into 1,4-cyclohexadiene proceeded under considerably milder conditions in that most reactions proceeded at room temperature without the need for slow addition of the diazoester, except in the reactions with less activated substrates such as 1,4-dihydronaphthalene and cycloheptatriene. There is little known about the reasons why iridium catalysts are offering unique reactivity, and in order to better understand iridium in carbene transfer reactions with the objective of achieving new synthetic methods we needed more information regarding the reactive iridium(III) phebox carbene intermediate. We were unable to characterize the iridium carbene during our experimental studies, so we initiated collaboration with Dr. Jamal Musaev at Emory University to help us computationally evaluate the structure and stability of this reactive intermediate, as well as gain insight into its mechanism of formation. The DFT calculations described below were performed by Dr. Jamal Musaev, Dr. Vyacheslav Boyarskikh, and Dr. Adrian Varela-Alvarez and communicated in our initial description of this chemistry.¹⁸⁰

3.5.1 DFT Analysis of the reactive carbene intermediate.

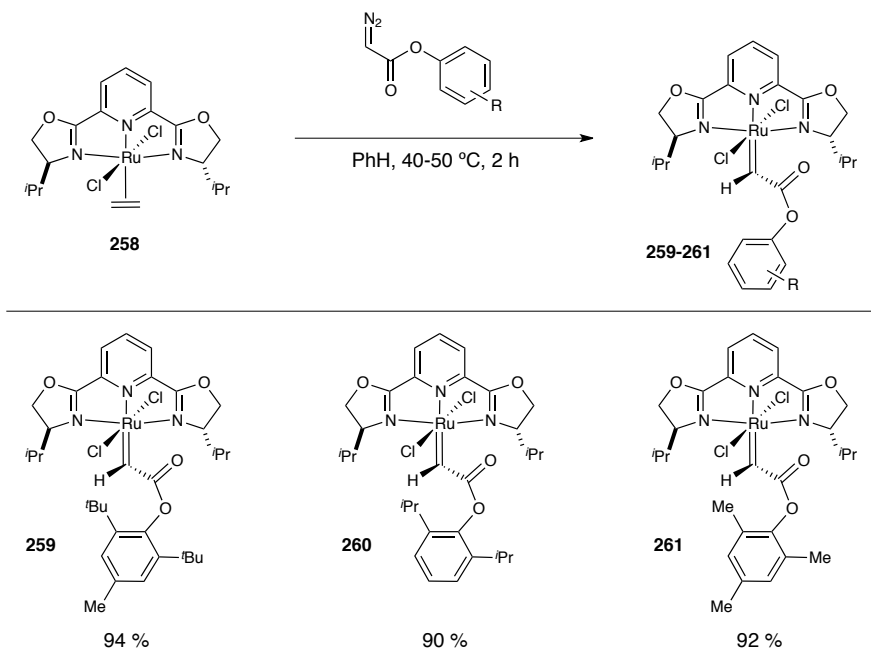
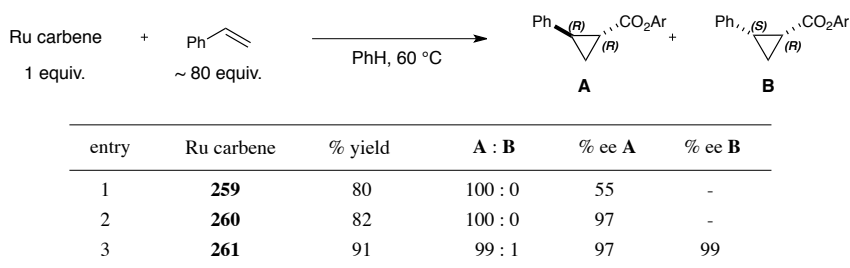
In these calculations the CPCM-M06L/BS1 level of theory was used to evaluate the lowest energy reaction pathway for iridium carbene formation (Figure 3.7).¹⁹⁸ The calculations were simplified using a modified version of catalyst **216**, where a methyl group replaced the 4-*tert*-butyl substituent. The energies of each intermediate and transition state are shown as both gas-phase enthalpies and Gibbs free energy in dichloromethane solution. The Gibbs free energies are in parentheses and are the ones discussed in the text. The resting state of the catalyst is shown as **18-eq**, and the energy zero is fixed to include methyl phenyldiazoacetate [N₂CPh(CO₂Me)]. The initial step of the reaction pathway was found to be dissociation of the equatorially bound water ligand with a barrier of 5.6 kcal/mol¹ to form the 16-electron intermediate **trans-20**. (In this context the term equatorial denotes coordination *trans* to the phenyl anion.) Upon water dissociation, two separate reaction pathways were found. The first involves initial coordination of the diazoester substrate with an energy barrier of 26.4 kcal mol⁻¹ to form **trans-TS2**. From this transition state, nitrogen gas extrusion is exergonic by 8.0 kcal mol⁻¹ relative to **18-eq**, and the equatorially bound carbene intermediate **19-eq** is formed. A second reaction pathway was found in which a chloride ligand in 16-electron intermediate **trans-20** could further isomerize to give **TS1** with an energy barrier of 16.4 kcal·mol⁻¹ relative to **trans-20**. From this transition state, the water ligand can again coordinate to the iridium metal center in the axial position *via* intermediate **cis-20** and form the axial aqua complex **18-ax** of the precatalyst **18-eq** (the term axial is used to denote coordination perpendicular to the plane of the phenyl carbanion). This axial aqua

Figure 3.7. Free energy profile for the formation of the axial and equatorial carbenes.



complex **18-ax** was found to be only $5.3 \text{ kcal}\cdot\text{mol}^{-1}$ less stable than the isolable equatorial **18-eq** species, which indicates that both isomers of the precatalysts are in equilibrium under the reaction conditions. This in turn means that isomers *trans*-**20** and *cis*-**20** are both accessible during the reaction. However, the diazoester substrate can begin to precoordinate with the iridium metal center before water re-coordination can occur, and this process has essentially no energy barrier at $1.9 \text{ kcal}\cdot\text{mol}^{-1}$ with respect to *cis*-**20**. Coordination of the diazoester follows and is exergonic by $11 \text{ kcal}\cdot\text{mol}^{-1}$. Then, an incredibly low nitrogen extrusion barrier of $0.7 \text{ kcal}\cdot\text{mol}^{-1}$ (*cis*-**TS3**) gives rise to the axial carbene **19-ax**. This axial carbene is thermodynamically more stable than the equatorially bound carbene **19-eq** by $18.6 \text{ kcal}\cdot\text{mol}^{-1}$.

Such a drastic energy difference between these two isomers and the preference for axial carbene formation was completely unexpected for multiple reasons. First, the stereochemical models used to predict olefin cyclopropanation by ruthenium(II) pybox catalysts with ethyl diazoacetate have always invoked an equatorially bound carbene intermediate. This notion was likely initiated by studies from Nishiyama in which air and moisture stable acceptor-only carbenes **259-261** were prepared in excellent yields by reacting ruthenium pybox **258** with 2,6-di-*tert*-butyl-4-methylphenyl diazoacetate, 2,6-diisopropylphenyl diazoacetate, and 2,4,6-trimethylphenyl diazoacetate (Table 3.6).¹⁹⁹

**Table 3.6.** Synthesis of ruthenium(II) pybox carbenes **259-261** by Nishiyama.**Table 3.7.** Cyclopropanation of styrene with ruthenium pybox carbenes **259-261**.

These carbene complexes were found to perform enantio- and diastereoselective cyclopropanation of styrene with very high yields and selectivities (Table 3.7). In fact, these values were identical to reactions that were performed with the standard ruthenium ethylene pybox catalyst **258** using the same carbene precursors, which strongly suggests that the equatorial carbene may be responsible for the stereoselectivity in the reaction. Density functional theory studies have also been conducted and are in solid agreement

with Nishiyama's proposed transition state and the experimental outcome, and the computation-derived model is depicted in Figure 3.8.²⁰⁰ It must also be noted that similar transition states have been proposed for the analogous copper pybox catalyzed cyclopropanation reactions.²⁰¹

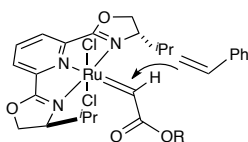
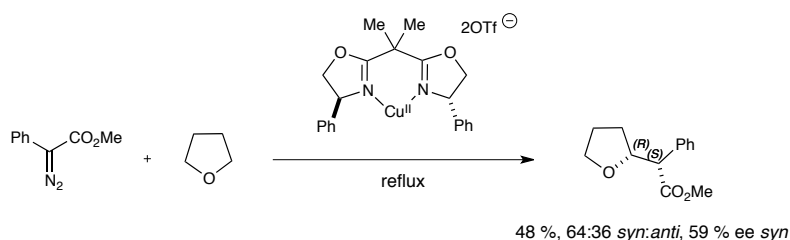


Figure 3.8. Predictive model for ruthenium pybox catalyzed cyclopropanation.

In addition, the Fraile group has reported that bidentate copper bisoxazoline complexes catalyze the intermolecular C-H insertion of donor/acceptor carbenes into cyclic ethers with moderate enantioselectivity (Scheme 3.44),^{202,203} and a computational study was carried out to probe the stereochemical outcome of the transformation.²⁰⁴ The transition state that was located for the insertion into the C-H bond alpha to oxygen in THF involves equatorial copper carbene formation and correctly predicts the observed major product of the reaction (Figure 3.9).



Scheme 3.44. Calculated transition state for copper bisoxazoline catalyzed C-H insertion of methyl phenyldiazoacetate into tetrahydrofuran.

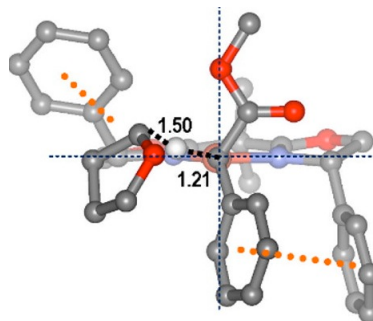


Figure 3.9. Calculated transition state for copper bisoxazoline catalyzed C-H insertion into THF.²⁰⁴

Despite the agreement between the stereochemical outcomes of both the cyclopropanation and C-H insertion reactions described above with their computed models and transition states, it remains unclear if the corresponding axial carbene geometries were considered for any of the ruthenium or copper reactive intermediates. In our case, the axial iridium carbene intermediate derived from methyl phenyldiazoacetate was found to be thermodynamically more stable by 18.6 kcal mol⁻¹. These data strongly suggest that an axial carbene intermediate should not be ruled out when designing pincer complexes for atom transfer reactions. This increased stability of the axial iridium carbene can be explained by the strong *trans* effect of the phenyl carbanion on the pincer ligand (Figure 3.10). When the carbene is equatorially bound, there is less σ -donation from the carbenic carbon and consequentially less *d*-electron overlapping, or back-donation, relative to the axial iridium carbene. This results in a longer Ir-C_{carbene} bond distance (2.037 Å calculated) relative to the axially bound carbene complex, which is calculated to be 1.927 Å. This calculated Ir-C_{carbene} bond distance is in strong agreement with the Ir-C_{carbene} bond distance obtained from the X-ray structure of

iridium(III) phebox complex **216** (1.924 Å, cf. Figure 3.4). The increased stability for **19-ax** is consistent with the shorter bond length.

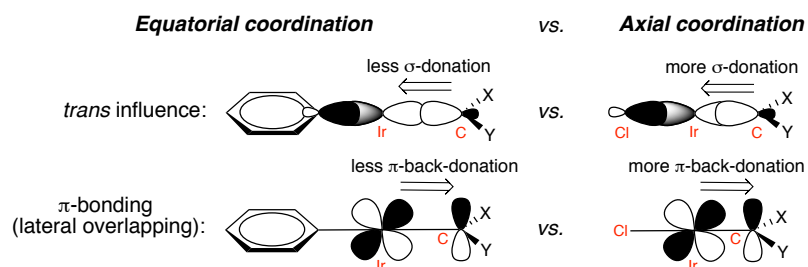


Figure 3.10. Relative stabilities of the axial and equatorial carbene intermediates as explained by the *trans* effect of the phenyl anion.

To probe the transition state of the C-H insertion reaction into 1,4-cyclohexadiene, a conformational analysis of the resultant axial carbene was performed (Figure 3.11). From the most stable axial carbene conformer **19-ax**, we were able to develop a model for predicting the observed selectivity for C-H insertion into 1,4-cyclohexadiene reaction using iridium(III) phebox complexes (Figure 3.12). Inspection of the calculated structure clearly enables one to envision the approach of cyclohexadiene from the *Re* face of the metallocarbene since the *Si* face is blocked by the benzyl substituent on the oxazoline ring of the complex. This facial trajectory leads to the (*R*) enantiomer of the C-H insertion product **217**.

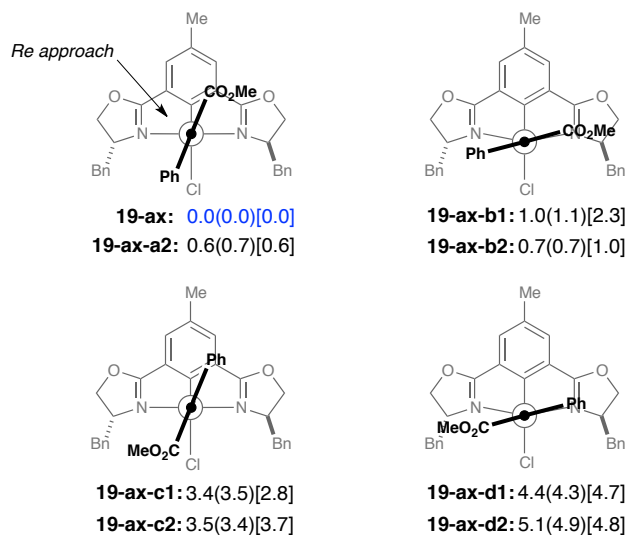


Figure 3.11. Conformational analysis of the potential isomers of the axial carbene. The $\Delta E(\Delta H)[\Delta G]$ values are in kcal mol⁻¹ and are relative to **19-ax**. The two sets of values under each conformer were obtained by rotation around the C_{carbene}-CO₂Me bond.

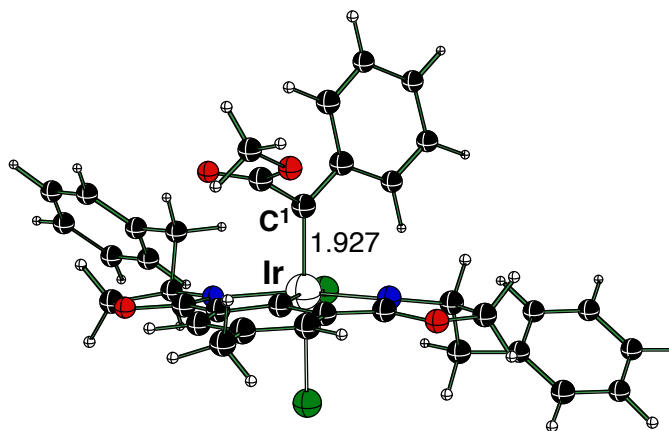
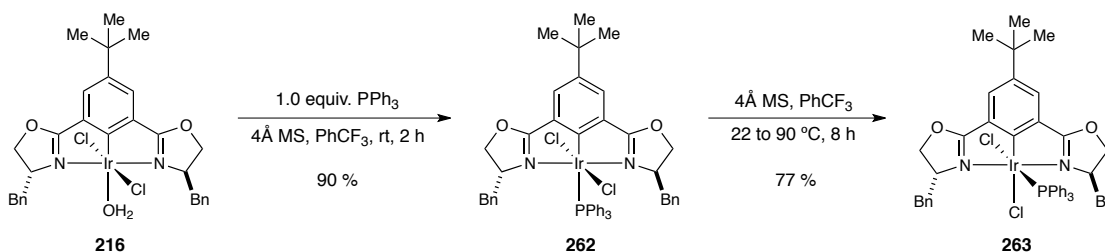


Figure 3.12. The predictive model for stereoinduction for the iridium phebox catalyzed C-H insertion reaction of methyl phenyldiazoacetate into 1,4-cyclohexadiene.

3.5.3 Attempts to experimentally validate the computation

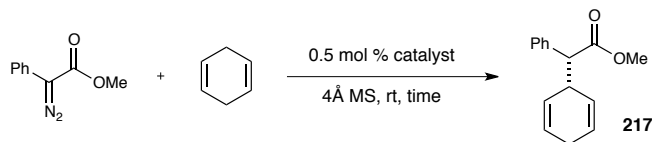
At this stage we wanted to experimentally support the predicted carbene geometry. As we could not obtain the axial iridium aqua complex, we hypothesized that synthesizing the equatorial triphenylphosphine complex and its axial analog would allow us to gain information regarding the geometry of the reactive intermediate. To do this, iridium phebox complex **216** was treated with 1 equivalent PPh₃ in the presence of molecular sieves at room temperature *via* a modified literature procedure²⁰⁵ and the equatorial triphenylphosphine complex **262** was obtained in 90 % yield (Scheme 3.45). The corresponding thermodynamically more stable axial triphenylphosphine complex **263** was synthesized in 77 % yield by thermal isomerization at 90 °C. The ¹H NMR indicated a loss of C₂-symmetry. These complexes were yellow in appearance, were purified by silica gel column chromatography, and stable to air and moisture.



Scheme 3.45. Synthesis of the equatorial and axial triphenylphosphine complexes **262** and **263**.

Their performance in the C-H insertion of methyl phenyldiazoacetate into 1,4-cyclohexadiene was evaluated by subjecting each catalyst to identical reaction conditions to those reported during our initial studies with the iridium aqua complexes.

For the equatorial (*trans*) triphenylphosphine complex **262** a 91 % yield and 98 % enantiomeric excess of product **217** was obtained after 44 hours (Table 3.8, entry 1). When this catalyst was added, the reaction mixture more slowly turned to the dark green color when compared to the reactions with the iridium phebox aqua complexes. For the axial (*cis*) triphenylphosphine complex **263**, decomposition of the diazoester was incredibly slow and the reaction did not go to completion after 1 week at room temperature (entry 2). Throughout this reaction the yellow color was preserved, unlike the reaction with the equatorially bound PPh₃ ligand. The crude reaction mixture was analyzed by ¹H NMR spectroscopy and a 1 : 0.6 : 0.1 ratio of insertion product **217** : methyl phenyldiazoacetate : dimer was detected. The lack of dark green color suggests that the carbene concentration is much lower than with the equatorial complex. The isolated yield of the insertion product **217** was not obtained since it overlapped with the unreacted methyl phenyldiazoacetate on TLC. However, analysis of the crude mixture by chiral HPLC indicated an enantiomeric excess of 89 %. The difference in enantioselectivity between the two catalysts does not support nor refute the calculated axial carbene intermediate. Assuming that the same reactive carbene isomer is accessible from either precatalyst under the reaction conditions, then identical enantioselectivities should be obtained (within error). Unfortunately this was not the case, and we have yet to experimentally or computationally investigate this. We are currently collaborating with Dr. John Berry at the University of Wisconsin to structurally characterize the intermediate responsible for the high enantioselectivity in this reaction, and their preliminary results are discussed in Section 3.5.



entry	catalyst	time (h)	% yield	% ee
1	262	44	91	98
2	263	173	ND	89

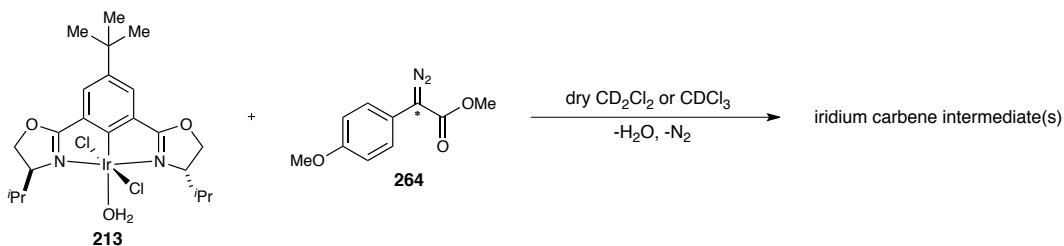
Table 3.8. C-H insertion of methyl phenyldiazoacetate into 1,4-cyclohexadiene using triphenylphosphine complexes **262** and **263**.

3.5 Structural Studies Performed by the Berry Group

3.5.1. Introduction

The Berry group undertook the challenge of characterizing and/or isolating the reactive iridium carbene intermediate to see if the axial or equatorial carbene was responsible for the high enantioselectivity observed in our reactions. All of the results described in this section are currently unpublished and used by permission from Dr. John Berry. We observed that the iridium(III) phebox **216** catalyzed C-H insertion reaction of methyl *p*-methoxyphenyldiazoacetate with 1,4-cyclohexadiene was very slow, taking four days to go to completion (Table 3.3, entry 9). We envisaged that this slow reaction time could be used to our advantage in that it could potentially allow for the iridium carbene intermediate to be isolated. Therefore, the reaction of ¹³C labeled methyl *p*-methoxyphenyldiazoacetate **264** with iridium(III) phebox complex **213** in dry CD₂Cl₂ or CDCl₃ was used for our studies (Scheme 3.46). The site of ¹³C labeling is denoted with an asterisk. The isopropyl-substituted iridium complex **213** was used

instead of the benzyl-substituted iridium complex **216** due to its relatively simplified ^{13}C NMR spectrum.



Scheme 3.46. Reaction used by the Berry group to conduct structural studies on the iridium carbene.

3.5.2. Variable temperature ^{13}C NMR studies

The ^{13}C NMR spectrum was collected at 14.5 °C and revealed two signals appearing at 293.6 ppm and 292.5 ppm in a 19 : 81 ratio, respectively (Figure 3.13) These signals are believed to represent the reactive iridium carbene intermediate(s). The ppm values lie in a similar range as those obtained for carbenes of $\text{Rh}_2(\text{O}_2\text{CCPh}_3)_4$ (240 ppm),²⁰⁶ PONOP-Ir=CH_2 (252.2 ppm),²⁰⁷ and $\text{Pybox-Ru=CHCO}_2\text{R}$ (305.7 ppm) (*cf.* Table 3.6).¹⁹⁹

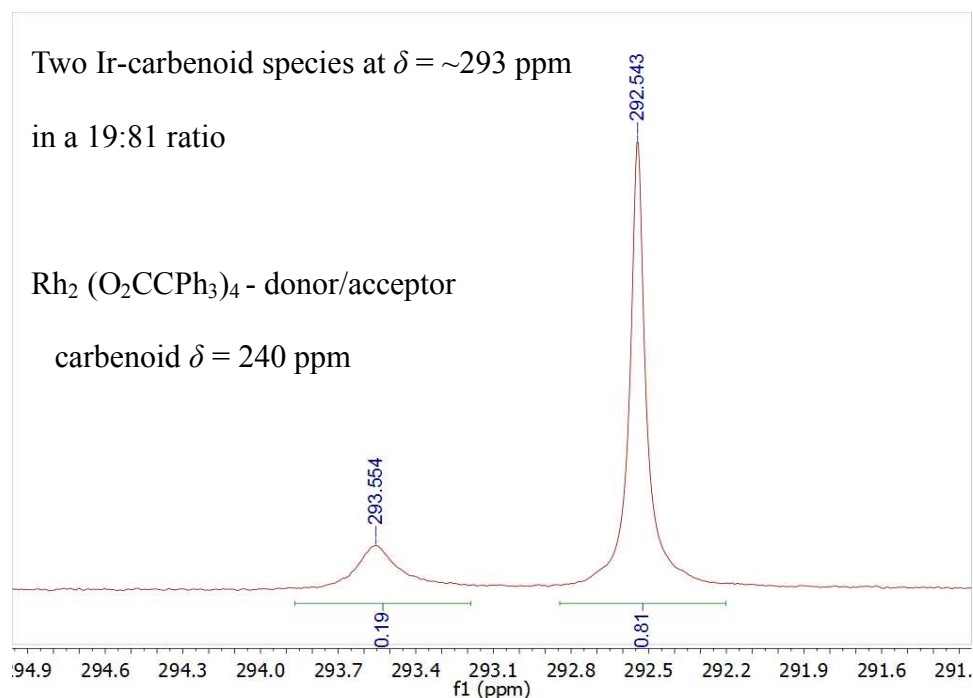


Figure 3.13. ^{13}C NMR spectrum of the reaction between iridium(III) phebox complex **213** and ^{13}C labeled methyl *p*-methoxyphenyl diazoacetate **264** at 14.5 °C in CDCl_3 .

If the two signals represent the equatorial and axial carbene isomers, then the ratio of the two signals should represent the ratio of enantiomers obtained in the catalytic reaction with 1,4-cyclohexadiene (8.5 : 91.5, Table 3.3, entry 9). This is not the case, but it may also be that rotational isomers of the axial or equatorial carbene exist in solution (*cf.* **19-ax** and **19-ax-a2**, Figure 3.11). Variable temperature ^{13}C NMR was used to probe this possibility, and the stacked spectra are shown in Figure 3.14.

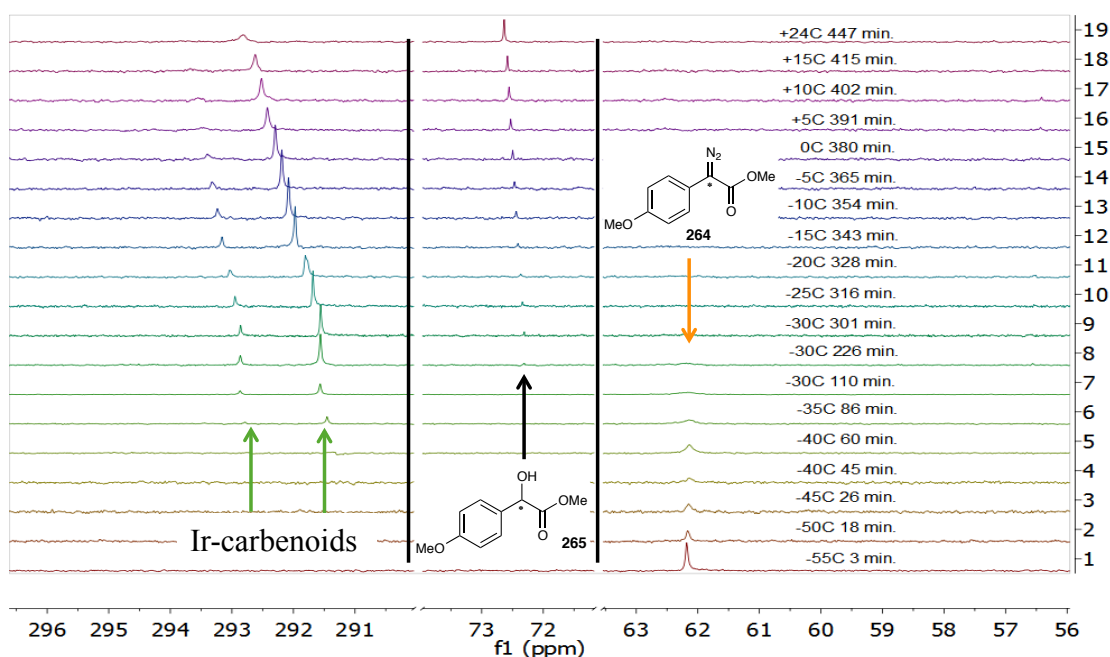


Figure 3.14. Variable temperature ^{13}C NMR spectra for the reaction of iridium(III) complex **213** with ^{13}C -labeled methyl *p*-methoxyphenyldiazoacetate **264**.

Nineteen ^{13}C NMR spectra were collected starting at $-55\text{ }^\circ\text{C}$ 15-20 minute intervals over 7.5 hours, and the temperature was gradually increased by $5\text{ }^\circ\text{C}$ at each time point. Figure 3.14 shows that as the signal for methyl *p*-methoxyphenyldiazoacetate decreases in intensity ($\sim 62\text{ ppm}$), the signals for the putative iridium carbenoids increase (292 ppm and 293 ppm). Furthermore, the signal for mandelic acid derivative **265**, which arises from O-H insertion of water into the carbene,²⁰⁸ begins to form at $\sim 72\text{ ppm}$. The qualitative comparison of the signal intensities at 292 ppm 293 ppm with the signal intensity of **265** at 72 ppm suggests that the signals at 292 ppm 293 ppm are indeed those of iridium carbenoids. Qualitative analysis of these signals appears to indicate that these are structural isomers since their relative intensities appear proportional throughout the experiment. However, integration of the signals at each time point would provide a

quantitative ratio of these isomers and reveal a clearer picture of the nature of the intermediates.

3.5.3. UV-Vis studies on the reaction of iridium(III) phebox **213** mediated decomposition of methyl *p*-methoxyphenyldiazoacetate **264**

UV-Vis spectroscopy was also used to investigate the reactive intermediate. The UV-Vis spectrum of the reaction in dichloromethane was acquired at ambient temperature at various time periods (Figure 3.15). A metastable intermediate was observed at 652 nm, and its peak absorbance was measured at 17.5 hours. Remarkably, this intermediate remained in the reaction mixture for nearly four days. The UV-Vis spectrum obtained for the spectroscopically characterized dirhodium(II) carbenoid **266** derived from $\text{Rh}_2(\text{O}_2\text{CCPh}_3)_4$ and methyl *p*-methoxyphenyl diazoacetate **264** showed a $\lambda_{\text{max}} \sim 700 \text{ nm}$.²⁰⁶ A solution of rhodium carbene **266** was found to be stable at 0 °C for 20 hours. The fact that the intermediate observed for the iridium phebox **213** mediated decomposition of methyl *p*-methoxyphenyldiazoacetate persisted for four days suggests that the iridium carbene intermediate can be isolated. Attempts to identify and structurally characterize the intermediate by X-ray crystallography are ongoing in the Berry laboratory.

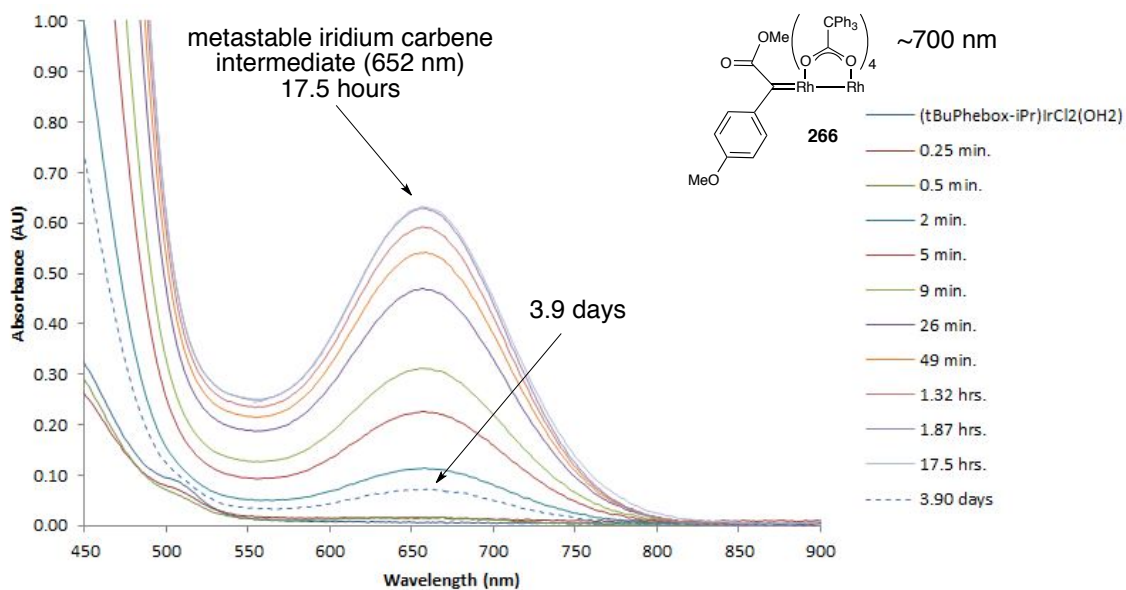


Figure 3.15. UV-Vis spectrum of the iridium(III) phebox **213** mediated decomposition of ^{13}C -labeled methyl *p*-methoxyphenyldiazoacetate **264**.

3.6 Conclusions

We have designed a series of new iridium(III) phebox complexes that are effective catalysts for highly enantioselective C-H functionalization of cyclic dienes using donor/acceptor carbenes derived from aryl diazoesters. The insertion reactions proceeded at room temperature without the need for slow addition of the diazoester, and carbene dimerization was not detected. The iridium phebox complexes were not as reactive towards insertion into THF when compared to dirhodium(II) tetracarboxylate and iridium(III) salen complexes. It became clear that the carbenes generated from the iridium(III) phebox complexes were significantly attenuated and prompted us to gain more information regarding the reactive intermediates by computational and structural studies. Density functional theory calculations provide convincing evidence of an axially

bound carbene intermediate that is vital for understanding the enantioselectivity in the iridium(III) phebox catalyzed C-H functionalization of 1,4-cyclohexadiene using aryl diazoesters. Further structural studies using UV-Vis spectroscopy and ^{13}C NMR analysis have generated evidence for an iridium carbene intermediate, and efforts are ongoing to isolate this reactive intermediate.

Chapter 4

Iridium(III) Phebox and Iridium(III) Phebim Catalyzed Acceptor-Only Metallo carbene C-H Functionalization

4.1 Introduction

As described in Chapter 3, our design of new and readily accessible iridium(III) phebox complexes has led to highly enantioselective C-H insertion of donor/acceptor iridium carbenes into cyclic 1,4-dienes. However, the substrate scope outside of these substrates for the donor/acceptor iridium carbene C-H insertion was limited. This reactivity profile suggests that the iridium metal and our ligand framework are indeed capable of attenuating the metallo carbene reactivity. This being the case, then we would expect a potential energy barrier for C-H insertion using acceptor-only carbenes generated from the iridium(III) phebox complexes to be higher than that which was calculated by Davies and Autschbach for dirhodium(II) tetracarboxylate catalyzed C-H insertion of ethyl diazoacetate into 1,4-cyclohexadiene, which was calculated as nearly barrierless at $1.2 \text{ kcal}\cdot\text{mol}^{-1}$.⁷ This would perhaps allow for a later transition state to be reached with the acceptor-only metallo carbenes generated by the iridium(III) phebox complexes, and possibly lead to selective C-H functionalization reactions using this class of metallo carbenes.

4.2 Iridium(III) Phebox Catalyzed Acceptor-only Atom Transfer

4.2.1 Insertion of ethyl diazoacetate into 1,4-cyclohexadiene

Ethyl diazoacetate represents the simplest and most accessible acceptor-only metallo-carbene precursor. Despite concerns over its safety,²⁰⁹ Monsanto²¹⁰ and Bristol-Meyers Squibb²¹¹ have used ethyl diazoacetate on industrial scale. Additionally, Clark and coworkers at Monsanto have evaluated its thermal stability and detonation properties by differential scanning calorimetry.^{212,213} They found that ethyl diazoacetate is thermally stable below 120 °C and exhibits non-detonative properties.

The ethyl diazoacetate in our studies was obtained from Sigma Aldrich and was used without further purification. However, the reagent always contained residual and varying amounts of dichloromethane. This amount was checked periodically by ¹H NMR using 1, 3, 5-trimethoxybenzene as the internal standard to ensure accurate and precise measurements were always made between each insertion reaction. In this way ethyl diazoacetate was accurately weighed by syringe, and stock solutions of ethyl diazoacetate were always freshly prepared.

Our studies were initiated by attempting the C-H insertion reaction of ethyl diazoacetate into 1,4-cyclohexadiene by adding 1 mol % iridium(III) phebox **216** in one portion to a mixture of 1,4-cyclohexadiene and 4 Å MS at room temperature (Table 4.1, entry 1). Ethyl diazoacetate was completely consumed within 2 hours, and the crude ¹H NMR indicated a 25 : 33 : 42 ratio of insertion product **A**, cyclopropane **B**, and dimerized carbene **C**. Although the reaction favored dimer formation, the product arising from C-H

insertion was significant when compared to the observations by Müller in which cyclopropanation was obtained almost exclusively with both $\text{Rh}_2(\text{OAc})_4$ and copper powder (Table 4.1, entry 2 and 3, respectively).²⁸ This result was promising in two ways. First, it provided evidence that the acceptor-only iridium carbene was capable of performing C-H insertion. Second, it indicated that our iridium catalyst system exhibited more chemoselectivity for C-H insertion over cyclopropanation when compared to the dirhodium and copper catalysts.

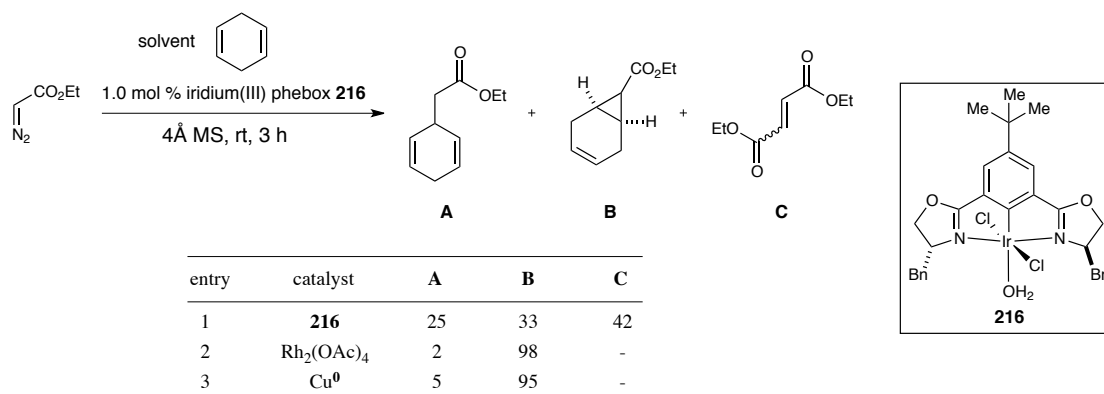
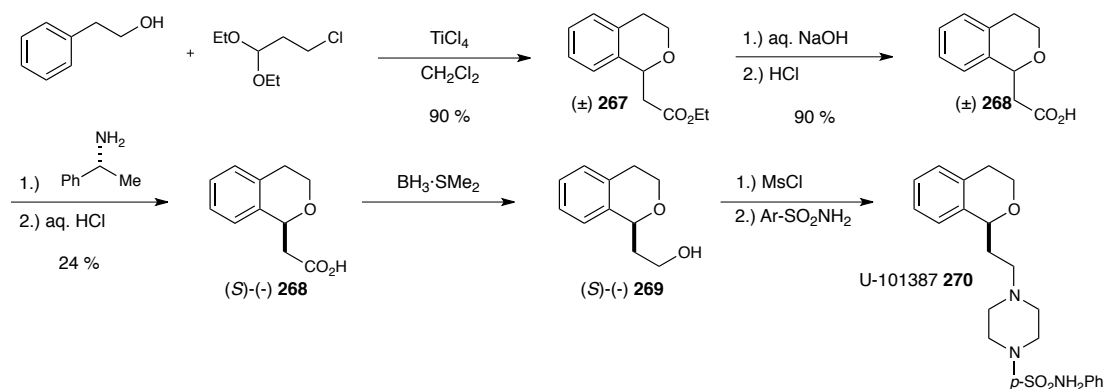


Table 4.1. Iridium(III) phebox catalyzed acceptor only C-H insertion into 1,4-cyclohexadiene.

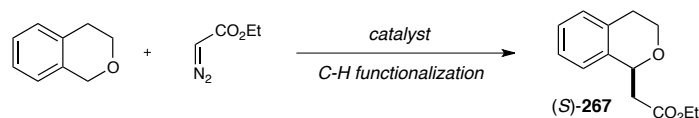
Given that the C-H insertion into 1,4-cyclohexadiene does not generate a chiral center, we did not invest any more time with this substrate. Instead, the reaction with a substrate containing prochiral methylene C-H bonds would quickly inform us of our iridium complexes' capabilities to perform enantioselective acceptor-only C-H functionalization.

4.2.2 Insertion of ethyl diazoacetate into tetrahydrofuran

The ability to enantioselectively functionalize C-H bonds alpha to heteroatoms using acceptor-only metallocarbenes would be a powerful method in the context of natural product and pharmaceutical synthesis and diversification. For example, U-101387 (Sonepiprazole) is a dopamine D₄ antagonist that was in clinical trials for the treatment of schizophrenia.²¹⁴ Its synthesis is outlined in Scheme 4.1 and involves hydrolysis of racemic ester **267** and a kinetic resolution to provide enantioenriched acid (S)-(-) **268**, which proceeded in only 24 % yield (50 % theoretical). A more economical approach to the chiral acid (S)-(-) **268** would involve the direct formation of the enantioenriched ester (S)-(-) **267** *via* catalytic, enantioselective C-H insertion into the benzylic/etheral C-H bond using ethyl diazoacetate (Scheme 4.2). Another example of the potential impact of this transformation was previously described in Chapter 1 Section 1.2.3, in which the molecule Baclofen could be readily synthesized *via* benzylic C-H insertion.



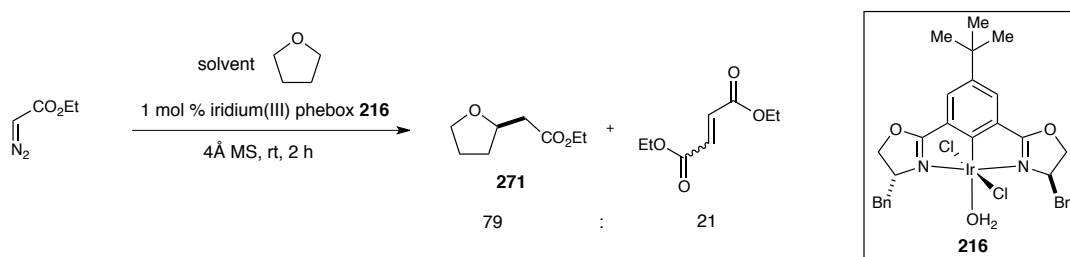
Scheme 4.1. Synthesis of U-101387 **270**.



Scheme 4.2. C-H functionalization approach to enantioenriched ester *S*-267.

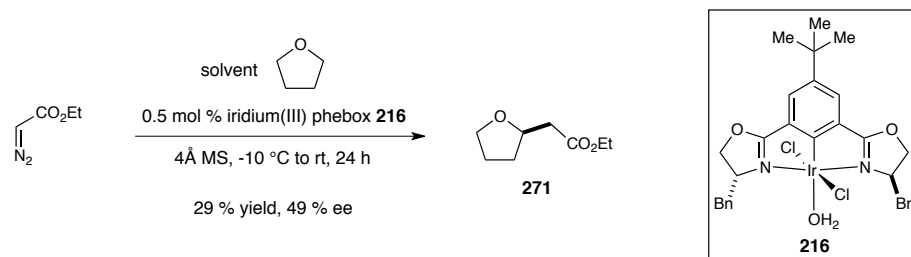
Tetrahydrofuran was initially chosen as the substrate for our investigation since it is cheap, readily available, and its motif is present in numerous natural products and biologically active molecules.²¹⁵ We selected ethyl diazoacetate as the acceptor-only metallocarbene precursor as it is the most widely used acceptor carbene precursor and is commercially available. Furthermore, it would allow for a direct comparison of our catalysts' performance with state of the art copper catalysis.

The first reaction entailed adding iridium(III) phebox catalyst **216** in one portion to a mixture of ethyl diazoacetate and 4 Å molecular sieves in THF (Scheme 4.3). Ethyl diazoacetate was consumed within two hours and a 79 : 21 mixture of C-H insertion product **271** to dimerization products was observed. Unfortunately, the reaction was run on a small scale (~25 mg) and **271** was unable to be isolated. It is also possible the product was lost when it was placed under vacuum.



Scheme 4.3. Iridium(III) phebox catalyzed acceptor-only C-H into tetrahydrofuran.

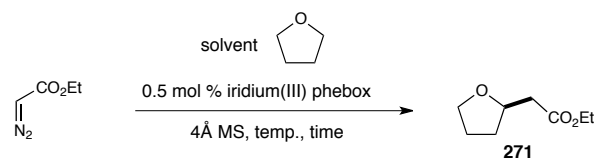
This outcome informed us that dimerization was a significant byproduct at room temperature. Low temperature and slow addition of the diazoester are known to suppress dimerization of the carbene.^{3,5,27,35} Therefore, a solution of ethyl diazoacetate in THF was added over the course of 5 hours to a -10 °C mixture of iridium complex **216** and 4 Å MS in THF. Ethyl diazoacetate was still not consumed after an additional 17 hours stirring at -10 °C. The mixture was then warmed to room temperature and stirred three hours, at which time the diazoester was consumed. Product **271** was then obtained in 29 % yield by ¹H NMR analysis with 1,3,5-trimethoxybenzene as the internal standard (Scheme 4.4). **271** was isolated in 29 % yield with 49 % enantiomeric excess after flash column chromatography,²¹⁶ and the product was never placed under high vacuum to avoid loss due to potential volatility. Notably, the insertion product is difficult to visualize by thin layer chromatography. It is not UV active but stains pink by anisaldehyde under prolonged heating (> 2 minutes); submerging the TLC plate into distilled water after heating significantly increases the intensity of the pink stain.



Scheme 4.4. Enantioselective intermolecular C-H insertion into THF using ethyl diazoacetate.

With this result in hand, nine additional iridium(III) phebox complexes were evaluated for their catalytic performance for the C-H insertion into THF. Complex **213**

performed the C-H insertion reaction in 71 % isolated yield and 49 % ee, and ethyl diazoacetate was consumed immediately upon complete addition (Table 4.2, entry 1). The dimethyl phebox complex **174** performed nearly equally as well, providing **271** in 63 % yield and 49 % enantiomeric excess (entry 5). *tert*-Butyl oxazoline substitution precluded decomposition of ethyl diazoacetate, and the crude ¹H NMR showed < 5 % conversion in each case (entries 2 and 6). Phenyl substitution on the oxazoline significantly decreased the enantioselectivity to 20 % ee and 19 % ee (entries 3 and 7). The reaction was significantly slower with catalyst **215** and required warming to room temperature and stirring for three days for complete ethyl diazoacetate consumption (entry 3). Benzyl substitution on the oxazoline provided enantioselectivities that were comparable to the isopropyl-substituted catalysts, but the reaction time was longer and the yields were lower (entries 4 and 8). Notably, the acetate complex **217** exerted similar behavior to the donor/acceptor C-H insertion reactions and did not decompose the diazoester (entry 9). Additionally, performing the reaction at -78 °C with catalyst **213** resulted in a 24 hour reaction time and did not improve the enantioselectivity (entry 10). Complex **213** provided the best yield, enantioselectivity, and shortest reaction time and was used in subsequent studies.



entry ^a	catalyst	temp	time	% yield ^b	% ee ^c
1	213	-10 °C	8	80 (71)	49
2	214	-10 °C to rt	24	≤ 5	-
3	215	-10 °C to rt	74	36 (33)	-20
4	216	-10 °C to rt	24	29 (29)	-49
5	174	-10 °C	6	79 (63)	49
6	201	-10 °C to rt	24	≤ 5	-
7	202	-10 °C	24	62 (48)	-19
8	203	-10 °C to rt	27	45 (45)	-47
9	217	-10 °C to rt	24	≤ 5	-
10	213	-78 °C	24	ND	49

^a Ethyl diazoacetate (0.88 mmol) was added as a solution in THF (0.29 M) via syringe pump over the course of 6 hours to a stirring mixture of iridium catalyst (4.1 μmol) and 4 Å MS (200mg/1mmol diazo) in THF (3 mL). ^b Yield determined by ¹H NMR using 1,3,5-trimethoxybenzene as the internal standard. The value in parentheses denotes isolated yield. ^c Determined by chiral HPLC.

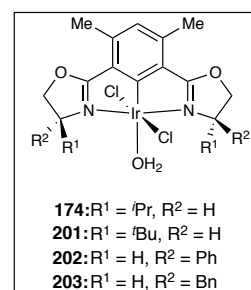
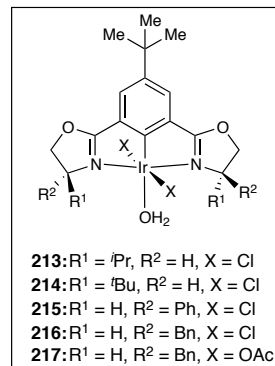
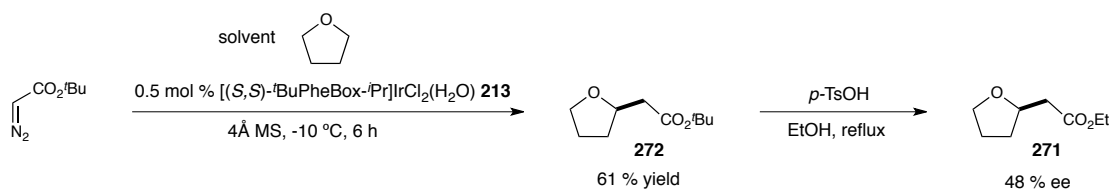


Table 4.2. Iridium(III) phebox catalyst evaluation for the enantioselective C-H functionalization of tetrahydrofuran using ethyl diazoacetate.

4.2.3. Evaluation of other acceptor-only metallocarbene precursors for C-H insertion into THF.

In our iridium(III) phebox catalyzed donor/acceptor C-H insertion into cyclic 1,4-dienes the size of the ester had minimal impact on the enantioselectivity of the reaction (cf. Chapter 3, Section 3.4.2), but it could not be predicted *a priori* that the acceptor-only C-H insertion would follow suit. Therefore, we investigated the effect on selectivity and yield for insertion into THF by changing the ethyl ester on the acceptor-only metallocarbene precursor. Slow addition of a THF solution of *tert*-butyl diazoacetate²¹⁷ to a mixture of iridium(III) phebox catalyst **213** and 4 Å MS at -10 °C provided **272** in 61 % isolated yield (Scheme 4.5). Obtaining a suitable HPLC assay to

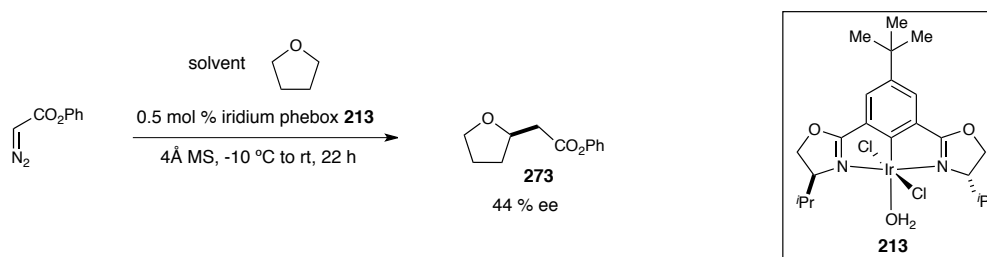
measure enantioselectivity was unsuccessful, therefore *tert*-butyl ester **272** was converted to the ethyl ester **271** by treatment with 1.2 equivalents *p*-TsOH in refluxing ethanol, and the ethyl ester **271** was found to have 48 % ee. To ensure racemization did not occur during the transesterification, the enantioenriched ethyl ester **271** was subjected to *p*-TsOH in refluxing ethanol, and subsequent HPLC analysis confirmed that its enantiopurity was not compromised during the transesterification. The yield and enantioselectivity using *tert*-butyl diazoacetate were comparable with the results obtained with ethyl diazoacetate as the metallo-carbene precursor and showed that increasing the steric bulk of the ester had minimal impact on the reaction outcome.



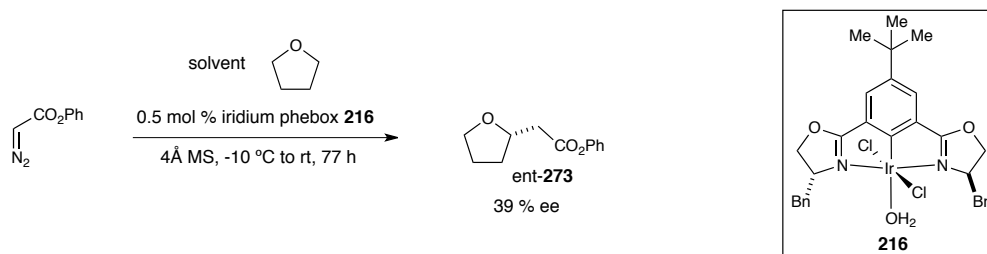
Scheme 4.5. Enantioselective intermolecular C-H insertion into THF using *tert*-butyl diazoacetate.

Other acceptor metallo-carbene precursors that have been used in atom-transfer reactions were also evaluated. Addition of phenyl diazoacetate over 5 hours to isopropyl-substituted catalyst **213** in THF resulted in the incomplete consumption of the diazoester. The reaction was then warmed to room temperature and stirred an additional 17 hours until the diazoester had been completely consumed, but only furnished the insertion product **273** in 44 % ee (Scheme 4.6). We imagined that secondary interactions between the phenyl diazoester and the benzyl substituents on catalyst **216** might increase

the selectivity, however this resulted in even lower enantioselectivity at 39 % ee with incomplete consumption of the diazoester (Scheme 4.7).



Scheme 4.6. Enantioselective intermolecular C-H insertion into THF using phenyl diazoacetate catalyzed by **213**.

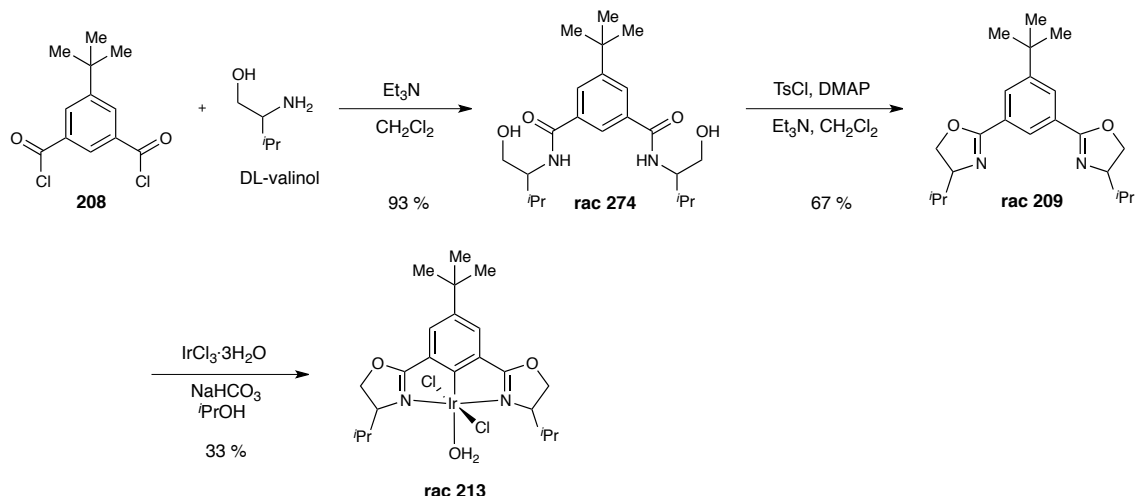


Scheme 4.7. Enantioselective intermolecular C-H insertion into THF using phenyl diazoacetate catalyzed by **216**.

Diazoacetamides²¹⁸ and succinimidyl diazoacetate²¹⁹⁻²²¹ have been shown to be effective acceptor-only carbene transfer reagents, however the reactions with our iridium(III) phebox catalyst **213** provided < 10 % conversion even at elevated temperatures (~ 40 °C).

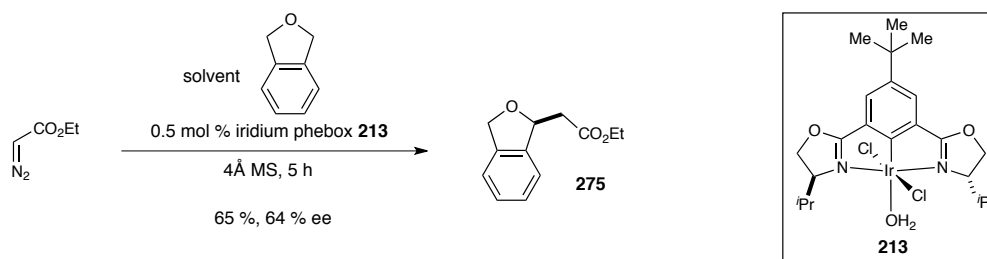
4.2.4. Iridium(III) phebox catalyzed enantioselective C-H functionalization of phthalan

We wanted to further understand our catalysts' reactivity by exploring other oxygen heterocycles as substrates. It was expected that phthalan (dihydroisobenzofuran) would be particularly amenable for C-H functionalization as it contains benzylic and etheral C-H bonds. For this substrate, it was more difficult to obtain the racemate of the insertion product **275** under $\text{Rh}_2(\text{OAc})_4$ catalysis (Scheme 4.9, *vide infra*). Therefore, the chiral/racemic iridium phebox complex **rac-213** was prepared from commercially available DL-valinol (Scheme 4.8). First, amide **rac-274** was formed in 93 % yield from the reaction of bis-acyl chloride **208** and DL-valinol with triethylamine in dichloromethane. The amide **rac-274** was cyclized to form ligand **rac-209** in 67 % yield by reacting it with tosyl chloride, DMAP, and Et_3N according to the method of Evans.²²² The ligand was metallated in the usual way with $\text{IrCl}_3 \cdot \text{H}_2\text{O}$ and the chiral/racemic iridium(III) phebox complex **rac-213** was formed in 33 % yield. This complex was used as the catalyst for the formation of racemic acceptor-only C-H insertion products throughout the rest of our experiments.



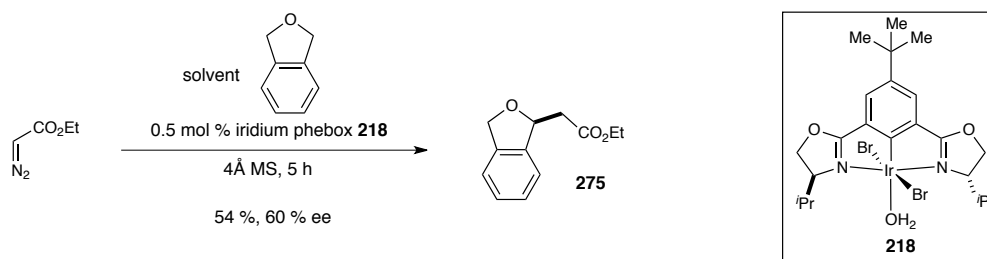
Scheme 4.8. Synthesis of chiral/racemic iridium(III) phebox complex **rac 213**.

With an HPLC assay for **275** in hand, a solution of ethyl diazoacetate in phthalan was added over 5 hours to a room temperature mixture of iridium(III) phebox catalyst **213**, phthalan, and 4Å MS. the insertion product **275** was obtained in 65 % isolated yield and 64 % enantiomeric excess (Scheme 4.9). This was a 15 % increase in enantioselectivity relative to the C-H insertion reaction into THF using the same catalyst (cf. Table 4.1, entry 1). It is worth noting that this reaction was conducted at room temperature because the melting point of phthalan is 6 °C.



Scheme 4.9. Iridium(III) chloro phebox **213** catalyzed enantioselective intermolecular C-H insertion into phthalan.

We were intrigued to see what impact bromide substitution on the iridium metal center would have on the reaction outcome. Using the analogous iridium(III) bromo complex **218** decreased the yield and enantiomeric excess of **275** to 54 % and 60 %, respectively (Scheme 4.10).



Scheme 4.10. Iridium(III) bromo phebox **218** catalyzed enantioselective intermolecular C-H insertion into phthalan.

When we began our investigations in acceptor-only C-H insertion chemistry, we assumed that a large excess of the substrate was necessary to help prevent the dimerization side reaction.²⁷ However, it is obvious that this approach is impractical if the methodology is to be employed in complex molecule synthesis. With this in mind, we added ethyl diazoacetate as a solution in trifluorotoluene over 5 hours to a -10 °C mixture of catalyst **213**, 4 Å molecular sieves, and only 4 equivalents of phthalan. Gratifyingly, the insertion product **275** was obtained in 81 % yield and 76 % enantioselectivity (Table 4.3, entry 1). This is a marked increase when compared to the reaction with phthalan as solvent. The amount of phthalan could be further decreased to 2 equivalents without compromising the enantioselectivity (entry 2). Adding an excess of ethyl diazoacetate could potentially increase the yield of this reaction, but this was not pursued.

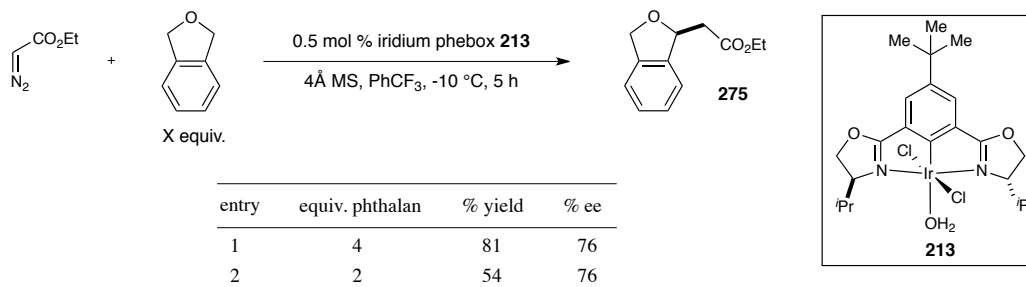


Table 4.3. Lowering the equivalents of phthalan for the iridium catalyzed intermolecular C-H insertion into phthalan using ethyl diazoacetate.

Trifluorotoluene was first used in the acceptor-only insertion reaction with 4 equivalents phthalan because it proved to be the best solvent for our donor/acceptor iridium carbene insertion reactions into cyclic 1,4-dienes. It could not be predicted that trifluorotoluene was the best solvent in the acceptor-only insertion reactions, therefore solvent effects as related to reaction enantioselectivity were also examined for the C-H insertion reaction of ethyl diazoacetate into phthalan. As in the case of the iridium phebox catalyzed C-H insertion of donor/acceptor diazoesters into 1,4-cyclohexadiene, trifluorotoluene proved to be the best solvent. Hexanes, dichloromethane, and benzene all provided inferior enantioselectivity (Table 4.4).

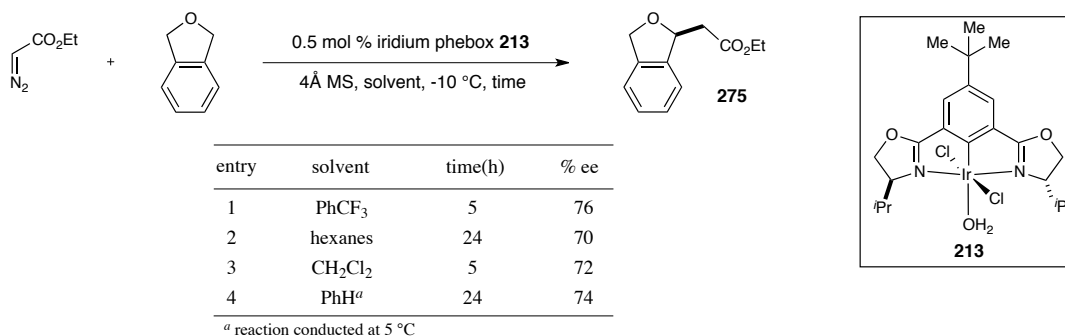
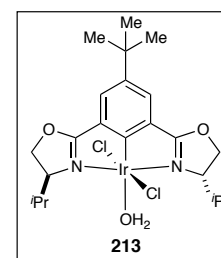
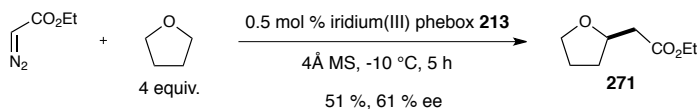


Table 4.4. Solvent evaluation for iridium phebox catalyzed C-H insertion of ethyl diazoacetate into phthalan.

4.2.5. Iridium(III) phebox catalyzed enantioselective C-H functionalization of tetrahydrofuran and 2,5-dihydrofuran.

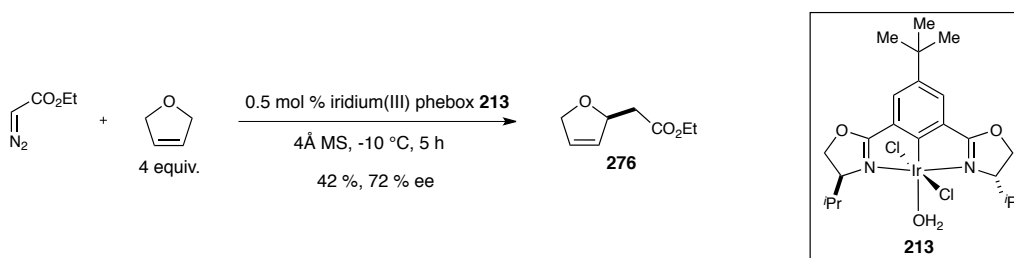
We were then curious if the enantioselectivity of the insertion into tetrahydrofuran would increase when lowering the equivalents of THF used in the reaction. Indeed, running the C-H insertion reaction with 4 equivalents THF and catalyst **213** in trifluorotoluene furnished the insertion product **271** in 51 % yield and 61 % ee (Scheme 4.11). Although the yield is lower than when the reaction was run with THF as solvent (80 %), the enantioselectivity is significantly higher at 61 % (versus 49 %).



Scheme 4.11. Iridium(III) phebox **213** catalyzed acceptor-only enantioselective C-H insertion using 4 equivalents THF.

Since the outcome of the reaction with 1,4-cyclohexadiene with ethyl diazoacetate and catalyst **213** provided a nearly 1 : 1 mixture of C-H insertion to cyclopropanation products (cf. Table 4.1), we hypothesized that our iridium phebox complexes had the potential to perform chemoselective C-H insertion over cyclopropanation. To this end, ethyl diazoacetate was added as a solution in PhCF₃ over the course of 5 hours to a stirring mixture of iridium(III) phebox catalyst **213**, 2,5-dihydrofuran, and 4 Å MS in

PhCF₃ at -10 °C (Scheme 4.12). To our satisfaction, C-H insertion alpha to oxygen was achieved to give **276** in 42 % yield with 72 % enantiomeric excess, and the corresponding cyclopropane was not detected in the crude ¹H NMR (Figure 4.1). The relatively low yield is likely attributed to the product's volatility since extra care was not taken to prevent loss under reduced pressure. This is a particularly powerful example of chemoselectivity imparted by our iridium(III) phebox catalysts since both Rh₂(OAc)₄²²³ and Cu^{II}(acac)₂²²⁴ catalysts are completely selective for cyclopropanation of the olefin within 2,5-dihydrofuran.



Scheme 4.12. Iridium phebox **213** catalyzed chemo- and enantioselective C-H insertion of ethyl diazoacetate into 2,5-dihydrofuran.

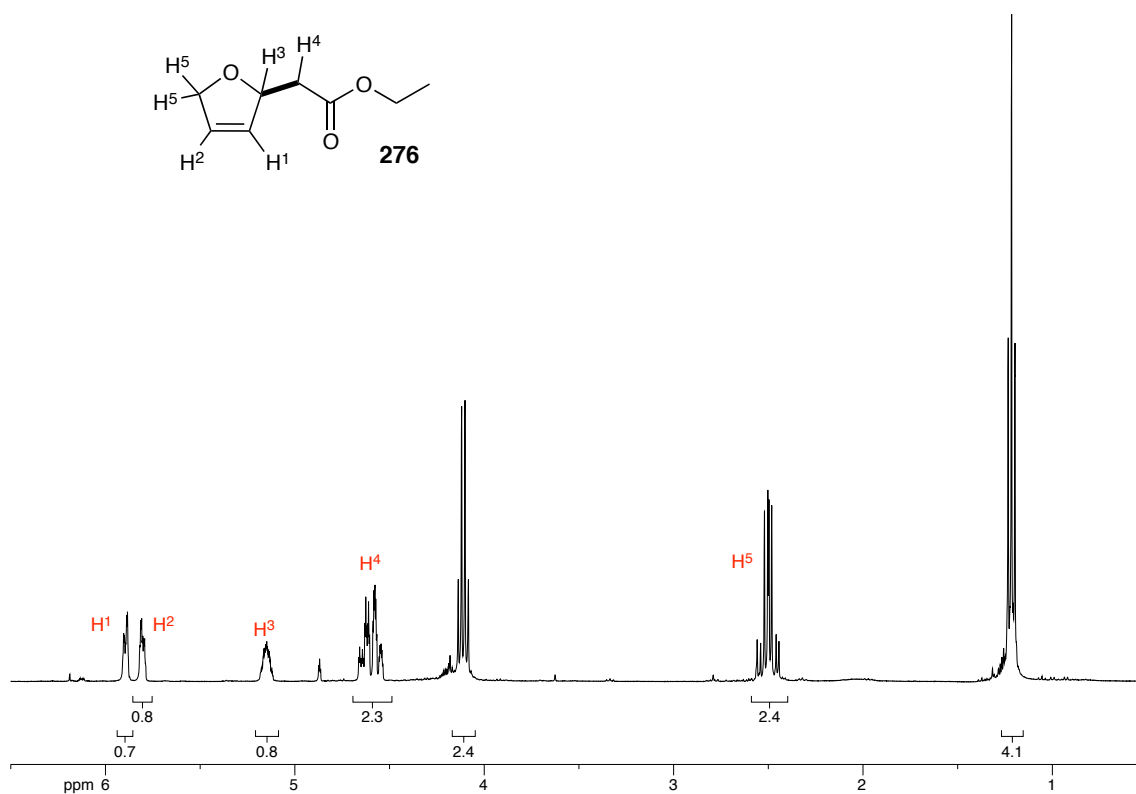


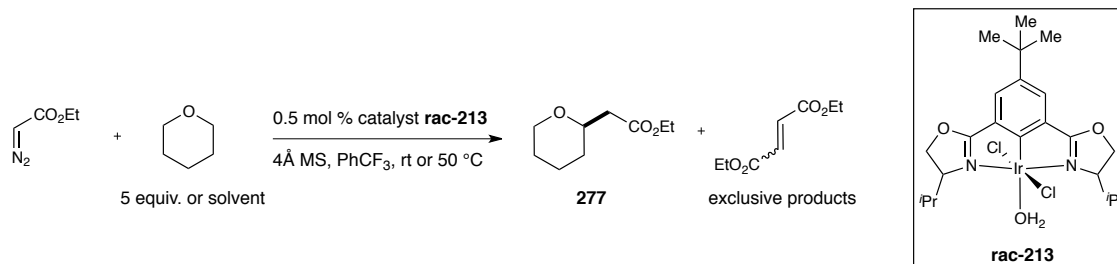
Figure 4.1. Crude ^1H NMR spectrum for the chemoselective C-H insertion of ethyl diazoacetate into 2,5-dihydrofuran.

4.2.6 Kinetic isotope effect for the C-H insertion of ethyl diazoacetate into tetrahydrofuran.

The measurement of primary kinetic isotope effects (KIE, $k_{\text{H}}/k_{\text{D}}$) is a common technique for studying reaction mechanisms.²²⁵ The primary KIE of our iridium(III) phebox **213** catalyzed insertion of ethyl diazoacetate into THF was determined to be 1.68 by reacting ethyl diazoacetate with iridium(III) phebox catalyst **213** in a 1:1 mixture of protio- and deuterio-THF in PhCF_3 . We were unable to quantify the ratio using ^1H NMR,

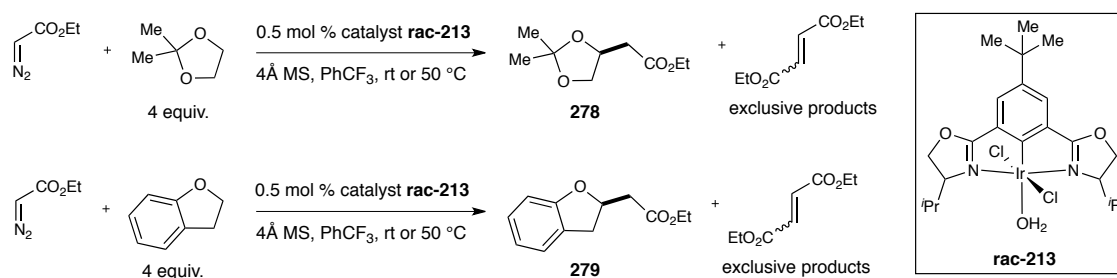
4.2.7. Attempts to perform C-H functionalization into other cyclic ethers.

We then directed our attention towards exploring the scope of cyclic ethers that could undergo C-H functionalization alpha to oxygen using our iridium(III) phebox complexes. Racemic iridium phebox complex **rac-213** was used to conduct these studies, as it would allow us to probe reactivity while potentially furnishing the racemic product necessary for HPLC analysis. The next substrate that was investigated was tetrahydropyran (THP), as it was shown to be a viable substrate for copper catalyzed C-H functionalization.²⁷ Unfortunately, adding ethyl diazoacetate over 12 hours to a mixture of THP, iridium complex **rac-213**, and 4Å MS in PhCF₃ at room temperature only led to formation of the diethyl maleate and diethyl fumarate dimers as determined by thin layer chromatography and ¹H NMR (Scheme 4.13). Running the reaction at 50 °C also led to exclusive carbene dimerization. In an effort to suppress dimerization of the carbene, the reaction was run with tetrahydropyran as solvent at room temperature, but even this tactic proved unsuccessful and the insertion product **277** was not observed by ¹H NMR in the crude reaction mixture. The lack of reactivity for tetrahydropyran may be due to the larger s-character at the carbon alpha to oxygen compared to tetrahydrofuran, and stabilizing positive charge buildup in the transition state is more difficult.²²⁷ Alternatively, the larger and more conformationally flexible six membered ring may geometrically prevent accessibility of the substrate to the metallo-carbene.



Scheme 4.13. Attempted C-H insertion into tetrahydropyran (**277** not formed).

Other cyclic ethers that were evaluated for C-H insertion using ethyl diazoacetate included 2,2-dimethyl dioxolane and 2,3-dihydrobenzofuran (Scheme 4.14). Each substrate was reacted with iridium(III) phebox complex **rac-213** at both $22\text{ }^\circ\text{C}$ and $50\text{ }^\circ\text{C}$ with slow addition of ethyl diazoacetate over five hours. $^1\text{H NMR}$ analysis of the crude reactions run with 2,2-dimethyl dioxolane indicated only dimer formation, and signals corresponding to the insertion product were not present.²²⁸ The lack of reactivity for this substrate may be due to steric hindrance or to the inductive electron withdrawal by the additional oxygen atom. 2,3-dihydrobenzofuran was also unreactive, and formation of the dimers dominated the reaction.

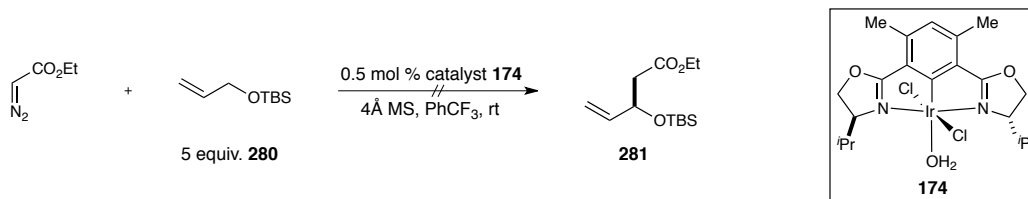


Scheme 4.14. Attempted C-H insertion into 2,2-dimethyl dioxolane and dihydrobenzofuran (**278** and **279** not formed).

4.2.8. Attempts to perform acceptor-only C-H functionalization into acyclic ethers

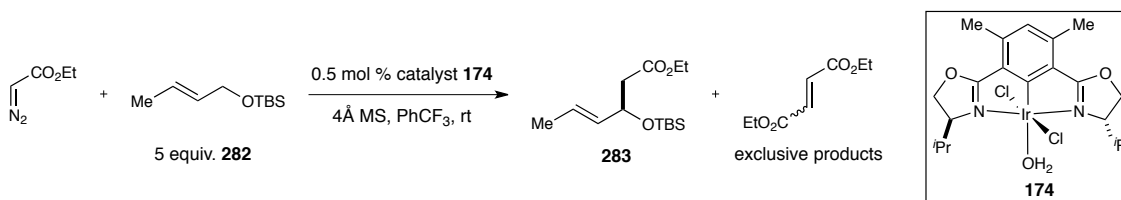
The ability to use acyclic ethers as substrates for acceptor-only C-H insertion using ethyl diazoacetate would significantly enhance the generality of the iridium(III) phebox complexes in catalysis. Since we found that insertion into cyclic ethers using ethyl diazoacetate was difficult, acyclic ethers would need to contain exceptionally reactive and accessible C-H bonds to be proper substrates for iridium(III) phebox catalyzed C-H insertion. The iridium catalyzed C-H insertion of ethyl diazoacetate into the allylic and ethereal 2° C-H bond of silyl protected allylic alcohols would provide a disconnection strategy that is equivalent to an aldol addition of ethyl acetate to an aldehyde,^{9,229} and the silicon-protecting group has been shown to enhance the reactivity of adjacent C-H bonds in dirhodium(II) catalyzed C-H insertion using donor/acceptor carbenes.^{21,229}

To begin our studies, a solution of ethyl diazoacetate in trifluorotoluene was added over six hours to a mixture of iridium(III) phebox catalyst **174**, 5 equivalents TBS-protected allylic alcohol **280**, and 4Å MS in trifluorotoluene (Scheme 4.15). Unfortunately ethyl diazoacetate was not consumed in the reaction even after stirring for 50 hours. We hypothesized that binding of the alkene substrate to the iridium metal center was inhibiting the decomposition of ethyl diazoacetate. In fact, olefin binding to iridium is a well-documented process.^{230,231}



Scheme 4.15. Attempted C-H insertion into TBS protected allylic alcohol **280**.

In an attempt to prevent this inhibitive binding, the *E*-2-butenol derived TBS ether **282** was employed as substrate for the reaction. Coordination of the *trans* alkene was expected to be minimal such that decomposition of ethyl diazoacetate would be allowed.^{94,131} This substrate has an additional level of complexity in that the 1° allylic C-H bonds are potentially reactive towards insertion. Reacting ethyl diazoacetate with TBS ether **282** and 0.5 mol % iridium(III) phebox complex **174** resulted in complete conversion of the diazoester. However, the sole reaction products arose from iridium carbene dimerization, and a mixture of diethyl fumarate and diethyl maleate esters was obtained (Scheme 4.16). This outcome suggests that the allylic methylene C-H bonds alpha to oxygen are either too sterically encumbered by the bulky silyl ether to undergo insertion or simply not reactive enough towards the iridium carbene.



Scheme 4.16. Attempted C-H insertion into TBS protected allylic alcohol **282**.

4.2.9. Conclusions

We found that our iridium(III) phebox complexes are effective catalysts for asymmetric acceptor-only intermolecular C-H insertion into phthalan, 2,5-dihydrofuran, and tetrahydrofuran, providing products in up to 76 % enantiomeric excess. A particularly powerful example of the selectivity of our catalysts was exemplified in the chemo- and enantioselective C-H functionalization of 2,5-dihydrofuran, a substrate that undergoes exclusive cyclopropanation under rhodium and copper catalysis. These are significant advances considering that acceptor-only intermolecular C-H insertion has been studied for over ten years, and asymmetric reactions have not been achieved until now. Unfortunately, we have not been able to extend the generality of these catalysts towards other cyclic or acyclic ethers, and it is unclear as to why the iridium phebox acceptor-only carbenes are so tame relative to the coinage metal-derived carbenes.

4.3 Computational Studies for Iridium(III) Phebox Catalyzed Acceptor-only C-H Insertion into THF and Phthalan

The fact that enantioselectivity is observed in the iridium(III) phebox catalyzed acceptor-only insertion reactions is remarkable considering that the calculated potential energy barriers for the rhodium(II) formate catalyzed C-H insertion of ethyl diazoacetate into 1,4-cyclohexadiene and cyclopentane were very small at $1.2 \text{ kcal}\cdot\text{mol}^{-1}$ and $3.5 \text{ kcal}\cdot\text{mol}^{-1}$, respectively.⁷ These small values are consistent with the low selectivity that is obtained for intermolecular C-H insertion with dirhodium(II) acceptor-only carbenes. Therefore we collaborated with Dr. Jamal Musaev and Dr. Shentan Chen at Emory University to understand the reactivity and selectivity of our iridium(III) phebox complexes by DFT analysis of the C-H insertion reactions of ethyl diazoacetate into phthalan and THF.²³²

4.3.1. DFT analysis of the geometry of the reactive acceptor-only carbene intermediate derived from ethyl diazoacetate

The first issue to address was the geometry of the reactive iridium carbene intermediate generated from ethyl diazoacetate. The geometry of the carbene was shown to play an essential role in determining the enantioselectivity in the iridium catalyzed donor/acceptor carbene (Chapter 3).¹⁸⁰ The free energy profile for the formation of both the equatorial and axial carbene intermediates are shown in Figure 4.3. The energies of each intermediate and transition state are shown as the Gibbs free energy and the

gas-phase enthalpy (in parentheses) in dichloromethane. The Gibbs free energies are the ones discussed in the text. The isopropyl-substituted iridium(III) phebox complex **213** was used in these calculations, and the resting state of the catalyst is denoted as **1-eq**. The energy zero was fixed to include **1-eq** and methyl diazoacetate as a simplified source of the resultant acceptor-only carbene.

The first step of the reaction pathway was found to be water dissociation to form the 16-electron intermediate **2-eq** with a barrier of 2.1 kcal·mol⁻¹. Upon water dissociation, two separate reaction pathways were found. One is the isomerization of **2-eq** to form the 16-electron intermediate **2-ax** with a barrier of 19.4 kcal·mol⁻¹. From here, the diazoester ethyl diazoacetate can coordinate to iridium in the axial position to form **4-ax**, a process that is exergonic by 14.9 kcal·mol⁻¹. Nitrogen gas extrusion *via* **TSN2-ax** occurs with a 5.1 kcal·mol⁻¹ energy barrier to form the axial iridium carbene **5-ax**. Formation of this species exergonic by 23.3 kcal·mol⁻¹, and isomerization of **2-eq** to **2-ax** was found to be the rate-limiting step for the formation of the axial acceptor-only carbene.

A second reaction pathway starting from the 16-electron intermediate **2-eq** was also found on the reaction coordinate. Coordination of methyl diazoacetate and subsequent nitrogen gas extrusion occurs with a lower potential energy barrier at 16.3 kcal·mol⁻¹ than does isomerization of a chloride ligand to form **TS1** (19.4 kcal·mol⁻¹). Thus, the formation of the equatorial acceptor carbene intermediate **5-eq** is kinetically favored under the reaction conditions and nitrogen gas extrusion is the rate-limiting step for its formation.

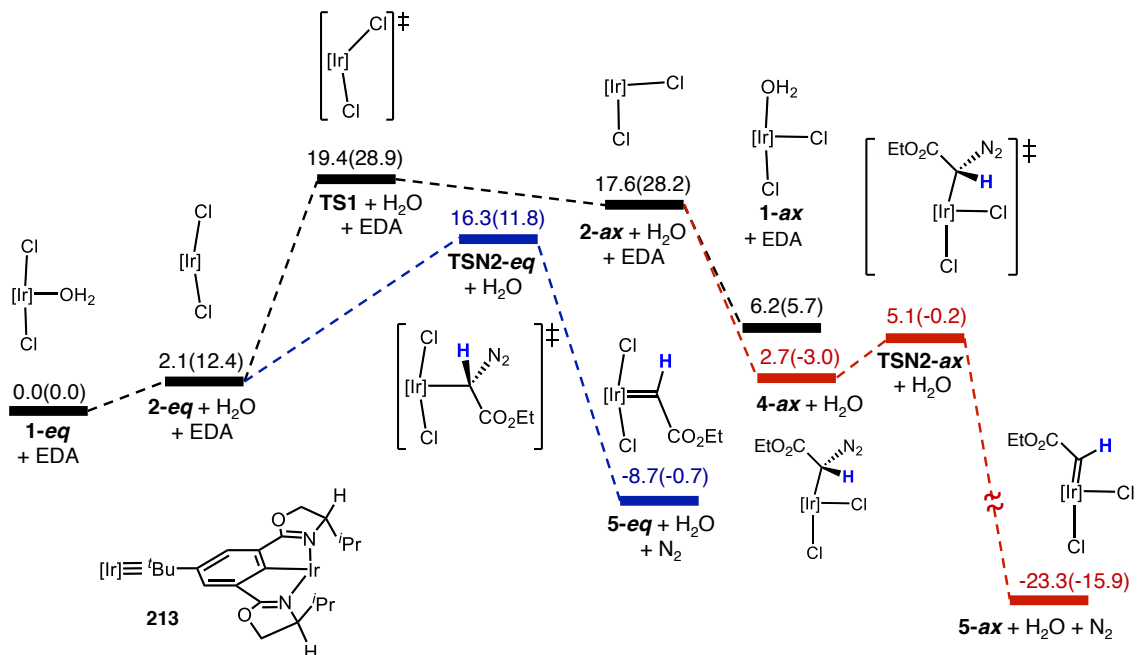


Figure 4.3. Free energy profile for axial and equatorial acceptor-only iridium carbene formation. All energy values $\Delta G(\Delta H)$ are given in kcal·mol⁻¹. EDA = ethyl diazoacetate.

4.3.2. Calculated transition state and intrinsic reaction coordinate for iridium(III) phebox catalyzed C-H insertion of ethyl diazoacetate into THF.

The calculations have shown that the equatorial iridium carbene isomer **5-*eq*** is the kinetically favored intermediate in the acceptor-only C-H insertion reaction into THF. From this intermediate the transition state **TSHT-*eq*** for the C-H functionalization of THF was located and is shown in Figure 4.4. The C-H functionalization barrier *via* transition state **TSHT-*eq*** was calculated to be 13.7 kcal·mol⁻¹. This number is astoundingly high compared to the calculated energy barriers for dirhodium tetracarboxylate catalyzed acceptor-only C-H functionalization of cyclopentane and

1,4-cyclohexadiene, which were calculated to be $3.5 \text{ kcal}\cdot\text{mol}^{-1}$ and $1.2 \text{ kcal}\cdot\text{mol}^{-1}$, respectively.^{7,233}

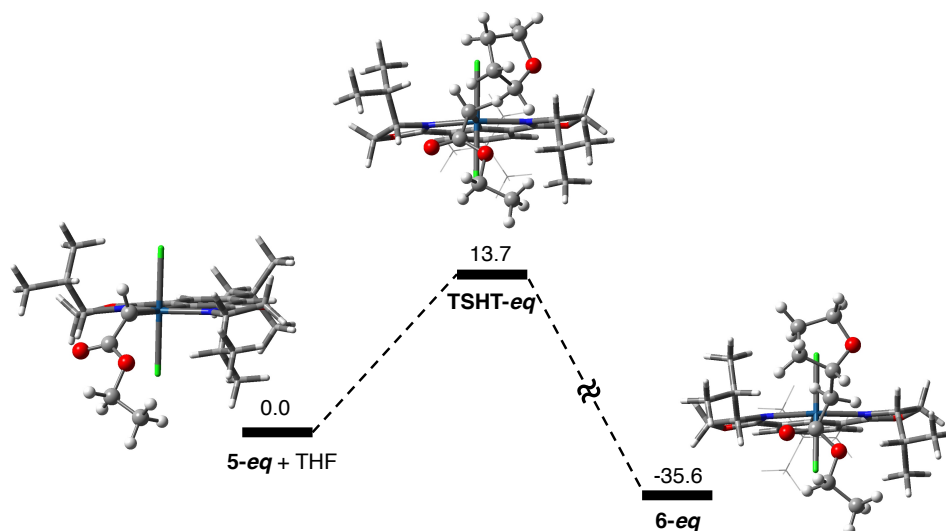


Figure 4.4. Lowest free energy profile for iridium phebox catalyzed acceptor-only C-H insertion into tetrahydrofuran *via* **TSHT-eq**.

To further our understanding of the reaction mechanism the intrinsic reaction coordinate was also calculated and is shown in Figure 4.5. **TSHT-eq** is shown at top left, and Mulliken population analysis²³⁴ revealed a $\delta_q(\text{THF})$ of +0.44 at the carbon alpha to oxygen in the tetrahydrofuran substrate. As the C-H bond begins to break the charge on the carbon containing the C-H bond becomes more positive, and $\delta_q(\text{THF}) = +0.82$ at **TSHT-eq**⁺. Before reaching a charge of +1.00, which would indicate the formation of a discrete carbocation intermediate, carbon-carbon bond formation rapidly occurs to give the insertion product **271** and regenerate the 16 electron iridium(III) phebox intermediate **2-eq** (**6-eq** is comprised of both **271** and **2-eq**). This calculated reaction coordinate is in

agreement with a mechanism that initially involves a strong hydride transfer component followed by asynchronous carbon-carbon bond formation.⁷

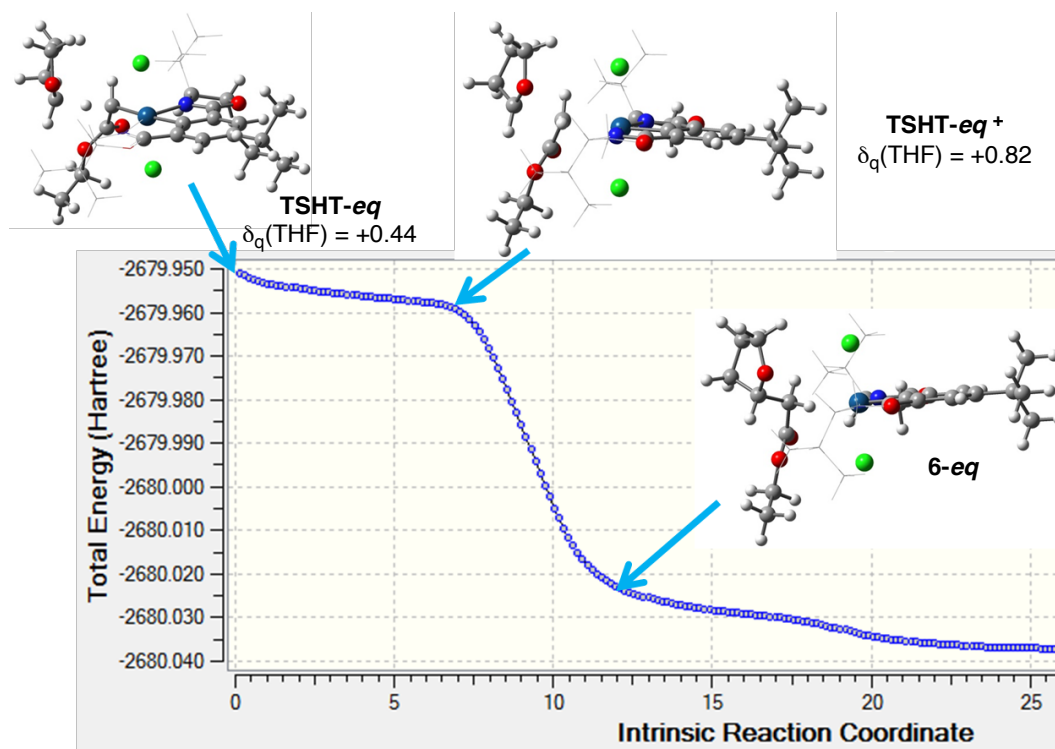


Figure 4.5. Intrinsic reaction coordinate for C-H insertion into THF *via* TSHT-eq.

4.3.3. Factors controlling the enantioselectivity for C-H insertion of ethyl diazoacetate into THF *via* TSHT-eq.

Since the equatorial acceptor iridium carbene geometry **5-eq** was calculated to be favored over the axial carbene geometry **5-ax**, discrimination of the two enantiotopic protons at the methylene site alpha to oxygen depends on the *Re* or *Si* approach of the THF substrate. The lowest energy transition state **TSHT-eq** shown above in Figure 4.4 leads to the (*S*) enantiomer of the insertion product **271**, and this transition state was shown to have a 13.7 kcal·mol⁻¹ energy barrier. In addition, a transition state involving

Re approach of THF was located on the reaction pathway (Figure 4.6). This transition state, denoted as **TSCH-R**, was calculated to have a potential energy barrier of 14.2 kcal·mol⁻¹. For **TSHT-*eq***, the existence of a short O1-H2 distance of 2.038 Å is the result of an electrostatic interaction, which is partially responsible for the lower energy transition state and increased selectivity for the *S* enantiomer of the product **271**.

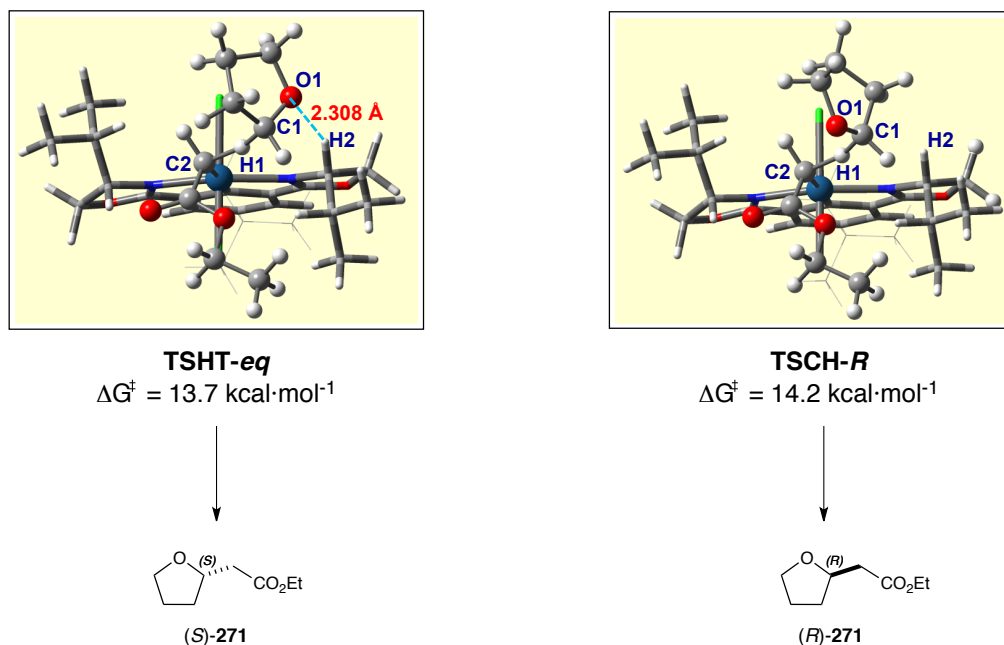


Figure 4.6. Comparison of the transition states leading to the *S* (**TSHT-*eq***) and *R* (**TSCH-R**) enantiomers of THF insertion product **271**.

Unfortunately we have not been able to determine the absolute configuration to support or refute the computationally predicted stereochemical outcome of the iridium(III) phebox catalyzed C-H insertion of ethyl diazoacetate into THF, but this remains an immediate priority in our investigations.

4.3.4. Factors controlling the enantioselectivity for C-H insertion of ethyl diazoacetate into phthalan.

The highest levels of enantioselectivity for acceptor-only C-H insertion were achieved with iridium(III) phebox complex **213** and the phthalan substrate. We were interested to investigate computationally the reasons for the higher selectivity for this substrate compared to THF. To this end, two transition states, **TSCHP-R** and **TSCHP-S**, were located that predict the *R* and *S* insertion products, respectively (Figure 4.7). As observed for the lowest energy THF insertion reaction transition state **TSHT-*eq*** (cf. Figure 4.6), the existence of a short O-H2 distance of 2.355 Å is the result of an electrostatic interaction that is responsible for the lower energy transition state **TSCHP-R**. The potential energy barrier for this transition state was calculated to be 14.9 kcal·mol⁻¹ and predicts the *R* enantiomer of the insertion product **275**. The difference in energy barriers ($\Delta\Delta G^\ddagger$) between **TSCHP-R** and **TSCHP-S**¹ for the C-H insertion of ethyl diazoacetate into phthalan is 3.7 kcal·mol⁻¹, whereas the $\Delta\Delta G^\ddagger$ for the C-H insertion into tetrahydrofuran is smaller at 0.5 kcal·mol⁻¹. Thus, the computationally determined $\Delta\Delta G^\ddagger$ values agree with the higher enantioselectivity observed for the C-H insertion for phthalan. Efforts are ongoing to determine the absolute stereochemistry of the phthalan insertion product **275**.

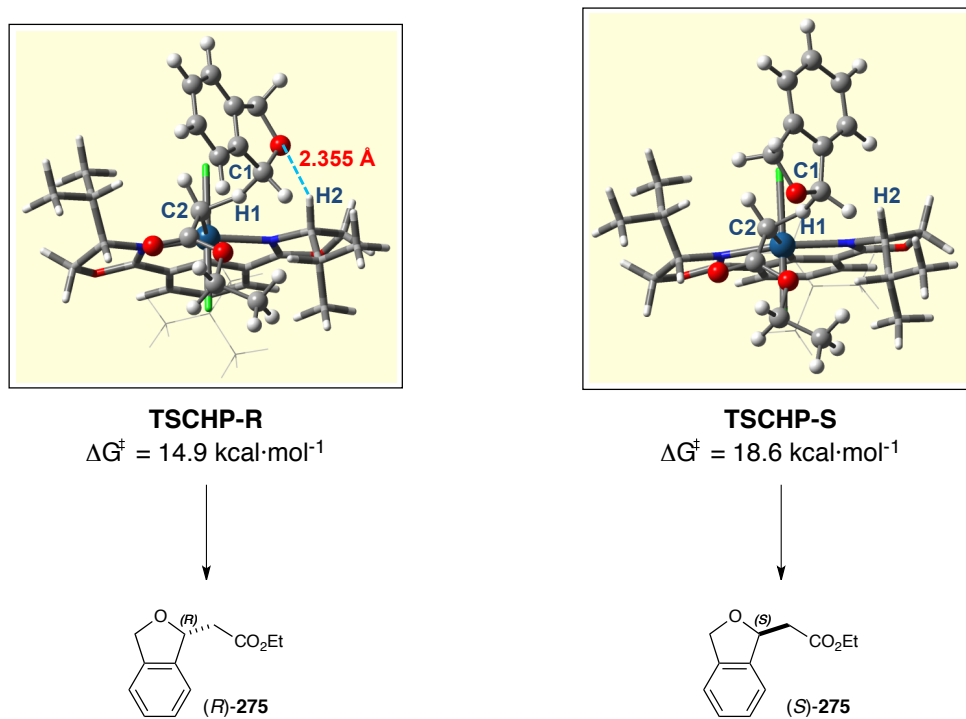


Figure 4.7. Comparison of the transition states leading to the *R* (**TSCHP-R**) and *S* (**TSCHP-S**) enantiomers of phthalan insertion product **275**.

4.4 Bis(imidazolinyl)phenyl (phebim) Iridium(III) Complexes

4.4.1. Introduction

Much like the case of the iridium phebox catalyzed C-H insertion using donor/acceptor carbenes, the substrate scope for the acceptor-only C-H insertion was not as general as we would have liked. Additionally, the enantioselectivity for the iridium phebox catalyzed C-H insertion could not be further increased using the library of phebox complexes we developed. The C-H insertion of ethyl diazoacetate into phthalan using iridium(III) phebox complex **213** to give the insertion product in 76 % ee constituted our best result.

We hypothesized that electronic modification on the iridium complex could potentially affect the enantioselectivity of the insertion reactions. The most direct way to influence the electronics at the iridium metal center would be to replace the *tert*-butyl substituent at the 4 position of the iridium phebox complex with electron donating or electron withdrawing groups. This approach would be difficult in that the substituent must also act to block the undesired cyclometallation reaction during the synthesis of the complex. Alternatively, an electron donating or withdrawing substituent could be added to the 4 position of the 3,5-dimethyl series of iridium(III) phebox complexes. However, synthesis of the requisite diacids containing such modifications would be lengthy, undermining our ability to rapidly access these new phebox catalysts.

To circumvent these concerns we recognized that further electronic and steric variation on the complexes could be achieved by synthesizing the

bis(imidazolinyl)phenyl (phebim) ligands (Figure 4.8). In these ligands the C_2 -symmetry and meridional coordination environment of the NCN pincer framework are preserved, which would provide a similar chiral environment around the metal center as that of the phebox complexes. Replacement of the oxygen atom with a substituted nitrogen atom would permit further tunability of both the electronic and steric environments on the ligand.

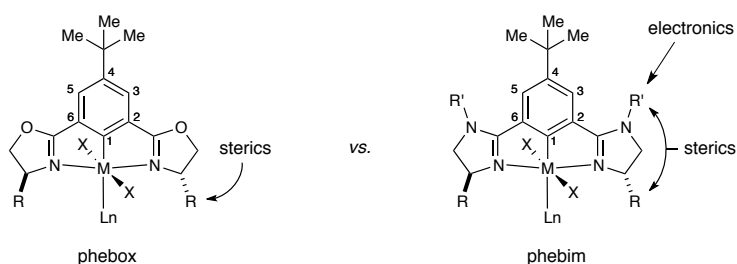
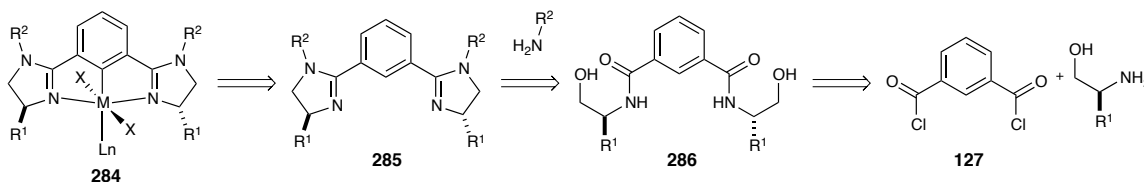


Figure 4.8. Structural differences between phebox and phebox ligands.

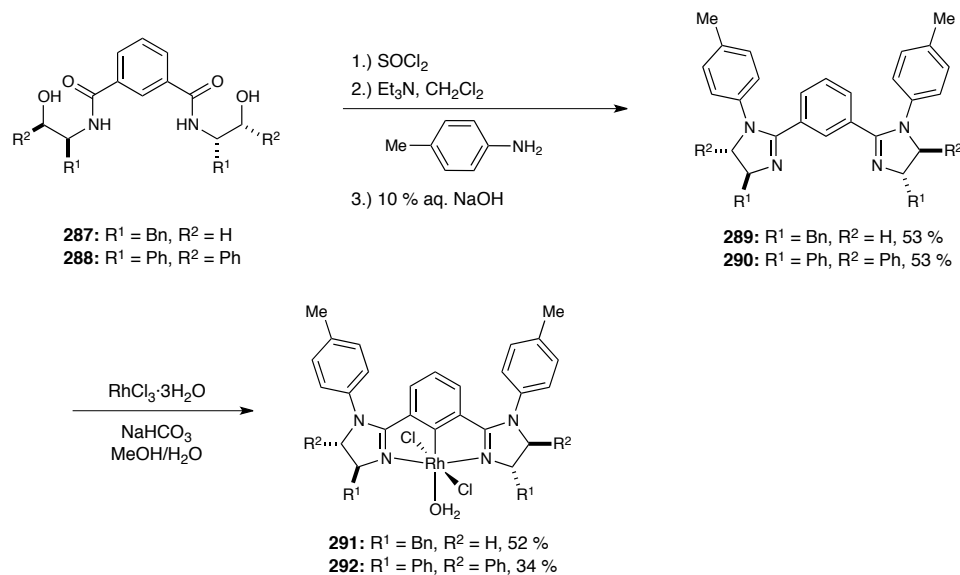
4.4.2. Synthesis of phebox ligands and rhodium(III) complexes thereof.

Phebox complexes **284** are obtained by cyclometallation of the phebox ligands of generic type **285**, which in turn is derived from reacting a primary amine with the bis-amido alcohol **286** (Scheme 4.17). The bis-amido alcohol is then synthesized by the condensation of isophthaloyl dichloride **127** with a chiral amino alcohol.

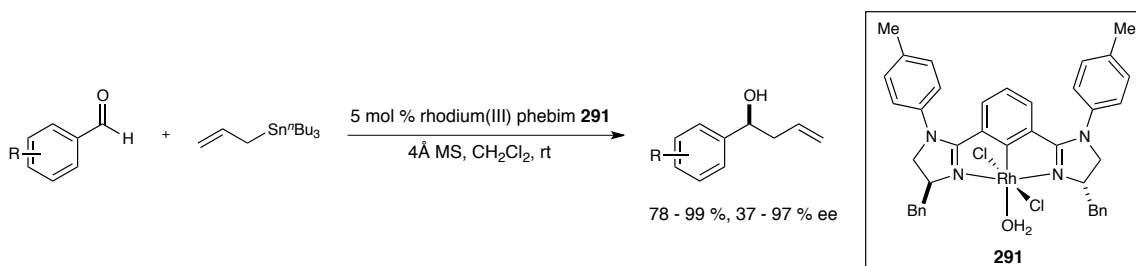


Scheme 4.17. Generalized synthesis of phebox metal complexes.

Despite their structural similarity to phebox ligands, phebox ligands have not been as extensively applied towards catalytic asymmetric reactions.²³⁵ The Song group has previously synthesized palladium,^{236,237} platinum,^{238,239} and nickel²⁴⁰ phebox complexes. Song also reported in 2013 the synthesis of rhodium(III) phebox complexes, which most directly pertain to our studies since catalyst synthesis was achieved by cyclometallation of the phebox ligand using RhCl₃ according to the method reported by Nishiyama.¹⁴¹ Two representative members of the chiral rhodium(III) phebox complexes were synthesized according to Scheme 4.18. The ligands **289** and **290** were synthesized in a one-pot three-step protocol by first refluxing amides **287** and **288** in thionyl chloride.²³⁷ After concentration, Et₃N and 4-methylaniline were added and the reaction was stirred overnight. Ligands **289** and **290** were both obtained in 53 % yield after workup with aqueous NaOH and purification by silica gel column chromatography. Metallation was realized by refluxing the ligand in rhodium trichloride to give rhodium(III) chloro phebox complexes **291** and **292** in 52 % and 34 % yields, respectively.^{170,241} Complex **291** was very effective for the catalytic enantioselective allylation of benzaldehydes, providing the allylic alcohols in up to 99 % yield and 97 % ee (Scheme 4.19).¹⁷⁰ The yields and enantioselectivities using the phebox complexes were generally higher yielding than those reported by Nishiyama for the analogous rhodium(III) phebox complexes (*cf.* Chapter 3, scheme 3.11).¹⁴⁶



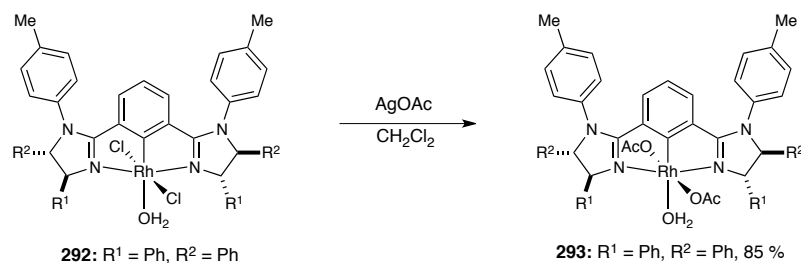
Scheme 4.18. Song's synthesis of rhodium(III) phebox complexes **291** and **292**.



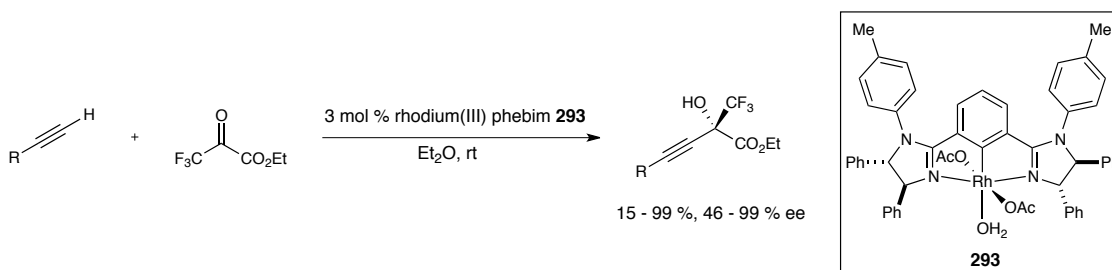
Scheme 4.19. Rhodium(III) phebox **291** catalyzed asymmetric allylation of benzaldehydes.

The chloride ligands could also be exchanged for acetate ligands by treating the phebox complex **292** with AgOAc in dichloromethane, giving rise to the acetate complex **293** in 85 % yield (Scheme 4.20).²⁴¹ The acetate complex **293** was found to catalyze the asymmetric alkynylation of trifluoropyruvates with terminal acetylenes in up to 99 % yield and 99 % enantioselectivity (Scheme 4.21). The acetate ligands on the complex

were necessary for reactivity, and the rhodium(III) chloro complexes were unreactive in this chemistry.



Scheme 4.20. Chloride ligand exchange in rhodium(III) phebox complex **292**.



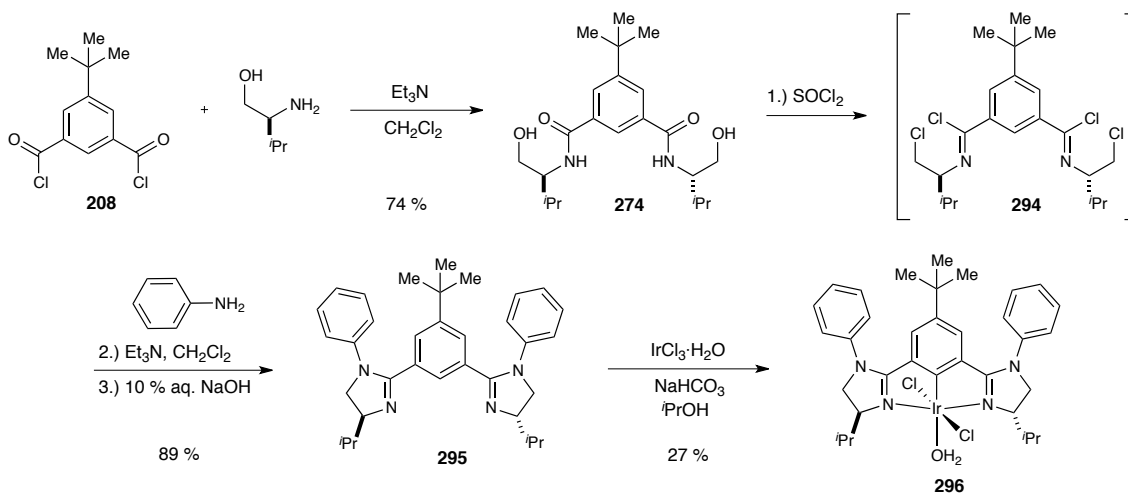
Scheme 4.21. Rhodium(III) phebox **293** catalyzed asymmetric alkylation of trifluoropyruvates.

4.4.3. Synthesis of phebox ligand **295** and its iridium(III) phebox complex **296**

With the precedence that the phebox ligand can be metallated in a similar fashion to the phebox ligands using RhCl_3 , we rationalized that the synthesis of iridium(III) phebox complexes could be achieved by metallating the phebox ligands with IrCl_3 . We sought to obtain the imidazoline ligand that retained the isopropyl functionality on the chiral portion of the ligand since this group provided the best enantioselectivity in the iridium(III) phebox catalyzed enantioselective intermolecular acceptor-only C-H

insertion using ethyl diazoacetate. Furthermore, we wanted to first incorporate an aromatic substituent on the nitrogen that was as electron neutral as possible.

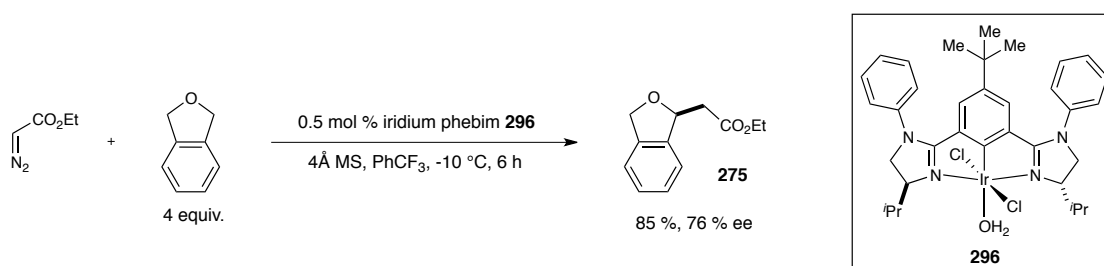
To this end, isopropyl substituted amide **274** was synthesized in 74 % yield from *tert*-butyl isophthaloyl dichloride and L-valinol (Scheme 4.22). Reacting the amide **274** with SOCl₂ formed the crude chloroimidate intermediate **294**. This intermediate was condensed directly with aniline in the presence of triethylamine, and upon workup with aqueous 10 % NaOH ligand **295** was formed in 89 % yield. Gratifyingly, the iridium(III) phebox complex *N*-Ph[(*S,S*)-^{*t*}BuPhebim-^{*i*}Pr]IrCl₂(OH₂) **296** was successfully synthesized by metallation of the ligand **295** with iridium trichloride, albeit in 27 % yield. This complex was stable to air and moisture and purified by silica gel column chromatography.



Scheme 4.22. Synthesis of phebox ligand **295** and its iridium(III) phebox complex **296**.

4.4.4. Enantioselective intermolecular C-H insertion of ethyl diazoacetate into phthalan catalyzed by iridium(III) phebox complex **296**

To ensure that these new iridium phebox complexes were competent catalysts for enantioselective intermolecular acceptor-only C-H insertion, we began by adding a solution of ethyl diazoacetate in PhCF₃ over the course of five hours to a -10 °C mixture of four equivalents phthalan, 0.5 mol % iridium(III) phebox complex **296**, and 4Å molecular sieves. We were pleased to find that complex **296** performed asymmetric C-H insertion using ethyl diazoacetate, and the insertion product **275** was formed in 85 % yield with 76 % enantioselectivity (Scheme 4.23). The yield and selectivity were nearly identical to that obtained by the analogous isopropyl substituted iridium(III) phebox complex **213**, which provided the insertion product in 81 % yield and 76 % ee (*cf.* Table 4.3). While this new phebox complex did not provide a significant increase in reaction yield or selectivity, it provided a suitable reference point for us to evaluate the effects of electronic variation on the aromatic ring of the substituted nitrogen on the imidazoline ligand.



Scheme 4.23. Iridium(III) phebox **296** catalyzed enantioselective acceptor-only C-H insertion of ethyl diazoacetate into phthalan.

4.4.5. Synthesis of electronically varied iridium(III) phebox ligands **295**, **297-300** and their iridium(III) phebox complexes **296**, **301-304**

A series of electron-rich and deficient ligands were synthesized in order to systematically investigate whether or not varying the electronics on the imidazoline nitrogen of the iridium(III) phebox complexes had a substantial impact on the yield and selectivity for the C-H insertion of ethyl diazoacetate into phthalan. A variety of electronically differentiated aniline derivatives were employed in the reaction sequence involving isopropyl-substituted amide **274**, and ligands **295**, **297-300** were synthesized in 78-89 % yields (Table 4.5).

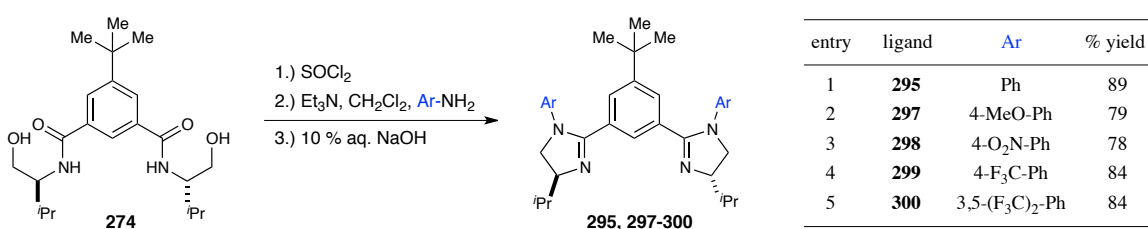


Table 4.5. Synthesis of electronically varied *N*-aryl isopropyl phebox ligands **295**, **297-300**.

Each of these ligands was metallated with iridium trichloride in the presence of sodium bicarbonate in refluxing isopropanol, and the corresponding iridium(III) phebox chloro complexes **296**, **301-304** were obtained in 15-61 % yields following purification by silica gel chromatography (Table 4.6). Complexes **301** and **302** were purified using preparative TLC since these complexes were obtained in unsatisfactory yield (< 5 %) upon purification by flash column chromatography.

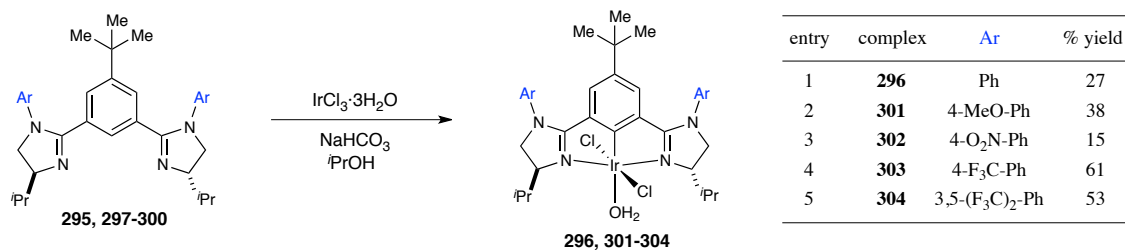
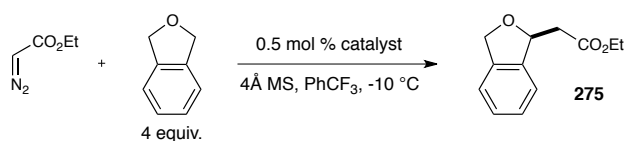


Table 4.6. Synthesis of iridium(III) phebox complexes **296**, **301-304**.

4.4.6. Catalytic activity of electronically varied iridium(III) phebox complexes **301-304** for C-H insertion of ethyl diazoacetate into phthalan

These new catalysts were then evaluated for their performance in the C-H insertion of ethyl diazoacetate into phthalan under our standard conditions. Electron-donating *para*-methoxyphenyl substituted iridium phebox complex **301** furnished the insertion product in only 26 % yield (Table 4.7, entry 2), however the enantioselectivity increased to 78 % from 76 % (entry 1). Placing a strongly electron-withdrawing nitro substituent on the aromatic ring provided an increase in enantioselectivity to 80 % with a 70 % yield (complex **302**, entry 3). Both the *para*-trifluoromethylphenyl (**303**, entry 4) and the 3,5-bis-(trifluoromethyl)phenyl (**304**, entry 5) iridium phebox complexes delivered **275** with identical enantioselectivity at 80 %, with the iridium complex **304** giving the better yield at 84 %. These results show that the iridium(III) phebox complexes with electron-withdrawing functionality on the imidazoline nitrogen perform the best in terms of enantioselectivity. While these studies do not provide a clear correlation for change in electronics on the catalyst with enantioselectivity, but it does show that increasing the electron density on the aryl

nitrogen substituent greatly impacts the yield of the reaction. Furthermore, the ability to make subtle changes on the iridium(III) phebox complexes by altering nitrogen substitution highlights the increased tunability of these complexes relative to the iridium(III) phebox complexes. While the *para*-nitrophenyl containing catalyst **302** gave **275** in 70 % yield and 80 % ee, it was not evaluated further due to the poor yield for the ligand metallation. Even though the 3,5-bis(trifluoromethyl)phenyl iridium phebox complex **304** provided the highest yield of product **275** with 80 % ee, we decided to move forward with the *para*-trifluoromethylphenyl functionality on the imidazoline nitrogen since the yield of the metallation to form **303** was slightly higher at 61 % compared to 53 % with complex **304**.



entry ^a	catalyst	Ar	% yield ^b	ee ^c
1	296	Ph	85	76
2	301	4-MeO-Ph	26	78
3	302	4-O ₂ N-Ph	70	80
4	303	4-F ₃ C-Ph	73	80
5	304	3,5-(F ₃ C) ₂ -Ph	84	80

^a A 0.29 M solution of ethyl diazoacetate in PhCF₃ was added over 5 hours to a -10 °C mixture of iridium catalyst, phthalan (4 equiv.), and 4 Å MS in PhCF₃. EDA was consumed immediately upon complete addition. ^b Isolated yield. ^c Determined by chiral HPLC. The absolute stereochemistry was not determined.

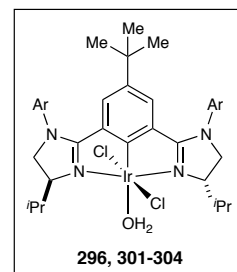
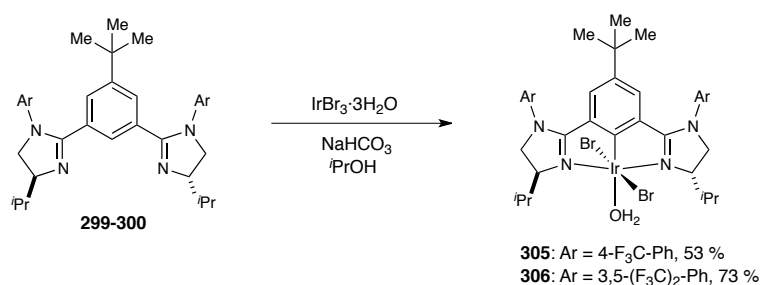


Table 4.7. Evaluation of electronic effects imparted by iridium(III) phebox chloro complexes **296**, **301-304** on the enantioselective C-H insertion of ethyl diazoacetate into phthalan.

4.4.7. Synthesis of iridium(III) bromo phebox complexes **305** and **306** and their reactivity towards C-H insertion of ethyl diazoacetate into phthalan

We were also curious to see if exchanging the chloride ligands for bromide ligands on the phebox complexes had an effect on yield and enantioselectivity. To this end, iridium(III) bromo phebox complexes **305** and **306** were synthesized by metallating ligands **299** and **300** with iridium tribromide (Scheme 4.24). C-H insertion into phthalan using ethyl diazoacetate with complex **305** proceeded in 83 % yield and 76 % ee (Table 4.8, entry 1), while the reaction with complex **306** furnished **275** in 45 % yield and 77 % ee (entry 2). In both cases, using the bromide complexes results in a lower enantioselectivity for the reaction when compared to the analogous chloro complexes **303** and **304** (Table 4.7). The same trend of decreasing enantioselectivity was observed in the iridium(III) phebox catalyzed C-H insertion of ethyl diazoacetate into phthalan (*cf.* Scheme 4.10).



Scheme 4.24. Synthesis of iridium(III) bromo phebox complexes **305** and **306**.

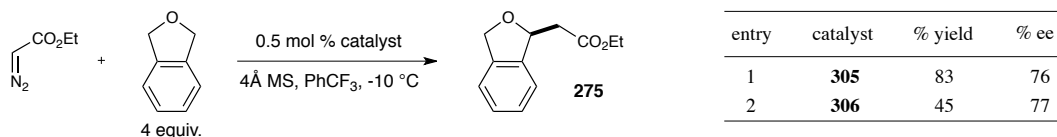


Table 4.8. C-H insertion of ethyl diazoacetate into phthalan using iridium(III) bromo phebox complexes **305** and **306**.

4.4.8. Synthesis of *sec*-butyl, cyclohexyl, *iso*-butyl, and CH₂-cyclohexyl iridium(III) chloro phebox complexes **311** - **314**

The isopropyl functionality was determined to be the best in terms of reaction enantioselectivity for the iridium(III) phebox catalyzed acceptor-only C-H insertion reactions. Having settled on the *N*-atom substituent and the chloride ligands on the phebox complexes, we decided to explore further steric variation on the imidazoline ligand framework that mimicked the chiral environment imposed by the isopropyl group. We identified the *sec*-butyl, cyclohexyl, *iso*-butyl, and CH₂-cyclohexyl chiral amino alcohols that fit this criterion (Figure 4.9). The isopropyl-mimicking portion of the substituent is highlighted in red. The amides **274**, **307-310** were synthesized in 54 - 99 % yield by stirring with the corresponding amino alcohol and **208** in triethylamine (condition **A**) or by stirring in aqueous potassium bicarbonate (condition **B**). The matching *N*-*para*-trifluoromethylphenyl substituted phebox ligands **299**, **311-314** were synthesized in 21 - 84 % yield.

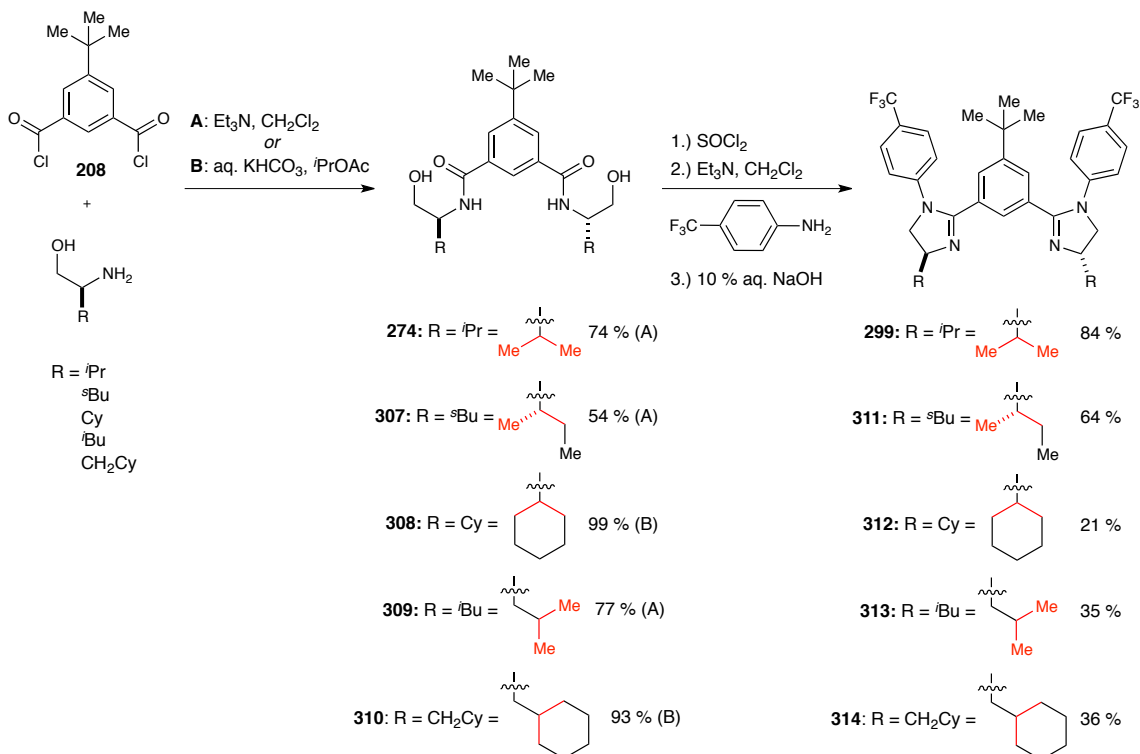
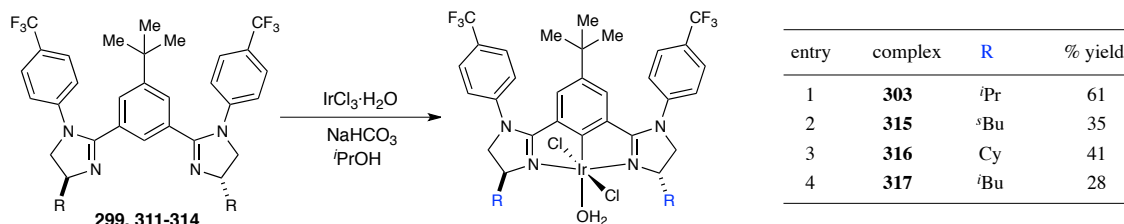


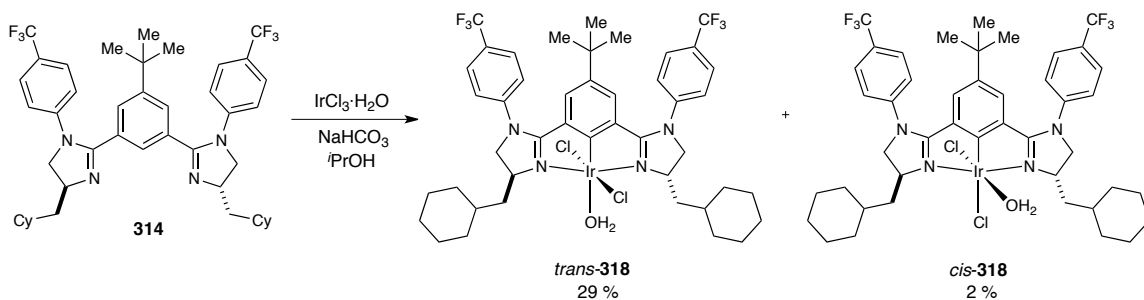
Figure 4.9. Synthesis of amides **274**, **307-310** and *N-para*-trifluoromethylphenyl phebox ligands **299**, **311-314**.

Each of these ligands was then metallated by refluxing them in IrCl₃·3H₂O in the presence of NaHCO₃, and the C₂-symmetric iridium(III) complexes bearing isopropyl (**303**), *sec*-butyl (**315**), cyclohexyl (**316**), and isobutyl (**317**) substituted imidazolines were formed in 28-61 % yield (Scheme 4.25) as red/orange solids following purification by either flash column chromatography or preparative thin-layer chromatography (Scheme 4.25). These complexes were stable to air and moisture and stored on the bench top.



Scheme 4.25. Synthesis of iridium(III) phebox complexes **303**, **315-317**.

An interesting result was obtained during the synthesis and purification of CH₂-cyclohexyl substituted iridium(III) phebox complex **318** by preparative thin-layer chromatography. The crude reaction mixture was purified by preparative thin layer chromatography and the anticipated complex *trans*-**318** eluted as the first orange band (R_f 0.63, 30 % EtOAc : hexanes), which was isolated in 29 % yield (Scheme 4.26). A second orange band at R_f 0.22 was also isolated, albeit in 2 % yield. This band corresponded to the *axial* aqua CH₂-cyclohexyl complex *trans*-**318**, where the water ligand is coordinated in the apical position, and was identified as such by ¹H NMR spectroscopy. The ¹H NMR spectrum showed a loss of C₂-symmetry as indicated by the six signals that integrate for 1 proton each between 4.8 and 4.0 ppm, which correspond to the protons located on the imidazoline ring. Figure 4.10 shows the overlaid ¹H NMR spectra of the C₂-symmetric “*trans*” complex *trans*-**318** (blue) with the isomerized “*cis*” complex *cis*-**318** (black).



Scheme 4.26. Synthesis of the *trans* and *cis* CH₂-cyclohexyl iridium phebox complexes *trans*-318 and *cis*-318.

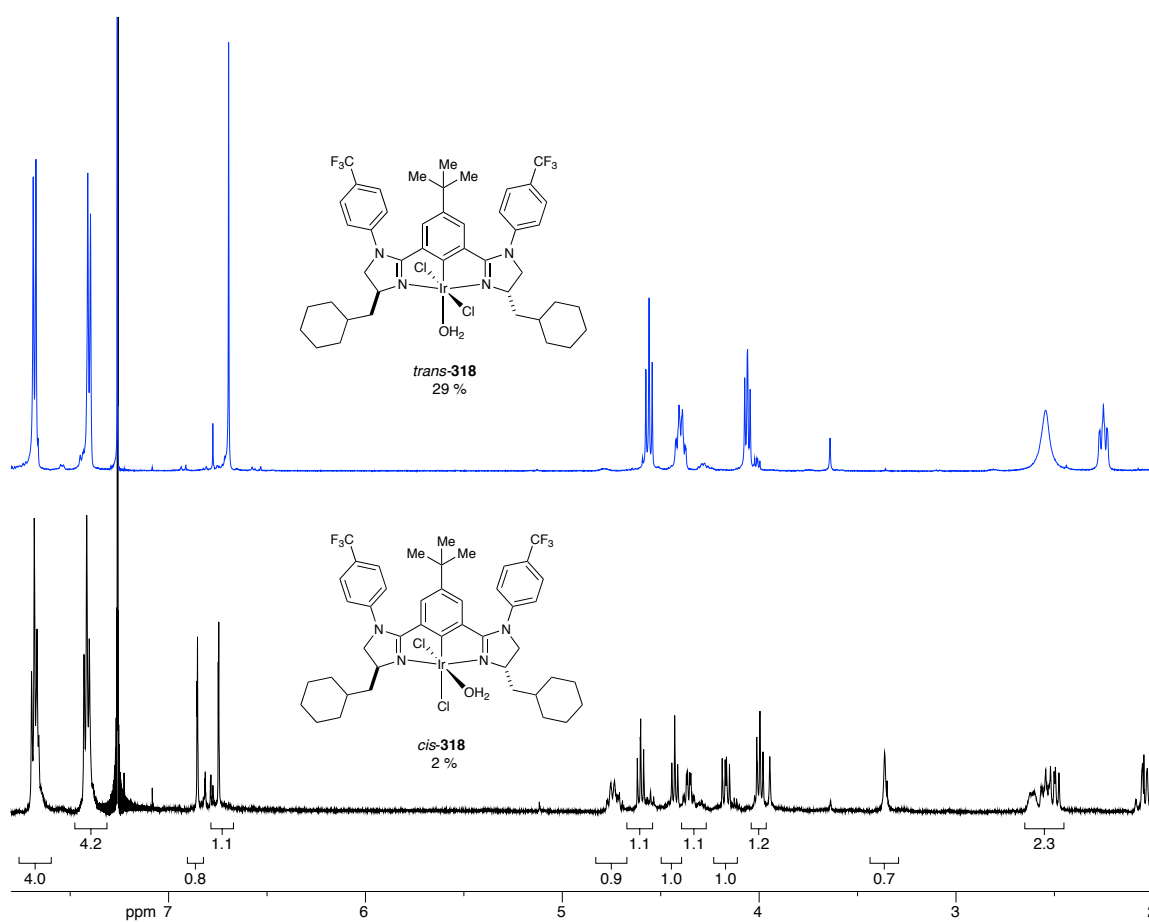
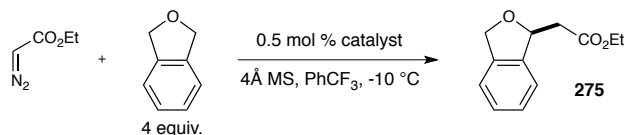


Figure 4.10. Stacked ¹H NMR spectra of the *trans* iridium(III) complex *trans*-318 (blue) and the *cis* iridium(III) phebox complex *cis*-318 (black).

4.4.9. Catalytic activity of *sec*-butyl, cyclohexyl, *iso*-butyl, and CH₂-cyclohexyl iridium(III) chloro phebox complexes 315-318

With these six new complexes in hand, their catalytic activity in the intermolecular C-H insertion of ethyl diazoacetate in phthalan was investigated (Table 4.9). Entry 1 shows the result obtained using the original isopropyl-substituted iridium(III) phebox complex **299**, which gave a 73 % yield and 80 % enantioselectivity. The *sec*-butyl substituted phebox complex **315** furnished **275** in 81 % yield and 83 % enantioselectivity (entry 2). Cyclohexyl substitution on the imidazoline framework provided the insertion product **275** in 83 % yield with 80 % enantioselectivity (**316**, entry 3). Using the *iso*-butyl substituted complex **317** resulted in a significant increase in both yield and enantioselectivity to 95 % and 89 %, respectively (entry 4). The *trans* CH₂-cyclohexyl catalyst *trans*-**318** provided an 80 % yield of **275** with the highest enantioselectivity at 90 % (entry 5). Intriguingly, the *cis*-CH₂-cyclohexyl catalyst *cis*-**318** also furnished the **275** in 89 % ee (entry 6).



entry ^a	catalyst	R	% yield ^b	ee ^c
1	299	ⁱ Pr	73	80
2	315	^t Bu	81	83
3	316	Cy	83	80
4	317	^t Bu	95	89
5	<i>trans</i> - 318	CH ₂ Cy	80	90
6	<i>cis</i> - 318	CH ₂ Cy	- ^d	89

^a A 0.29 M solution of ethyl diazoacetate in PhCF₃ was added over 5 hours to a -10 °C mixture of iridium catalyst, phthalan (4 equiv.), and 4 Å MS in PhCF₃. EDA was consumed immediately upon complete addition. ^b Isolated yield. ^c Determined by chiral HPLC. The absolute stereochemistry was not determined. ^d The yield was not determined.

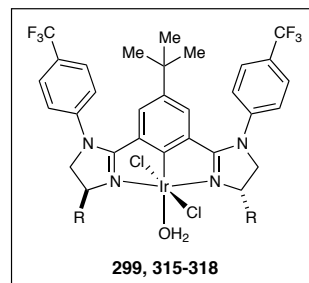


Table 4.9. Evaluation of iridium(III) phebox complexes **299**, **315-318** for the enantioselective C-H insertion of ethyl diazoacetate into phthalan.

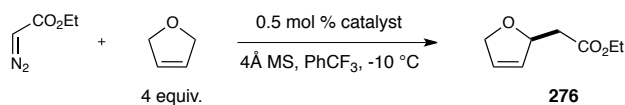
The results for entries 5 and 6 are interesting because they imply that the same reactive carbene isomer, which ultimately controls the selectivity for the insertion reaction, is accessible from both the *cis* and *trans* isomers of the CH₂-cyclohexyl precatalysts. There is no significant difference in selectivity between the two catalysts, and it seems unlikely that both the *cis* and *trans* carbene geometries provide nearly identical selectivity. This unfortunately does not provide any further insight into the reactive geometry of the carbene intermediate, but is consistent with the hypothesis that isomerization is possible under the reaction conditions.

4.4.10. C-H insertion of ethyl diazoacetate into 2,5-dihydrofuran and THF.

As we had obtained the highest combination of yield and enantioselectivity with the isobutyl iridium(III) phebox complex **317** for the C-H insertion reaction of ethyl

diazoacetate into phthalan, we wanted to test the generality of this catalyst for the insertion into other substrates that contained doubly activated (ethereal/allylic, ethereal/benzylic) prochiral methylene C-H bonds.

The first substrate we evaluated was 2,5-dihydrofuran, which contained both allylic and ethereal C-H bonds. In fact, catalyst **317** provided the insertion product **276** in 76 % yield and 74 % ee (entry 1, Table 4.10). Both of these values are higher relative to the isopropyl iridium(III) phebox **213** catalyzed C-H insertion, which exhibited a 42 % yield and 72 % ee (*cf.* Scheme 4.12). The reaction with the isopropyl substituted iridium(III) phebox complex **299** has not yet been performed, so unfortunately a direct comparison between the two catalyst systems cannot be made. The reaction with the CH₂-cyclohexyl substituted iridium(III) phebox complex *trans*-**318** further increased the yield and enantioselectivity to 77 % and 76 %, respectively. The trend in increasing enantioselectivity for insertion into this substrate was also observed for the C-H insertion of ethyl diazoacetate into phthalan. Once again, cyclopropanation of the olefin was not observed in the crude reaction mixture.



entry	complex	R	% yield	% ee
1	317	<i>i</i> Bu	76	74
2	<i>trans</i> - 318	CH ₂ Cy	77	76

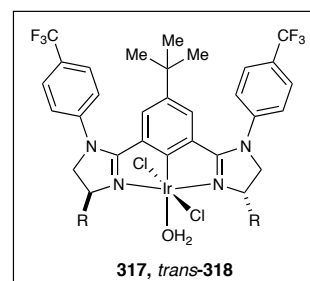
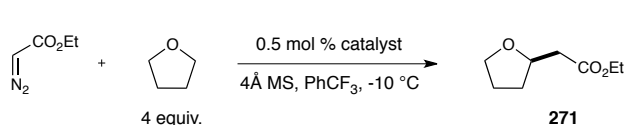


Table 4.10. Performance of iridium(III) phebox complexes **317** and *trans*-**318** for the enantioselective C-H insertion of ethyl diazoacetate into 2,5-dihydrofuran.

As described in section 4.2.5, the C-H insertion of ethyl diazoacetate into THF using iridium(III) phebox catalysts proceeded in 51 % yield with 61 % enantioselectivity. We expected that the iridium(III) phebox complexes would give an increased enantioselectivity for the insertion into THF since this trend was observed for the insertion reactions into both phthalan and 2,5-dihydrofuran. Disappointingly, the reaction of ethyl diazoacetate and THF in the presence of isobutyl-substituted iridium(III) phebox complex **317** resulted in 53 % yield of product **271** with a dramatic drop in enantioselectivity to 37 % (Table 4.11, entry 1). Furthermore, the reaction with CH₂-cyclohexyl substituted iridium(III) phebox complex *trans*-**318** was poorly yielding at 14 % with a 36 % enantiomeric excess (entry 2). It is obvious that these iridium(III) phebox complexes are inferior catalysts for this substrate when compared to iridium phebox complex **213**. However, a direct comparison with the phebox and phebox catalysts cannot be made since the *N-p*-F₃CPh isopropyl-substituted phebox complex **299** has not been evaluated for its catalytic activity for the C-H insertion of ethyl diazoacetate into THF. The direct comparison between these catalyst families will be the subject of future work.



entry	catalyst	R	% yield	% ee
1	317	<i>i</i> Bu	53	37
2	<i>trans</i> - 318	CH ₂ Cy	14	36

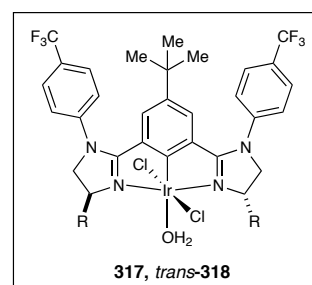
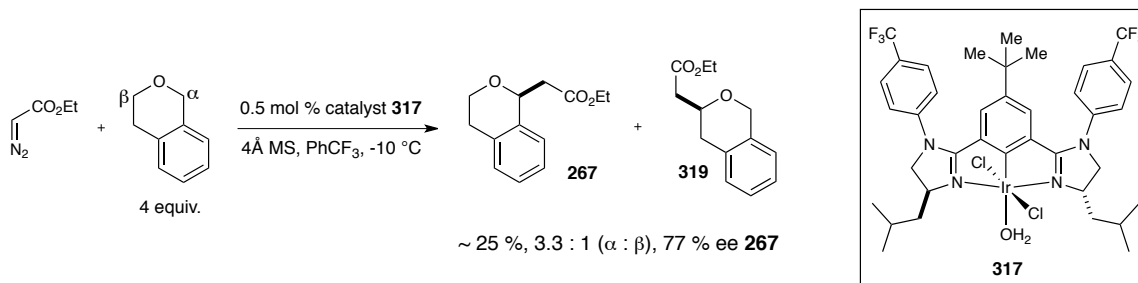


Table 4.11. Performance of iridium(III) phebox complexes **317** and *trans*-**318** for the enantioselective C-H insertion of ethyl diazoacetate into tetrahydrofuran.

4.4.11. Iridium(III) phebim catalyzed C-H insertion of ethyl diazoacetate into isochroman.

The studies conducted so far with the iridium(III) phebim catalysts have been conducted using substrates that contained C-H bonds alpha to oxygen within a five membered ring system. We know that the iridium(III) phebox catalysts cannot perform acceptor-only insertion into the ethereal C-H bonds of saturated six membered *O*-heterocycles. We were curious if using a substrate containing a doubly activated site would enable C-H insertion using ethyl diazoacetate. To this end, we chose isochroman as the substrate to test iridium(III) phebim catalyst **317**, since the most likely site for C-H insertion is the benzylic/ethereal site, or alpha position. Additionally, the product from insertion would be the common intermediate (*S*)-**267** for the synthesis of dopamine D₄ antagonist Sonopiprazole (cf., Scheme 4.1 and 4.2). For this substrate however, there is also a potentially competing site for insertion at the non-benzylic methylene site alpha to oxygen, or beta position. Performing the insertion reaction with ethyl diazoacetate, 4 equivalents isochroman, 0.5 mol % iridium(III) phebim complex **317**, and 4 Å MS in PhCF₃ resulted in ~ 25 % yield of 3.3:1 mixture of inseparable regioisomers **267** and **319** after column chromatography, favoring insertion at the alpha position (Scheme 4.27). Some of the diethyl maleate dimer was also present in the mixture. Notably, this reaction required an additional 14 hours of stirring at -10 °C for complete consumption of ethyl diazoacetate. The enantiomeric excess of ester **267** was determined by reduction to the alcohol (cf. Scheme 4.28 and Figure 4.12, *vide infra*).



Scheme 4.27. Iridium(III) phebox **317** catalyzed C-H insertion of ethyl diazoacetate into isochroman. The absolute stereochemistry was not determined.

The ratio of alpha to beta insertion products **267** and **319** was determined using ^1H NMR by integration of the methine protons at the sites of insertion. The signal corresponding to the alpha insertion product **267** appears as a multiplet between 3.79 and 3.84 ppm (Figure 4.11) and is in agreement with the literature.²¹⁴ The signal corresponding to the beta insertion product **319** appears at 3.90 ppm.

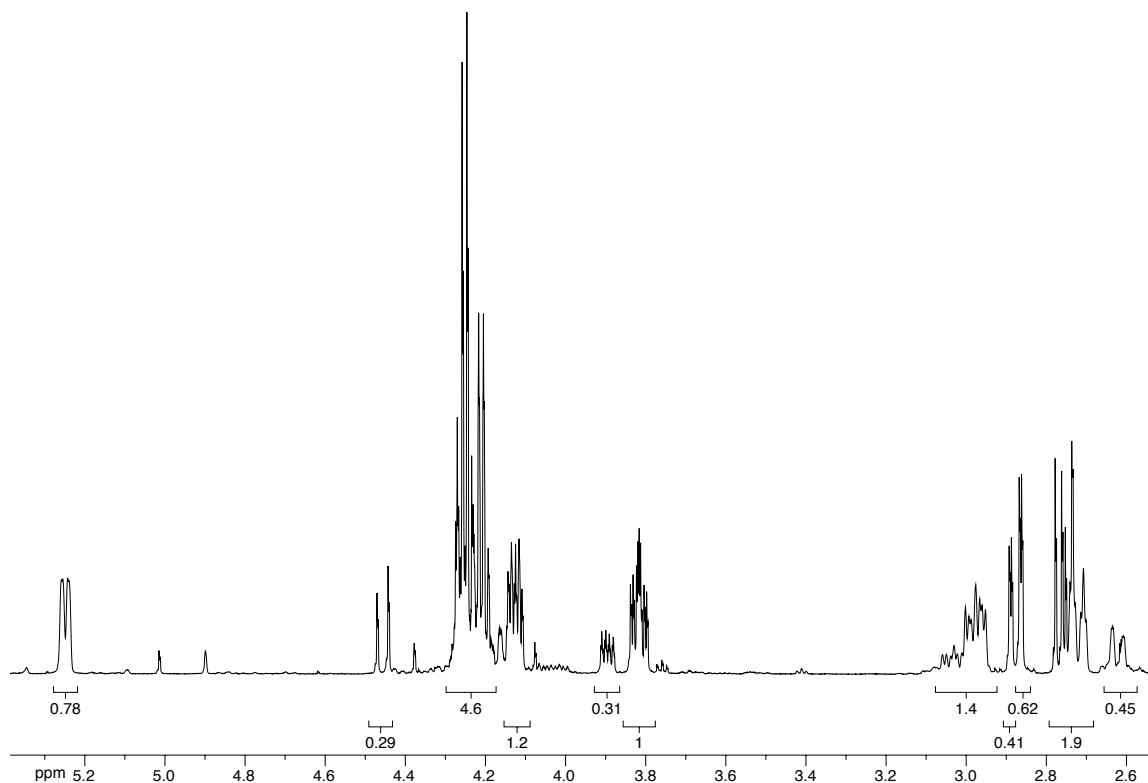
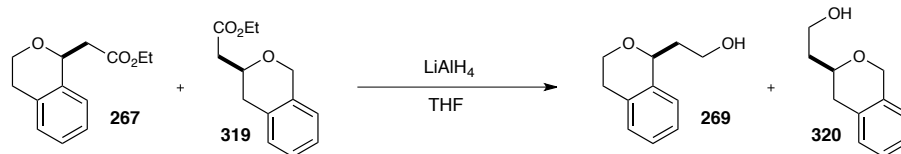
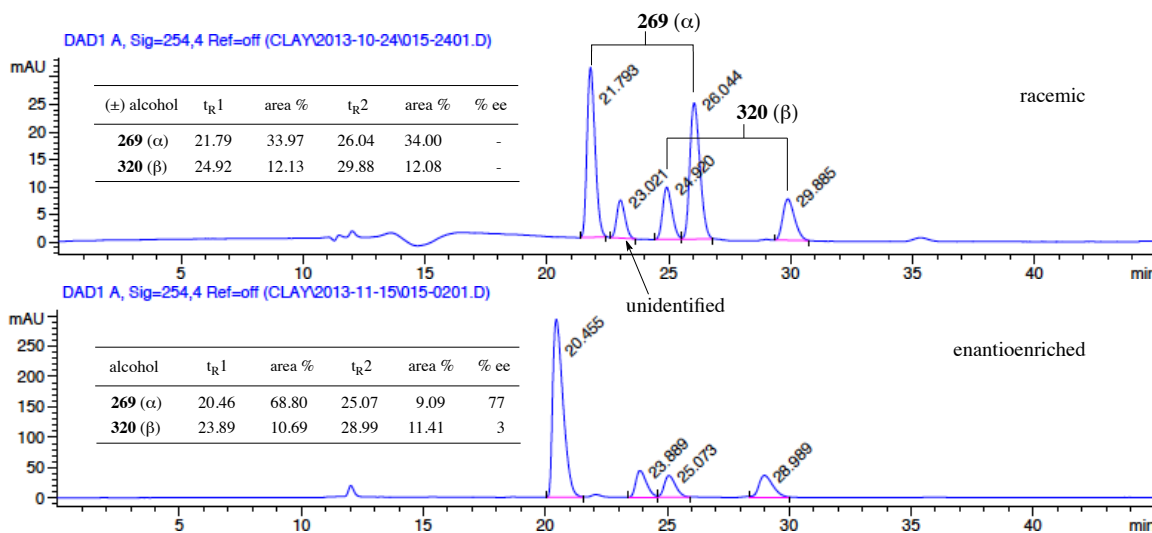


Figure 4.11. ^1H NMR spectrum of the combined insertion products **267** and **319**.

In an effort to obtain an HPLC assay for each regioisomeric ester, **267** and **319** were reduced to their corresponding alcohols **320** and **321** using LiAlH_4 in THF (Scheme 4.28). Using this tactic, both regioisomers and their diastereomers were separated, and the HPLC chromatograms are shown in Figure 4.12. The alpha insertion product **269** was formed in 77 % ee (20.46 and 25.07 min), while the beta insertion product **320** was formed in only 3 % ee (23.89 and 28.99 min). The signal at 23.021 min in the HPLC trace of the racemic sample was unidentified, but the signals corresponding to the alcohol products were confirmed by spiking the enantioenriched sample with racemic material.

Scheme 4.28. Reduction of esters **267** and **319** using LiAlH₄.Figure 4.12. HPLC chromatograms for the determination of enantiopurity of alcohols **269** and **320**.

4.5 Conclusions

We have discovered that our iridium(III) phebox complexes are competent catalysts for asymmetric acceptor-only intermolecular C-H functionalization of phthalan, tetrahydrofuran, and 2,5-dihydrofuran. The reaction with 2,5-dihydrofuran is remarkably chemoselective for C-H insertion over cyclopropanation. However, extension to other cyclic and acyclic ethers using these catalysts has not been achieved.

DFT calculations have been performed to help elucidate the nature of the reactive intermediates for iridium(III) phebox catalyzed acceptor-only C-H insertion into THF and phthalan. The results show that the equatorial iridium carbene is likely the reactive intermediate in these reactions. Furthermore, the potential energy barriers for C-H functionalization of THF and phthalan using our iridium phebox catalysts are markedly higher than those calculated for dirhodium(II) tetracarboxylate catalyzed acceptor-only C-H insertion into cyclopentane and 1,4-cyclohexadiene.⁷ This increased energy barrier for C-H insertion helps explain why enantioselective intermolecular C-H insertion is achievable using ethyl diazoacetate as the carbene source under iridium phebox catalysis.

The development of the more tunable iridium(III) phebox complexes has led to increased levels of enantioselectivity for C-H insertion into phthalan and 2,5-dihydrofuran in up to 90 % ee and 76 % ee, respectively. This new class of iridium(III) phebox complexes offers an extra point of modification compared to the iridium(III) phebox complexes. Further modification on the iridium phebox complex framework may indeed allow for increased substrate scope and enhanced reactivity towards enantioselective intermolecular acceptor-only C-H functionalization.

Chapter 5

Iridium(III) Phebox Catalyzed C-H Amination

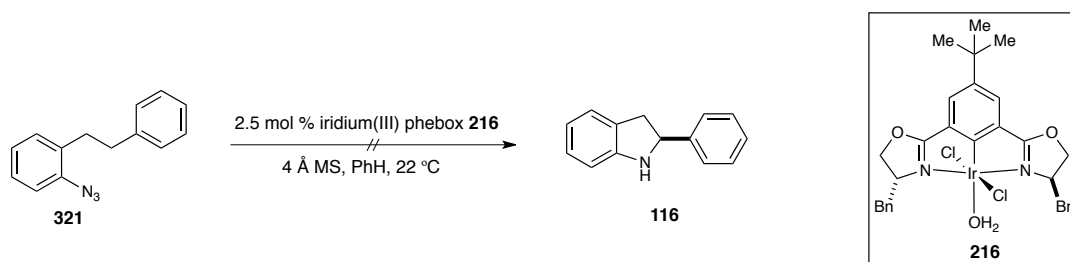
As outlined in Chapter 2, the field of iridium catalyzed metallonitrene C-H amination is far less developed than iridium catalyzed metallocarbene C-H functionalization. Katsuki established iridium(III) salen complexes as efficient catalysts for intramolecular C-H amination using aryl sulfonyl azides as nitrene precursors.¹³⁰ The Driver group demonstrated that iridium(I) salt $[\text{Ir}(\text{cod})\text{OMe}]_2$ was an effective catalyst for intramolecular benzylic C-H amination using simple aryl azides as the metallonitrene precursors.¹³⁷ This was the first reported example of simple aryl azides, which did not contain an electron-withdrawing group directly attached to the azide, undergoing C-H amination *via* a metallonitrene.

The main focus of our research has involved the development and use of new iridium(III) phebox and iridium(III) phevim complexes for enantioselective intermolecular metallocarbene C-H functionalization. During our initial exploration of iridium(III) metallocarbene reactivity, we simultaneously investigated the catalytic activity of iridium(III) phebox complexes **216**, **174**, and **201** for metallonitrene mediated C-H amination.

5.1 Iridium(III) phebox catalyzed intramolecular C-H amination using aryl azides

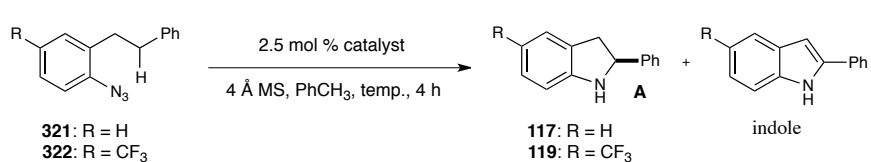
Driver observed that the indoline products from the azide amination reaction were formed in good yields, and placing the electron poor CF_3 group *para* to the azide resulted in the highest yield of the indoline product. However, electron-donating substituents on the aromatic ring that contained the azide were not amenable for this reaction. Additionally, formation of the indole product was a problematic side reaction. Enantioenriched indolines are present in numerous biologically active molecules, but methods for their synthesis remain scarce.²⁴²⁻²⁴⁵ Therefore we were curious to investigate if the iridium(III) phebox catalysts could perform enantioselective metllonitrene atom transfer using simple aryl azides as the nitrene precursors.

Our studies initiated by reacting aryl azide **321**¹³⁷ with 2.5 mol % iridium(III) phebox complex **216** in the presence of 4Å MS in benzene at room temperature (Scheme 5.1). Unfortunately, no reaction occurred and the starting azide **321** remained fully intact as determined by ¹H NMR analysis of the crude mixture.



Scheme 5.1. Reaction of iridium(III) phebox complex **216** with aryl azide **321** at room temperature.

We were pleased to find that running the reaction with complex **216** in toluene at 80 °C resulted in an 11 % conversion of the azide **321** and a 12 : 1 ratio of indoline **117** to indole as determined by ¹H NMR analysis, although the enantiopurity of the indoline was low at 35 % ee (Table 5.1, entry 1). Refluxing the reaction in toluene led to 98 % conversion of the aryl azide (entry 2), but the ratio of indoline to indole decreased to 1.6:1 and the enantioselectivity dropped to 28 % ee. For Blakey's ruthenium(II) pybox catalyzed enantioselective intramolecular C-H amination of sulfamate esters, a catalytic amount of silver triflate was added to abstract a halide from the catalyst.⁷⁸ This additive was crucial for increasing the reaction yield and enantioselectivity. In an effort to achieve the same effect in our system we added 2.5 mol % AgOTf to the reaction mixture, but the conversion and enantioselectivity of the reaction both decreased to 10 % (entry 3). Aryl azides are also known to undergo thermally induced C-N bond formation.^{246,133} To ensure the reaction of the azide with the iridium(III) phebox complex was truly catalytic a control experiment was ran in the absence of complex **216** (entry 4). Indeed, no reaction was observed and the azide was the sole component after refluxing the reaction. Placing an electron-withdrawing trifluoromethyl group *para* to the azide led to the highest conversion in Driver's iridium(I) catalyzed C-H amination. We investigated trifluoromethyl-substituted azide **322** towards C-H amination using iridium(III) complex **216** and a 51 % conversion and 18 % ee were observed (entry 5). During these studies we had also synthesized the dimethyl substituted phebox complexes **174** and **201**, and these complexes were evaluated for their catalytic activity for intramolecular C-H amination using azide **322** (entries 6 and 7). Unfortunately the conversions were poor with these catalysts (6 % and 2 %, respectively).



entry	catalyst	R	product	temp (°C)	% conversion ^a	A : indole ^a	% ee ^b
1	216	H	117	80	11	12 : 1	35
2	216	H	117	110	98	1.6 : 1	28
3 ^c	216	H	117	110	10	1.8 : 1	10
4	-	H	117	110	0	-	-
5	216	CF ₃	119	110	51	4 : 1	18
6	174	CF ₃	119	110	6	1.7 : 1	18
7	201	CF ₃	119	110	2	1 : 1	ND

^a Determined by ¹H NMR. ^b As determined by chiral HPLC. The absolute stereochemistry was not determined ^c 2.5 mol % AgOTf was added.

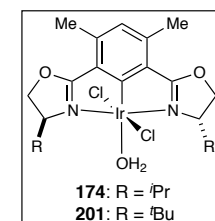
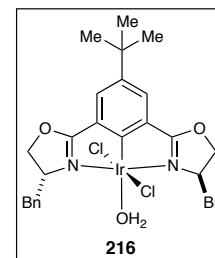


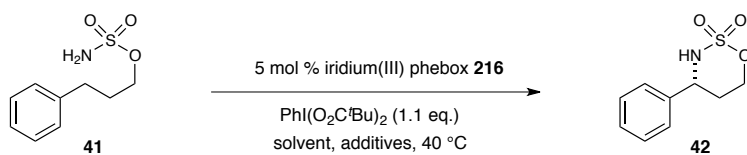
Table 5.1. Iridium(III) phebox catalyzed asymmetric intramolecular benzylic C-H amination using aryl azides.

5.2 Iridium(III) phebox catalyzed intramolecular C-H amination using sulfamate esters

In the midst of our research on intramolecular amination using aryl azides we were probing the efficacy of our iridium(III) phebox complexes in intramolecular C-H amination using sulfamate esters. We hypothesized that the phebox framework would be capable of inducing asymmetry due to the isosteric and isoelectronic similarities to the ruthenium(II) pybox catalyzed complexes.

Sulfamate ester **41** was chosen as the test substrate for this investigation. Reacting **41** with 5 mol % iridium(III) complex **216** and 1.1 equivalents hypervalent iodine oxidant PhI(O₂C^tBu)₂ in benzene led to 52 % conversion of the sulfamate ester (entry 1). The six-member ring **42** was produced in 32 % enantiomeric excess. 4 Å molecular sieves were added to remove adventitious water from the reaction. Doing this increased the

conversion and enantioselectivity to 61 % and 40 %, respectively (entry 2). Adding silver triflate to the reaction further increased the conversion, but the enantioselectivity decreased to 37 % (entry 3). Dichloromethane and trifluorotoluene were also evaluated as solvents for the reaction, with trifluorotoluene providing the best combined conversion and enantioselectivity at 74 % and 41 %, respectively (entry 5). These experiments indicate that additives and solvent only marginally affect the enantioselectivity of the reaction. It is likely that catalyst choice will influence the outcome of the C-H amination of sulfamate esters more substantially, but iridium(III) phebox complex **216** was the only catalyst available during this investigation.



entry	solvent	additive(s)	% conversion ^{a,b}	% ee ^b
1	PhH	-	52	32
2	PhH	4Å MS	61	40
3	PhH	4Å MS, AgOTf ^c	75	37
4	CH ₂ Cl ₂	4Å MS, AgOTf ^c	63	36
5	PhCF ₃	4Å MS, AgOTf ^c	74	41

^a As determined by ¹H NMR of the crude reaction mixture. ^b Determined by chiral HPLC. ^c 5 mol %. ^d The absolute configuration was determined by comparison to the optical rotation value reported in the literature.

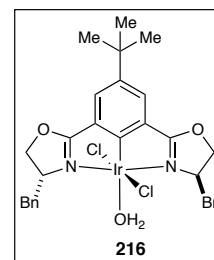


Table 5.2. Iridium(III) phebox catalyzed asymmetric intramolecular benzylic C-H amination using sulfamate esters.

5.3 Conclusions

These preliminary results indicate that the iridium(III) phebox complexes are capable of performing asymmetric C-H amination reactions of simple aryl azides and sulfamate esters. The asymmetric C-H amination using aryl azides is perhaps the most

exciting of the results described in this chapter, but 35 % ee is the highest enantioselectivity we have achieved so far using the iridium(III) phebox complexes that were investigated. Although this enantioselectivity is currently moderate, numerous iridium(III) phebox and iridium(III) phevim complexes have since been synthesized. It is likely that enantioselectivity for this reaction can be increased by systematic evaluation of these catalysts, and this is an active area of research in our laboratory.

Chapter 6 - Experimental Procedures

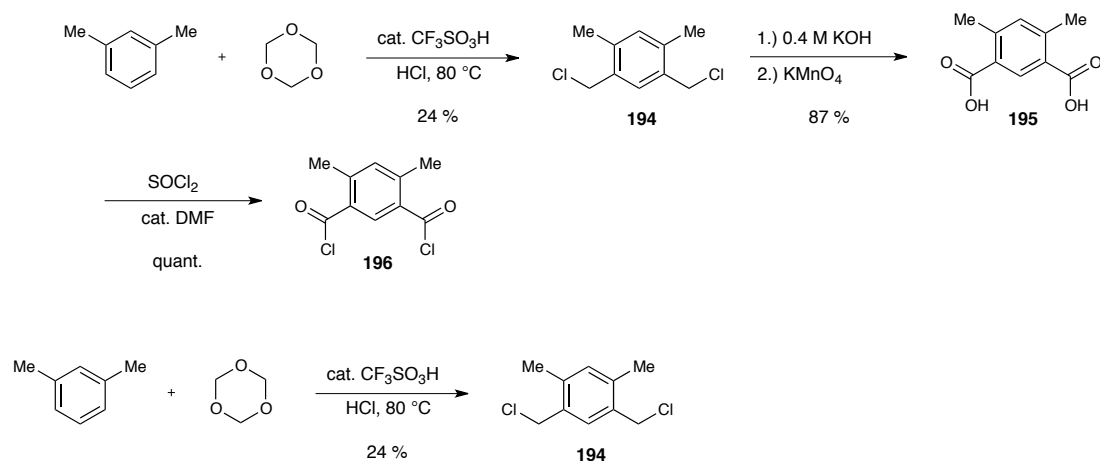
6.1 General Information

^1H and ^{13}C NMR spectra were recorded on a Varian Inova 600 spectrometer (600 MHz ^1H , 150 MHz ^{13}C), a Varian Unity plus 600 spectrometer (600 MHz ^1H , 150 MHz ^{13}C), and a Varian Inova 400 spectrometer (400 MHz ^1H , 100 MHz ^{13}C) at room temperature in CDCl_3 (neutralized and dried with anhydrous K_2CO_3) with internal CHCl_3 as the reference (7.26 ppm for ^1H and 77.23 ppm for ^{13}C), unless otherwise stated. Chemical shifts (δ values) were reported in parts per million (ppm) and coupling constants (J values) in Hz. Multiplicity was indicated using the following abbreviations: s = singlet, d = doublet, t = triplet, q = quartet, qn = quintet, m = multiplet, b = broad. Infrared (IR) spectra were recorded using a Thermo Electron Corporation Nicolet 380 FT-IR spectrometer. High-resolution mass spectra were obtained using a Thermo Electron Corporation Finigan LTQFTMS (at the Mass Spectrometry Facility, Emory University). Melting points were taken using a Fisher Johns melting point apparatus and are uncorrected (dec. = decomposition). High-pressure liquid chromatography (HPLC) was carried out on a Varian Prostar 210 equipped with Daicel OD, OJ, OD-H, OJ-H, AD-H, and SS Whelk columns and a variable wavelength detector or an Agilent 1100 Series equipped with Daicel AD-H, AS-H, OD-H, and OJ-H columns and a variable wavelength detector. Analytical thin layer chromatography (TLC) was performed on precoated glass backed EMD 0.25 mm silica gel 60 plates. TLC visualization was accomplished by fluorescence quenching and staining with ethanolic anisaldehyde or KMnO_4 . Flash

column chromatography was carried out using Silicycle SiliaFlash® F60 silica gel (40-63 μm). All reactions were conducted in oven dried and nitrogen charged glassware. Anhydrous solvents were obtained by passage through activated alumina columns using a *Glass Contours* solvent purification system unless otherwise noted. Solvents used in workup, extraction, and column chromatography were used as received from commercial suppliers without further purification. Chloroform used in chromatography was neutralized with anhydrous K_2CO_3 prior to use. All reagents were purchased from Sigma Aldrich or Strem and used as received unless otherwise noted. 1,4-cyclohexadiene (Sigma Aldrich) contained ~ 0.1-0.2 % of hydroquinone or BHT (3,5-di-*tert*-butyl-4-hydroxytoluene) radical inhibitors. All diazoesters were prepared according to the literature procedure.¹ 4Å powdered molecular sieves were activated by heating to 100 °C under reduced pressure (0.2 torr) for at least 12 hours. We acknowledge the use of shared instrumentation provided by grants from the National Institutes of Health and the National Science Foundation.

6.2 Chapter 3 Procedures and Characterization

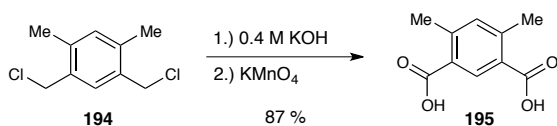
6.2.1 Synthesis of 4,6-dimethylisophthaloyl dichloride **196**



A procedure was adapted from the literature as follows; a 250 mL round-bottomed flask was charged with *m*-xylene (7.7 mL, 62.3 mmol), trioxane (14.1 g, 156 mmol), and concentrated HCl (26 mL, 312 mmol). Trifluoromethylsulfonic acid (0.5 mL, 6.2 mmol) was added and the suspension was stirred at $80\text{ }^\circ\text{C}$ for 5 hours. The solution was allowed to cool to room temperature, filtered through celite, and extracted with cyclohexane. The filter cake was washed until the filtrate became colorless. The organic phase was collected, dried over Na_2SO_4 , filtered, and concentrated. The crude solid was triturated with hexanes (x 5) until the supernatant became colorless. The solid was filtered off and dried on high vacuum to give 1,3-bis(chloromethyl)-4,6-dimethylbenzene **194** as a gray-white solid (3.0 g, 24 %). The spectral data match the literature.¹⁸¹

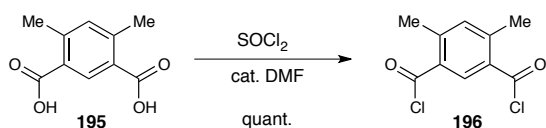
^1H NMR (400 MHz; CDCl_3): 7.26 (s, 1H), 7.05 (s, 1H), 4.58 (s, 4H), 2.39 (s, 6H). **^{13}C NMR** (100 MHz, CDCl_3): δ 138.1, 133.7, 133.5, 131.4, 44.6, 18.6. **HRMS** [+ APCI] calculated for 167.0622, found 167.0621 [$\text{M}-\text{Cl}$]⁺ **IR** (thin film, cm^{-1}) ν = 3010, 2973,

1258, 656



A procedure was adapted from the literature as follows; a 500 mL two-neck roundbottom flask was charged with 1,3-bis(chloromethyl)-4,6-dimethylbenzene **194** (3.2 g, 16 mmol) and 0.4 M aq. KOH (160 mL, 64 mmol). The mixture was refluxed for 3 hours until all starting material had dissolved. The reaction was cooled gradually at which time solid KMnO_4 (0.95 g, 6.0 mmol) was added in portions. The mixture was allowed to stir for 14 hours at room temperature. Formalin was added (~ 100 mL) and the resulting mixture was filtered through a celite pad. The filtrate was acidified with conc. HCl until pH=1. The 2,4-dimethylisophthalic acid **195** was collected as a white solid by vacuum filtration and dried overnight on high vacuum (2.7 g, 87 %). The spectral data match the literature.²

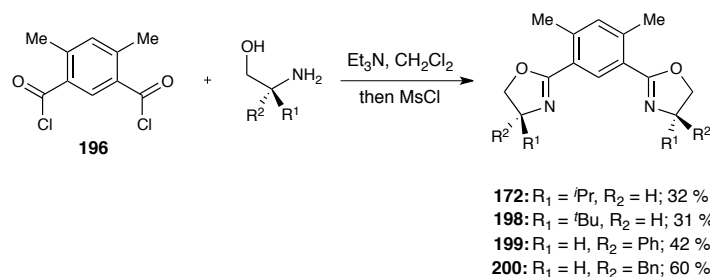
$^1\text{H NMR}$ (400 MHz; DMSO): 12.96 (s, 2H), 8.35 (s, 1H), 7.25 (s, 1H), 2.54 (s, 6H)



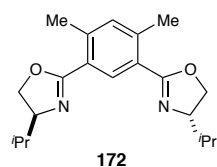
A suspension of 2,4-dimethylisophthalic acid **195** (3.5 g, 18 mmol) in SOCl_2 (28 mL, 378 mmol) and DMF (0.1 mL) was refluxed for 9 hours. The mixture was then concentrated and dried on high vacuum overnight to give 4.1 g **196** as a pale yellow solid which was used without further purification (4.1 g, 99 %).

6.2.2 Synthesis of phebox ligands and iridium(III) phebox complexes

General procedure A for the synthesis of 4,6-dimethyl phebox ligands **172**, **198-200**



A procedure was adapted from the literature as follows:³ a solution of 4,6-dimethylisophthaloyldichloride **196** (1.0 equiv.) in CH₂Cl₂ (0.25 M in acid chloride) was slowly added to a solution of amino alcohol (2.0 equiv.) and Et₃N (15 equiv.) in anhydrous CH₂Cl₂ (0.25 M in amino alcohol) at 0° C. The solution was warmed to room temperature and stirred for one hour. The mixture was again cooled to 0° C and methanesulfonyl chloride (2.2 equiv.) was added dropwise. The mixture was allowed to warm to room temperature and stirred 5.5 hours. Then, 1M K₂CO₃ (~50 mL/1g acid chloride) was added at 0° C and the mixture was extracted with ethyl acetate. The organic phase was washed with brine, dried over Na₂SO₄, filtered, and concentrated. The residue was purified as indicated.



Prepared according to general procedure A; 4,6-dimethylisophthaloyl chloride (1.2 g, 5.2 mmol) in CH₂Cl₂ (21 mL), L-valinol (1.10 g, 10.4 mmol), Et₃N (11 mL, 78 mmol) in

CH₂Cl₂ (42 mL), and methanesulfonyl chloride (0.90 mL, 11.4 mmol)) gave (*S,S*)-diMePhebox-^{*i*}Pr **172** as a colorless oil following purification by flash chromatography (SiO₂, 15 % → 20 % → 30 % EtOAc:pentane) (550 mg, 32 %)

¹H NMR (600 MHz; CDCl₃): δ 8.20 (s, 1H), 7.10 (s, 1H), 4.32 (dd, *J* = 9.4, 8.0, 2H), 4.10 (ddd, *J* = 9.4, 7.7, 6.3, 2H), 4.04 (t, *J* = 7.7, 2H), 2.58 (s, 6H), 1.82 (oct, *J* = 6.6, 2H), 1.01 (d, *J* = 6.8, 6H), 0.92 (d, *J* = 6.8, 6H)

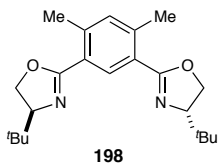
¹³C NMR (150 MHz, CDCl₃): δ 163.2, 141.3, 134.4, 131.5, 125.0, 73.4, 69.4, 33.1, 21.9, 19.1, 18.5

HRMS [+ APCI] calculated for 329.2224, found 329.2222 [M+H]⁺

IR (thin film, cm⁻¹) ν = 2959, 2952, 1646, 1067, 999, 570

[α]_D²² -108 (*c* = 1.00, CHCl₃)

R_f 0.42 (30 % EtOAc:hexanes)



Prepared according to general procedure **A**, with anhydrous THF as solvent; 4,6-dimethylisophthaloyl chloride (1.0 g, 4.3 mmol) in THF (9 mL), (*S*)-*tert*-leucinol (1.0 g, 8.6 mmol), Et₃N (17 mL, 123 mmol) in THF (26 mL), and methanesulfonyl chloride (1.8 mL, 22.4 mmol) gave (*S,S*)-diMePhebox-^{*t*}Bu **198** as a pale yellow oil which solidified upon standing following purification by flash chromatography (SiO₂, 10 % → 15 % → 30 % EtOAc:pentane) (460 mg, 31 %).

¹H NMR (400 MHz; CDCl₃): δ 8.19 (s, 1H), 7.11 (s, 1H), 4.26 (dd, *J* = 10.1, 8.5, 2H),

4.14 (t, $J = 8.0$, 2H), 4.06 (dd, $J = 10.1$, 7.6, 2H), 2.60 (s, 6H), 0.90 (s, 18H)

^{13}C NMR (100 MHz, CDCl_3): δ 163.0, 141.4, 134.4, 131.4, 124.9, 77.1, 67.9, 34.1, 26.1, 21.9

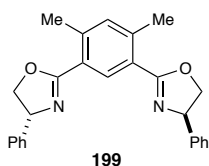
HRMS [+ ESI] calculated for 357.2537, found 357.2532 $[\text{M}+\text{H}]^+$

IR (thin film, cm^{-1}) $\nu = 2955, 2902, 2868, 1648, 1364, 1078, 1007, 955$

$[\alpha]_{\text{D}}^{22} -103$ ($c = 1.00$, CHCl_3)

m.p. 91-92 °C

R_f 0.43 (15 % EtOAc:hexanes)



Prepared according to general procedure A; 4,6-dimethylisophthaloyl chloride (700 mg, 3.0 mmol) in CH_2Cl_2 (12 mL), D-phenylglycinol (820 mg, 6.0 mmol), Et_3N (6.4 mL, 45 mmol) in CH_2Cl_2 (24 mL), and methanesulfonyl chloride (0.52 mL, 6.6 mmol) gave (*S,S*)-diMePhebox-Ph **199** as a white solid following purification by flash chromatography (SiO_2 , 20 % \rightarrow 30 % EtOAc:pentane) (500 mg, 42 %).

^1H NMR (600 MHz; CDCl_3): δ 8.50 (s, 1H), 7.39-7.29 (m, 10H), 7.22 (s, 1H), 5.46 (dd, $J = 10.1, 8.3$, 2H), 4.75 (dd, $J = 10.1, 8.3$, 2H), 4.21 (t, $J = 8.3$, 2H), 2.72 (s, 6H)

^{13}C NMR (150 MHz, CDCl_3): δ 164.5, 142.8, 142.1, 134.7, 132.0, 128.9, 127.7, 126.8, 124.5, 74.1, 70.8, 22.2

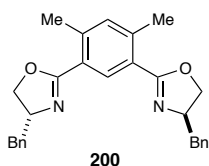
HRMS [+ APCI] calculated for 397.1911, found 397.1909 $[\text{M}+\text{H}]^+$

IR (thin film, cm^{-1}) $\nu = 3057, 2894, 1634, 1064, 1033, 760, 696, 535$

$[\alpha]_{\text{D}}^{22} +80.6$ ($c = 1.00$, CHCl_3)

m.p. 103-104 °C

R_f 0.40 (30 % EtOAc:hexanes)



Prepared according to general procedure **A**; 4,6-dimethylisophthaloyl chloride (500 mg, 2.16 mmol) in CH_2Cl_2 (9 mL), D-phenylalaninol (650 mg, 4.32 mmol), Et_3N (4.4 mL, 32 mmol) in CH_2Cl_2 (18 mL), and methanesulfonyl chloride (0.37 mL, 4.8 mmol) gave (*R,R*)-diMePhebox-Bn **200** as an off-white solid following purification by flash chromatography (SiO_2 , 30 % \rightarrow 50 % EtOAc:pentane) (550 mg, 60 %).

$^1\text{H NMR}$ (400 MHz; CDCl_3): δ 8.23 (s, 1H), 7.32-7.20 (m, 10H), 7.11 (s, 1H), 4.59 (tdd, $J = 8.9, 7.1, 5.3$, 2H), 4.27 (t, $J = 8.9$, 2H), 4.08 (dd, $J = 8.4, 7.2$, 2H), 3.20 (dd, $J = 13.7, 5.2$, 2H), 2.75-2.70 (m, 2H), 2.56 (s, 6H)

$^{13}\text{C NMR}$ (100 MHz, CDCl_3): δ 163.8, 141.6, 138.3, 134.5, 131.8, 129.5, 128.7, 126.7, 124.8, 71.0, 68.6, 42.1, 21.9

HRMS [+ APCI] calculated for 425.2224, found 425.2219 $[\text{M}+\text{H}]^+$

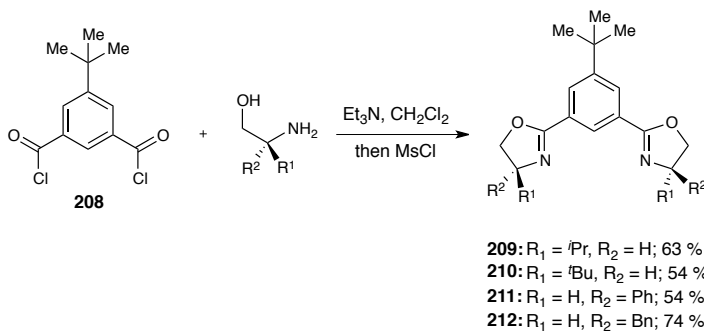
IR (thin film, cm^{-1}) $\nu = 3026, 2923, 1642, 1347, 700$

$[\alpha]_{\text{D}}^{22} +9.1$ ($c = 1.00$, CHCl_3)

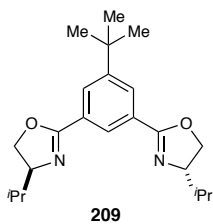
m.p. 92-93 °C

R_f 0.30 (30 % EtOAc:hexanes)

General procedure B for the synthesis of 5-*tert*-butyl phebox ligands 209-212



A solution of 5-*t*-butylisophthaloyl dichloride (1.0 equiv.) in anhydrous CH₂Cl₂ (0.25 M in acid chloride) was slowly added to a solution of amino alcohol (2.0 equiv.) and Et₃N (15 equiv.) in CH₂Cl₂ (0.25 M in amino alcohol) at 0° C. The solution was warmed to room temperature and stirred for one hour. The mixture was again cooled to 0° C and methanesulfonyl chloride (2.2 equiv.) was added dropwise. The mixture was allowed to warm to room temperature and stirred 5.5 hours. Then, 1M K₂CO₃ (~50 mL/1g acid chloride) was added at 0° C and the mixture was extracted with ethyl acetate. The organic phase was washed with brine, dried over Na₂SO₄, filtered, and concentrated. The residue was purified as indicated.



Prepared according to general procedure **B**; 5-*t*-butylisophthaloyl dichloride (2.6 g, 10 mmol) in CH₂Cl₂ (40 mL), L-valinol (2.00 g, 19.5 mmol), Et₃N (21.0 mL, 151 mmol) in CH₂Cl₂ (80 mL), and methanesulfonyl chloride (1.7 mL, 22 mmol) gave (*S,S*)-

^tBuPhebox-ⁱPr **209** as a white solid following purification by flash chromatography (SiO₂, 30 % EtOAc:pentane) (2.2 g, 63 %).

¹H NMR (400 MHz; CDCl₃): δ 8.34 (t, *J* = 1.6, 1H), 8.09 (d, *J* = 1.6, 2H), 4.43-4.39 (m, 2H), 4.17-4.09 (m, 4H), 1.90-1.85 (m, 2H), 1.37 (s, 9H), 1.04 (d, *J* = 6.8, 3H), 0.93 (d, *J* = 6.8, 3H)

¹³C NMR (100 MHz; CDCl₃): δ 163.3, 151.8, 128.1, 125.8, 72.9, 70.3, 35.2, 33.0, 31.5, 19.2, 18.2

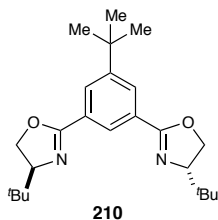
HRMS [+ APCI] calculated for calculated for 357.25366, found 357.25349 [M+H]⁺

IR (thin film, cm⁻¹) ν = 2959, 2903, 1653, 1593, 1235, 983

[α]_D²² -95.0 (*c* = 1.00, CHCl₃)

m.p. 84-86 °C

R_f 0.15 (3 % EtOAc:CH₂Cl₂)



Prepared according to general procedure **B**; 5-^tbutylisophthaloyl dichloride (2.3 g, 9.0 mmol) in CH₂Cl₂ (35 mL), *L*-*tert*-leucinol (2.1 g, 18 mmol), Et₃N (19.0 mL, 134 mmol) in CH₂Cl₂ (75 mL), and methanesulfonyl chloride (1.6 mL, 20 mmol) gave (*S,S*)-^tBuPhebox-^tBu **210** as a white solid following purification by flash chromatography (SiO₂, 30 % EtOAc:pentane) (1.7 g, 54 %)

¹H NMR (400 MHz; CDCl₃): δ 8.37 (t, *J* = 1.6, 1H), 8.06 (d, *J* = 1.6, 2H), 4.35 (dd, *J* = 10.1, 8.6, 2H), 4.24 (dd, *J* = 8.6, 7.6, 2H), 4.06 (dd, *J* = 10.1, 7.6, 2H), 1.37 (s, 9H), 0.96 (s, 18H)

¹³C NMR (100 MHz; CDCl₃): δ 163.1, 151.7, 128.1, 125.8, 76.4, 68.8, 35.1, 34.2, 26.0

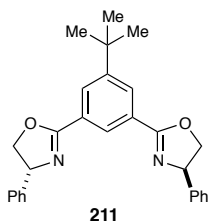
HRMS [+ APCI] calculated for 385.2846, found 385.2850 [M+H]⁺

IR (thin film, cm⁻¹) ν = 2954, 1650, 1360, 1245, 1113, 976, 593

[α]_D²² -103 (*c* = 1.00, CHCl₃)

m.p. 166-168 °C

R_f 0.26 (3 % EtOAc:CH₂Cl₂)



Prepared according to general procedure **B**; 5-*t*-butylisophthaloyl dichloride (2.6 g, 10 mmol) in CH₂Cl₂ (40 mL), D-phenylglycine (2.74 g, 20.0 mmol), Et₃N (21.0 mL, 150 mmol) in CH₂Cl₂ (80 mL), and methanesulfonyl chloride (0.90 mL, 11 mmol) gave (*R,R*)-*t*-BuPhebox-Ph **211** as a white solid following purification by flash chromatography (SiO₂, 30 % → 50 % EtOAc:pentane) (1.34 g, 54 %).

¹H NMR (400 MHz; CDCl₃): δ 8.51 (t, *J* = 1.6, 1H), 8.23 (d, *J* = 1.6, 2H), 7.39-7.28 (m, 10H), 5.41 (dd, *J* = 10.1, 8.2, 2H), 4.81 (dd, *J* = 10.1, 8.4, 2H), 4.29 (t, *J* = 8.3, 2H), 1.39 (s, 9H)

¹³C NMR (100 MHz, CDCl₃): δ 164.7, 142.5, 129.0, 128.8, 127.9, 127.0, 126.2, 75.2, 70.5, 35.3, 31.5.

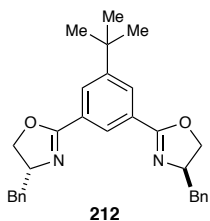
HRMS [+ APCI] calculated for 425.22235, found 425.22210 [M+H]⁺

IR (thin film, cm⁻¹) ν = 3030, 2962, 2897, 1646, 1236, 980, 697, 574

$[\alpha]_D^{22}$ +66.1 (c = 1.00, CHCl₃)

m.p. 152-154 °C

R_f 0.39 (50 % EtOAc:hexanes)



Prepared according to general procedure **B**; 5-*t*-butylisophthaloyl dichloride (1.3 g, 5.0 mmol) in CH₂Cl₂ (20 mL), D-phenylalaninol (1.51 g, 10.0 mmol), Et₃N (10.4 mL, 75 mmol) in CH₂Cl₂ (40 mL), and methanesulfonyl chloride (0.9 mL, 11 mmol) gave (*R,R*)-*t*BuPhebox-Bn **212** as an amorphous solid following purification by flash chromatography (SiO₂, 30 % → 50 % EtOAc:pentane) (1.7 g, 74 %).

¹H NMR (400 MHz; CDCl₃): δ 8.38 (t, J = 1.5, 1H), 8.18 (d, J = 1.5, 2H), 7.37-7.25 (m, 10H), 4.64 (tdd, J = 9.2, 7.3, 4.9, 2H), 4.38 (t, J = 8.9, 2H), 4.19 (dd, J = 8.4, 7.4, 2H), 3.32 (dd, J = 13.7, 4.9, 2H), 2.76 (dd, J = 13.7, 9.2, 2H), 1.43 (s, 9H)

¹³C NMR (100 MHz, CDCl₃): δ 164.0, 152.0, 138.2, 129.5, 128.8, 128.4, 128.1, 126.8, 125.8, 72.1, 68.3, 42.1, 35.2, 31.5

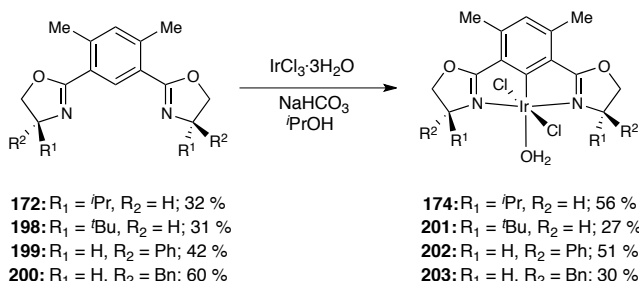
HRMS [+ APCI] calculated for 453.2534, found 453.2537 [M+H]⁺

IR (thin film, cm⁻¹) ν = 3026, 2963, 1648, 1239, 977, 701

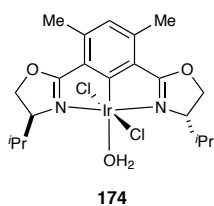
$[\alpha]_D^{22}$ -13.2 (c = 1.00, CHCl₃)

R_f 0.40 (30 % EtOAc:hexanes)

General procedure C for the synthesis of 3,5-dimethyl iridium(III) phebox complexes 174, 201-203



A procedure was adapted from the literature as follows:⁴ A round-bottom flask was charged with IrCl₃·3H₂O (1.1 equiv.), NaHCO₃ (1.1 equiv.), and diMePhebox ligand (1.0 equiv.). Isopropanol (0.03 M) was added and the mixture was refluxed for the indicated time. The crude reaction mixture was concentrated, adsorbed onto SiO₂ using a rotary evaporator, and immediately purified by column chromatography (SiO₂, eluent as indicated). The residue was then crystallized or triturated as indicated to give the iridium diMePhebox complexes **174, 201-203**.



Following general procedure C, a mixture of (*S,S*)-diMePheBox-ⁱPr **172** (350 mg, 1.0 mmol), IrCl₃·3H₂O (300 mg, 1.0 mmol), sodium bicarbonate (84 mg, 1.0 mmol), and isopropanol (30 mL) was refluxed for 11 hours. The resulting mixture was purified by

flash column chromatography (SiO₂, 20 % → 50 % EtOAc:hexanes). The orange fractions at R_f 0.33 (50 % EtOAc:hexanes) were collected and concentrated. The oil was crystallized by slow evaporation of a concentrated CH₂Cl₂ solution to give [(*S,S*)-diMePhebox-^{*t*}Pr]IrCl₂(H₂O) **174** as an orange solid (320 mg, 56 %).

¹H NMR (400 MHz; 50 °C, CDCl₃): δ 6.64 (s, 1H), 4.83-4.75 (m, 4H), 4.20 (t, *J* = 6.4, 2H), 2.63 (s, 6H), 2.45 (s, 2H), 2.25 (s, 2H), 0.97 (dd, *J* = 10.4, 7.0, 12H)

¹³C NMR (150 MHz; CDCl₃): δ 176.2, 141.2, 126.7, 126.2, 71.0, 67.3, 29.1, 19.7, 18.9, 15.5

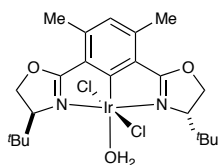
HRMS [+ APCI] calculated for 596.16558, found 596.16548 [M-Cl, -H₂O, +CH₃CN]⁺

IR (thin film, cm⁻¹) ν = 3364, 2958, 2930, 1603, 1383, 1219, 943, 570

[α]_D²² +232 (*c* = 0.46, CHCl₃)

m.p. 200 °C (dec.)

R_f 0.33 (50 % EtOAc:hexanes)



201

Following general procedure **C**, a mixture of (*S,S*)-diMePheBox-^{*t*}Bu **198** (350 mg, 0.98 mmol), IrCl₃·3H₂O (330 mg, 1.1 mmol), NaHCO₃ (90 mg, 1.1 mmol), and isopropanol (33 mL) was refluxed for 12 hours. The resulting mixture was purified by flash column chromatography (SiO₂, 30 % → 50 % → 65 % EtOAc:hexanes) followed by trituration with dry Et₂O to give [(*S,S*)-diMePhebox-^{*t*}Bu]IrCl₂(H₂O) **201** as an orange solid (174 mg, 27 %).

¹H NMR (600 MHz; CDCl₃): δ 6.60 (s, 1H), 4.99-4.94 (m, 2H), 4.78-4.73 (m, 2H), 4.13-4.08 (m, 2H), 2.61 (s, 6H), 2.19 (s, 2H), 1.22 (s, 18H)

¹³C NMR (100 MHz; CDCl₃): δ 177.1, 141.9, 127.2, 126.4, 72.9, 71.9, 34.1, 26.8, 19.1

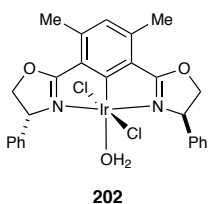
HRMS [+ APCI] calculated for 656.22309, found 656.22242 [M-Cl, -H₂O, +CH₃CN, +MeOH]⁺

IR (thin film, cm⁻¹) ν = 2962, 2880, 1594, 1488, 1392, 1323, 1220, 1072, 945, 855

[α]_D²² +408 (c = 1.00, CHCl₃)

m.p. 340 °C (dec.)

R_f 0.21 (30 % EtOAc:hexanes)



Following general procedure **C**, a mixture of (*R,R*)-diMePhebox-Ph **199** (300 mg, 0.76 mmol), IrCl₃·3H₂O (250 mg, 0.84 mmol), NaHCO₃ (70 mg, 0.84 mmol), and isopropanol (25 mL) was refluxed for 10 hours. The resulting mixture was purified by flash column chromatography (SiO₂, 30 % → 50 % EtOAc:hexanes). The orange fractions at R_f 0.46 (30 % EtOAc:hexanes) were collected and concentrated to give an orange powder which was crystallized by slow diffusion of pentane into a saturated CHCl₃ solution to give [(*R,R*)-diMePhebox-Ph]IrCl₂(H₂O) **202** as an orange solid (254 mg, 51 %).

¹H NMR (400 MHz; CDCl₃): δ 7.50-7.49 (m, 4H), 7.37-7.33 (m, 6H), 6.68 (s, 1H), 5.28-5.17 (m, 4H), 4.63-4.58 (m, 2H), 2.70 (s, 6H), 1.86 (bs, 2H)

^{13}C NMR (100 MHz; CDCl_3): δ 181.2, 142.2, 137.8, 129.1, 129.0, 126.3, 126.2, 77.9, 67.1, 19.1

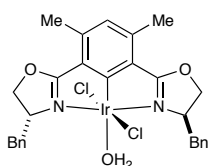
HRMS [+ APCI] calculated for 656.22309, found 656.22242 [M-Cl, -H₂O, +CH₃CN, +MeOH]⁺

IR (thin film, cm^{-1}) ν = 3273, 2967, 1599, 1480, 1386, 1218, 1020, 753, 698.

$[\alpha]_{\text{D}}^{22}$ -464 (c = 1.01, CHCl_3)

m.p. 195 °C (dec.)

R_f 0.46 (30 % EtOAc:hexanes)



203

Following general procedure C, a mixture of (*R,R*)-diMePheBox-Bn **S4** (120 mg, 0.28 mmol), $\text{IrCl}_6 \cdot 6\text{H}_2\text{O}$ (160 mg, 0.31 mmol), NaHCO_3 (77 mg, 0.92 mmol, 3.3 equiv.), and isopropanol (11 mL) was refluxed for 8 hours. The resulting mixture was purified by flash column chromatography (SiO_2 , 30 % EtOAc:hexanes). The orange fractions at R_f 0.33 (5 % EtOAc: CH_2Cl_2) (SiO_2 , 30 % EtOAc:hexanes) were collected and concentrated to give [(*R,R*)-diMePhebox-Bn] $\text{IrCl}_2(\text{H}_2\text{O})$ **4** as an orange solid (60 mg, 30 %).

^1H NMR (600 MHz; CDCl_3): δ 7.35-7.21 (m, 10H), 6.66 (s, 1H), 4.75 (t, J = 8.9, 2H), 4.61 (t, J = 7.8, 2H), 4.55-4.52 (m, 2H), 3.64 (dd, J = 14.0, 3.9, 2H), 2.83 (dd, J = 14.1, 10.4, 2H), 2.64 (s, 6H), 2.17 (bs, 2H)

^{13}C NMR (100 MHz; CDCl_3): δ 177.9, 141.7, 137.3, 129.4, 129.1, 127.1, 126.2, 75.2, 63.7, 40.5, 19.0

HRMS [+ APCI] calculated for 615.16099, found 615.16100 [M-2Cl, -H₂O]⁺

IR (thin film, cm⁻¹) ν = 3303, 3026, 2963, 1602, 1482, 1388, 1219, 751, 702

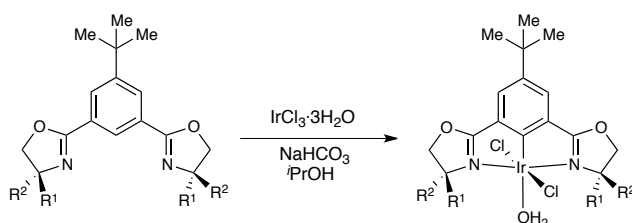
[α]_D²² -123 (*c* = 0.50, CHCl₃)

m.p. 216 °C (dec.)

R_f 0.33 (5 % EtOAc:CH₂Cl₂)

General procedure D for the synthesis of 4-*tert*-butyl iridium(III) phebox complexes

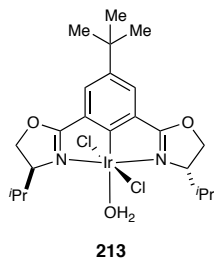
213-216



209: R₁ = *t*Pr, R₂ = H; 63 %
210: R₁ = *t*Bu, R₂ = H; 54 %
211: R₁ = H, R₂ = Ph; 54 %
212: R₁ = H, R₂ = Bn; 74 %

213: R₁ = *t*Pr, R₂ = H; 41 %
214: R₁ = *t*Bu, R₂ = H; 27 %
215: R₁ = H, R₂ = Ph; 14 %
216: R₁ = H, R₂ = Bn; 54 %

A procedure was adapted from the literature⁵ as follows: A round-bottom flask was charged with IrCl₃·3H₂O (1.1 equiv.), NaHCO₃ (1.1 equiv.), and *t*BuMePhebox ligand (1.0 equiv.). Isopropanol (0.03 M) was added and the mixture was refluxed for the indicated time. The crude reaction mixture was concentrated then adsorbed onto SiO₂ using a rotary evaporator, immediately purified by column chromatography (SiO₂, eluent as indicated), and crystallized as indicated to give the iridium *t*BuPhebox iridium complexes **213-216**.



Following general procedure **D**, a mixture of (*S,S*)-^tBuPhebox-^tPr **209** (200 mg, 0.561 mmol), IrCl₃·3H₂O (219 mg, 0.62 mmol), sodium bicarbonate (52 mg, 0.62 mmol), and isopropanol (22 mL) was refluxed for 2 hours. The resulting mixture was purified by flash column chromatography (SiO₂, 30 % EtOAc:hexanes → 50 % → 75 %). The orange fractions at R_f 0.33 (30 % EtOAc:hexanes) were collected and concentrated to give [(*S,S*)-^tBuPhebox-^tPr]IrCl₂(H₂O) **213** as an orange solid (147 mg, 41 %).

¹H NMR (600 MHz; CDCl₃): δ 7.50 (s, 2H), 4.82 (d, *J* = 7.6, 4H), 4.27-4.09 (bm, 2H), 2.43 (bs, 2H), 1.36 (s, 9H), 0.94 (bs, 12H)

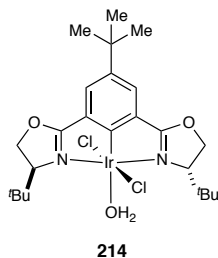
¹³C NMR (150 MHz, CDCl₃): δ 176.6, 145.1, 129.1, 125.5, 71.3, 68.0, 35.1, 32.0, 29.2, 19.7, 15.4 HRMS [+ APCI] calculated for 548.20148, found 548.19698 [M-2Cl,-H₂O]⁺

IR (thin film, cm⁻¹) ν = 3321, 2955, 1620, 1442, 1377, 1285, 968

[α]_D²² +188 (*c* = 1.00, CHCl₃)

m.p. 204 °C (dec.)

R_f 0.33 (30 % EtOAc:hexanes)



Following general procedure **D**, a mixture of (*S,S*)-*t*BuPhebox-*t*Bu **210** (216 mg, 0.561 mmol), IrCl₃·3H₂O (219 mg, 0.62 mmol), sodium bicarbonate (52 mg, 0.62 mmol), and isopropanol (22 mL) was refluxed for 4.5 hours. The resulting mixture was purified by flash column chromatography (SiO₂, 30 % EtOAc:hexanes). The orange fractions at R_f 0.15 (30 % EtOAc:hexanes, 2 runs) were collected and concentrated to give [(*S,S*)-*t*BuPhebox-*t*Bu]IrCl₂(H₂O) **214** as a bright orange solid (100 mg, 27 %).

¹H NMR (600 MHz; CDCl₃): δ 7.48 (d, *J* = 1.3, 2H), 4.89-4.87 (d, *J* = 8.4, 4H), 3.98 (m, 2H), 2.92 (s, 2H), 1.37 (s, 9H), 1.16 (m, 18H)

¹³C NMR (150 MHz, CDCl₃): δ 177.4, 145.2, 129.4, 125.9, 73.4, 72.3, 35.0, 34.7, 31.9, 26.6

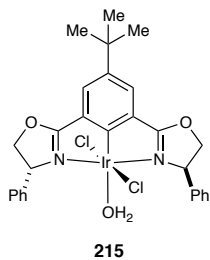
HRMS [+ APCI] calculated for 576.22844, found 575.22470 [M-2Cl,-H₂O]

IR (thin film, cm⁻¹) ν = 3338, 2954, 1695, 1447, 1379, 1261, 982

[α]_D²² +174 (*c* = 0.10, CHCl₃)

m.p. 370 °C (dec.)

R_f 0.15 (30 % EtOAc:hexanes, 2 runs)



Following general procedure **D**, a mixture of (*R,R*)-^tBuPhebox-Ph **211** (84 mg, 0.20 mmol), IrCl₃·3H₂O (78 mg, 0.22 mmol), sodium bicarbonate (19 mg, 0.22 mmol), and isopropanol (8 mL) was refluxed for 7 hours. The resulting mixture was purified by flash column chromatography (SiO₂, 30 % EtOAc:hexanes). The orange fractions at R_f 0.28 (3 % EtOAc:CHCl₃) was collected and concentrated to give [(*R,R*)-^tBuPhebox-Ph]IrCl₂(H₂O) **215** as an orange solid (20 mg, 14 %).

¹H NMR (600 MHz; CDCl₃): δ 7.63 (s, 2H), 7.46-7.45 (m, 4H), 7.35-7.30 (m, 6H), 5.30-5.22 (m, 4H), 4.67-4.61 (m, 2H), 1.65 (bs, 4H), 1.39 (s, 9H)

¹³C NMR (100 MHz; CDCl₃): δ 180.6, 145.1, 138.0, 129.2, 129.0, 128.9, 128.4, 126.2, 78.5, 67.3, 35.1, 32.0

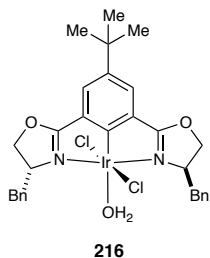
HRMS [+ APCI] calculated for 616.17018, found 616.16588 [M-2Cl,-H₂O]⁺

IR (thin film, cm⁻¹) ν = 3321, 3032, 2963, 1618, 1549, 1476, 1444, 1379, 1289, 981, 730, 699

[α]_D²² -372 (c = 0.50, CHCl₃)

m.p. 202 °C (dec.)

R_f 0.28 (3 % EtOAc:CHCl₃)



Following general procedure **D**, a mixture of (*R,R*)-^tBuPhebox-Bn **212** (1.60 g, 3.54 mmol), IrCl₃·3H₂O (1.37 g, 3.89 mmol), sodium bicarbonate (330 mg, 3.89 mmol), and isopropanol (118 mL) was refluxed for 2 hours. The resulting mixture was purified by flash column chromatography (SiO₂, 3 % → 6 % → 8 % → 10 % EtOAc:CH₂Cl₂). The orange fractions at R_f 0.38 (30 % EtOAc:hexanes) were collected and concentrated to give an orange powder which was crystallized by slow diffusion of pentane into a saturated CH₂Cl₂ solution to give [(*R,R*)-^tBuPhebox-Bn]IrCl₂(H₂O) **216** as an orange solid (1.4 g, 54 %).

¹H NMR (400 MHz; CDCl₃): δ 7.54 (s, 2H), 7.31-7.20 (m, 10H), 4.79 (m, 2H), 4.60 (m, 4H), 3.64 (dd, *J* = 13.8, 3.1, 2H), 2.84 (dd, *J* = 14.1, 9.7, 2H), 2.20 (s, 2H), 1.35 (s, 9H)

¹³C NMR (150 MHz, CDCl₃): δ 177.4, 145.0, 137.2, 129.4, 126.9, 125.6, 75.4, 64.1, 40.3, 35.0, 31.9

HRMS [+ APCI] calculated for 643.1931, found 643.1933 [M-2Cl, -H₂O]⁺

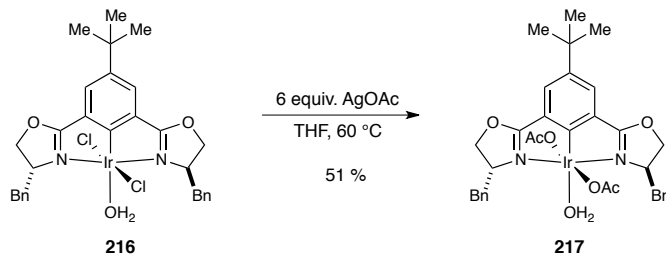
IR (thin film, cm⁻¹) ν = 3330, 2957, 1619, 1447, 1378, 1286, 975, 728, 699

[α]_D²² -142 (*c* = 0.50, CHCl₃)

m.p. 220 °C (dec.)

R_f 0.38 (30 % EtOAc:hexanes)

Synthesis of [(*R,R*)-^tBuPhebox-Bn]IrCl₂(OAc) **217**



An aluminum foil wrapped 25 mL round bottom flask was charged with [(*R,R*)-^tBuPhebox-Bn]IrCl₂(H₂O) **216** (100 mg, 0.136 mmol) and AgOAc (136 mg, 0.816 mmol), fitted with a reflux condenser, and evacuated and backfilled with dry nitrogen (3 cycles). 3 mL THF was added and the flask was submerged in a preheated oil bath at 60 °C. Starting complex **216** was consumed after 2.5 hours as judged by TLC. The crude reaction mixture was cooled to room temperature, concentrated, and purified by flash column chromatography (SiO₂, 50 % → 75 % EtOAc:pentane) to give [(*R,R*)-^tBuPhebox-Bn]IrCl₂(OAc) **217** as a light orange solid (54 mg, 51 %).

¹H NMR (600 MHz; CDCl₃): δ 7.54 (s, 2H), 7.33 (t, *J* = 7.6, 4H), 7.29-7.24 (m, 7H), 4.81 (t, *J* = 8.3, 2H), 4.70-4.64 (m, 4H), 3.72 (dd, *J* = 13.9, 3.4, 2H), 2.66 (dd, *J* = 13.9, 10.0, 2H), 1.74 (s, 6H), 1.40 (s, 9H)

¹³C NMR (150 MHz, CDCl₃): δ 183.8, 178.5, 165.7, 145.0, 137.2, 130.0, 129.6, 129.0, 127.0, 125.3, 75.5, 64.9, 40.3, 35.2, 32.0, 23.4

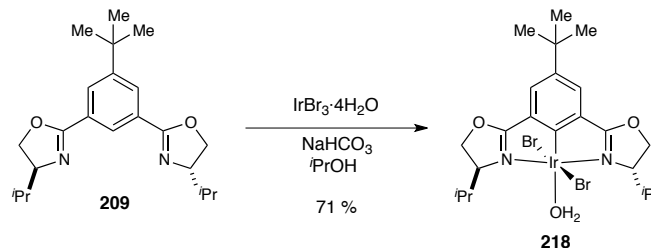
HRMS [+ ESI] calculated for 763.2359, found 763.2397 [M-H₂O+H]⁺

IR (thin film, cm⁻¹) ν = 3315, 2960, 1610, 1447, 1378, 1286, 976, 751

[α]_D²² -248 (*c* = 0.10, CHCl₃)

R_f 0.42 (50 % EtOAc:hexanes)

Synthesis of [(*S,S*)-^tBuPhebox-ⁱPr]IrBr₂(OH₂) **218**



A 50 mL round bottom flask was charged with phebox ligand **209** (250 mg, 0.70 mmol), IrBr₃·4H₂O (388 mg, 0.77 mmol), and NaHCO₃ (65 mg, 0.77 mmol). The flask was fitted with a reflux condenser, and evacuated and backfilled with dry nitrogen (3 cycles). 23 mL isopropanol was added and the mixture was refluxed for 8.5 hours. The reaction mixture was cooled to room temperature, adsorbed onto silica gel, and immediately purified by flash column chromatography (SiO₂, 20 % → 30 % → 50 % EtOAc:hexanes) to give [(*S,S*)-^tBuPhebox-ⁱPr]IrBr₂(OH₂) **218** as a red/orange solid (359 mg, 71 %).

¹H NMR (400 MHz; CDCl₃): δ 7.51 (s, 2H), 4.85-4.77 (m, 4H), 4.21 (bs, 2H), 2.45 (bs, 2H), 1.37 (s, 9H), 0.95 (bs, 12H)

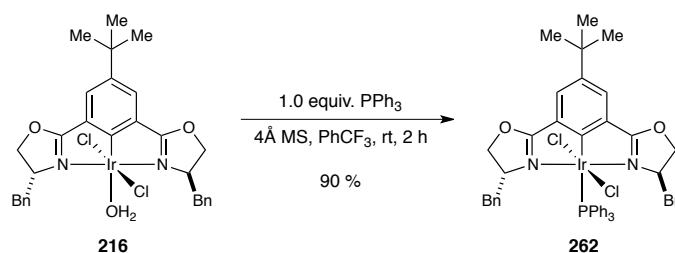
¹³C NMR (100 MHz, CDCl₃): δ 176.3, 145.0, 129.0, 125.5, 109.9, 71.4, 68.3, 35.0, 32.0, 28.9, 19.7, 15.7

HRMS [+ APCI] calculated for 706.0376, found 706.0359 [M-H₂O]⁺

R_f 0.21 (20 % EtOAc:hexanes)

6.2.3 Synthesis of triphenylphosphine iridium(III) phebox complexes **262** and **263** and their NMR spectra

Synthesis of *trans*-[(*R,R*)-^tBuPhebox-Bn]IrCl₂(PPh₃) **262**



Toluene (1.0 mL, 0.029 M) was added to a mixture of [(*R,R*)-^tBuPheBox-Bn]IrCl₂(H₂O) **216** (21.3 mg, 0.029 mmol), triphenylphosphine (7.6 mg, 0.082 mmol), and 4Å powdered molecular sieves (42.4 mg). The mixture was stirred at room temperature for ~30 minutes until complex **216** was consumed as determined by thin-layer chromatography (20 % EtOAc:hexanes, R_f **216** = 0.15). The mixture was filtered through a plug of Celite, and the filter cake was washed with CHCl₃ until the filtrate ran clear. Purification by flash column chromatography (SiO₂, 10 % → 30 % EtOAc:hexanes) gave *trans*-[(*R,R*)-^tBuPheBox-Bn]IrCl₂(PPh₃) **262** as a yellow solid (25.6 mg, 90 %).

¹H NMR (400 MHz; CDCl₃): δ 8.05-8.00 (m, 6H), 7.64 (d, *J* = 1.9, 2H), 7.33-7.31 (m, 9H), 7.13-7.11 (m, 6H), 6.47-6.45 (m, 4H), 4.56 (app t, *J* = 8.6, 2H), 4.42 (dd, *J* = 8.6, 3.9, 2H), 4.16 (ddt, *J* = 11.6, 8.0, 3.9, 2H), 2.84 (dd, *J* = 14.6, 3.9, 2H), 2.29 (dd, *J* = 14.6, 11.3, 2H), 1.39 (s, 9H)

¹³C NMR (100 MHz, CDCl₃): δ 179.7, 146.3, 136.9, 135.1, 135.0, 134.8, 134.4, 130.0, 129.2, 128.6, 128.5, 128.3, 128.2, 126.6, 126.3, 126.2, 74.2, 64.8, 39.5, 35.2, 31.9

HRMS [+ ESI] calculated for 941.2609, found 941.2629 [M-Cl]⁺

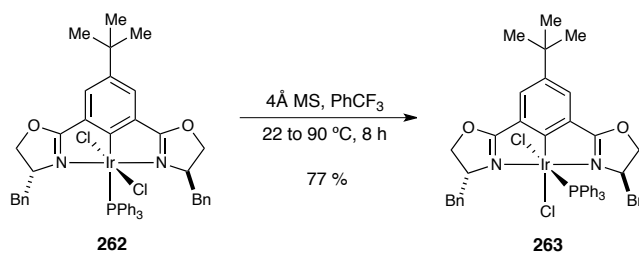
IR (thin film, cm^{-1}) $\nu = 3057, 2962, 1621, 1480, 1450, 1378, 1295, 977, 911, 731, 697$

$[\alpha]_{\text{D}}^{22} -107.8$ ($c = 0.40, \text{CHCl}_3$)

m.p. 280 °C (dec.)

R_f 0.33 (20 % EtOAc:hexanes)

Synthesis of *cis*-[(*R,R*)-^tBuPhebox-Bn]IrCl₂(PPh₃) **263**



α, α, α -trifluorotoluene (5 mL, 0.1 M) was added to a mixture of *trans*[(*R,R*)-^tBuPheBox-Bn]IrCl₂(PPh₃) **262** (51.2 mg, 0.0524 mmol) and 4 Å powdered molecular sieves (102 mg) at room temperature. The mixture was stirred at room temperature for 5 minutes then submerged into a preheated oil bath at 60 °C. After stirring for 15 minutes at 60 °C, the temperature was gradually raised to 90 °C. Stirring was continued for 7 hours until complex **262** was consumed as determined by thin-layer chromatography (20 % EtOAc:hexanes, R_f **262** = 0.33). The mixture was filtered through a plug of Celite, and the filter cake was washed with CHCl₃ until the filtrate ran clear. Purification by flash column chromatography (SiO₂, 10 % → 30 % → 50 % EtOAc:hexanes) gave *cis*-[(*R,R*)-^tBuPheBox-Bn]IrCl₂(PPh₃) **263** as a yellow solid (39.5 mg, 77 %).

¹H NMR (400 MHz; CDCl₃): δ 7.65-7.60 (m, 5H), 7.47-7.43 (m, 1H), 7.38-7.32 (m, 7H), 7.28-7.08 (m, 13H), 4.68-4.46 (m, 6H), 4.17-4.08 (m, 2H), 2.93-2.87 (m, 1H), 1.30-1.29 (s, 9H), 1.06-0.96 (m, 2H)

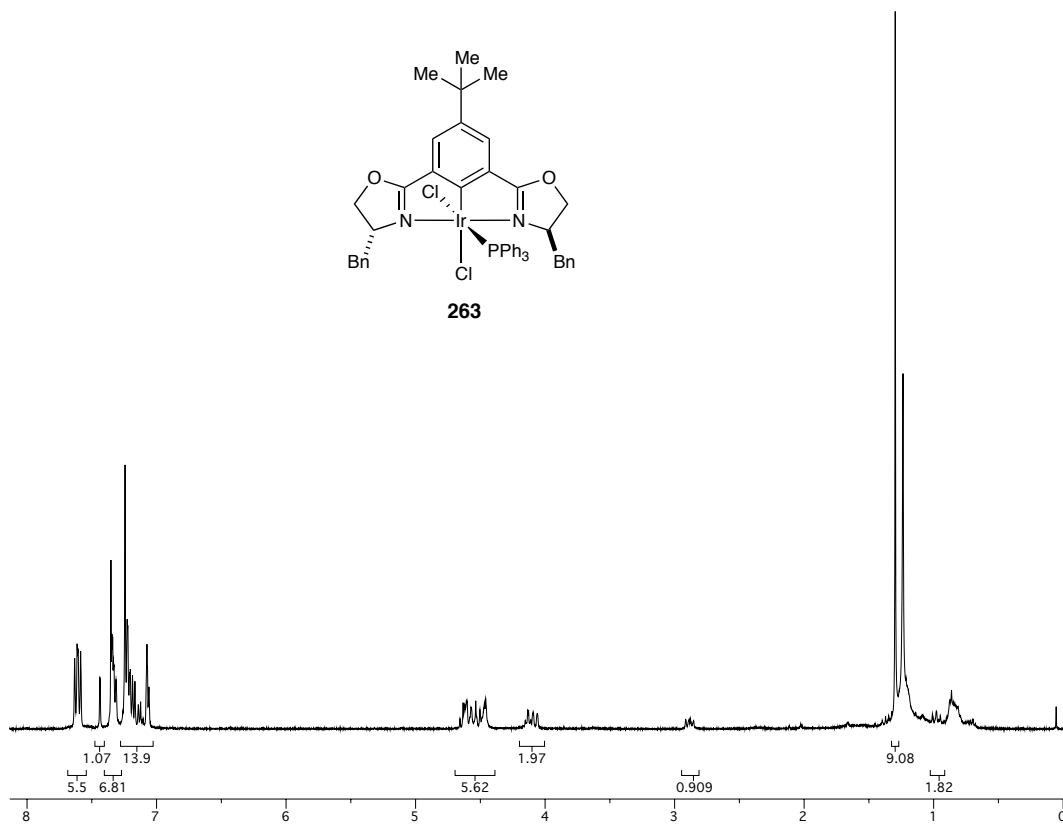
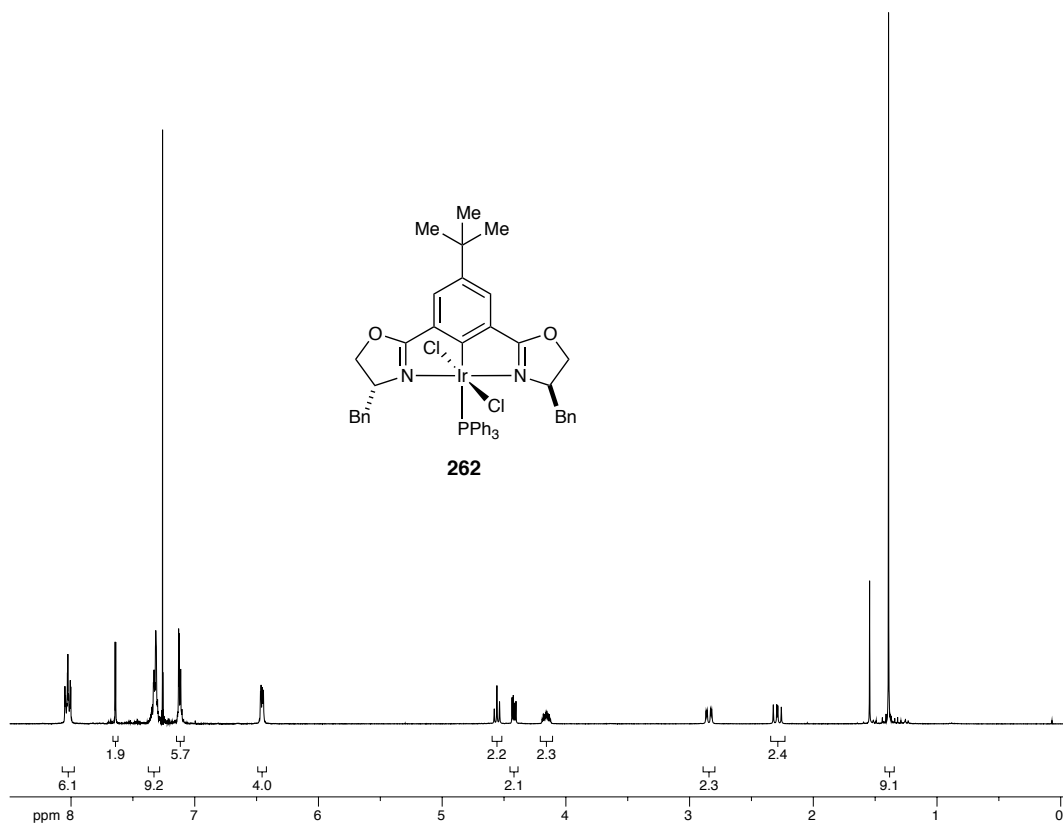
¹³C NMR (100 MHz, CDCl₃): δ 178.8, 178.3, 145.5, 138.4, 138.2, 134.4, 134.3, 131.4, 130.8, 130.4, 129.4, 129.0, 128.9, 128.8, 128.6, 128.1, 128.0, 126.7, 126.6, 126.5, 76.1, 65.9, 65.4, 40.6, 38.6, 35.2, 32.0, 29.9

HRMS [+ ESI] calculated for 941.2609, found 941.2609 [M-Cl]⁺

IR (thin film, cm⁻¹) ν = 3058, 2964, 1619, 1550, 1478, 1451, 1435, 1379, 1287, 977, 746, 697

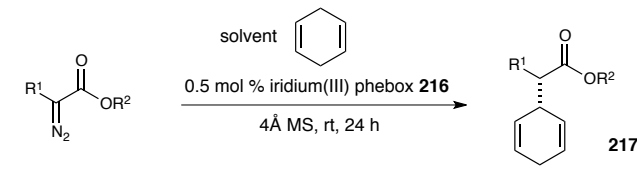
m.p. 320 °C (dec.)

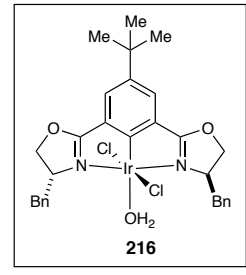
R_f 0.30 (30 % EtOAc:pentane)



6.2.4 Procedures and characterization data for C-H insertion reactions using donor/acceptor carbenes

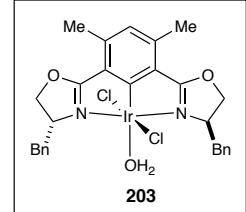
Table 3.3





216

entry ^a	R ¹	R ²	product	% yield ^b	% ee ^c
1	C ₆ H ₅	Me	217	93	97
2	C ₆ H ₅	Et	218	93	96 ^d
3	C ₆ H ₅	ⁱ Pr	219	86	96 ^d
4	C ₆ H ₅	^t Bu	220	71	88 ^d
5	2-naphthyl	Me	221	97	95 ^d
6	<i>p</i> -ClC ₆ H ₄	Me	222	99	83
7 ^e	<i>p</i> -ClC ₆ H ₄	Me	223	87	94
8	<i>p</i> -F ₃ CC ₆ H ₄	Me	224	88	88 ^d
9 ^f	<i>p</i> -MeOC ₆ H ₄	Me	225	74	83
10	<i>m</i> -ClC ₆ H ₄	Me	226	99	91
11	<i>m</i> -MeOC ₆ H ₄	Me	227	88	99
12 ^g	<i>o</i> -ClC ₆ H ₄	Me	228	10	-
13	3,4-Cl ₂ C ₆ H ₃	Me	229	99	93

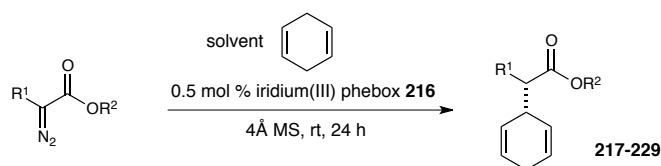


203

^a Reactions carried out on a 0.82 mmol scale. ^b Isolated yield. ^c Determined by chiral HPLC.

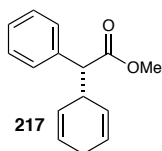
^d The absolute configuration was assigned by analogy. ^e Reaction carried out using 0.5 mol % catalyst **203**. ^f Reaction stirred for 4 days. ^g Reaction stirred for 6 days.

General procedure for the C-H insertion of aryl diazoacetates into 1,4-cyclohexadiene.



A dry 7 mL vial was charged with aryldiazoester (0.82 mmol), 4 Å powdered molecular sieves (164 mg, 200 mg/1 mmol diazo) and a PTFE coated magnetic stir bar. The vial was capped with a PTFE lined septum then evacuated and backfilled with dry nitrogen

three times. 1,4-cyclohexadiene (1.64 mL, 0.5 M in diazo) was added via syringe. The cap was removed and the iridium catalyst (0.5 mol %, 4.1 μmol) was added in a single portion. The cap was quickly replaced, the vial headspace purged with dry nitrogen, and the mixture was stirred for 24 hours (unless noted otherwise) at ambient temperature ($\sim 22\text{ }^\circ\text{C}$). The reaction mixture was concentrated and the residue was purified by flash column chromatography (SiO_2 , 5 % Et_2O :pentane) to furnish the title compound. The enantiomeric excess of the product was determined by chiral HPLC.



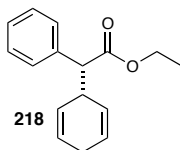
methyl (*R*)-(2,5-cyclohexadienyl)phenylacetate,¹⁰² colorless oil, 93 %, 97 % ee.

^1H NMR (400 MHz; CDCl_3): δ 7.34-7.23 (m, 5H), 5.80 (m, 1H), 5.73-5.65 (m, 2H), 5.27-5.23 (m, 1H), 3.66 (s, 3H), 3.47 (m, 1H), 3.41 (d, $J = 10.4$, 1H), 2.62-2.58 (m, 2H)

^{13}C NMR (100 MHz; CDCl_3): δ 173.6, 136.9, 128.8, 128.7, 127.6, 126.8, 126.5, 126.1, 126.0, 58.5, 52.2, 38.7, 26.6

HPLC (Daicel OJ, 230 nm detection, 0.5 % 2-propanol:hexanes, 1 mL/min); $t_{\text{R}} = 8.72$ min (major) and 10.32 min (minor)

$[\alpha]_{\text{D}}^{22}$ -105.5 ($c = 1.00$, CHCl_3)



ethyl (*R*)-(2,5-cyclohexadienyl)phenylacetate; colorless oil, 93 %, 96 % ee.

¹H NMR (400 MHz; CDCl₃): δ 7.35-7.23 (m, 5H), 5.81-5.77 (m, 1H), 5.74-5.64 (m, 2H), 5.27-5.22 (m, 1H), 4.21-4.04 (m, 2H), 3.50-3.44 (m, 1H), 3.38 (d, *J* = 10.4, 1H), 2.62-2.58 (m, 2H), 1.21 (t, *J* = 7.1, 3H)

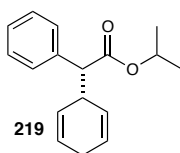
¹³C NMR (100 MHz; CDCl₃): δ 173.1, 137.0, 128.8, 128.7, 127.5, 126.8, 126.4, 126.1, 126.0, 60.9, 58.7, 38.7, 26.6, 14.4

HRMS [+ APCI] calculated for 169.10118, found 169.10098 [M-CO₂Et]⁺

IR (thin film, cm⁻¹) ν = 3030, 2980, 1729, 1153, 697

HPLC (Daicel OD, 230 nm detection, 0.5 % 2-propanol:hexanes, 1 mL/min); *t*_R = 6.68 min (major) and 8.77 min (minor)

[α]_D²² -95.0 (*c* = 1.00, CHCl₃)



isopropyl (*R*)-(2,5-cyclohexadienyl)phenylacetate; colorless oil, 86 %, 96 % ee.

¹H NMR (400 MHz; CDCl₃): δ 7.34-7.22 (m, 5H), 5.81-5.77 (m, 1H), 5.74-5.70 (m, 1H), 5.68-5.63 (m, 1H), 5.28-5.23 (m, 1H), 5.00 (sept, *J* = 6.3, 1H), 3.51-3.42 (m, 1H), 3.35 (d, *J* = 10.4, 1H), 2.62-2.57 (m, 2H), 1.23 (d, *J* = 6.3, 3H), 1.13 (d, *J* = 6.3, 3H)

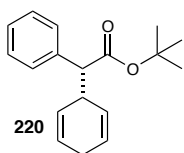
¹³C NMR (100 MHz; CDCl₃): δ 172.6, 137.2, 128.8, 128.6, 127.4, 126.9, 126.3, 126.2, 125.9, 68.3, 58.9, 38.8, 26.6, 22.0, 21.8

HRMS [+ APCI] calculated for 215.10666, found 215.10649 [M-((H₃C)₂CH)+H]⁺

IR (thin film, cm⁻¹) ν = 3030, 2979, 1725, 1163, 1106, 697

HPLC (Daicel AD-H, 230 nm detection, 0.3 % 2-propanol:hexanes, 1 mL/min); t_R = 6.35 min (minor) and 6.99 min (major)

$[\alpha]_D^{22}$ -78.7 (c = 2.00, CHCl₃)



tert-butyl (*R*)-(2,5-cyclohexadienyl)phenylacetate; pale yellow oil, 71 %, 88 % ee.

¹H NMR (400 MHz; CDCl₃): δ 7.33-7.22 (m, 5H), 5.81-5.73 (m, 2H), 5.67-5.63 (m, 1H), 5.26-5.22 (m, 1H), 3.46-3.37 (m, 1H), 3.29 (d, J = 10.4, 1H), 2.61-2.57 (m, 2H), 1.40 (s, 9H)

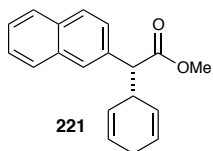
¹³C NMR (100 MHz; CDCl₃): δ 172.3, 137.5, 128.8, 128.5, 127.3, 127.0, 126.4, 126.1, 125.8, 81.0, 59.6, 38.8, 28.2, 26.6

HRMS [+ APCI] calculated for 169.10118, found 169.10091 [M-CO₂^tBu]⁺

IR (thin film, cm⁻¹) ν = 3030, 2926, 2856, 1725, 1143, 697

HPLC (Daicel OJ-H, 230 nm detection, 0.5 % 2-propanol:hexanes, 1 mL/min); t_R = 4.25 min (major) and 4.69 min (minor)

$[\alpha]_D^{22}$ -59.5 (c = 1.00, CHCl₃)



methyl-(*R*)-(2,5-cyclohexadienyl)-(2-naphthalenyl)acetate; pale-yellow wax, 97 %, 95 % ee.

¹H NMR (400 MHz; CDCl₃): δ 7.84-7.81 (m, 3H), 7.79 (d, *J* = 1.5, 1H), 7.52 (dd, *J* = 8.6, 1.8, 1H), 7.49-7.46 (m, 2H), 5.87-5.82 (m, 1H), 5.80-5.76 (m, 1H), 5.68 (dtd, *J* = 10.2, 3.3, 1.6, 1H), 5.30-5.26 (m, 1H), 3.69 (s, 3H), 3.64-3.59 (m, 2H), 2.66-2.61 (m, 2H)

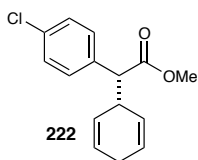
¹³C NMR (100 MHz; CDCl₃): δ 173.6, 134.4, 128.4, 128.08, 127.95, 127.83, 126.8, 126.6, 126.5, 126.3, 126.20, 126.1, 126.0, 58.7, 52.2, 38.7, 26.6

HRMS [+ APCI] calculated for 279.13796, found 279.13773 [M+H]⁺

IR (thin film, cm⁻¹) ν = 3028, 2950, 1733, 1156, 754

HPLC (Daicel AD-H, 230 nm detection, 0.3 % 2-propanol:hexanes, 1 mL/min); t_R = 10.90 min (major) and 12.70 min (minor)

[α]_D²² -159.2 (*c* = 1.00, CHCl₃)



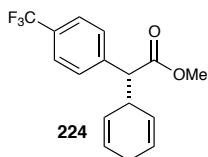
methyl (*R*)-(2,5-cyclohexadienyl)(4-chlorophenyl)acetate;¹⁰² colorless oil, 93 %, 97 % ee.

¹H NMR (400 MHz; CDCl₃): δ 7.29-7.23 (m, 4H), 5.81-5.76 (m, 1H), 5.70-5.63 (m, 2H), 5.28-5.23 (m, 1H), 3.66 (s, 3H), 3.45-3.38 (m, 2H), 2.60-2.55 (m, 2H)

¹³C NMR (100 MHz; CDCl₃): δ 173.2, 135.3, 133.5, 130.2, 128.8, 126.7, 126.5, 126.4, 125.5, 57.7, 52.3, 38.7, 26.5

HPLC (Daicel OD, 230 nm detection, 0.5 % 2-propanol:hexanes, 1 mL/min); $t_R = 5.30$ min (minor) and 7.36 min (minor)

$[\alpha]_D^{22} -147.9$ ($c = 1.00$, CHCl_3)



methyl (*R*)-(2,5-cyclohexadienyl)(4-trifluoromethylphenyl)acetate; colorless oil, 88 %, 88 % ee.

$^1\text{H NMR}$ (400 MHz; CDCl_3): δ 7.58 (d, $J = 8.2$, 2H), 7.46 (d, $J = 8.2$, 2H), 5.83-5.80 (m, 1H), 5.73-5.67 (m, 2H), 5.26-5.23 (m, 1H), 3.69 (s, 3H), 3.51 (s, 2H), 2.61-2.57 (m, 2H).

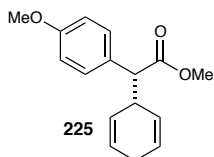
$^{13}\text{C NMR}$ (100 MHz; CDCl_3): 172.9, 140.9, 129.3, 126.9, 126.8, 126.3, 125.6, 125.3, 58.2, 52.4, 38.8, 26.5.

HRMS [+APCI] calculated for 237.08856, found 237.08869 $[\text{M}-\text{CO}_2\text{Me}]^+$

IR (thin film, cm^{-1}) $\nu = 3031, 2954, 1736, 1324, 1160, 1124, 1069, 834, 696$.

HPLC (Daicel OD-H, 230 nm detection, 0.3% IPA:hexane, 0.8 mL/min); $t_R = 4.88$ min (minor) and 5.75 min (major).

$[\alpha]_D^{22} -83.3$ ($c = 3.00$, CHCl_3)



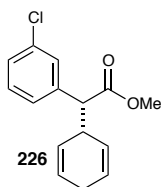
methyl (*R*)-(2,5-cyclohexadienyl)(4-methoxyphenyl)acetate,¹⁰² colorless oil, 74 %, 83 % ee.

¹H NMR (400 MHz; CDCl₃): δ 7.25-7.22 (m, 2H), 6.86-6.82 (m, 2H), 5.80-5.76 (m, 1H), 5.71-5.64 (m, 2H), 5.29-5.24 (m, 1H), 3.76 (s, 3H), 3.65 (s, 3H), 3.47-3.39 (m, 1H), 3.35 (d, *J* = 10.4, 1H), 2.62-2.57 (m, 2H)

¹³C NMR (100 MHz; CDCl₃): δ 173.9, 159.1, 129.8, 129.0, 126.9, 126.4, 126.1, 126.0, 114.1, 57.6, 55.4, 52.1, 38.8, 26.6

HPLC (Daicel OJ, 230 nm detection, 0.5 % 2-propanol:hexanes, 1 mL/min); *t_R* = 13.68 min (major) and 17.88 min (minor)

[α]_D²² -111.7 (*c* = 1.00, CHCl₃)



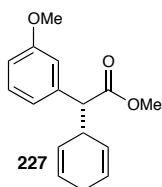
methyl-(*R*)-(2,5-cyclohexadienyl)(3-chlorophenyl)acetate;⁵ colorless oil, 99 %, 91 % ee.

¹H NMR (400 MHz; CDCl₃): δ 7.32 (s, 1H), 7.24-7.19 (m, 3H), 5.81-5.77 (m, 1H), 5.72-5.64 (m, 2H), 5.27-5.22 (m, 1H), 3.67 (s, 3H), 3.48-3.40 (m, 1H), 3.38 (d, *J* = 10.2, 1H), 2.61-2.56 (m, 2H)

¹³C NMR (100 MHz; CDCl₃): δ 173.1, 138.8, 134.5, 129.9, 129.0, 127.8, 127.1, 126.8, 126.6, 126.4, 125.5, 58.0, 52.3, 38.7, 26.5

HPLC (Daicel OD-H, 230 nm detection, 0.5 % 2-propanol:hexanes, 1 mL/min); $t_R =$ 4.26 min (minor) and 4.90 min (major)

$[\alpha]_D^{22} -105.3$ ($c = 2.00$, CHCl_3)



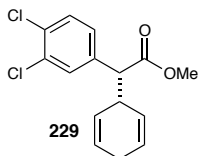
methyl (*R*)-(2,5-cyclohexadienyl)-(3-methoxyphenyl)acetate;¹⁰² colorless oil, 88 %, 99 % ee.

$^1\text{H NMR}$ (400 MHz; CDCl_3): δ 7.24 (t, $J = 7.9$, 1H), 6.93-6.90 (m, 2H), 6.82 (ddd, $J = 8.2$, 2.5, 1.0, 1H), 5.81 (m, 1H), 5.70 (m, 2H), 5.27 (m, 1H), 3.80 (s, 3H), 3.68 (s, 3H), 3.46 (m, 1H), 3.38 (d, $J = 10.6$, 1H), 2.62 (m, 2H)

$^{13}\text{C NMR}$ (100 MHz; CDCl_3): δ 173.5, 159.8, 138.4, 129.7, 126.8, 126.5, 126.0, 121.2, 114.3, 113.0, 58.5, 55.4, 52.2, 38.7, 26.6

HPLC (Daicel AD-H, 230 nm detection, 0.5 % 2-propanol:hexanes, 1 mL/min); $t_R =$ 11.25 min (major) and 18.24 min (minor)

$[\alpha]_D^{22} -122.4$ ($c = 2.00$, CHCl_3)



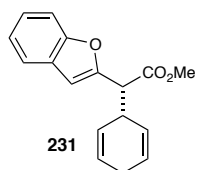
methyl (*R*)-(2,5-cyclohexadienyl)(3,4-dichlorophenyl)acetate;¹⁰² colorless oil, 99 %, 93 % ee.

¹H NMR (400 MHz; CDCl₃): δ 7.43 (d, *J* = 2.1, 1H), 7.39 (d, *J* = 8.3, 1H), 7.18 (dd, *J* = 8.3, 2.1, 1H), 5.81 (dtt, *J* = 10.1, 3.3, 1.7, 1H), 5.73 (dtt, *J* = 10.2, 3.3, 1.7, 1H), 5.67-5.62 (m, 1H), 5.32-5.27 (m, 1H), 3.70 (s, 3H), 3.46-3.38 (m, 2H), 2.62-2.56 (m, 2H)

¹³C NMR (100 MHz; CDCl₃): δ 172.8, 137.0, 132.7, 131.8, 130.9, 130.5, 128.3, 127.0, 126.9, 126.2, 125.2, 57.4, 52.4, 38.8, 26.5

HPLC (Daicel OD-H, 230 nm detection, 0.5 % 2-propanol:hexanes, 0.5 mL/min); *t_R* = 8.24 min (minor) and 10.23 min (major)

[α]_D²² -120.9 (*c* = 1.00, CHCl₃)



methyl (*R*)-2-(benzofuran-2-yl)-2-(cyclohexa-2,5-dien-1-yl)acetate; colorless oil, 46 %, 10 % ee

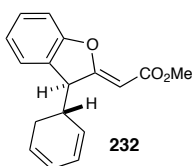
¹H NMR (400 MHz; CDCl₃): δ 7.54-7.51 (m, 1H), 7.47-7.45 (m, 1H), 7.27-7.19 (m, 2H), 6.67 (s, 1H), 5.81 (dtt, *J* = 17.4, 10.1, 3.4, 1.7, 2H), 5.70 (dq, *J* = 10.1, 2.7, 2.0, 1H), 5.53 (dq, *J* = 10.1, 2.7, 2.0, 1H), 3.82 (d, *J* = 8.7, 1H), 3.74 (s, 3H), 3.70-3.63 (m, 1H), 2.67-2.62 (m, 2H)

^{13}C NMR (100 MHz; CDCl_3): 170.9, 154.9, 153.3, 128.6, 126.9, 126.8, 125.8, 125.6, 124.1, 122.9, 121.0, 111.4, 105.2, 52.5, 52.0, 37.3, 26.5

HRMS [+APCI] calculated for 269.11722, found 269.11697 $[\text{M}+\text{H}]^+$

IR (thin film, cm^{-1}) ν = 3031, 2951, 1740, 1454, 1251, 1155, 749.

HPLC (Daicel OJ-H, 230 nm detection, 2% IPA:hexane, 1.0 mL/min); t_{R} = 43.09 min (minor) and 52.39 min (major).



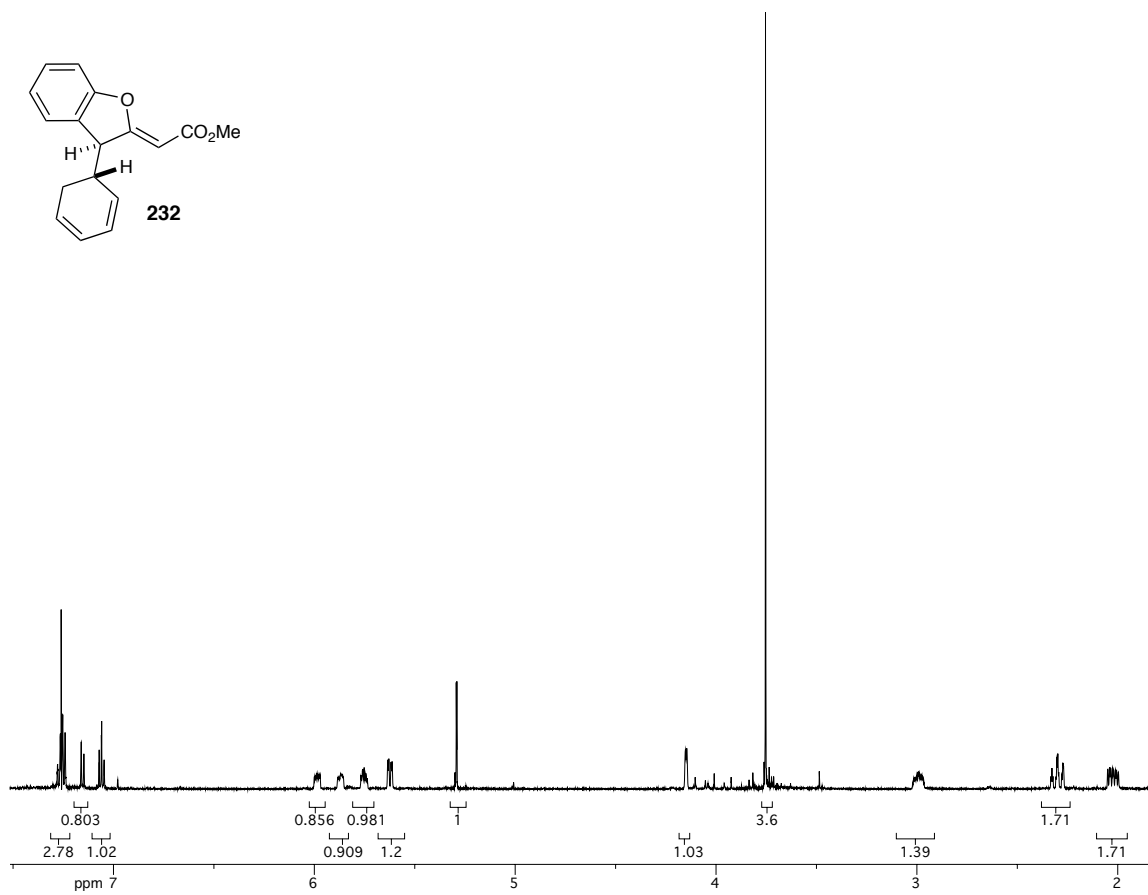
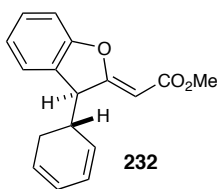
(*Z*)-methyl 2-((*S*)-3-((*S*)-cyclohexa-2,4-dien-1-yl)benzofuran-2(3*H*)-ylidene)acetate **232**; colorless oil, 29 %.

^1H NMR (600 MHz; CDCl_3): δ 7.28-7.24 (m, 2H), 7.15 (d, J = 8.0, 1H), 7.06 (td, J = 7.5, 0.8, 1H), 5.99 (ddd, J = 9.1, 5.6, 3.1, 1H), 5.88-5.86 (m, 1H), 5.77-5.74 (m, 1H), 5.62 (dd, J = 9.8, 3.1, 1H), 5.29 (dd, J = 1.7, 0.7, 1H), 4.15 (d, J = 4.2, 1H), 3.75 (s, 3H), 3.02-2.96 (m, 1H), 2.33-2.27 (m, 2H), 2.02 (ddd, J = 17.4, 8.7, 5.4, 2H)

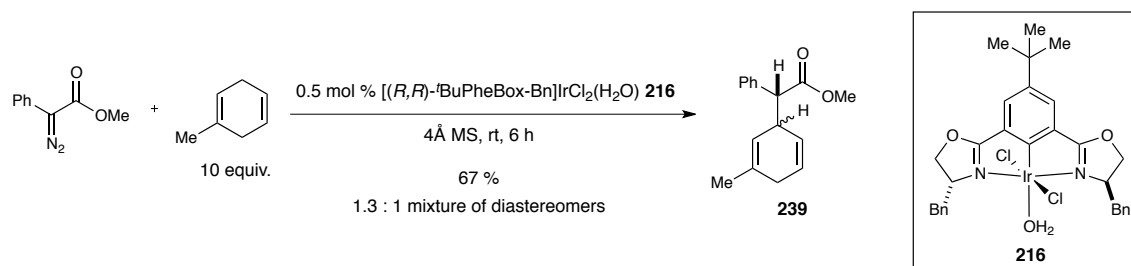
^{13}C NMR (100 MHz; CDCl_3): δ 170.8, 165.4, 157.8, 129.1, 127.1, 126.7, 125.8, 124.7, 124.4, 123.5, 110.8, 94.9, 51.3, 50.4, 39.7, 25.0

HRMS [+APCI] calculated for 209.09664, found 209.05976 $[\text{M}-\text{CO}_2\text{Me}+\text{H}]^+$

IR (thin film, cm^{-1}) ν = 2924, 2852, 1718, 1462, 1156, 752



Procedures for the C-H insertion of aryl diazoacetates into substituted cyclic 1,4-dienes

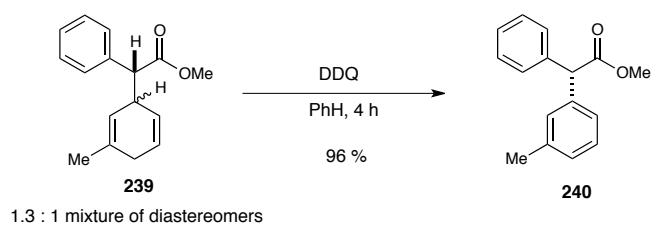
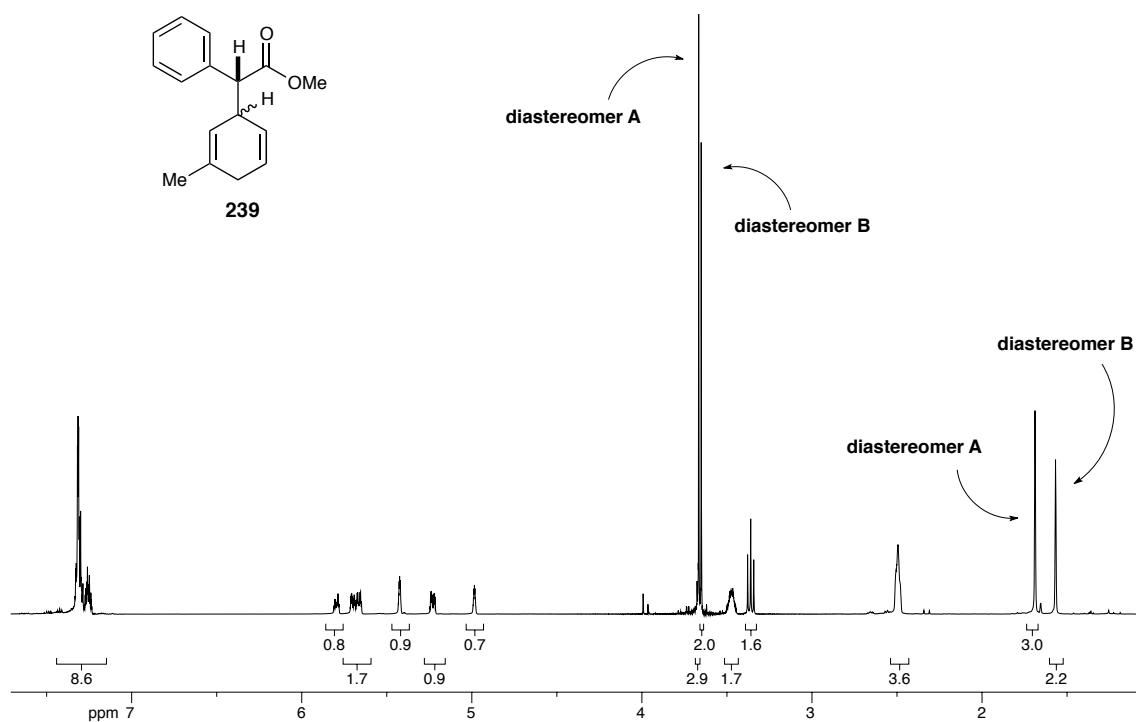


(2R)-methyl 2-(3-methylcyclohexa-2,5-dien-1-yl)-2-phenylacetate **239**

A dry 7 mL vial was charged with methyl phenyldiazoacetate (144 mg, 0.82 mmol), 4 Å powdered molecular sieves (164 mg, 200 mg/1 mmol diazo) and a PTFE coated magnetic stir bar. The vial was capped with a PTFE septum then evacuated and backfilled with dry nitrogen three times. 1-methyl-1,4-cyclohexadiene (772 mg, 8.2 mmol) and α - α -trifluorotoluene (0.82 mL, 1 M in diazo) were added via syringe. The cap was removed and iridium catalyst **216** (0.5 mol %, 3.0 mg, 4.1 μmol) was added in a single portion. The cap was quickly replaced, the vial headspace purged with dry nitrogen, and the mixture was stirred for 6 hours at ambient temperature (~ 22 °C). The reaction mixture was concentrated and the residue was purified by flash column chromatography to give a colorless oil (SiO_2 , 5 % Et_2O :pentane, R_f 0.37). ^1H NMR analysis indicated a 1.3:1 mixture of inseparable diastereomers (133 mg, 67 %).

^1H NMR (600 MHz; CDCl_3): δ 7.33-7.24 (m, 8H), 5.81-5.78 (m, 1H), 5.71-5.65 (m, 2H), 5.43 (td, $J = 3.2, 1.6$, 1H), 5.24-5.22 (m, 1H), 4.98 (dt, $J = 3.2, 1.6$, 1H), 3.67 (s, 2.90H, major diastereomer A), 3.65 (s, 2.0H, minor diastereomer B), 3.50-3.45 (m, 2H), 3.36 (t,

$J = 10.8$, 2H), 2.51-2.48 (m, 4H), 1.69 (s, 3.0H, major diastereomer A), 1.57 (s, 2.2H, minor diastereomer B)



methyl-(*S*)-2-phenyl-2-(3-methylphenyl)acetate **240**; colorless oil, 96 %

Diene **239** (63 mg, 0.26 mmol) was dissolved in benzene (9 mL, 0.03 M) and 2,3-dichloro-5,6-dicyano-1,4-benzoquinone (125 mg, 0.55 mmol) was added in a single portion. The mixture was stirred for 10 minutes then filtered through Celite, washing with

CHCl₃ until the filtrate ran clear. The filtrate was concentrated and the residue was purified by flash column chromatography (SiO₂, 5 % → 10 % Et₂O:pentane) to give methyl-(*S*)-2-phenyl-2-(3-methylphenyl)acetate **240** as a colorless oil (60 mg, 95 %, 64 % over two steps).

¹H NMR (400 MHz; CDCl₃): δ 7.31-7.28 (m, 4H), 7.26-7.18 (m, 2H), 7.10-7.05 (m, 3H), 4.98 (s, 1H), 3.73 (s, 3H), 2.31 (s, 3H)

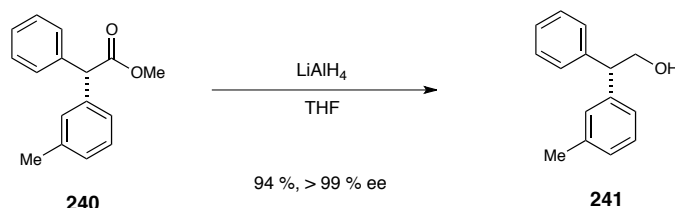
¹³C NMR (100 MHz; CDCl₃): 173.3, 138.9, 138.7, 138.5, 129.5, 128.8, 128.70, 128.3, 127.4, 125.8, 57.1, 52.5, 21.7

HRMS [+NSI] calculated for 279.0781, found 279.0781 [M+K]⁺

IR (thin film, cm⁻¹) ν = 3028, 2950, 1736, 1159, 700

[α]_D²² +12.3 (c = 1.00, CHCl₃)

R_f 0.19 (5 % Et₂O:pentane)



(*S*)-2-phenyl-2-(3-methylphenyl)ethanol **241**.

A solution of LiAlH₄ in Et₂O (1.0 M, 0.38 mL, 0.38 mmol) was added slowly to a solution of **240** (60 mg, 0.25 mmol) in THF (1.5 mL, 0.17 M) at room temperature and the reaction mixture was stirred for 14 hours. At room temperature, water (0.5 mL), 1M NaOH (0.6 mL), diethyl ether (6 mL), and water (2 mL) were added sequentially and the mixture was stirred for 5 minutes. The phases were separated and the aqueous phase was extracted with diethyl ether (3 x 5 mL). The ethereal phases were combined, dried over

Na₂SO₄, and concentrated. The residue was purified by flash column chromatography (SiO₂, 20 % → to 30 % EtOAc:hexanes) to give (*S*)-2-phenyl-2-(3-methylphenyl)ethanol **241** as a colorless oil (50 mg, 94 %, > 99 % ee).

¹H NMR (600 MHz; CDCl₃): δ 7.32-7.30 (m, 2H), 7.26-7.19 (m, 4H), 7.06-7.03 (m, 3H), 4.16-4.14 (m, 3H), 2.31 (s, 3H), 1.49 (bs, 1H)

¹³C NMR (150 MHz; CDCl₃): 141.6, 141.4, 138.6, 129.3, 128.9, 128.8, 128.5, 127.8, 127.0, 125.4, 66.4, 53.8, 21.7

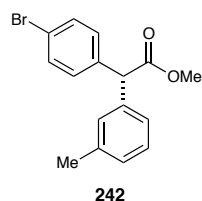
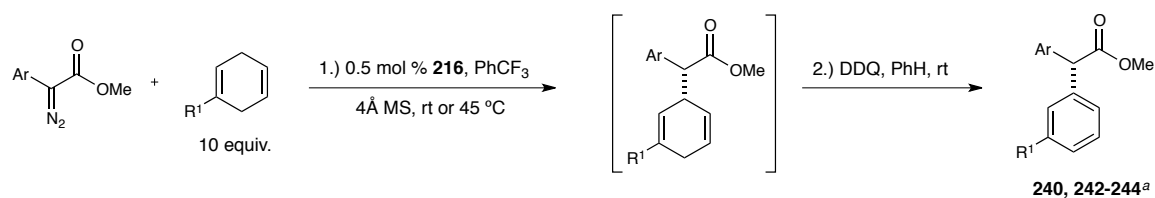
HRMS [+NSI] calculated for 235.1093, found 235.1092 [M+Na]⁺

IR (thin film, cm⁻¹) ν = 3370, 3026, 2922, 1604, 1492, 1059, 700

HPLC (Daicel OJ, 230 nm detection, 10 % 2-propanol:hexanes, 0.7 mL/min); t_R = 29.50 min (major) and 33.95 min (minor)

[α]_D²² +1.0 (c = 0.50, CHCl₃)

R_f 0.24 (20 % EtOAc:hexanes)



methyl-(*S*)-2-(4-bromophenyl)-2-(3-methylphenyl)acetate **242**.

A dry 7 mL vial was charged with methyl *p*-bromophenyldiazoacetate (105 mg, 0.41 mmol), 4 Å powdered molecular sieves (82 mg, 200 mg/1 mmol diazo) and a PTFE

coated magnetic stir bar. The vial was capped with a PTFE septum then evacuated and backfilled with dry nitrogen three times. 1-methyl-1,4-cyclohexadiene (386 mg, 4.1 mmol) and α - α - α -trifluorotoluene (0.2 mL, 1 M in diazo) were added via syringe. The cap was removed and iridium catalyst **216** (0.5 mol %, 1.5 mg, 2.1 μ mol) was added in a single portion. The cap was quickly replaced, the vial headspace purged with dry nitrogen, and the mixture was stirred for 17 hours at ambient temperature (~ 22 °C). The reaction mixture was concentrated and the residue was purified by flash column chromatography (SiO₂, 5 % Et₂O:pentane, R_f 0.57). ¹H NMR analysis indicated a 1.3:1 mixture of inseparable diastereomers as a colorless oil (128 mg, 97 %). A portion of the oil (62 mg, 0.19 mmol) was dissolved in benzene (6.5 mL, 0.03 M) and 2,3-dichloro-5,6-dicyano-1,4-benzoquinone (52 mg, 0.23 mmol) was added in a single portion. The mixture was stirred for 2 hours then filtered through Celite, washing with CHCl₃ until the filtrate ran clear. The filtrate was concentrated and the residue was purified by flash column chromatography (SiO₂, 5 % \rightarrow 10 % Et₂O:pentane) to give methyl-(*S*)-2-(4-bromophenyl)-2-(3-methylphenyl)acetate **242** as a colorless oil (62 mg, 99 %, 95 % ee, 96 % over two steps).

¹H NMR (400 MHz; CDCl₃): δ 7.43 (d, J = 8.5, 2H), 7.24-7.21 (m, 1H), 7.18 (d, J = 8.5, 2H), 7.07 (t, J = 6.2, 3H), 4.93 (s, 1H), 3.73 (s, 3H), 2.32 (s, 3H)

¹³C NMR (100 MHz; CDCl₃): 172.8, 138.7, 138.1, 137.9, 131.9, 130.6, 129.3, 128.8, 128.5, 125.6, 121.5, 56.5, 52.7, 21.7

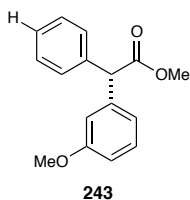
HRMS [+APCI] calculated for 259.01169, found 259.01192 [M-CO₂Me]⁺

IR (thin film, cm⁻¹) ν = 2950, 1738, 1488, 1161, 1011

HPLC (Daicel SS WHELK, 230 nm detection, 1.0 % 2-propanol:hexanes, 1 mL/min); t_R = 11.35 min (minor) and 14.68 min (major)

$[\alpha]_D^{22} +19.8$ ($c = 1.00$, CHCl_3)

R_f 0.29 (5 % Et_2O :pentane)



methyl-(*S*)-2-phenyl-2-(3-methoxyphenyl)acetate **243**.

A dry 7 mL vial was charged with methyl phenyldiazoacetate (72 mg, 0.41 mmol), 4Å powdered molecular sieves (82 mg, 200 mg/1 mmol diazo) and a PTFE coated magnetic stir bar. The vial was capped with a PTFE septum then evacuated and backfilled with dry nitrogen three times. 1-methoxy-1,4-cyclohexadiene (534 mg, 4.1 mmol) and α - α - α -trifluorotoluene (0.2 mL, 1 M in diazo) were added via syringe. The cap was removed and iridium catalyst **216** (0.5 mol %, 1.5 mg, 2.1 μmol) was added in a single portion. The cap was quickly replaced, the vial headspace purged with dry nitrogen, and the mixture was stirred for 6.5 hours at ambient temperature (~ 22 °C). The reaction mixture was concentrated and the residue was filtered through a pad of silica, washing first with hexanes (to remove excess diene) then washing with 1:1 Et_2O :pentane to collect the insertion product (5 % Et_2O :pentane, R_f 0.21) as a colorless oil. ^1H NMR of the mixture showed a 1.1:1 mixture of inseparable diastereomers. The oil was dissolved in benzene (10 mL, 0.04 M) and 2,3-dichloro-5,6-dicyano-1,4-benzoquinone (111 mg, 0.49 mmol) was added in a single portion. The mixture was stirred for 2 hours then filtered

through Celite, washing with CHCl_3 until the filtrate ran clear. The filtrate was concentrated and the residue was purified by flash column chromatography (SiO_2 , 5 % \rightarrow 10 % Et_2O :pentane) to give methyl-(*S*)-2-phenyl-2-(3-methoxyphenyl)acetate **243** as a colorless oil (103 mg, 98 %, 94 % ee).

$^1\text{H NMR}$ (400 MHz; CDCl_3): δ 7.31-7.29 (m, 4H), 7.27-7.21 (m, 3H), 6.89-6.87 (m, 1H), 6.86-6.85 (m, 1H), 6.81-6.78 (m, 1H), 4.99 (s, 1H), 3.76 (s, 3H), 3.73 (s, 3H)

$^{13}\text{C NMR}$ (100 MHz; CDCl_3): 173.1, 159.9, 140.2, 138.6, 129.8, 128.8, 127.5, 121.2, 114.8, 112.7, 57.1, 55.4, 52.6

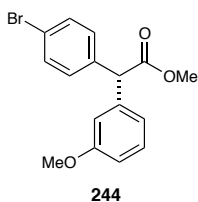
HRMS [+NSI] calculated for 295.07310, found 295.07297 $[\text{M}+\text{K}]^+$

IR (thin film, cm^{-1}) ν = 2950, 1733, 1597, 1489, 1261, 1144, 696

HPLC (Daicel ChiralPak AS-H, 230 nm detection, 1.0 % 2-propanol:hexanes, 0.5 mL/min); t_{R} = 16.69 min (major) and 18.56 min (minor)

$[\alpha]_{\text{D}}^{22}$ +10.4 (c = 1.00, CHCl_3)

R_{f} 0.24 (10 % Et_2O :pentane)



methyl-(*S*)-2-(4-bromophenyl)-2-(3-methoxyphenyl)acetate **244**.

A dry 7 mL vial was charged with methyl *p*-bromophenyldiazoacetate (105 mg, 0.41 mmol), 4Å powdered molecular sieves (82 mg, 200 mg/1 mmol diazo) and a PTFE coated magnetic stir bar. The vial was capped with a PTFE septum then evacuated and backfilled with dry nitrogen three times. 1-methoxy-1,4-cyclohexadiene (452 mg, 4.1 mmol) and α - α - α -trifluorotoluene (0.2 mL, 1 M in diazo) were added via syringe. The

cap was removed and iridium catalyst **216** (0.5 mol %, 1.5 mg, 2.1 μmol) was added in a single portion. The cap was quickly replaced, the vial headspace purged with dry nitrogen, and the mixture was stirred for 2 hours at ambient temperature ($\sim 22\text{ }^\circ\text{C}$). The reaction mixture was concentrated and the residue was filtered through a pad of silica, washing first with hexanes (to remove excess diene) then washing with 1:1 Et_2O :pentane to collect the insertion product (10 % Et_2O :pentane, R_f 0.33) as a colorless oil. ^1H NMR of the mixture showed a 4.3:1 mixture of inseparable diastereomers. The oil was dissolved in benzene (14 mL, 0.03 M) and 2,3-dichloro-5,6-dicyano-1,4-benzoquinone (111 mg, 0.49 mmol) was added in a single portion. The mixture was stirred for 8 hours then filtered through Celite, washing with CHCl_3 until the filtrate ran clear. The filtrate was concentrated and the residue was purified by flash column chromatography (SiO_2 , 5 % \rightarrow 10 % Et_2O :pentane) to give methyl-(*S*)-2-(4-bromophenyl)-2-(3-methoxyphenyl)acetate **244** as a colorless oil (113 mg, 82 %, 90 % ee).

^1H NMR (400 MHz; CDCl_3): δ 7.44 (d, $J = 8.5$, 2H), 7.27-7.23 (m, 2H), 7.19 (m, $J = 8.5$, 2H), 6.87-6.85 (m, 1H), 6.83-6.80 (m, 2H), 4.95 (s, 1H), 3.78 (s, 3H), 3.75 (s, 3H)

^{13}C NMR (100 MHz; CDCl_3): δ 172.6, 160.0, 139.7, 137.7, 131.9, 130.5, 130.0, 121.6, 121.0, 114.7, 112.8, 56.5, 55.4, 52.7

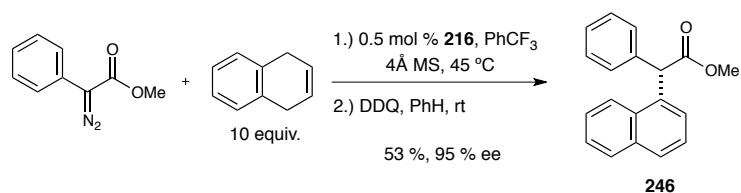
HRMS [+NSI] calculated for 372.98362, found 372.98351 $[\text{M}+\text{K}]^+$

IR (thin film, cm^{-1}) $\nu = 2951, 1737, 1489, 1262, 1162, 1011$

HPLC (Chiralcel OJ-H, 230 nm detection, 25 % 2-propanol:hexanes, 1 mL/min); $t_R = 20.66$ min (minor) and 22.74 min (major)

$[\alpha]_D^{22} +20.5$ ($c = 1.00$, CHCl_3)

R_f 0.23 (10 % Et_2O :pentane)



methyl-(*S*)-2-(1-naphthalenyl)-2-phenylacetate **246**.

A dry 7 mL vial was charged with 4Å powdered molecular sieves (84 mg, 200 mg/1 mmol diazo), 1,4-dihydronaphthalene (549 mg, 4.22 mmol), iridium catalyst **216** (0.5 mol %, 3.0 mg, 4.2 μmol) and a PTFE coated magnetic stir bar. The vial was capped with a PTFE septum then evacuated and backfilled with dry nitrogen three times. The mixture was submerged in a preheated 45 °C oil bath, then a solution of methyl phenyldiazoacetate (74 mg, 0.42 mmol) and 1,4-dihydronaphthalene (0.11 mL, 0.26 M in diazo) in α - α - α -trifluorotoluene (0.73 mL, 0.58 M in diazo) was added over the course of 42 hours *via* syringe pump. The mixture was allowed to stir an additional 18 hours then filtered through a plug of silica gel, washing with a 1:1 mixture of Et₂O:pentane. The filtrate was concentrated and the residue was purified by flash column chromatography [SiO₂, 0 % → 5 % Et₂O:pentane (*R_f* 0.37 in 5 % Et₂O:pentane)] to collect the insertion product as a colorless oil (68 mg, 58 %). ¹H NMR of the oil showed a 8:1 mixture of inseparable diastereomers. The oil was dissolved in benzene (14 mL, 0.03 M) and 2,3-dichloro-5,6-dicyano-1,4-benzoquinone (111 mg, 0.50 mmol) was added in a single portion. The mixture was stirred for 2 hours, then a second portion of 2,3-dichloro-5,6-dicyano-1,4-benzoquinone (76 mg, 0.34 mmol) was added. The mixture was stirred for 4 hours then a third portion of 2,3-dichloro-5,6-dicyano-1,4-benzoquinone (26 mg, 0.11 mmol) was added. The reaction was stirred an additional 14 h, at which time the entire mixture was filtered through a pad of silica gel, washing with a 1:1 mixture of

Et₂O:pentane until the filtrate ran clear. The filtrate was concentrated and the residue was purified by flash column chromatography (SiO₂, 0 % → 5 % → 10 % Et₂O:pentane) to give methyl-(*S*)-2-(1-naphthalenyl)-2-phenylacetate **246** as a colorless oil (62 mg, 53 %, 95 % ee)

¹H NMR (400 MHz; CDCl₃): δ 8.01-7.98 (m, 1H), 7.89-7.87 (m, 1H), 7.81 (d, *J* = 8.2, 1H), 7.52-7.48 (m, 2H), 7.44 (t, *J* = 7.7, 1H), 7.37-7.27 (m, 6H), 5.81 (s, 1H), 3.77 (s, 3H)

¹³C NMR (100 MHz; CDCl₃): 173.5, 138.1, 134.6, 134.2, 131.8, 129.2, 128.9, 128.4, 127.6, 126.8, 126.5, 125.9, 125.6, 123.3, 77.4, 53.8, 52.7

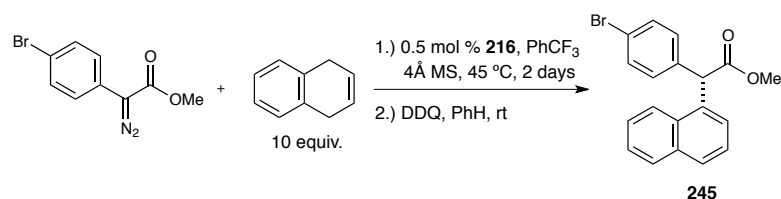
HRMS [+APCI] calculated for 299.10425, found 299.10414 [M+Na]⁺

IR (thin film, cm⁻¹) ν = 3060, 2950, 1735, 1195, 1151, 778, 698

HPLC (Daicel Chiralpak AS-H, 210 nm detection, 1.0 % 2-propanol:hexanes, 1 mL/min); t_R = 6.53 min (major) and 7.54 min (minor)

[α]_D²² +7.4 (*c* = 1.00, CHCl₃)

R_f 0.40 (10 % Et₂O:pentane)



methyl-(*S*)-2-(4-bromophenyl)-2-(1-naphthalenyl)acetate **245**.

A dry 7 mL vial was charged with 4 Å powdered molecular sieves (42 mg, 200 mg/1 mmol diazo), 1,4-dihydronaphthalene (275 mg, 2.11 mmol), iridium catalyst **216** (0.5 mol %, 1.5 mg, 2.1 μmol) and a PTFE coated magnetic stir bar. The vial was capped with a

PTFE septum then evacuated and backfilled with dry nitrogen three times. The mixture was submerged in a preheated 45 °C oil bath, then a solution of methyl 4-bromophenyldiazoacetate (54 mg, 0.21 mmol) in α - α - α -trifluorotoluene (0.42 mL, 0.5 M in diazo) was added over the course of 42 hours *via* syringe pump. The mixture was allowed to stir an additional 24 hours then filtered through a pad of silica gel, washing with a 1:1 mixture of Et₂O:pentane. The filtrate was concentrated and the residue was purified by flash column chromatography [SiO₂, 0 % \rightarrow 5 % Et₂O:pentane (R_f 0.28 in 5 % Et₂O:pentane)] to collect the insertion product as a colorless oil (68 mg, 58 %). The oil was dissolved in benzene (7 mL, 0.03 M) and 2,3-dichloro-5,6-dicyano-1,4-benzoquinone (57 mg, 0.50 mmol) was added in a single portion. The mixture was stirred for 2 hours, then a second portion of 2,3-dichloro-5,6-dicyano-1,4-benzoquinone (25 mg, 0.11 mmol) was added. The mixture was stirred for an additional 16 hours, at which time the entire mixture was filtered through a pad of silica gel, washing with a 1:1 mixture of Et₂O:pentane until the filtrate ran clear. The filtrate was concentrated and the residue was purified by flash column chromatography (SiO₂, 0 % \rightarrow 5 % \rightarrow 10 % Et₂O:pentane) to give methyl-(*S*)-2-(4-bromophenyl)-2-(1-naphthalenyl)acetate **245** as a colorless oil (37 mg, 52 %, 88 % ee).

¹H NMR (600 MHz; CDCl₃): δ 7.93-7.91 (m, 1H), 7.88-7.87 (m, 1H), 7.82 (d, J = 8.3, 1H), 7.50-7.48 (m, 2H), 7.45 (dt, J = 8.0, 3.8, 3H), 7.35 (d, J = 7.1, 1H), 7.19 (d, J = 8.3, 2H), 5.74 (s, 1H), 3.77 (s, 3H)

¹³C NMR (150 MHz; CDCl₃): 173.1, 137.2, 134.2, 134.0, 132.0, 131.6, 130.9, 129.3, 128.7, 126.9, 126.3, 126.1, 125.6, 123.3, 121.7, 53.2, 52.9

HRMS [+NSI] calculated for 392.98870, found 392.98858 [M+K]⁺

IR (thin film, cm^{-1}) $\nu = 3049, 2950, 1735, 1487, 1162, 778$

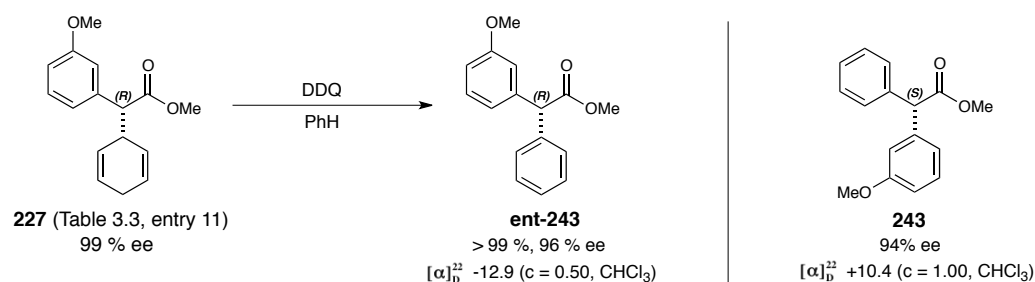
HPLC (Daicel Chiralcel OJ-H, 230 nm detection, 25 % 2-propanol:hexanes, 1 mL/min);

$t_R = 15.79$ min (major) and 19.39 min (minor)

$[\alpha]_D^{22} -1.6$ ($c = 1.00, \text{CHCl}_3$)

R_f 0.39 (10 % Et₂O:pentane)

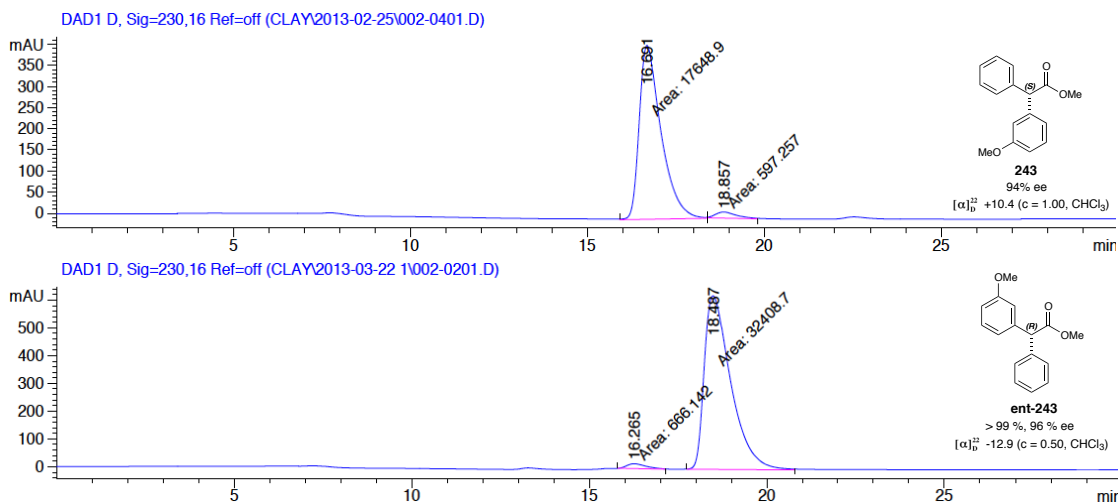
Confirmation of the predicted facial selectivity for insertion into methyl phenyldiazoacetate into 1-methoxy-1,4-cyclohexadiene



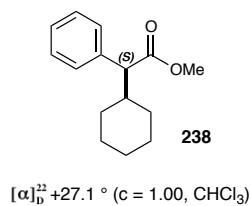
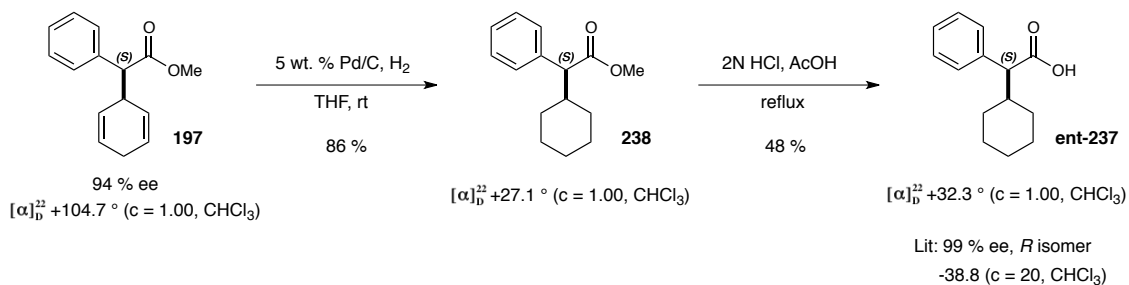
2,3-dichloro-5,6-dicyano-1,4-benzoquinone (44 mg, 0.19 mmol) was added in a single portion to a stirring mixture of methyl-(*R*)-(2,5-cyclohexadienyl)-(3-methoxyphenyl)acetate **227** (41 mg, 0.16 mmol). The mixture was stirred for 18 hours, and the entire mixture was filtered through a pad of silica gel, washing with a 1:1 mixture of Et₂O:pentane until the filtrate ran clear. The filtrate was concentrated and the residue was purified by flash column chromatography (SiO₂, 5 % → 10 % Et₂O:pentane) to give methyl-(*R*)-2-phenyl-2-(3-methoxyphenyl)acetate (**ent-243**) as a colorless oil (41 mg, > 99 %, 96 % ee).

HPLC (Daicel ChiralPak AS-H, 230 nm detection, 1.0 % 2-propanol:hexanes, 0.5 mL/min); $t_R = 16.27$ min (minor) and 18.48 min (major).

$[\alpha]_D^{22}$ -12.9 ($c = 0.50$, CHCl_3).



Determination of the absolute stereochemistry for the C-H insertion of methyl phenyldiazoacetate into 1,4-cyclohexadiene



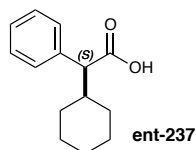
(*R*)-methyl-2-cyclohexyl-2-phenylacetate **238**; colorless oil, 86 %.

A mixture of methyl-(*R*)-(2,5-cyclohexadienyl)phenylacetate **197** (158 mg, 0.69 mmol, 94 % ee, $[\alpha]_D^{22} +104.7$ ($c = 1.0$, CHCl_3) and 5 wt. % Pd/C (146 mg, 0.069 mmol Pd) in THF (7 mL, 1M) was stirred under 1 atm H_2 (balloon) for 20 hours. The mixture was filtered through a pad of celite, washing with Et_2O (~ 50 mL). The filtrate was concentrated under reduced pressure to give (*R*)-methyl-2-cyclohexyl-2-phenylacetate **238** as a colorless oil (138 mg, 86 %).

$^1\text{H NMR}$ (400 MHz; CDCl_3): δ 7.34-7.22 (m, 5H), 3.63 (s, 3H), 3.23 (d, $J = 10.7$, 1H), 2.02 (qt, $J = 11.1, 3.3$, 1H), 1.83-1.72 (m, 2H), 1.65-1.58 (m, 2H), 1.36-1.27 (m, 2H), 1.19-1.00 (m, 3H), 0.74 (qd, $J = 12.2, 3.4$, 1H).

HRMS [+APCI] calculated for 233.15361, found 233.15347 $[\text{M}+\text{H}]^+$

$[\alpha]_D^{22} +27.1$ ($c = 1.0$, CHCl_3).



$[\alpha]_D^{22} +32.3^\circ$ ($c = 1.00$, CHCl_3)

Lit: 99 % ee, *R* isomer
-38.8 ($c = 20$, CHCl_3)

(*S*)-2-cyclohexyl-2-phenylacetic acid **ent-237**; amorphous solid, 48 %.

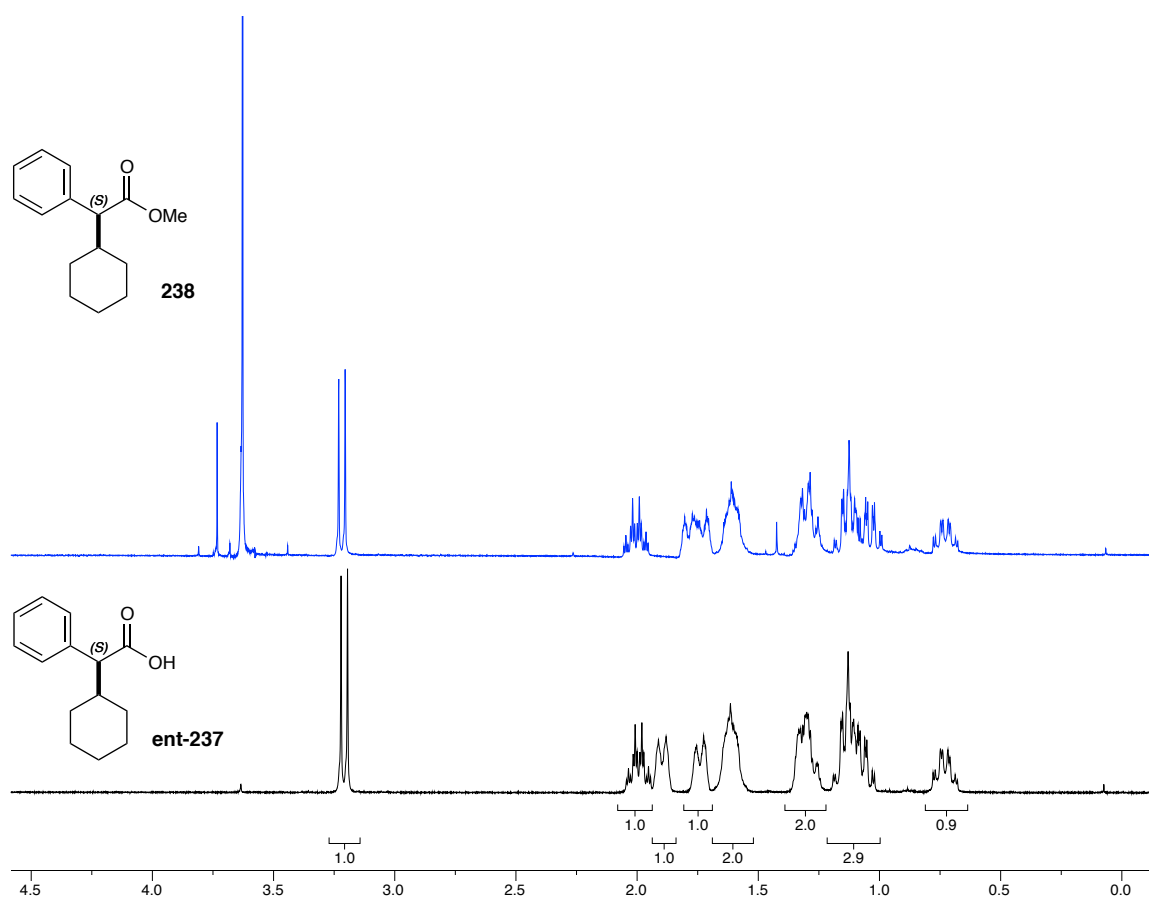
A procedure was adapted from the literature as follows:⁶ A mixture of ester **238**, 2N HCl (1.3 mL), and glacial acetic acid (3.2 mL) was refluxed overnight. The mixture was cooled to room temperature and concentrated. Water was added (5 mL) and the mixture was extracted with CH_2Cl_2 (8 x 5 mL). The extracts were combined, dried over Na_2SO_4 , and concentrated to give **ent-237** as an amorphous solid (42 mg, 48 %). The spectral data match the literature.

$^1\text{H NMR}$ (400 MHz; CDCl_3): δ 11.18 (bs, 1H), 7.33-7.24 (m, 5H), 3.21 (d, $J = 11.0$, 1H), 1.99 (qt, $J = 11.0$, 3.4, 1H), 1.90 (app d, $J = 12.7$, 1H), 1.76-1.72 (m, 1H), 1.65-1.58 (m, 2H), 1.35-1.24 (m, 2H), 1.19-1.02 (m, 3H), 0.73 (qd, $J = 12.2$, 3.4, 1H)

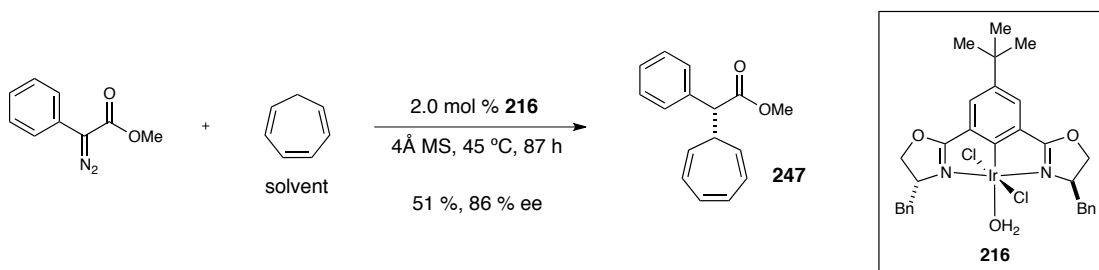
$^{13}\text{C NMR}$ (100 MHz; CDCl_3): 180.5, 137.5, 128.92, 128.74, 127.6, 59.1, 59.0, 40.9, 32.1, 30.5, 26.5, 26.1

IR (thin film, cm^{-1}) $\nu = 3029, 2923, 2851, 1699, 1291, 699$

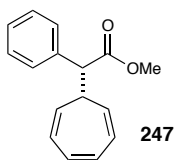
$[\alpha]_{\text{D}}^{22} +32.3$ ($c = 1.00, \text{CHCl}_3$)



Procedure for the C-H insertion of methyl phenyldiazoacetate into cycloheptatriene



A solution of **9** (72 mg, 0.41 mmol) in cycloheptatriene (1.44 mL) was added over the course of 72 hours to a stirring mixture of iridium catalyst **8** (6.0 mg, 8.2 μ mol, 2.0 mol %), 4Å powdered molecular sieves (82 mg, 200 mg/1 mmol diazo), and cycloheptatriene (0.82 mL) at 45 °C. Upon addition of the diazoester, the reaction was stirred for an additional 15 hours. The reaction mixture was filtered through Celite, the filter cake was washed with CHCl₃, and the filtrate was concentrated. The residue was purified by flash column chromatography (SiO₂, 5 % Et₂O:pentane) to give methyl-(*R*)-2-(cyclohepta-2,4,6-trien-1-yl)-2-phenylacetate **247** as a colorless oil (50 mg, 51 %, 86 % ee).



methyl-(*R*)-2-(cyclohepta-2,4,6-trien-1-yl)-2-phenylacetate **247**.

¹H NMR (400 MHz; CDCl₃): δ 7.35-7.26 (m, 5H), 6.68 (qd, J = 11.7, 5.4, 2H), 6.27 (dd, J = 9.5, 5.4, 1H), 6.10 (dd, J = 9.5, 5.5, 1H), 5.37 (dd, J = 9.5, 6.1, 1H), 5.00 (dd, J = 9.5, 6.1, 1H), 3.84 (d, J = 11.7, 1H), 3.67 (s, 3H), 2.67 (dt, J = 11.7, 6.0, 1H).

¹³C NMR (100 MHz; CDCl₃): 173.7, 137.2, 131.21, 131.10, 128.9, 128.8, 127.8, 125.9, 125.7, 124.4, 123.4, 53.2, 52.3, 41.9.

HRMS [+NSI] calculated for 241.12231, found 241.12220 [M+H]⁺

IR (thin film, cm^{-1}) $\nu = 3016, 2951, 1733, 1155, 695$.

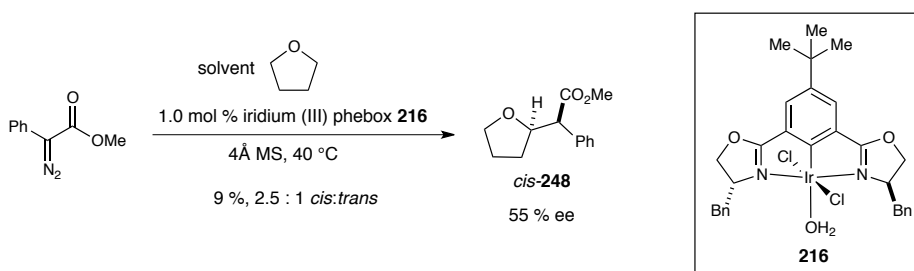
HPLC (Daicel Chiralcel OJ-H, 210 nm detection, 5.0 % 2-propanol:hexanes, 1 mL/min);

$t_R = 15.40$ min (major) and 25.64 min (minor).

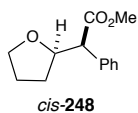
$[\alpha]_D^{22} +8.0$ ($c = 0.50, \text{CHCl}_3$).

R_f 0.32 (5 % Et₂O:pentane)

Procedure for the C-H insertion of methyl phenyldiazoacetate into tetrahydrofuran



A solution of methyl phenyldiazoacetate (100 mg, 0.57 mmol) in THF (100 mg / 1 mL) was added over 6 hours via syringe pump to a stirring mixture of iridium catalyst **216** (3.7 mg, 5 μm , 1 mol %) and 4 Å MS (115 mg) in THF (3 mL) at 40 °C. The mixture was stirred for an additional 63 hours at 40 °C. The mixture was filtered through a plug of celite and concentrated. The residue was submitted for crude NMR analysis to obtain the diastereomeric ratio (2.5 : 1). After recovery of the NMR sample, the residue was purified by flash column chromatography (SiO₂, 10 % EtOAc:hexanes) to obtain the major diastereomer *cis*-**248** as a colorless oil (9 %, 55 % ee).



Methyl-(α ,*S*,*2R*)-(tetrahydrofuran-2-yl)phenylacetate *cis*-**238**;⁵ colorless oil, 9 %, 55 % ee.

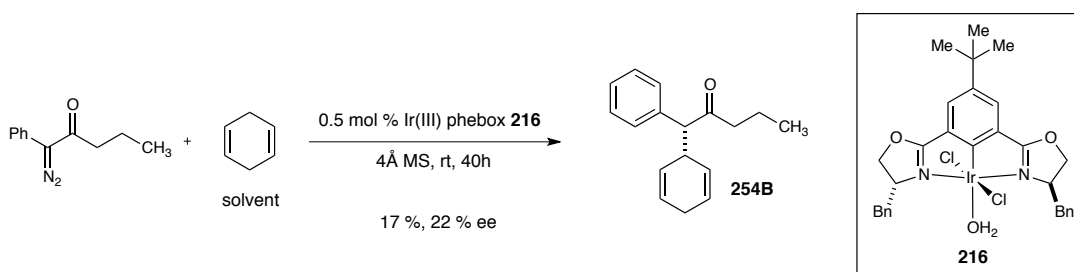
¹H NMR (400 MHz; CDCl₃): δ 7.38-7.24 (m, 5H), 4.45 (q, J = 8.4, 1H), 3.79 (dt, J = 8.2, 6.8, 1H), 3.70 (dt, J = 8.2, 6.8, 1H), 3.66 (s, 3H), 3.62 (d, J = 8.4, 1H), 2.15-2.07 (m, 1H), 1.90-1.82 (m, 2H), 1.71-1.62 (m, 1H).

¹³C NMR (150 MHz; CDCl₃): δ 172.7, 136.8, 128.76, 128.72, 127.7, 80.2, 68.5, 57.0, 52.2, 30.3, 25.8.

HPLC (Chiralcel OD-H, 230 nm detection, 0.1 % 2-propanol:hexanes, 0.5 mL/min); t_R = 17.67 min (major) and 24.90 min (minor).

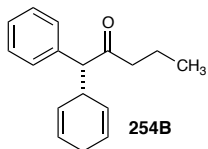
$[\alpha]_D^{22}$ -27.6 (c = 0.5, CHCl₃)

Procedures for the C-H insertion of donor/acceptor C-H insertion into 1,4-cyclohexadiene using ketone and trifluoromethyl acceptor



A 7 mL vial was charged with phenyl diazopentanone (154 mg, 0.82 mmol), 4Å powdered molecular sieves (164 mg) and a PTFE coated magnetic stir bar. The vial was capped with a PTFE septum, and evacuated and backfilled with dry nitrogen three times. 1,4-cyclohexadiene (1.64 mL, 0.5 M in diazo) was added via syringe. The cap was removed, and the iridium catalyst **216** (0.5 mol %, 3.0 mg, 4.1 μ mol) was added in a

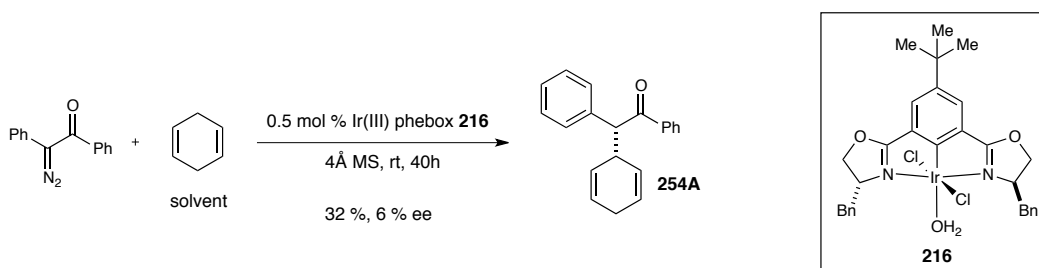
single portion. The vial was capped and the mixture was stirred for 40 hours at room temperature ($\sim 22\text{ }^{\circ}\text{C}$). The reaction mixture was filtered through celite and concentrated. The residue was purified by flash column chromatography (SiO_2 , 5 % Et_2O :pentane) to furnish 1-(2,5-cyclohexadienyl)-1-phenyl-2-pentanone **254B** as a colorless oil (33.5 mg, 17 %, 22 % ee).



1-(2,5-cyclohexadienyl)-1-phenyl-2-pentanone **254B**;⁷ as a colorless oil, 17 %, 22 % ee).

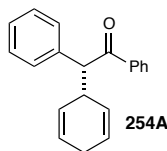
$^1\text{H NMR}$ (400 MHz; CDCl_3): δ 7.34-7.21 (m, 5H), 5.77-5.58 (m, 3H), 5.20-5.16 (m, 1H), 2.62-2.59 (m, 2H), 2.37-2.33 (m, 2H), 1.59-1.53 (m, 2H), 0.79 (t, $J = 7.4$, 2H).

HPLC (Chiralcel AD-H, 230 nm detection, 0% to 0.1 % IPA:hexane, 0.5 mL/min); $t_R =$ 13.74 min (minor) and 14.68 min (major).



A 7 mL vial was charged with phenyl diazoacetophenone (182 mg, 0.82 mmol), 4Å powdered molecular sieves (164 mg) and a PTFE coated magnetic stir bar. The vial was capped with a PTFE septum, and evacuated and backfilled with dry nitrogen three times. 1,4-cyclohexadiene (1.64 mL, 0.5 M in diazo) was added via syringe. The cap was removed, and the iridium catalyst **216** (0.5 mol %, 3.0 mg, 4.1 μmol) was added in a single portion. The vial was capped and the mixture was stirred for 40 hours at room

temperature (~ 22 °C). The reaction mixture was filtered through celite and concentrated. The residue was submitted for crude NMR analysis to obtain the insertion:cyclopropanation ratio (2.5:1). After recovery of the NMR sample, the residue was purified by flash column chromatography (SiO₂, 5 % Et₂O:pentane) to obtain (*R*)-2-(cyclohexa-2,5-dien-1-yl)-1,2-diphenylethanone **254A** as a colorless oil (72.6 mg, 32 %, 6 % ee).

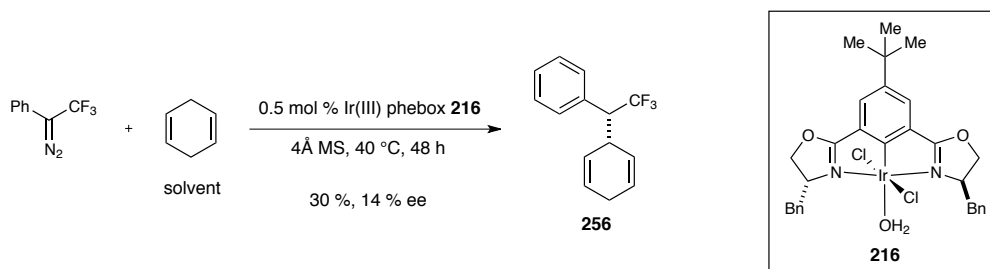


(*R*)-2-(cyclohexa-2,5-dien-1-yl)-1,2-diphenylethanone **254A**,⁷ colorless oil, 32 %, 6 % ee)

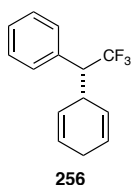
¹H NMR (400 MHz; CDCl₃): δ 7.95 (d, *J* = 8.3, 2H), 7.49-7.45 (m, 1H), 7.39-7.33 (m, 4H), 7.30-7.24 (m, 3H), 7.22-7.18 (m, 1H), 5.72-5.67 (m, 3H), 5.26-5.23 (m, 1H), 4.46 (d, *J* = 10.2, 1H), 3.76-3.68 (m, 1H), 2.64-2.61 (m, 2H).

¹³C NMR (100 MHz; CDCl₃): δ 199.5, 137.4, 137.0, 133.1, 129.15, 128.98, 128.86, 128.73, 127.7, 127.4, 125.99, 125.81, 60.5, 38.9, 26.6.

HPLC (Chiralcel AS-H, 230 nm detection, 0% to 0.1 % IPA:hexane, 0.5 mL/min); T_R = 8.26 min (major) and 8.94 min (minor).



A 10 mL flask was charged with trifluoromethyl phenyldiazomethane (143 mg, 0.77 mmol), 4Å powdered molecular sieves (164 mg, 200 mg/1 mmol diazo) and a PTFE coated magnetic stir bar. The flask was fitted with a reflux condenser then purged with dry nitrogen. 1,4-cyclohexadiene (1.64 mL, 0.5 M in diazo) was added via syringe, and the iridium catalyst **216** (0.5 mol %, 3.0 mg, 4.1 μmol) was added in a single portion. The mixture was stirred for 48 hours at 40 °C. The reaction mixture was cooled then filtered through celite and concentrated. The residue was submitted for crude NMR analysis to obtain the insertion:cyclopropanation ratio (3.5:1). After recovery of the NMR sample, the residue was purified by flash column chromatography (SiO₂, pentane) to obtain 1-(2,5-cyclohexadienyl)-2,2,2-trifluoroethylbenzene **256** as a colorless oil (54 mg, 30 %, 14 % ee)



1-(2,5-cyclohexadienyl)-2,2,2-trifluoroethylbenzene **256**; colorless oil, 30 %, 14 % ee)

¹H NMR (400 MHz; CDCl₃): δ 7.34-7.24 (m, 5H), 5.77-5.69 (m, 3H), 5.57-5.54 (m, 1H), 3.51-3.48 (m, 1H), 3.29 (qd, *J* = 10.2, 6.7, 1H), 2.54-2.31 (m, 2H).

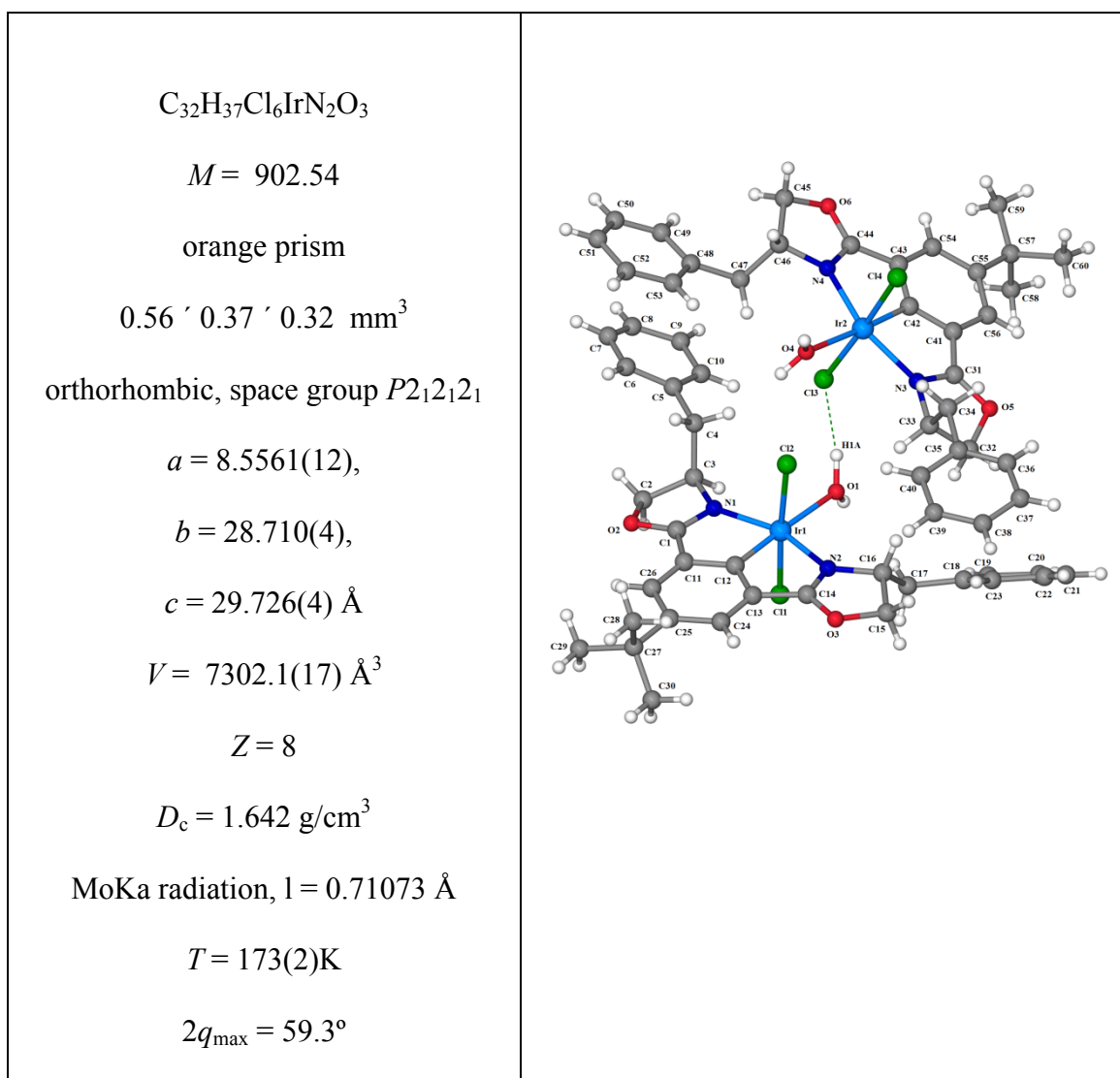
¹³C NMR (100 MHz; CDCl₃): δ 133.9, 129.8, 128.4, 128.0, 127.3, 126.9, 126.2, 125.3, 55.6 (q, *J* = 24.6), 36.2, 26.1

HPLC (Chiralcel OJ-H, 210 nm detection, 0% to 0.1 % IPA:hexane, 0.5 mL/min); t_R = 11.23 min (minor) and 12.94 min (major).

6.2.5 X-ray Crystallographic Data for [(*R,R*)-^tBuPhebox-Bn]IrCl₂(H₂O) **216**

Crystal structure data for the absolute structure determination of [(*R,R*)-^tBuPheBox-Bn]IrCl₂(H₂O) **216** has been deposited in the Cambridge Crystallographic Data Centre (CCDC) and is available free of charge. The CIF file is available separately.

CCDC #904665



<p>54198 reflections collected, 20318 unique Numerical absorption correction $R_{\text{int}} = 0.0413$ Final $Goof = 1.050$ $R1 = 0.0465$ $wR2 = 0.1062$ 814 parameters, 75 restraints $\mu = 4.130 \text{ mm}^{-1}$</p>	
---	--

General Information

There are two iridium molecules in the asymmetric unit. There are also two CH₂Cl₂ molecules that have been omitted for clarity. The absolute structure is correct, and the atoms C3, C16, C33 and C46 are the chiral centres and have the (*R*) configuration.

The crystals grew as large orange prisms. A suitable single crystal was selected from the sample and mounted onto a nylon fibre with paratone oil and placed under a cold stream at 173K. Single crystal X-ray data were collected on a Bruker APEX2 diffractometer with 1.6 kW graphite monochromated Mo radiation. The detector to crystal distance was 5.1 cm. Exposure times of 10s per frame and scan widths of 0.5° were used throughout the data collection. The data collection was performed using a combination of 2 sets of ω scans with different φ values yielding data in the θ range 1.97 to 29.63° and with an average completeness of 99.7%. The frames were integrated with the SAINT v7.68a (Bruker, 2009).¹ A numerical absorption correction was carried out using the program SADABS V2008-1 (Bruker, 2008)². The structure was solved and refined with Olex2³ and SHELX (Sheldrick, 2008).⁴ In the final cycles of refinement all

non-hydrogen atoms, except the disordered atoms were refined anisotropically. The structure contains disordered phenyl rings, t-butyl groups and dichloromethane solvent molecules of crystallisation. The disorder for each disordered group was treated the same way: modeled using two components with similarity restraints and restraints/constraints on thermal parameters for individual split atoms. The populations of individual components were refined or fixed at 50%. For clarity, Figure 1 shows the plot of only one of the two molecules in the asymmetric unit.

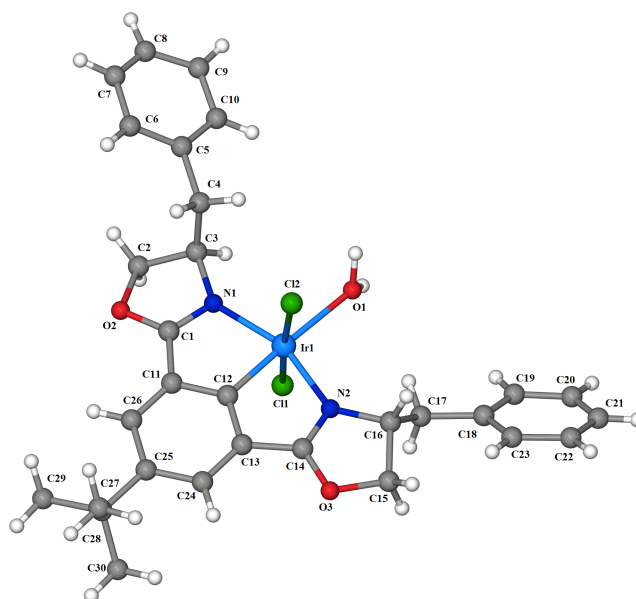


Figure 6.1. X-ray structure of $[(R,R)\text{-}^t\text{BuPhebox-Bn}]\text{IrCl}_2(\text{OH}_2)$ complex **216**.

References

- (1) Bruker (2009). SAINT V7.68a, BRUKER AXS Inc., Madison, WI, USA.
- (2) Bruker (2008), SADABS V2008-1, BRUKER AXS Inc., Madison, WI, USA.

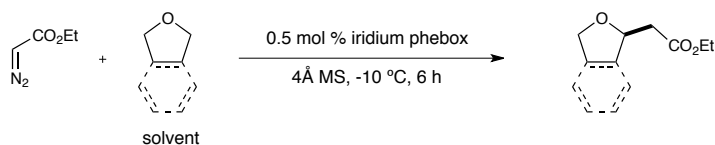
- (3) O. V. Dolomanov, L. J. Bourhis, R. J. Gildea, J. A. K. Howard and H. Puschmann (2009). OLEX2: a complete structure solution, refinement and analysis program. *J. Appl. Cryst.* 42, 339-341. *Supramol. Chem.* **2001**, 1, 189-191
- (4) Sheldrick, G.M. (2008). *Acta Cryst.* A64, 112-122.

6.3 Chapter 4 Procedures and Characterization

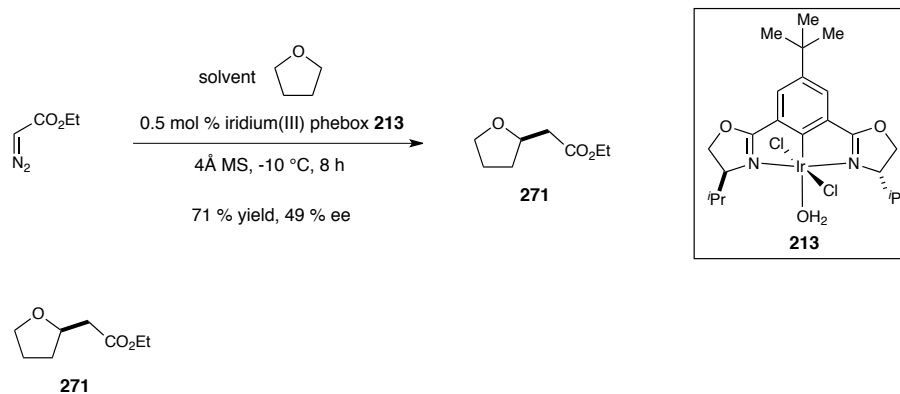
6.3.1 Iridium(III) phebox catalyzed enantioselective C-H insertion of acceptor-only metallocarbenes

General considerations.

The ethyl diazoacetate (EDA) in our studies was obtained from Sigma Aldrich and used without further purification. However, the reagent always contained residual dichloromethane. This amount was checked periodically by ^1H NMR using 1, 3, 5-trimethoxybenzene as the internal standard to ensure accurate and precise measurements were made between each insertion reaction. EDA was measured by mass in a syringe during preparation of the stock solution, and the amounts (mmol) in the experimental procedures listed below are corrected for the residual amount of dichloromethane.

General procedure A for the iridium phebox catalyzed enantioselective C-H insertion of acceptor-only diazoacetates into cyclic ethers (solvent).

A freshly prepared solution of diazoacetate (0.75 mmol corrected) in cyclic ether (3 mL, 0.29 M) was added over 6 hours via syringe pump to a stirring mixture of iridium phebox catalyst (4.4 μ m, 0.5 mol %) and 4 Å MS (176 mg) in the cyclic ether substrate (3 mL) at -10 °C (salt/ice bath). The temperature of the reaction mixture was maintained between -10 °C and -5 °C. Ethyl diazoacetate was consumed immediately after addition unless otherwise noted. The mixture was filtered through a plug of celite, and the filter cake was washed with Et₂O until the filtrate ran clear. The filtrate was carefully concentrated on a rotary evaporator such that the water bath temperature never exceeded 30 °C. The residue was purified as indicated to give the insertion product as a colorless/pale yellow oil.

Synthesis of 271 using general procedure A (THF as solvent).

Ethyl diazoacetate was used, purification by flash column chromatography (SiO₂, 30 % Et₂O:pentane) gave ethyl 2-(tetrahydrofuran-2-yl)acetate **271** as a pale yellow oil (71 %, 49 % ee).

¹H NMR (400 MHz; CDCl₃): δ 4.22 (pseudo-qn, *J* = 6.8, 1H), 4.12 (pseudo-q, *J* = 7.1, 2H), 3.85 (m, 1H), 3.72 (m, 1H), 2.56 (dd, *J* = 15.2, 7.3, 1H), 2.43 (dd, *J* = 15.2, 6.0, 1H), 2.10-2.02 (m, 1H), 1.92-1.83 (m, 2H), 1.52 (m, 1H), 1.23 (td, *J* = 7.1, 0.6, 3H).

¹³C NMR (100 MHz; CDCl₃): δ 171.5, 75.5, 75.4, 40.9, 31.4, 25.7, 14.3.

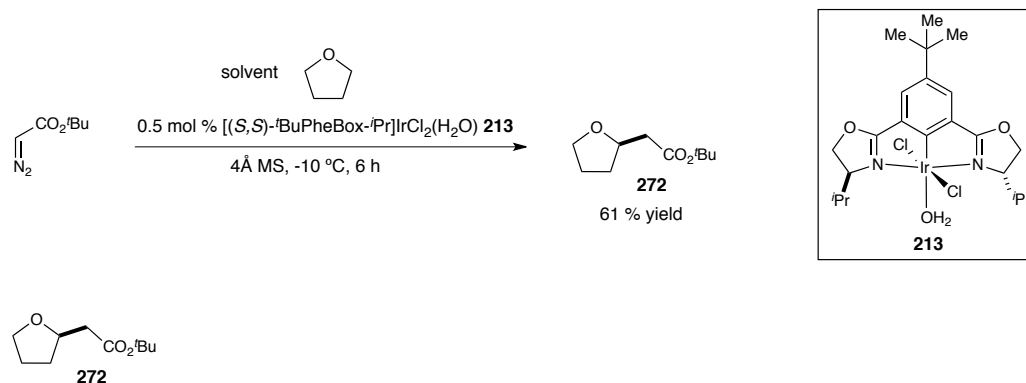
IR (thin film, cm⁻¹) *v* = 2979, 1734, 1065.

HRMS [+APCI] calculated for 159.10157, found 159.10147 [M+H]⁺

HPLC (Daicel OD-H, 230 nm detection, 1 % 2-propanol:hexanes, 1.0 mL/min); t_R = 6.43 min (minor) and 7.58 min (major).

[α]_D²² -2.0 (*c* = 1.0, CHCl₃).

R_f 0.45 (30 % Et₂O:pentane)

Synthesis of 272 using general procedure A (THF as solvent).

tert-Butyl diazoacetate was used. Purification by flash column chromatography (SiO₂, 30 % Et₂O:pentane) gave *tert*-butyl 2-(tetrahydrofuran-2-yl)acetate **272** as a colorless oil (61 %, 48 % ee). The enantiomeric excess was determined by conversion to the ethyl ester.

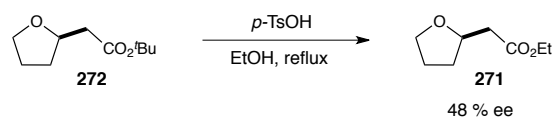
¹H NMR (400 MHz; CDCl₃): δ 4.18 (qn, *J* = 6.9, 1H), 3.87-3.82 (m, 1H), 3.75-3.69 (m, 1H), 2.51 (dd, *J* = 15.2, 7.2, 1H), 2.34 (dd, *J* = 15.2, 6.4, 1H), 2.05 (m, 1H), 1.92-1.81 (m, 2H), 1.57-1.48 (m, 1H), 1.42-1.42 (m, 9H).

¹³C NMR (150 MHz; CDCl₃): δ 170.8, 80.7, 75.7, 68.1, 42.1, 31.3, 28.3, 25.8

IR (thin film, cm⁻¹) ν = 2976, 1727, 1367, 1149, 1063.

HRMS [+ ESI] calculated for 209.11482, found 209.11471 [M+Na]⁺

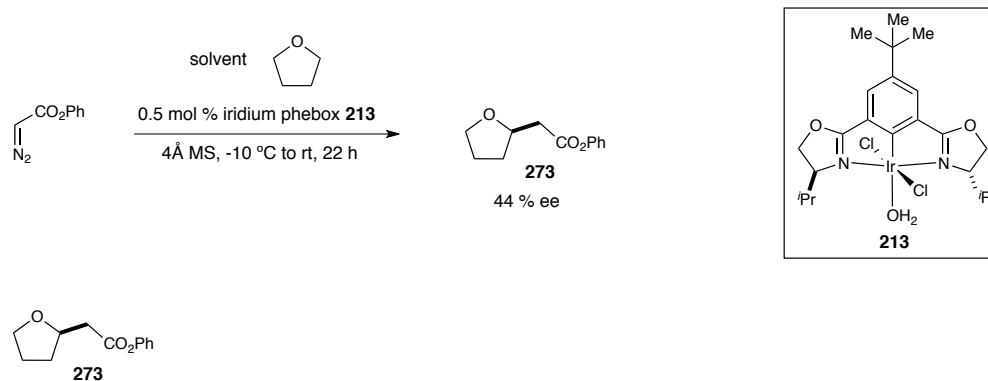
R_f 0.62 (30 % Et₂O:pentane)

Transesterification of 272 to ethyl ester 271

A solution of *tert*-butyl-2-(tetrahydrofuran-2-yl)acetate **272** (85 mg, 0.46 mmol) and *para*-toluenesulfonic acid (105 mg, 0.55 mmol) in anhydrous ethanol (9 mL, 0.05 M) was

refluxed for 16 hours then concentrated. The residue was taken up in Et₂O (10 mL) and washed with saturated aqueous NaHCO₃ (2 x 10 mL). The ethereal phase was washed with H₂O (10 mL), brine (10 mL) then dried over Na₂SO₄ and concentrated. The residue was purified by filtration through a plug of silica gel washing with 20% Et₂O:pentane to give ethyl 2-(tetrahydrofuran-2-yl)acetate **271** as a pale yellow oil. The yield was not determined.

Synthesis of **273** using general procedure A (THF as solvent).

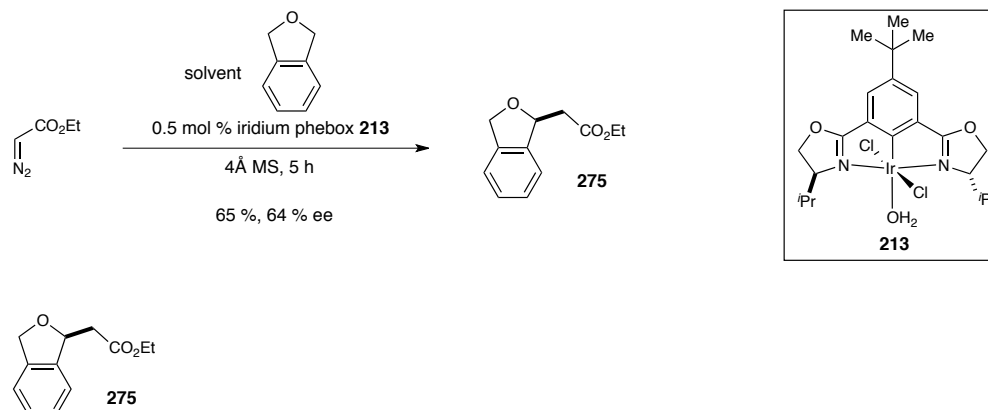


Phenyl diazoacetate was used.⁸ Purification by flash column chromatography (SiO₂, 15 % EtOAc:hexanes) gave phenyl 2-(tetrahydrofuran-2-yl)acetate **273** as a colorless oil (44 % ee).

¹H NMR (600 MHz; CDCl₃): δ 7.39-7.35 (m, 2H), 7.23-7.21 (m, 1H), 7.10-7.08 (m, 2H), 4.38 (quintet, *J* = 6.7, 1H), 3.94 (dd, *J* = 14.6, 7.2, 1H), 3.80 (td, *J* = 7.9, 6.3, 1H), 2.84 (dd, *J* = 15.2, 7.2, 1H), 2.73 (dd, *J* = 15.2, 6.0, 1H), 2.20-2.14 (m, 1H), 1.99-1.91 (m, 2H), 1.69-1.63 (m, 1H)

HPLC (Daicel AS-H, 210 nm detection, 1 % 2-propanol:hexanes, 1.0 mL/min); t_R = 11.80 min (minor) and 14.62 min (major).

R_f 0.24 (10 % EtOAc:hexanes)

Synthesis of 275 using general procedure A (phthalan as solvent).

Ethyl diazoacetate was used. Purification by flash column chromatography (SiO₂, 30 % Et₂O:pentane) gave ethyl 2-(2,5-dihydroisobenzofuranyl)acetate **275** as a colorless oil, 65 %, 64 % ee.

¹H NMR (400 MHz; CDCl₃): δ 7.29-7.16 (m, 4H), 5.66-5.63 (m, 1H), 5.15-5.03 (m, 2H), 4.18 (q, *J* = 7.1, 2H), 2.74 (qd, *J* = 14.5, 6.4, 2H), 1.25 (t, *J* = 7.1, 3H)

¹³C NMR (100 MHz; CDCl₃): δ 170.9, 140.8, 139.3, 128.0, 127.5, 121.27, 121.17, 80.4, 72.8, 60.8, 41.8, 14.3

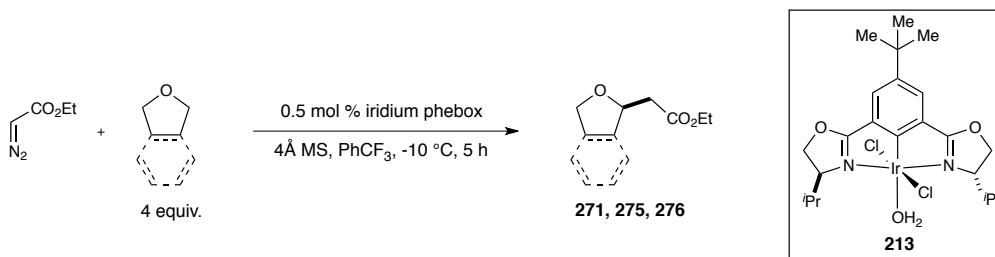
IR (thin film, cm⁻¹) *v* = 2980, 2858, 1729, 1158, 1036, 750

HRMS [+NSI] calculated for 207.10157, found 207.10188 [M+H]⁺

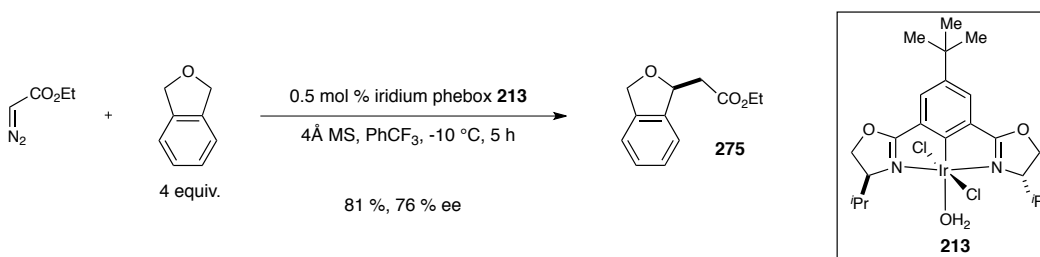
HPLC (Daicel OJ-H, 210 nm detection, 1 % 2-propanol:hexanes, 1.0 mL/min); *t_R* = 17.52 min (minor) and 24.85 min (major).

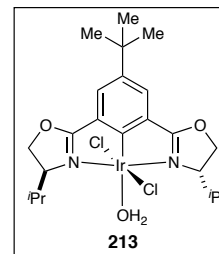
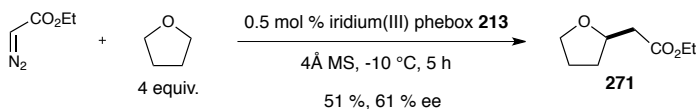
R_f 0.26 (20 % Et₂O:pentane)

General procedure B for the iridium phebox **213 catalyzed enantioselective C-H insertion of ethyl diazoacetate into cyclic ethers (4 equivalents).**

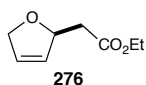
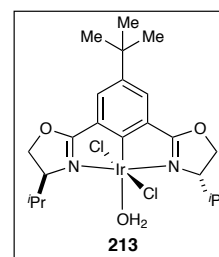
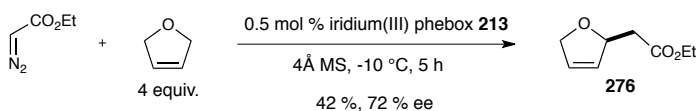


A 25 mL round bottom flask was charged with iridium phebox catalyst **213** (0.5 mol %, 4.4 μmol), 4Å molecular sieves (176 mg) and a stir bar, then evacuated and backfilled with dry nitrogen three times. Substrate (3.52 mmol, 4 equiv) and 2 mL anhydrous PhCF₃ were added via syringe and the reaction mixture was cooled to -10 °C in an ice/salt bath. A freshly prepared solution of ethyl diazoacetate in anhydrous PhCF₃ (0.29M, 0.75 mmol, 3.0mL) was added over 5 hours via syringe pump. The temperature of the reaction mixture was maintained between -10 °C and -5 °C. After addition, ethyl diazoacetate was completely consumed as judged by TLC (20 % Et₂O:hexanes, R_f 0.37). The mixture was carefully concentrated on a rotary evaporator such that the water bath temperature never exceeded 30 °C. The residue was purified as indicated to give the insertion product as a colorless/pale yellow oil. The characterization data for **275** and **271** are the same as above.





Synthesis of **276** using general procedure B.



Purification by flash column chromatography (SiO₂, 30 % Et₂O:pentane) gave ethyl 2-(2,5-dihydroisobenzofuranylmethyl)acetate **275** as a colorless oil, 65 %, 64 % ee.

¹H NMR (400 MHz; CDCl₃): δ 5.90-5.88 (m, 1H), 5.82-5.79 (m, 1H), 5.18-5.13 (m, 1H), 4.66-4.53 (m, 2H), 4.11 (q, *J* = 7.2, 2H), 2.56-2.44 (m, 2H), 1.22 (t, *J* = 7.2, 3H)

¹³C NMR (100 MHz; CDCl₃): δ 171.0, 128.8, 127.5, 82.4, 75.3, 60.6, 41.3, 14.3

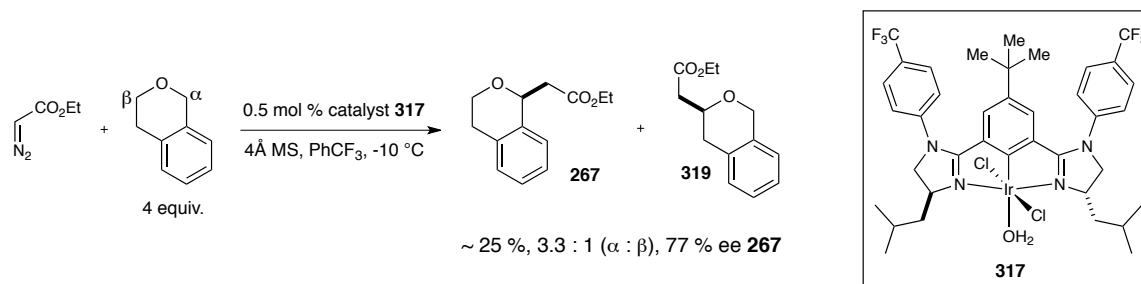
IR (thin film, cm⁻¹) *v* = 2983, 1731, 1179, 1028

HRMS [+NSI] calculated for 155.0703, found 155.0704 [M-H₂]⁺

HPLC (Daicel OJ-H, 210 nm detection, 1 % 2-propanol:hexanes, 0.7 mL/min); *t*_R = 14.57 min (minor) and 15.87 min (major).

R_f 0.31 (20 % Et₂O:pentane)

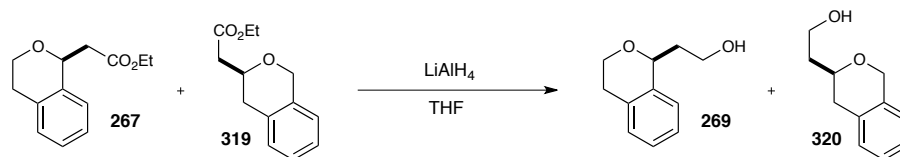
Synthesis of **267** and **319** using general procedure B.



Purification by flash column chromatography (SiO₂, 10 % to 20 % Et₂O:pentane) gave a 3.3:1 mixture of esters **267** and **319** as a colorless oil, 25 % yield combined, 77 % ee **267**.

¹H NMR (600 MHz; CDCl₃): δ 7.29-7.23 (m, 1H), 7.19-7.14 (m, 2H), 7.12-7.12 (m, 1H), 7.05-7.04 (m, 1H), 5.25 (dd, J = 9.4, 2.1 Hz, 1H), 4.47-4.44 (m, 0.3H), 4.29-4.17 (m, 4.6H), 4.16-4.11 (m, 1.2H), 3.91-3.88 (m, 0.3H), 3.84-3.76 (m, 1H), 3.06-2.95 (m, 1.3H), 2.89-2.71 (m, 1H), 2.78-2.71 (m, 2H), 2.64-2.61 (m, 0.3), 1.32-1.26 (m, 6.6H).

Reduction of **267** and **319** to form alcohols **269** and **320**.



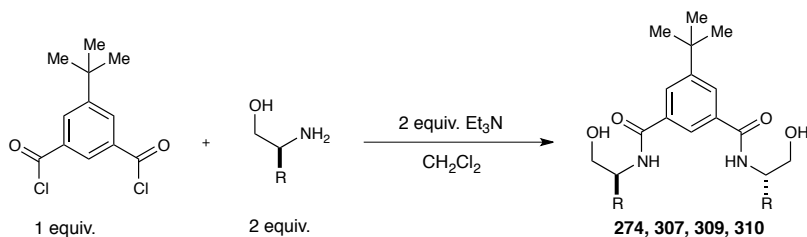
A 1M solution of LiAlH₄ in Et₂O (2.3 mmol, 10 equiv.) was added to a mixture of alcohols **267** and **319** (0.20 mmol) in THF (5.4 mL) at room temperature and stirred for 3 hours. The reaction was quenched with 1 mL H₂O and 3 mL 1N NaOH at 0 °C. 5 mL Et₂O were added, the layers were separated, and the organic phase collected. The aqueous phase was extracted with Et₂O (2x3mL). The organics were combined and filtered

through a plug of SiO₂, washing with 50 % to 70 % EtOAc:hexanes to give a crude mixture of esters **269** and **320** (~1.3-1) as a colorless oil.

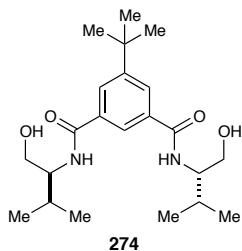
¹H NMR (600 MHz; CDCl₃): δ 7.26-7.21 (m, 1.6H), 7.19-7.14 (m, 2.1H), 7.11-7.10 (m, 1.2H), 7.04-7.03 (m, 1.2H), 4.99-4.97 (m, 1H), 4.18-4.15 (m, 1.3H), 3.97-3.92 (m, 0.7H), 3.86-3.80 (m, 2.8H), 3.78-3.72 (m, 3H), 3.68-3.66 (m, 0.6H), 3.05-3.00 (m, 1.6H), 2.77-2.76 (m, 1H), 2.69-2.65 (m, 1.5H), 2.25-2.19 (m, 1.3H), 2.07-2.01 (m, 1.3H), 1.84-1.82 (m, 1.3H), 1.67-1.65 (m, 1H).

6.3.2 Synthesis of amides **274**, **307**-**310**

General procedure A for the synthesis of amides **274**, **307**, **309**



A procedure was adapted from the literature as follows;⁹ A 0.5 M solution of **208** (1.0 equiv.) in CH₂Cl₂ was added dropwise to a 0 °C mixture of amino alcohol (2.0 equiv.) and Et₃N (2.0 equiv.) in CH₂Cl₂ (0.29 M in **208**). The reaction mixture was warmed to ambient temperature and stirred approximately 20 hours. Water was added (5 mL/1 mmol **208**) and the mixture was stirred for ten minutes. The phases were separated and the organic phase was dried over Na₂SO₄ and concentrated. The resulting solid was purified as indicated to give the title amide.

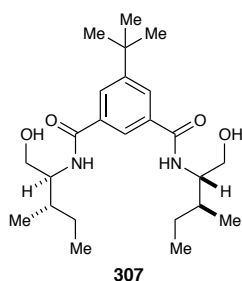


Prepared according to general procedure **A**; 5-*tert*-butylisophthaloyl chloride **208** (518 mg, 2.0 mmol) in CH₂Cl₂ (4 mL), L-valinol (413 mg, 4.0 mmol), and Et₃N (0.55 mL, 4.0 mmol) in CH₂Cl₂ (7 mL) furnished amide **274** as a white flaky solid following recrystallization from boiling Et₂O : CH₂Cl₂ (582 mg, 74 %).

¹H NMR (400 MHz; CDCl₃): δ 7.89 (s, 1H), 7.79 (s, 2H), 6.95-6.93 (m, 2H), 3.98-3.92 (m, 2H), 3.87-3.68 (m, 6H), 1.98 (dq, *J* = 13.5, 6.8, 2H), 1.25 (s, 9H), 0.99 (t, *J* = 6.3, 12H)

¹³C NMR (100 MHz; CDCl₃): δ 168.9, 152.1, 134.8, 127.5, 63.3, 58.0, 35.0, 31.3, 29.7, 19.7, 19.5

HRMS [+APCI] calculated for 393.2748, found 393.2743 [M+H]⁺

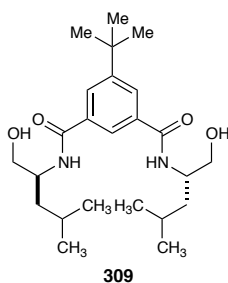


Prepared according to general procedure **A**; 5-*tert*-butylisophthaloyl chloride **208** (518 mg, 2.0 mmol) in CH₂Cl₂ (4 mL), (*S*)-isoleucinol (472 mg, 4.0 mmol), and Et₃N (0.55 mL, 4.0 mmol) in CH₂Cl₂ (7 mL) furnished amide **307** as a white flaky solid following recrystallization from boiling Et₂O : CH₂Cl₂ (454 mg, 54 %).

¹H NMR (400 MHz; CDCl₃): δ 7.97 (t, *J* = 1.4, 1H), 7.81 (d, *J* = 1.4, 2H), 7.32 (d, *J* = 8.7, 2H), 4.05-3.99 (m, 2H), 3.85-3.76 (m, 4H), 3.07 (q, *J* = 7.3, 2H), 1.80-1.73 (m, 2H), 1.59-1.49 (m, 2H), 1.31 (t, *J* = 7.3, 2H), 1.22 (s, 9H), 0.95 (d, *J* = 6.8, 6H), 0.89 (t, *J* = 7.4, 6H)

¹³C NMR (100 MHz; CDCl₃): δ 168.7, 152.0, 134.7, 127.8, 122.0, 62.8, 56.7, 46.4, 36.1, 35.0, 31.3, 26.2, 15.6, 11.5, 8.8

HRMS [+APCI] calculated for 421.30608, found 421.30601 [M+H]⁺

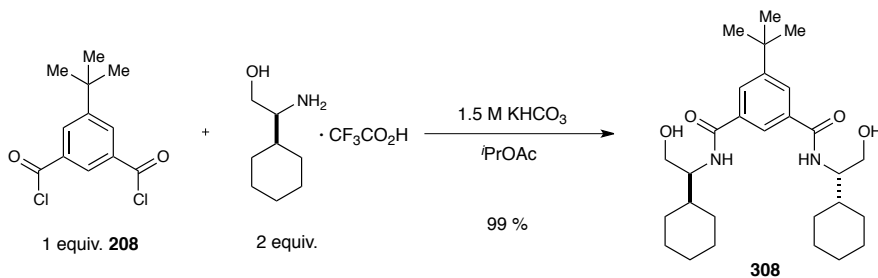


Prepared according to general procedure A; 5-*tert*-butylisophthaloyl chloride **208** (1.04 g, 4.0 mmol) in CH₂Cl₂ (8 mL), (*S*)-leucinol (943 mg, 1.03 mL, 8.0 mmol), and Et₃N (1.16 mL, 8.0 mmol) in CH₂Cl₂ (14 mL) furnished amide **309** as a white powder following recrystallization from boiling toluene : CH₂Cl₂ (1.30 g, 77 %).

¹H NMR (400 MHz; CDCl₃): δ 7.85 (bs, 1H), 7.77 (bs, 2H), 6.93 (bs, 2H), 4.28 (bs, 2H), 3.82 (dd, *J* = 11.3, 3.2, 2H), 3.66 (dd, *J* = 11.0, 6.5, 2H), 3.08-3.05 (m, 2H), 1.67 (dq, *J* = 13.6, 6.7, 2H), 1.59-1.52 (m, 2H), 1.43-1.37 (m, 2H), 1.23 (s, 9H), 0.94 (d, *J* = 6.5, 12H)

IR (thin film, cm⁻¹) ν = 3291, 2957, 2870, 1637, 1543

HRMS [+APCI] calculated for 421.30608, found 421.30596 [M+H]⁺

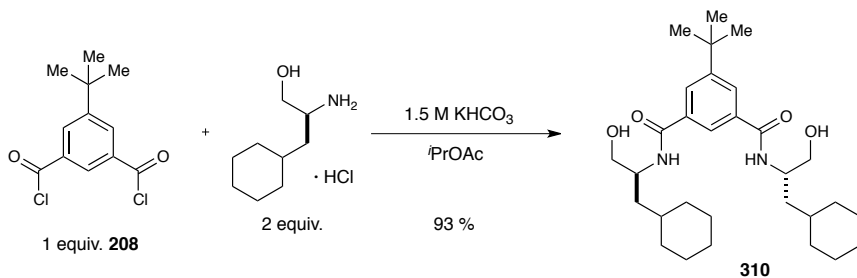
Synthesis of cyclohexyl substituted amide **308**

A procedure was adapted from the literature as follows:¹⁰ A round bottom flask was charged with (*S*)-2-amino-2-cyclohexylethanol·TFA salt (10 mmol) and evacuated and backfilled with dry nitrogen (3 cycles), and isopropyl acetate was added (40 mL, 0.13M in acyl chloride). The mixture was heated to 65 °C with vigorous stirring, and aqueous 1.5M KHCO₃ (35 mL, 50 mmol, 10 equiv.) was added. 5-*tert*-Butyl isophthaloyl dichloride **208** (1.3 g, 5.0 mmol) was added as a solid in three equal portions over the course of 30 minutes, and the mixture was aged at 65 °C for 12 hours. The mixture was cooled to room temperature and poured into a separatory funnel. The flask was rinsed 40 mL isopropyl acetate, which was also added to the separatory funnel. (If needed, additional isopropyl acetate or dichloromethane can be added to dissolve any remaining solids.) The phases were separated, and the aqueous phase was extracted with isopropyl acetate (x 3). The organics were combined, dried over sodium sulfate, filtered, and concentrated. The resulting amide **308** was obtained as a white powder. (2.34 g, 99 %).

¹H NMR (600 MHz; CDCl₃): δ 7.85 (bs, 1H), 7.82 (bs, 2H), 6.69 (d, *J* = 7.4, 2H), 4.30 (bs, 2H), 3.82 (d, *J* = 10.5, 2H), 3.66-3.64 (m, 2H), 3.47-3.45 (m, 2H), 3.18 (s, 2H), 1.83-1.34 (m, 18H), 1.28 (s, 9H), 1.24-1.12 (m, 8H), 1.00-0.87 (m, 4H)

HRMS [+APCI] calculated for 455.32682, found 455.32664 [M-OH]⁺

Synthesis of CH₂-cyclohexyl substituted amide **310**

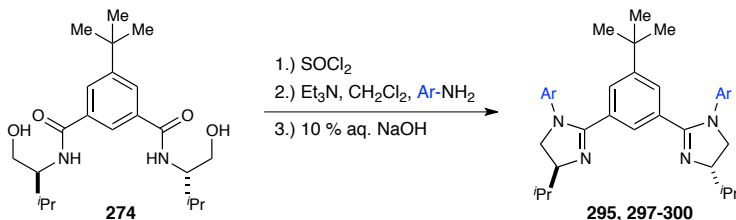


A procedure was adapted from the literature as follows:¹⁰ A round bottom flask was charged with (*S*)-2-amino-3-cyclohexylpropanol hydrochloride (387 mg, 2.0 mmol), evacuated and backfilled with dry nitrogen (3 cycles), and isopropyl acetate was added (8 mL, 0.13M in acyl chloride). The mixture was heated to 65 °C with vigorous stirring, and aqueous 1.5M KHCO₃ (7 mL, 10 mmol, 10 equiv.) was added. 5-*tert*-Butyl isophthaloyl dichloride (259 mg, 1.0 mmol) was added as a solid in three equal portions over the course of 30 minutes, and the mixture was aged at 65 °C for approximately 7 hours. The mixture was cooled to room temperature and poured into a separatory funnel. The flask was rinsed with 20 mL isopropyl acetate, which was also added to the separatory funnel. (If needed, additional isopropyl acetate or dichloromethane can be added to dissolve any remaining solids.) The phases were separated, and the aqueous phase was extracted with isopropyl acetate (x 3). The organics were combined, dried over sodium sulfate, filtered, and concentrated. Diethyl ether (20 mL) was added to the crude solid with stirring, and the solid was collected by vacuum filtration to give amide **310** as a white powder (438 mg, 93 %).

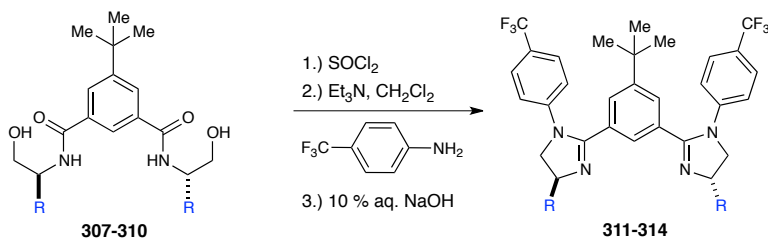
¹H NMR (600 MHz; CDCl₃): δ 8.15-8.05 (m, 1H), 7.86 (bs, 1H), 7.77 (bs, 1H), 7.01-6.80 (m, 1H), 4.67 (bs, 2H), 4.37-4.17 (m, 2H), 3.77-3.47 (m, 4H), 1.76-0.82 (m, 36H).

HRMS [+APCI] calculated for 501.36868, found 501.36851 [M+H]⁺

6.3.3 Synthesis of phehim ligands 295, 297-300, 311-314



entry	ligand	Ar	% yield
1	295	Ph	89
2	297	4-MeO-Ph	79
3	298	4-O ₂ N-Ph	78
4	299	4-F ₃ C-Ph	84
5	300	3,5-(F ₃ C) ₂ -Ph	84



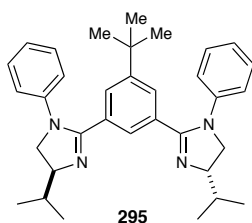
entry	ligand	R	% yield
1	311	^t Bu	64
2	312	Cy	21
3	313	ⁱ Bu	35
4	314	CH ₂ Cy	36

General procedure for the synthesis of phehim ligands

A procedure was adapted from the literature as follows:⁹ A 10 mL flask was charged with hydroxy amide (1.0 equiv.) fitted with a reflux condenser, and evacuated and backfilled with dry nitrogen (3 cycles). SOCl₂ (1M, excess) was added via syringe and the mixture was refluxed for approximately 7 hours (Note A). Excess SOCl₂ was removed directly under high vacuum for at least 30 minutes until bubbling ceased (Note B). The condenser was removed and replaced with a rubber septum, and the flask was evacuated and backfilled with dry nitrogen (3 cycles). The residue was dissolved in dry CH₂Cl₂ (0.18 M) and cooled to 0 °C. Et₃N (6.0 equiv.) and the primary aniline (2.2 equiv.) were added sequentially via syringe, and the mixture was stirred overnight (12-20 h) at ambient temperature (Note C). Three mL 10 % aqueous NaOH was added and stirred for at least 10 minutes and up to 3 hours. The phases were separated, and the aqueous was extracted with CH₂Cl₂ (10 mL x 3). The combined organics were dried over Na₂SO₄, filtered, and

concentrated. The residue was purified by flash column chromatography on silica gel as indicated to give the title compound.

Notes: A) Thionyl chloride was added by quickly removing the condenser, injecting it *via* syringe, and quickly replacing the condenser. B) Once the SOCl₂ is removed, the resulting residue is usually a sticky amorphous solid and may take sonication to get it to dissolve in CH₂Cl₂ for the next step. C) If the aniline reagent is a solid, you can add it directly to the crude residue, and then dissolve them both in CH₂Cl₂.



Prepared according to the general procedure using amide **274** (200 mg, 0.51 mmol), SOCl₂ (0.6 mL), Et₃N (0.43 mL, 3.1 mmol), CH₂Cl₂ (2.8 mL), aniline (104 mg, 1.12 mmol), and 10 % aq. NaOH (3 mL). Phebim ligand **295** was obtained as a light brown amorphous solid following purification by flash column chromatography (SiO₂, EtOAc → 10 % MeOH:EtOAc) (230 mg, 89 %).

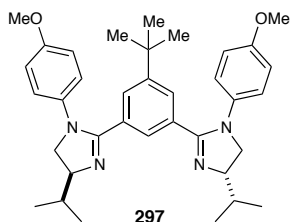
¹H NMR (400 MHz; CDCl₃): δ 7.80 (s, 1H), 7.25 (d, *J* = 1.5, 2H), 7.13 (t, *J* = 7.9, 4H), 6.98 (t, *J* = 7.4, 2H), 6.74 (d, *J* = 7.6, 4H), 4.22-4.08 (m, 4H), 3.63 (dd, *J* = 8.9, 6.8, 2H), 1.99-1.91 (m, 3H), 1.01 (d, *J* = 6.8, 6H), 0.93 (d, *J* = 6.8, 6H), 0.89 (s, 9H)

¹³C NMR (100 MHz; CDCl₃): δ 175.0, 161.8, 150.7, 142.2, 123.0, 128.9, 128.4, 127.3, 124.3, 123.5

IR (thin film, cm⁻¹) ν = 2957, 2871, 1577, 1495, 1253, 730, 695

HRMS [+APCI] calculated for 507.34822, found 507.34790 [M+H]⁺

R_f 0.08 (10 % MeOH:EtOAc)



Prepared according to the general procedure using amide **274** (200 mg, 0.51 mmol), SOCl₂ (0.6 mL), Et₃N (0.43 mL, 3.1 mmol), CH₂Cl₂ (2.8 mL), *p*-methoxyaniline (138 mg, 1.12 mmol), and 10 % aq. NaOH (3 mL). Phebim ligand **297** was obtained as a light grey amorphous solid following purification by flash column chromatography (SiO₂, 10 % → 20 % → 30 % MeOH:acetone) (229 mg, 79 %).

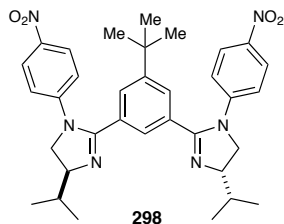
¹H NMR (400 MHz; CDCl₃): δ 7.77 (s, 1H), 7.25 (s, 2H), 6.73 (d, *J* = 8.9, 4H), 6.67 (d, *J* = 8.9, 4H), 4.12-4.01 (m, 4H), 3.69 (s, 5H), 3.49 (t, *J* = 7.1, 2H), 1.99-1.89 (m, 2H), 1.00 (d, *J* = 6.8, 6H), 0.92 (d, *J* = 6.8, 6H), 0.90 (s, 9H)

¹³C NMR (100 MHz; CDCl₃): δ 162.3, 156.9, 128.3, 127.4, 125.8, 114.3, 56.9, 55.7, 34.6, 33.1, 30.9, 19.0, 17.8

IR (thin film, cm⁻¹) ν = 2957, 1510, 1244

HRMS [+APCI] calculated for 567.36935, found 567.36890 [M+H]⁺

R_f 0.13 (20 % MeOH:acetone)



Prepared according to the general procedure using amide **274** (200 mg, 0.51 mmol), SOCl₂ (0.6 mL), Et₃N (0.43 mL, 3.1 mmol), CH₂Cl₂ (3.0 mL), *p*-nitroaniline (155 mg, 1.12 mmol), and 10 % aq. NaOH (3 mL). Phebim ligand **298** was obtained as a bright yellow solid following purification by flash column chromatography (SiO₂, EtOAc → 5 % → 7 % MeOH:EtOAc) (238 mg, 78 %).

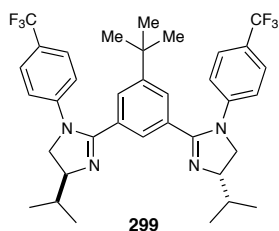
¹H NMR (400 MHz; CDCl₃): δ 8.00 (d, *J* = 9.0, 4H), 7.74 (s, 1H), 7.40 (s, 2H), 6.70 (d, *J* = 9.0, 4H), 4.23-4.18 (m, 2H), 4.14-4.07 (m, 2H), 3.77 (dd, *J* = 9.0, 7.1, 2H), 1.97-1.90 (m, 2H), 1.05 (s, 9H), 1.03 (d, *J* = 6.8, 6H), 0.93 (d, *J* = 6.8, 6H)

¹³C NMR (100 MHz; CDCl₃): δ 159.0, 152.1, 147.5, 141.8, 131.3, 128.1, 124.8, 119.8, 70.5, 55.4, 34.9, 33.0, 31.0, 19.0, 18.1

IR (thin film, cm⁻¹) ν = 2960, 1590, 1504, 1327

HRMS [+NSI] calculated for 597.31838, found 597.31823 [M+H]⁺

R_f 0.55 (5 % MeOH:EtOAc)



Prepared according to the general procedure using amide **274** (200 mg, 0.51 mmol), SOCl₂ (0.6 mL), Et₃N (0.43 mL, 3.1 mmol), CH₂Cl₂ (3.0 mL), *p*-trifluoromethylaniline

(180 mg, 1.12 mmol), and 10 % aq. NaOH (3 mL). Phebim ligand **299** was obtained as a light yellow amorphous solid following purification by flash column chromatography (SiO₂, 5 % → 10 % MeOH:EtOAc) (274 mg, 84 %).

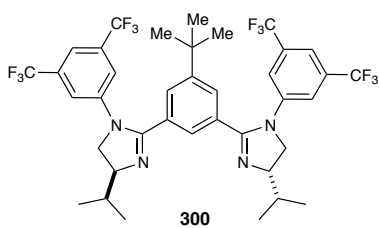
¹H NMR (400 MHz; CDCl₃): δ 7.76 (t, *J* = 0.7, 1H), 7.35 (d, *J* = 8.7, 4H), 7.30 (dd, *J* = 1.5, 0.8, 2H), 6.74 (d, *J* = 8.7, 4H), 4.18 (app t, *J* = 9.7, 2H), 4.11-4.05 (m, 2H), 3.67 (dd, *J* = 9.0, 6.9, 2H), 1.95-1.87 (m, 2H), 1.01 (d, *J* = 6.7, 6H), 0.97 (s, 9H), 0.92 (d, *J* = 6.7, 6H)

¹³C NMR (100 MHz; CDCl₃): δ 160.1, 151.3, 145.4, 131.0, 128.1, 126.6, 125.8, 121.5, 70.3, 55.4, 34.7, 33.0, 30.8, 19.0, 18.0

IR (thin film, cm⁻¹) *v* = 2960, 1613, 1324, 1121, 1072

HRMS [+NSI] calculated for 643.32299, found 643.32112 [M+H]⁺

R_f 0.50 (5 % MeOH:EtOAc)



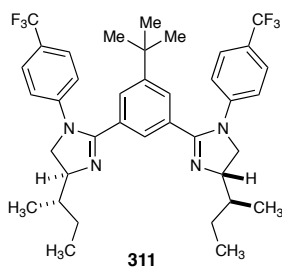
Prepared according to the general procedure using amide **274** (200 mg, 0.51 mmol), SOCl₂ (0.6 mL), Et₃N (0.43 mL, 3.1 mmol), CH₂Cl₂ (3.0 mL), *p*-3,5-bis(trifluoromethyl)aniline (180 mg, 1.12 mmol), and 10 % aq. NaOH (3 mL). Phebim ligand **300** was obtained as a pale yellow amorphous solid following purification by flash column chromatography (SiO₂, 50 % EtOAc:hexanes) (333 mg, 84 %).

$^1\text{H NMR}$ (400 MHz; CDCl_3): δ 8.02 (s, 1H), 7.40 (s, 2H), 7.26 (s, 2H), 7.09 (s, 4H), 4.25 (t, $J = 9.7$, 2H), 4.14-4.08 (m, 2H), 1.91 (dq, $J = 13.1, 6.7$, 2H), 1.02 (d, $J = 6.7$, 6H), 0.95-0.93 (m, 15H)

$^{13}\text{C NMR}$ (100 MHz; CDCl_3): δ 158.6, 151.4, 143.7, 132.2 (q, $^2J_{\text{FC}} = 33.4$), 130.3, 128.1, 127.1, 124.4, 121.7, 120.7, 115.7, 70.3, 55.7, 34.7, 33.1, 30.7, 18.9, 18.1

HRMS [+NSI] calculated for 779.29776, found 779.29723 $[\text{M}+\text{H}]^+$

R_f 0.36 (50 % EtOAc:hexanes)



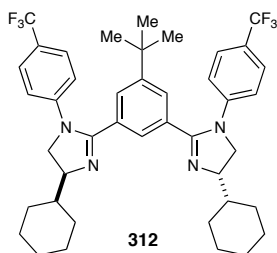
Prepared according to the general procedure using amide **307** (215 mg, 0.51 mmol), SOCl_2 (0.6 mL), Et_3N (0.43 mL, 3.1 mmol), CH_2Cl_2 (3.0 mL), *p*-trifluoromethylaniline (180 mg, 1.12 mmol), and 10 % aq. NaOH (3 mL). Phebim ligand **311** was obtained as a white amorphous solid following purification by flash column chromatography (SiO_2 , EtOAc \rightarrow 5 % MeOH:EtOAc \rightarrow 10 % MeOH:EtOAc) (220 mg, 64 %).

$^1\text{H NMR}$ (600 MHz; CDCl_3): δ 8.12 (s, 1H), 7.46 (d, $J = 8.3$, 4H), 7.19 (s, 2H), 7.07 (s, 4H), 4.42-4.32 (m, 4H), 3.87 (t, $J = 8.3$, 2H), 1.95 (s, 2H), 1.59-1.55 (m, $J = 5.6$, 2H), 1.26 (dt, $J = 14.7, 7.4$, 2H), 0.95 (app t, $J = 7.4$, 12H), 0.82 (s, 9H)

$^{13}\text{C NMR}$ (150 MHz; CDCl_3): δ 187.1, 173.6, 161.9, 151.6, 142.4, 129.5, 126.4, 124.4, 122.6, 64.3, 54.9, 38.3, 34.4, 30.2, 25.5, 13.6, 11.4

HRMS [+APCI] calculated for 671.35429, found 671.35404 $[\text{M}+\text{H}]^+$

R_f 0.61 (5 % MeOH:EtOAc)



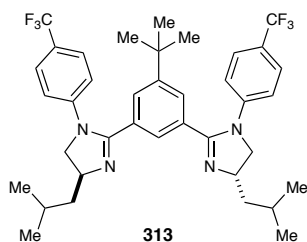
Prepared according to the general procedure using amide **308** (482 mg, 1.02 mmol), SOCl₂ (1.2 mL), Et₃N (0.86 mL, 6.2 mmol), CH₂Cl₂ (6.0 mL), *p*-trifluoromethylaniline (362 mg, 2.24 mmol), and 10 % aq. NaOH (6 mL). Phebim ligand **312** was obtained as a light brown amorphous solid following purification by flash column chromatography (SiO₂, EtOAc → 2 % MeOH:EtOAc → 5 % MeOH:EtOAc) (155 mg, 21 %).

¹H NMR (600 MHz; CDCl₃): δ 7.80 (s, 1H), 7.34 (d, *J* = 8.6 Hz, 4H), 7.27 (d, *J* = 1.2 Hz, 2H), 6.73 (d, *J* = 8.4 Hz, 4H), 4.16 (t, *J* = 9.7 Hz, 2H), 4.07 (dt, *J* = 9.7, 6.6 Hz, 2H), 3.71 (dd, *J* = 8.9, 7.4 Hz, 2H), 1.92 (d, *J* = 12.2 Hz, 2H), 1.76 (t, *J* = 11.2 Hz, 5H), 1.68 (d, *J* = 12.2 Hz, 4H), 1.59 (dtd, *J* = 14.8, 7.4, 3.1 Hz, 3H), 1.30-1.22 (m, 4H), 1.19-1.14 (m, 2H), 1.05 (dq, *J* = 24.2, 12.1, 3.2 Hz, 4H), 0.95 (s, 9H).

¹³C NMR (150 MHz; CDCl₃): δ 160.0, 151.2, 145.4, 131.0, 128.1, 126.6, 125.8, 125.2, 123.4, 121.4, 69.5, 55.7, 43.1, 34.7, 30.8, 29.6, 28.5, 26.7, 26.3, 26.2

HRMS [+APCI] calculated for 723.38611, found 723.38635 [M+H]

R_f 0.13 (EtOAc)

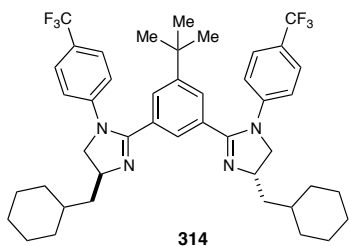


Prepared according to the general procedure using amide **309** (215 mg, 0.51 mmol), SOCl₂ (1.0 mL), Et₃N (0.43 mL, 3.1 mmol), CH₂Cl₂ (3.0 mL), *p*-trifluoromethylaniline (180 mg, 1.12 mmol), and 10 % aq. NaOH (3 mL). Phebim ligand **313** was obtained as a colorless oil following purification by flash column chromatography (SiO₂, 50 % EtOAc:hexanes) (119 mg, 35 %).

¹H NMR (400 MHz; CDCl₃): δ 7.77 (t, *J* = 1.2 Hz, 1H), 7.34 (d, *J* = 8.7 Hz, 4H), 7.26 (s, 1H), 6.73 (d, *J* = 8.6 Hz, 3H), 4.32-4.24 (m, 2H), 4.18 (t, *J* = 9.2 Hz, 2H), 3.65 (t, *J* = 8.3 Hz, 2H), 1.88-1.72 (m, *J* = 7.3 Hz, 4H), 1.45-1.37 (m, 2H), 1.00-0.98 (m, 12H), 0.96 (s, 9H).

¹³C NMR (100 MHz; CDCl₃): δ 159.8, 151.2, 145.4, 131.1, 128.1, 126.7, 125.9, 121.1, 63.1, 58.8, 46.1, 34.7, 30.8, 25.5, 23.2, 22.8

R_f 0.66 (50 % EtOAc:hexanes)



Prepared according to the general procedure using amide **310** (241 mg, 0.51 mmol), SOCl₂ (0.6 mL), Et₃N (0.43 mL, 3.1 mmol), CH₂Cl₂ (3.0 mL), *p*-trifluoromethylaniline (180 mg, 1.12 mmol), and 10 % aq. NaOH (3 mL). Phebim ligand **314** was obtained as a

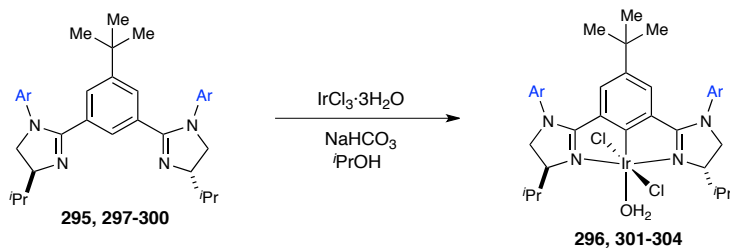
white amorphous solid following purification by flash column chromatography (SiO₂, 30 % → 50 % → 70 % EtOAc:hexanes) (154 mg, 36 %).

¹H NMR (600 MHz; CDCl₃): δ 7.80 (s, 1H), 7.34 (d, *J* = 8.6 Hz, 4H), 7.25 (s, 2H), 6.73 (d, *J* = 8.6 Hz, 4H), 4.31 (dt, *J* = 15.9, 7.8 Hz, 2H), 4.19 (t, *J* = 9.3 Hz, 2H), 3.64 (t, *J* = 8.3 Hz, 2H), 1.82-1.62 (m, 12H), 1.55-1.50 (m, 2H), 1.40 (dt, *J* = 13.7, 7.0 Hz, 2H), 1.30-1.16 (m, 6H), 1.00-0.95 (m, 13H)

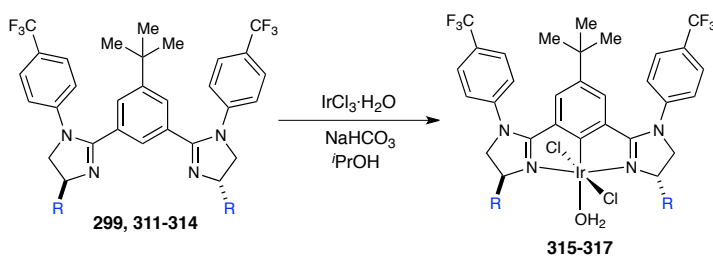
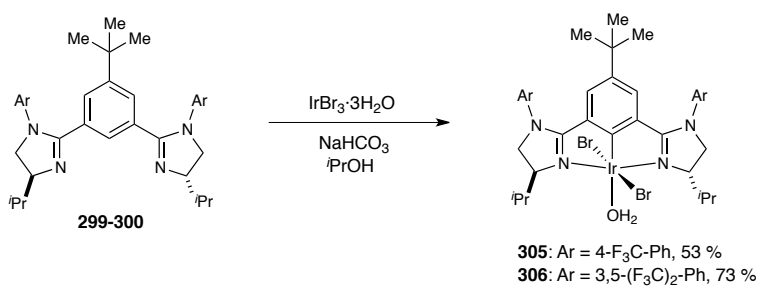
¹³C NMR (150 MHz; CDCl₃): δ 187.4, 159.7, 145.5, 131.2, 128.0, 126.7, 125.8, 121.05, 121.05, 62.5, 58.9, 44.8, 34.9, 33.9, 33.5, 30.8, 26.8, 26.4

R_f 0.57 (70 % EtOAc:hexanes)

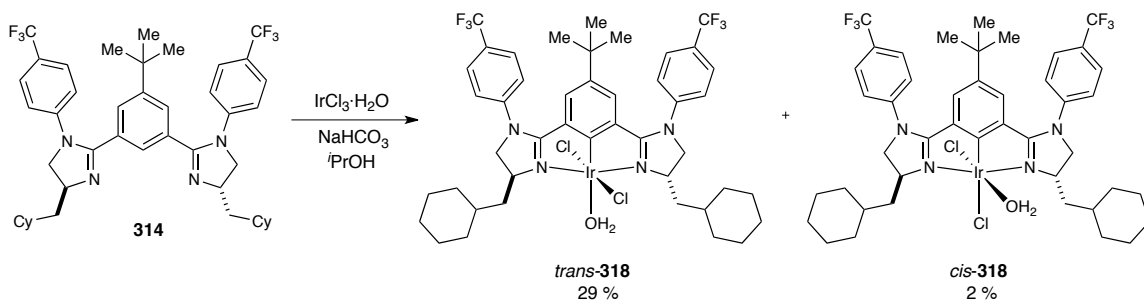
6.3.4 Synthesis of iridium(III) phebim complexes **296**, **301-306**, **299**, **315-317**, *trans*-**318**, *cis*-**318**



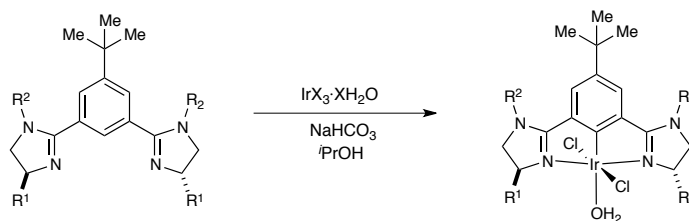
entry	complex	Ar	% yield
1	296	Ph	27
2	301	4-MeO-Ph	38
3	302	4-O ₂ N-Ph	15
4	303	4-F ₃ C-Ph	61
5	304	3,5-(F ₃ C) ₂ -Ph	53



entry	complex	R	% yield
1	315	ⁱ Bu	35
2	316	Cy	41
3	317	ⁱ Bu	28

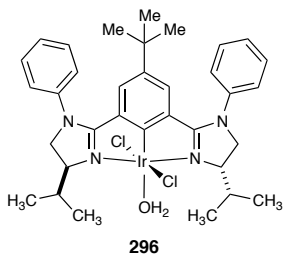


General procedure for the synthesis of iridium(III) phebim complexes, and select NMR spectra



A dry round bottom flask was charged with ligand (1.0 equiv.), $\text{IrCl}_3 \cdot 3\text{H}_2\text{O}$ or $\text{IrBr}_3 \cdot 4\text{H}_2\text{O}$ (1.1 equiv.), and NaHCO_3 (1.1 equiv.). The flask was fitted with a reflux condenser and evacuated and backfilled with dry nitrogen three times. Isopropanol (0.03 M) was added and the mixture was refluxed until the ligand was consumed as judged by thin-layer chromatography or ^1H NMR (see note below). The reaction mixture was cooled to 40 °C and concentrated on a rotary evaporator. The crude solid was purified by flash column chromatography on silica gel or by preparative TLC as indicated to give the iridium phebim complex as a dark orange/red solid).

Note: A small aliquot was taken from the reaction mixture, placed in a vial, concentrated on high vacuum, then dissolved in a small amount of CHCl_3 or CDCl_3 (which have been neutralized and dried over anhydrous K_2CO_3) for TLC/NMR analysis.



Prepared according to the general procedure using ligand **295** (139 mg, 0.274 mmol), $\text{IrCl}_3 \cdot 3\text{H}_2\text{O}$ (106 mg, 0.30 mmol), and NaHCO_3 (25 mg, 0.30 mmol). The reaction was refluxed in isopropanol (9 mL) for 5.5 hours to give iridium(III) phehim complex **296** as a dark red solid following purification by flash column chromatography (SiO_2 , 50 % EtOAc:hexanes) (154 mg, 36 %).

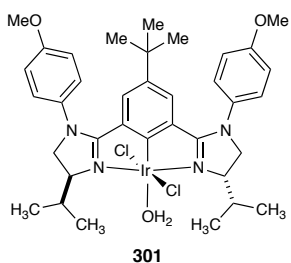
$^1\text{H NMR}$ (600 MHz; CDCl_3): δ 7.42 (t, $J = 7.8$ Hz, 4H), 7.31 (m, 6H), 6.54 (s, 2H), 4.41 (dd, $J = 11.1, 9.4$ Hz, 2H), 4.08-4.04 (m, 2H), 2.94 (bs, 2H), 2.54-2.50 (m, 2H), 1.01 (d, $J = 6.8$ Hz, 6H), 0.97 (d, $J = 6.8$ Hz, 6H).

$^{13}\text{C NMR}$ (150 MHz; CDCl_3): δ 170.5, 141.3, 132.2, 129.4, 127.3, 126.4, 125.5, 68.0, 54.9, 34.4, 31.4, 29.7, 19.4, 15.4

IR (thin film, cm^{-1}) $\nu = 3353, 2954, 1493, 1288, 730, 696$

HRMS [+NSI] calculated for 768.23320, found 768.23158 [$\text{M} + \text{H}_2\text{O}$]

R_f 0.67 (50 % EtOAc:hexanes)



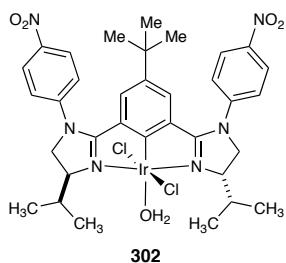
Prepared according to the general procedure using ligand **297** (35 mg, 0.062 mmol), $\text{IrCl}_3 \cdot 3\text{H}_2\text{O}$ (24 mg, 0.068 mmol), and NaHCO_3 (6 mg, 0.068 mmol). The reaction was relaxed in isopropanol (2 mL) for 12 hours to give iridium(III) phebin complex **301** as a dark red/brown solid following purification by preparative TLC (SiO_2 , 60 % EtOAc:hexanes) (20 mg, 38 %).

$^1\text{H NMR}$ (600 MHz; CDCl_3): δ 7.23 (d, $J = 8.8$ Hz, 4H), 6.93 (d, $J = 8.8$ Hz, 4H), 6.41 (s, 2H), 4.33-4.25 (m, 4H), 4.01 (dd, $J = 8.8, 5.6$ Hz, 2H), 3.83 (s, 6H), 2.52-2.47 (m, 2H), 2.33 (bs, 2H), 1.02 (d, $J = 6.7$ Hz, 6H), 0.97 (d, $J = 6.7$ Hz, 6H), 0.81 (s, 9H).

$^{13}\text{C NMR}$ (150 MHz; CDCl_3): δ 187.4, 170.8, 159.0, 142.6, 134.1, 132.3, 128.4, 125.3, 114.7, 68.0, 55.9, 55.1, 34.4, 31.4, 29.9, 19.4, 15.5

IR (thin film, cm^{-1}) $\nu = 3353, 2956, 1510, 1244, 1033, 749$

R_f 0.67 (50 % EtOAc:hexanes).



Prepared according to the general procedure using ligand **298** (44 mg, 0.074 mmol), $\text{IrCl}_3 \cdot 3\text{H}_2\text{O}$ (29 mg, 0.081 mmol), and NaHCO_3 (6 mg, 0.081 mmol). The reaction was

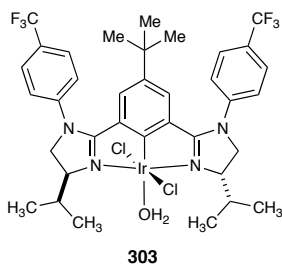
relaxed in isopropanol (3 mL) for 12 hours to give iridium(III) phebim complex **302** as a dark red/brown solid following purification by preparative TLC (SiO₂, 50 % EtOAc:hexanes, 2 runs) (10 mg, 15 %).

¹H NMR (600 MHz; CDCl₃): δ 8.30 (d, *J* = 9.0 Hz, 4H), 7.36 (d, *J* = 9.0 Hz, 4H), 7.03 (s, 2H), 4.59 (t, *J* = 10.2 Hz, 3H), 4.34 (bs, 2H), 4.13-4.08 (m, 3H), 2.52 (s, 2H), 1.02 (app s, 15H), 0.91 (d, *J* = 6.8 Hz, 6H)

¹³C NMR (150 MHz; CDCl₃): δ 195.5, 187.4, 146.7, 144.7, 132.1, 125.8, 125.0, 123.4, 68.4, 54.6, 34.9, 31.7, 29.9, 29.4, 19.5, 15.3

IR (thin film, cm⁻¹) ν = 3357, 2957, 1595, 1519, 1323, 1111, 752

R_f 0.48 (60 % EtOAc:hexanes)



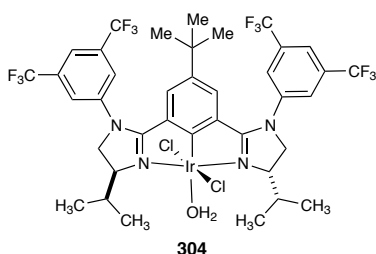
Prepared according to the general procedure using ligand **299** (177 mg, 0.28 mmol), IrCl₃·3H₂O (109 mg, 0.31 mmol), and NaHCO₃ (26 mg, 0.31). The reaction was relaxed in isopropanol (9 mL) for 4.5 hours to give iridium(III) phebim complex **303** as a dark red/brown solid following purification by flash column chromatography (SiO₂, 30% → 50 % EtOAc:hexanes) (157 mg, 61 %).

^1H NMR (400 MHz; CDCl_3): δ 7.68 (d, $J = 8.3$ Hz, 4H), 7.38 (d, $J = 8.3$ Hz, 4H), 6.73 (s, 3H), 4.49 (t, $J = 10.1$ Hz, 2H), 4.35 (bs, 2H), 4.11-4.04 (m, 3H), 3.10 (bs, 3H), 2.54 (s, 3H), 0.99 (d, $J = 6.9$ Hz, 6H), 0.96 (d, $J = 6.9$ Hz, 6H), 0.89 (s, 9H).

^{13}C NMR (100 MHz; CDCl_3): δ 170.3, 144.5, 143.0, 132.4, 128.6, 128.3, 126.5, 125.6, 125.2, 122.7, 68.3, 54.6, 34.6, 31.4, 29.6, 19.6, 15.5

HRMS [+APCI] calculated for 904.20797, found 904.20898 $[\text{M}-\text{H}_2\text{O}]^+$

R_f 0.64 (50 % EtOAc:hexanes)



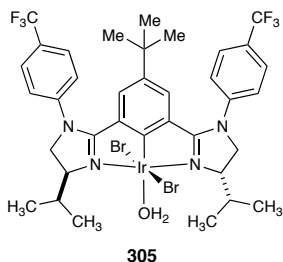
Prepared according to the general procedure using ligand **300** (90 mg, 0.12 mmol), $\text{IrCl}_3 \cdot 3\text{H}_2\text{O}$ (46 mg, 0.13 mmol), and NaHCO_3 (11 mg, 0.13). The reaction was refluxed in isopropanol (4 mL) for 3 hours to give iridium(III) phebim complex **304** as a dark orange/red solid following purification by flash column chromatography (SiO_2 , 30% \rightarrow 50 % \rightarrow 70 % EtOAc:hexanes) (67 mg, 53 %).

^1H NMR (600 MHz; CDCl_3): δ 7.78 (s, 2H), 7.70 (s, 4H), 6.75 (s, 2H), 4.54 (t, $J = 10.1$ Hz, 2H), 4.37 (bs, 2H), 4.14 (dd, $J = 9.0, 5.7$ Hz, 2H), 3.20 (bs, 2H), 2.57 (s, 2H), 1.02 (d, $J = 6.7$ Hz, 6H), 0.98 (d, $J = 6.7$ Hz, 6H), 0.92 (s, 9H).

^{13}C NMR (150 MHz; CDCl_3): δ 187.4, 169.4, 142.6, 133.2, 132.2, 125.2, 124.4, 123.8, 122.0, 119.7, 68.2, 54.9, 34.5, 31.3, 29.5, 19.5, 15.4

HRMS [+APCI] calculated for 1040.18274, found 1040.18437 $[\text{M}-\text{H}_2\text{O}]^+$

R_f 0.57 (50 % EtOAc:hexanes)



Prepared according to the general procedure using ligand **299** (54 mg, 0.084 mmol), IrBr₃·4H₂O (47 mg, 0.092 mmol), and NaHCO₃ (7.7 mg, 0.092). The reaction was relaxed in isopropanol (3 mL) for 7.5 hours to give iridium(III) phehim complex **305** as a dark red solid following purification by flash column chromatography (SiO₂, 30% → 50 % EtOAc:hexanes) (45 mg, 53 %).

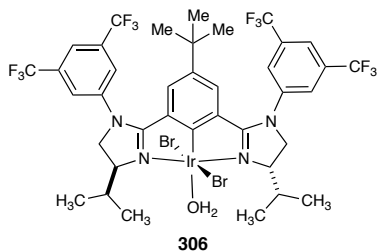
¹H NMR (400 MHz; CDCl₃): δ 7.68 (d, *J* = 8.2 Hz, 4H), 7.37 (d, *J* = 8.2 Hz, 4H), 6.75 (s, 2H), 4.52 (t, *J* = 10.1 Hz, 2H), 4.33 (s, 2H), 4.08-4.05 (m, 2H), 2.52 (s, 2H), 0.98 (app t, *J* = 7.6 Hz, 12H), 0.90 (s, 9H)

¹³C NMR (100 MHz; CDCl₃): δ 169.9, 144.5, 143.1, 132.2, 128.5, 126.5, 125.5, 125.0, 122.6, 68.5, 54.8, 34.5, 31.4, 29.3, 19.6, 15.7

IR (thin film, cm⁻¹) ν = 3374, 2959, 1321, 1614, 1484, 1125, 1068, 845, 733

HRMS [+NSI] calculated for 930.19189, found 930.21394 [M-HBr]⁺

R_f 0.30 (30 % EtOAc:hexanes)



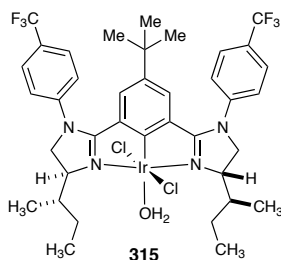
Prepared according to the general procedure using ligand **299** (164 mg, 0.21 mmol), IrBr₃·4H₂O (117 mg, 0.23 mmol), and NaHCO₃ (20 mg, 0.23). The reaction was refluxed in isopropanol (7.5 mL) for 3 hours to give iridium(III) phebim complex **306** as a dark red solid following purification by flash column chromatography (SiO₂, 30% → 50 % EtOAc:hexanes) (45 mg, 53 %).

¹H NMR (400 MHz; CDCl₃): δ 7.68 (d, *J* = 8.2 Hz, 4H), 7.37 (d, *J* = 8.2 Hz, 4H), 6.75 (s, 2H), 4.52 (t, *J* = 10.1 Hz, 2H), 4.33 (s, 2H), 4.08-4.05 (m, 2H), 2.52 (s, 2H), 0.98 (app t, *J* = 7.6 Hz, 12H), 0.90 (s, 9H)

¹³C NMR (100 MHz; CDCl₃): δ 169.0, 142.6, 133.3, 133.0, 132.2, 125.2, 124.2, 121.6, 199.6, 68.4, 55.0, 34.5, 31.3, 29.3, 19.6, 18.7, 15.6

HRMS [+NSI] calculated for 1153.06998, found 1153.07094 [M-H₂O+Na]⁺

R_f 0.42 (30 % EtOAc:hexanes)



Prepared according to the general procedure using ligand **311** (100 mg, 0.15 mmol), IrCl₃·3H₂O (60 mg, 0.17 mmol), and NaHCO₃ (15 mg, 0.17 mmol). The reaction was

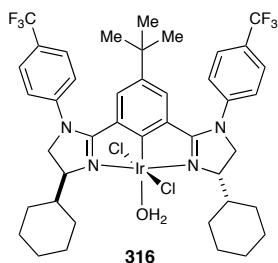
relaxed in isopropanol (5 mL) for 7.5 hours to give iridium(III) phebim complex **315** as a dark red/brown solid following purification by flash column chromatography (SiO₂, 50 % → 70 % EtOAc:hexanes) (50 mg, 35 %).

¹H NMR (600 MHz; CDCl₃): δ 7.67 (d, *J* = 8.2 Hz, 4H), 7.37 (d, *J* = 8.2 Hz, 4H), 6.71 (s, 2H), 4.47 (t, *J* = 10.1 Hz, 2H), 4.40 (s, 2H), 4.10-4.04 (m, 2H), 2.62 (bs, 2H), 2.25 (s, 2H), 1.41-1.35 (m, 2H), 1.31-1.22 (m, 4H), 1.01 (t, *J* = 7.2 Hz, 6H), 0.94 (d, *J* = 6.3 Hz, 6H), 0.88 (s, 9H).

¹³C NMR (150 MHz; CDCl₃): δ 187.4, 173.0, 144.4, 126.4, 125.5, 125.2, 66.9, 54.6, 36.4, 34.5, 31.3, 26.9, 12.3

HRMS [+APCI] calculated for 932.23927, found 932.24028 [M-H₂O]⁺

R_f 0.36 (50 % EtOAc:hexanes)



Prepared according to the general procedure using ligand **312** (139 mg, 0.192 mmol), IrCl₃·3H₂O (75 mg, 0.212 mmol), and NaHCO₃ (18 mg, 0.212 mmol). The reaction was relaxed in isopropanol (6.5 mL) for 4.5 hours to give iridium(III) phebim complex **316** as a dark red solid following purification by preparative TLC (SiO₂, 30 % EtOAc:hexanes) (80 mg, 41 %).

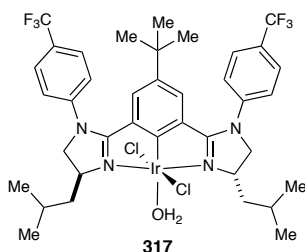
¹H NMR (600 MHz; CDCl₃): δ 7.67 (d, *J* = 8.5 Hz, 4H), 7.36 (d, *J* = 8.5 Hz, 4H), 6.71 (s, 2H), 4.49 (t, *J* = 10.2 Hz, 2H), 4.23-4.20 (m, 2H), 4.14-4.10 (m, 2H), 2.98 (s, 2H),

2.15 (td, $J = 12.0, 2.4$ Hz, 2H), 1.95 (d, $J = 11.7$ Hz, 2H), 1.80 (d, $J = 12.9$ Hz, 2H), 1.70-1.65 (m, 6H), 1.40-1.33 (m, 2H), 1.27-1.22 (m, 4H), 1.14-1.02 (m, 4H), 0.88 (s, 9H).

^{13}C NMR (150 MHz; CDCl_3): δ 171.4, 169.7, 144.4, 143.2, 132.1, 128.3 (q, $^2J_{\text{C-F}} = 33.0$)
126.4, 125.4, 68.1, 60.6, 55.3, 39.6, 34.5, 31.3, 30.1, 26.1 (dd, $^1J_{\text{C-F}} = 178$, $^2J_{\text{C-F}} = 33.0$),
21.2, 18.7, 14.4

HRMS [+APCI] calculated for 984.27057, found 984.27243 $[\text{M}-\text{H}_2\text{O}]^+$

R_f 0.36 (50 % EtOAc:hexanes)



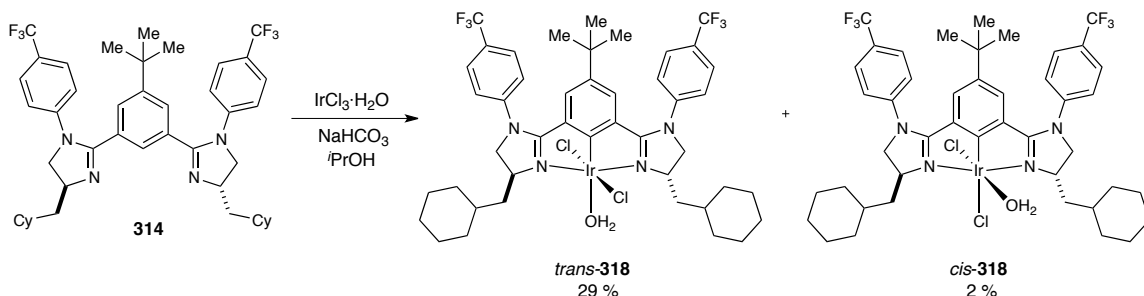
Prepared according to the general procedure using ligand **313** (110 mg, 0.164 mmol), $\text{IrCl}_3 \cdot 3\text{H}_2\text{O}$ (64 mg, 0.18 mmol), and NaHCO_3 (15 mg, 0.18 mmol). The reaction was refluxed in isopropanol (6 mL) for 8 hours to give iridium(III) phebim complex **317** as a dark red/brown solid following purification by flash column chromatography (SiO_2 , 30 % \rightarrow 50 % EtOAc:hexanes) (43 mg, 28 %).

^1H NMR (600 MHz; CDCl_3): δ 7.68 (d, $J = 8.3$ Hz, 4H), 7.41 (d, $J = 8.3$ Hz, 4H), 6.69 (s, 2H), 4.55 (t, $J = 9.6$ Hz, 2H), 4.37-4.34 (m, 2H), 2.77 (s, 2H), 2.20-2.17 (m, 2H), 1.70 (t, $J = 10.5$ Hz, 4H), 1.02 (t, $J = 6.5$ Hz, 12H), 0.87 (s, 9H).

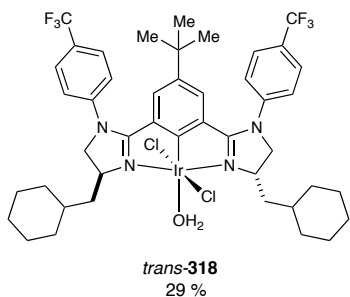
^{13}C NMR (150 MHz; CDCl_3): δ 169.7, 144.4, 142.9, 132.2, 128.4, 126.4, 125.44, 125.31, 123.0, 62.3, 60.0, 43.7, 34.4, 31.2, 25.7, 24.1, 21.8, 18.6

HRMS [+APCI] calculated for 932.23927, found 932.24003 $[\text{M}-2\text{Cl}-\text{H}_2\text{O}]^+$

R_f 0.56 (30 % EtOAc:hexanes)



Prepared according to the general procedure using ligand **314** (98 mg, 0.131 mmol), $\text{IrCl}_3 \cdot 3\text{H}_2\text{O}$ (53 mg, 0.15 mmol), and NaHCO_3 (13 mg, 0.15 mmol). The reaction was refluxed in isopropanol (5 mL) for 3.5 hours. The crude mixture was analyzed by ^1H NMR and revealed *trans*-**318** as the exclusive product. The mixture was subjected to preparative TLC on SiO_2 (50 % EtOAc:hexanes) and *trans*-**318** eluted first as an orange band (R_f 0.40, 50 % EtOAc:hexanes). Upon isolation, *trans*-**318** was obtained as a bright orange solid (39 mg, 29 %). *cis*-**318** was obtained as an orange solid after isolation of the second orange band (R_f 0.22, 50 % EtOAc:hexanes) (2 mg, 2 %).



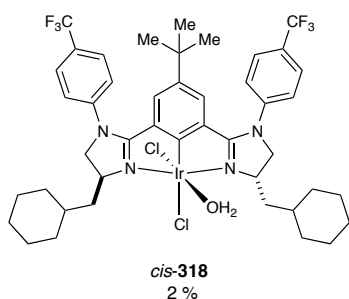
^1H NMR (600 MHz; CDCl_3): δ 7.68 (d, $J = 8.4$ Hz, 4H), 7.40 (d, $J = 8.4$ Hz, 4H), 6.70 (s, 2H), 4.56 (t, $J = 9.7$ Hz, 2H), 4.42-4.37 (m, 2H), 4.06 (t, $J = 8.3$ Hz, 2H), 2.54 (bs,

2H), 2.27-2.23 (m, 2H), 1.87 (d, $J = 12.8$ Hz, 2H), 1.77-1.67 (m, 8H), 1.25-1.03 (m, 12H), 0.88 (s, 9H), 1.40-1.34 (m, 2H).

^{13}C NMR (150 MHz; CDCl_3): δ 187.5, 169.6, 144.5, 143.1, 132.2, 128.5, 126.5, 125.5, 124.9, 123.1, 61.9, 60.2, 42.6, 35.4, 34.7, 34.5, 32.7, 31.4, 26.6

HRMS [+APCI] calculated for 1012.30402, found 1012.30069 $[\text{M}-\text{H}_2\text{O}]^+$

R_f 0.63 (30 % EtOAc:hexanes)



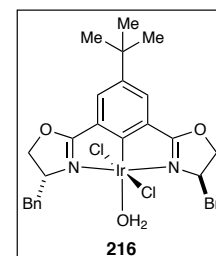
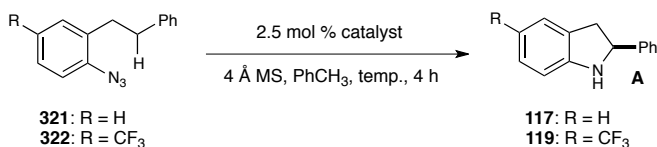
^1H NMR (600 MHz; CDCl_3): δ 7.68 (t, $J = 8.3$ Hz, 4H), 7.42 (t, $J = 8.3$ Hz, 4H), 6.85 (d, $J = 1.5$ Hz, 1H), 6.75 (d, $J = 1.5$ Hz, 1H), 4.77-4.69 (m, 1H), 4.62-4.55 (m, 1H), 4.43 (t, $J = 9.0$ Hz, 1H), 4.36 (qd, $J = 10.0, 3.5$ Hz, 1H), 4.17 (dd, $J = 13.2, 9.0$ Hz, 1H), 4.00 (t, $J = 9.5$ Hz, 1H), 3.36 (s, 1H), 2.62-2.48 (m, 2H), 2.09-1.99 (m, 1H), 1.94-1.84 (m, 3H), 1.75-1.30 (m, 20H), 0.92 (s, 9H)

IR (thin film, cm^{-1}) $\nu = 3440, 2925, 1614, 1321, 1068, 752$

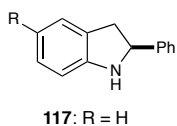
R_f 0.22 (30 % EtOAc:hexanes)

6.4 Chapter 5 Procedures and Characterization

Procedure for azide amination

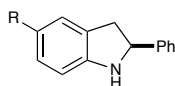


A 10 mL round bottom flask was charged with a magnetic stir bar, substrate (1 eq.), catalyst **216** (2.5 mol %), 4Å crushed molecular sieves (MS) (1 mg/1 mmol substrate), and equipped with a reflux condenser. Solvent (0.05 M) was added and the reaction was immersed in a preheated oil bath and refluxed for four hours. The reaction mixture was cooled and filtered through a plug of dry celite. The filter cake was washed with toluene (1 x 2 mL), CH₂Cl₂ (1 x 1 mL) and EtOAc (1 x 1 mL). The filtrate was concentrated on a rotary evaporator, and analysis of the crude oil provided percent conversion and ratio of indoline:indole (see general information). In the case of isolated yields, the indoline and indole products were purified by column chromatography (SiO₂, 5 % EtOAc:pentane). Enantiomeric excess of the product was determined by HPLC. The spectral data match the literature.¹³⁷



¹H NMR (400 MHz; CDCl₃): δ 7.46-7.28 (m, 5H), 7.12-7.07 (m, 2H), 6.76 (td, J = 7.4, 1.0, 1H), 6.69 (d, J = 7.3, 1H), 4.97 (t, J = 9.0, 1H), 4.16 (s, 1H), 3.46 (dd, J = 15.7, 9.2,

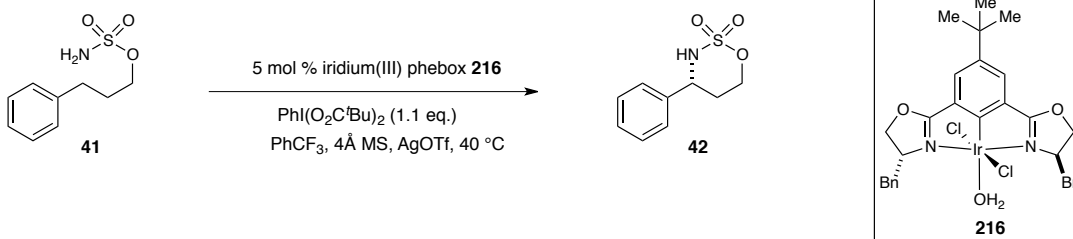
1H), 3.01 (dd, $J = 15.6, 8.9, 1\text{H}$). **HPLC** (Daicel OD-H, 210 nm detection, 3 % 2-propanol:hexanes, 1 mL/min); t_R (major = 18.01 min, minor = 29.06 min) 35 % ee.



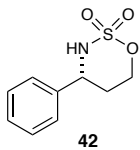
119: R = CF₃

¹H NMR (400 MHz; CDCl₃): δ 8.54 (s, 1H), 7.92 (s, 1H), 7.70-7.67 (m, 2H), 7.50-7.36 (m, 5H), 6.90 (s, 1H). **HPLC** (Chiracel AD-H, 280 nm detection, 5 % 2-propanol:hexanes, 1 mL/min); $t_R = 17.99$.

Procedure for sulfamate ester amination



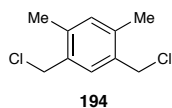
A 4 mL vial was charged with a magnetic stir bar, **41** (0.009 g, 0.04 mmol, 1 eq.), bis(*tert*-butylcarbonyloxy)-iodobenzene (0.018 g, 0.044 mmol, 1.1 eq.), catalyst **216** (0.002 mmol, 5 mol %), silver triflate (1 mg), and 4Å molecular sieves (20 mg / 0.4 mmol sulfamate ester **41**). The vial was evacuated and backfilled with argon (x 3). PhCF₃ (0.3 mL, 0.14 M in substrate) was added and the resulting suspension was stirred at 40 °C for 12 hours. The reaction mixture was then filtered through a plug of silica gel, eluting with CH₂Cl₂ (2 x 3 mL) and EtOAc (3 x 3 mL). The conversion of the reaction was determined by ¹H NMR and enantiomeric excess of the product was determined by HPLC. The spectral data match the literature.⁷⁸



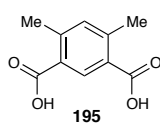
¹H NMR (CDCl₃, 400 MHz) δ 7.43-7.34 (m, 5H), 4.86 (t, 2H, *J*= 11.7 Hz), 4.66 (ddd, 1H, *J*= 11.3, 4.7, 1.2 Hz), 4.51 (d, 1H, *J*= 9.4 Hz), 2.25 (qd, 1H, *J*= 14.5, 4.7 Hz), 2.00 (dq, 1H, *J*= 14.5, 2.4 Hz)

Appendix – List of Synthesized Compounds

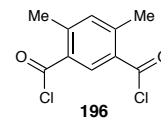
Thesis Page: 190



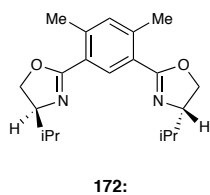
Thesis Page: 190



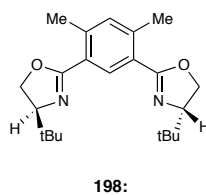
Thesis Page: 190



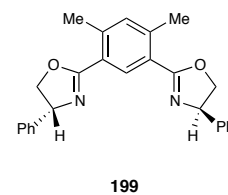
Thesis Page: 192



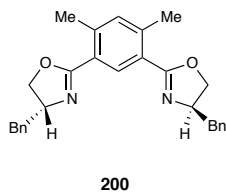
Thesis Page: 193



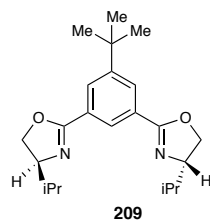
Thesis Page: 194



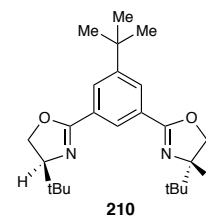
Thesis Page: 195



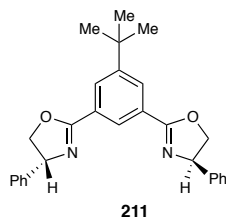
Thesis Page: 196



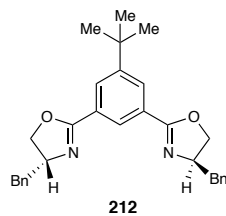
Thesis Page: 190



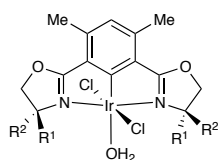
Thesis Page: 198



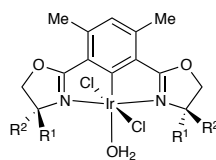
Thesis Page: 199



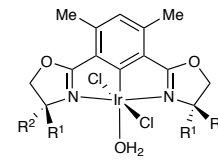
Thesis Page: 200

174: R¹ = *i*-Pr, R² = H

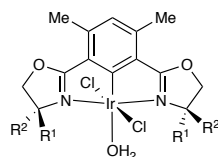
Thesis Page: 201

201: R¹ = *t*Bu, R² = H

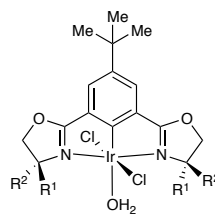
Thesis Page: 202

202: R¹ = H, R² = Ph

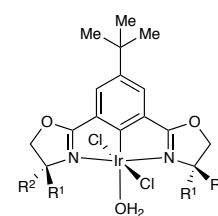
Thesis Page: 203

203: R¹ = H, R² = Bn

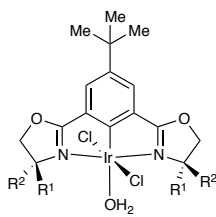
Thesis Page: 205

213: R¹ = *i*-Pr, R² = H; 41 %

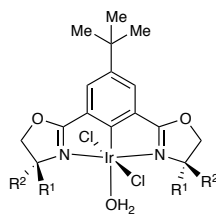
Thesis Page: 206

214: R¹ = *t*Bu, R² = H; 27 %

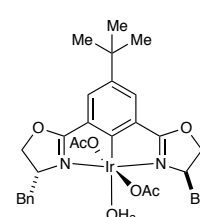
Thesis Page: 207

215: R¹ = H, R² = Ph; 14 %

Thesis Page: 208

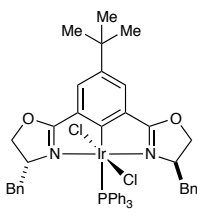
216: R¹ = H, R² = Bn; 54 %

Thesis Page: 209



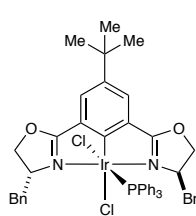
217

Thesis Page: 211



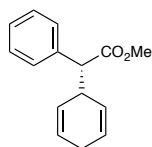
262

Thesis Page: 212



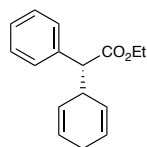
263

Thesis Page: 216



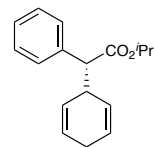
217

Thesis Page: 217



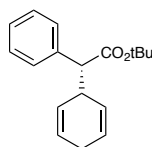
218

Thesis Page: 217



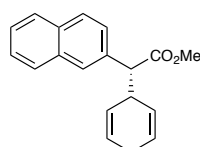
219

Thesis Page: 218



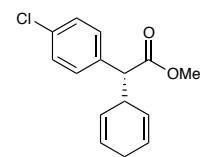
220

Thesis Page: 219



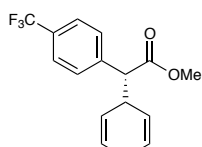
221

Thesis Page: 219



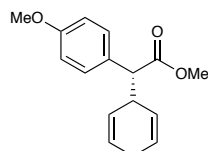
222

Thesis Page: 207



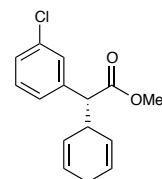
224

Thesis Page: 221



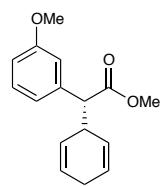
225

Thesis Page: 221



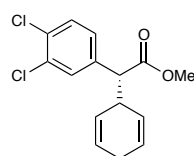
226

Thesis Page: 222



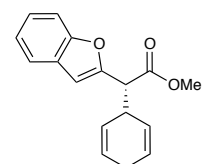
227

Thesis Page: 223



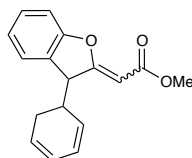
229

Thesis Page: 223



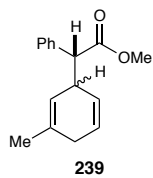
231

Thesis Page: 224

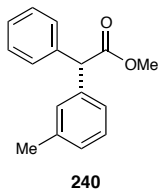


232

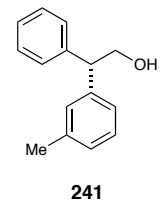
Thesis Page: 226



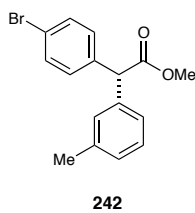
Thesis Page: 227



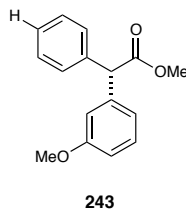
Thesis Page: 228



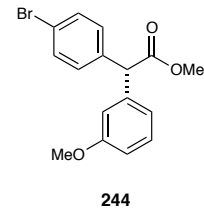
Thesis Page: 229



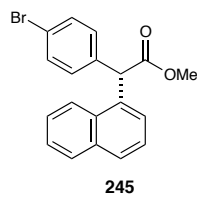
Thesis Page: 231



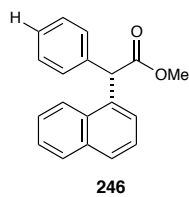
Thesis Page: 232



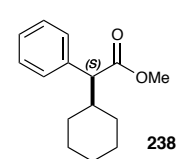
Thesis Page: 235



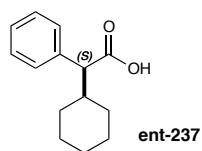
Thesis Page: 234



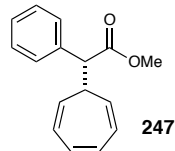
Thesis Page: 238



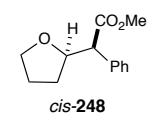
Thesis Page: 239



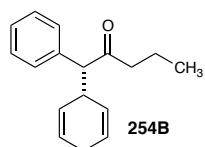
Thesis Page: 241



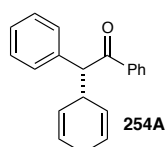
Thesis Page: 242



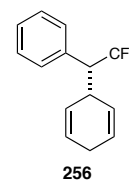
Thesis Page: 243



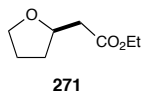
Thesis Page: 244



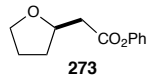
Thesis Page: 246



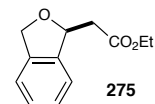
Thesis Page: 255



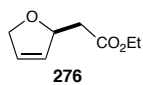
Thesis Page: 257



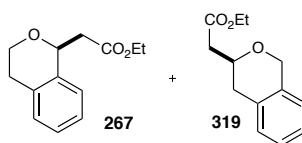
Thesis Page: 258



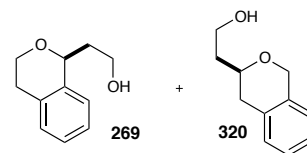
Thesis Page: 260



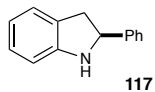
Thesis Page: 261



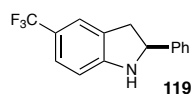
Thesis Page: 261



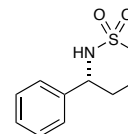
Thesis Page: 288



Thesis Page: 289

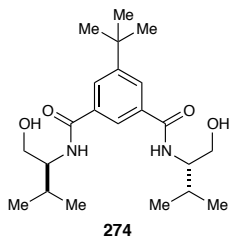


Thesis Page: 289

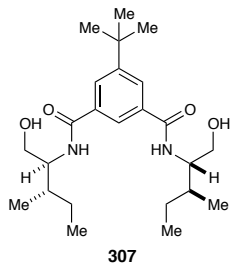


Amides

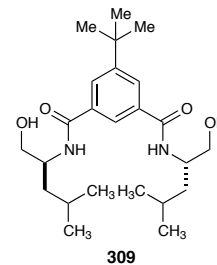
Thesis Page: 263



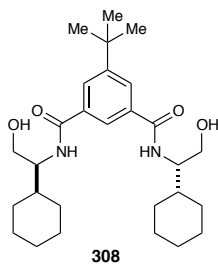
Thesis Page: 263



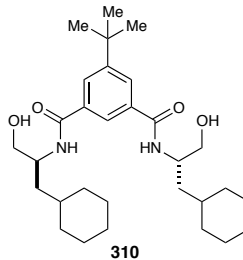
Thesis Page: 264



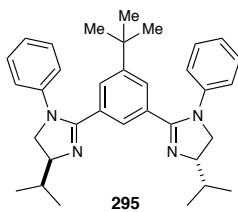
Thesis Page: 265



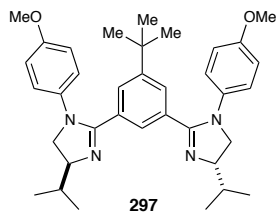
Thesis Page: 266

**Ligands**

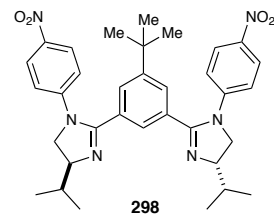
Thesis Page: 268



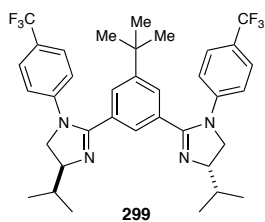
Thesis Page: 269



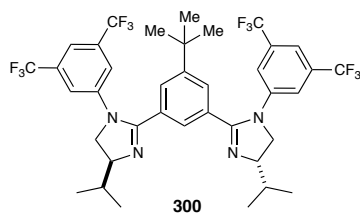
Thesis Page: 270



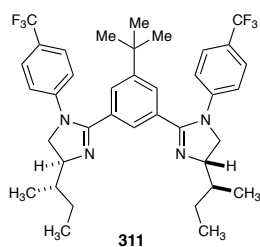
Thesis Page: 270



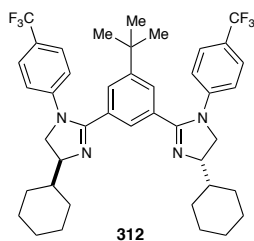
Thesis Page: 271



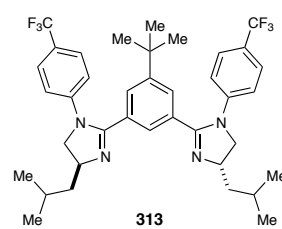
Thesis Page: 272



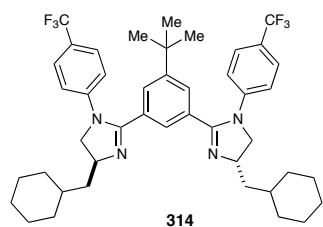
Thesis Page: 273



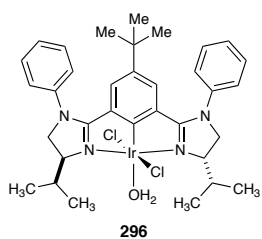
Thesis Page: 274



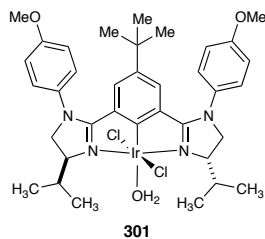
Thesis Page: 274

**Complexes**

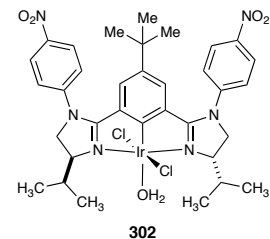
Thesis Page: 278



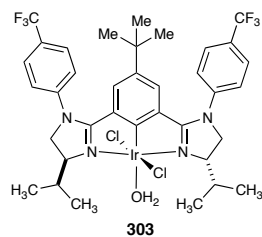
Thesis Page: 279



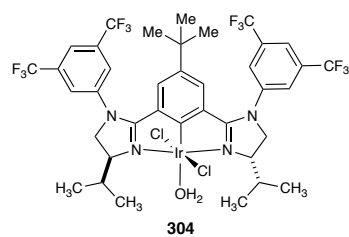
Thesis Page: 279



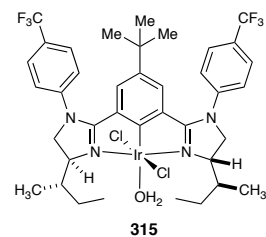
Thesis Page: 280

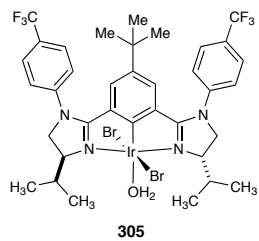
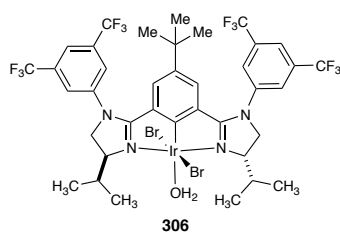
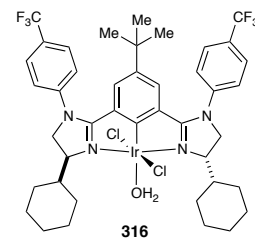
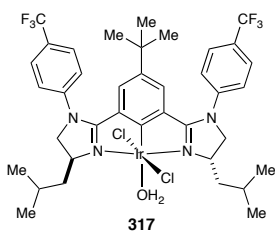
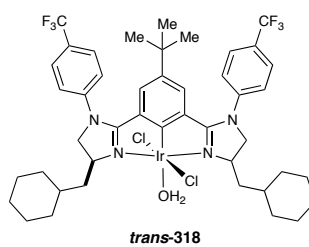
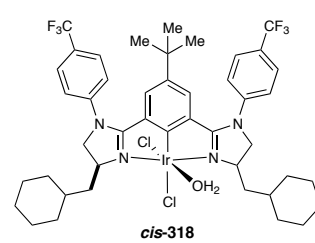


Thesis Page: 281



Thesis Page: 283



Complexes (continued)**Thesis Page: 282****Thesis Page: 283****Thesis Page: 284****Thesis Page: 285****Thesis Page: 286****Thesis Page: 287**

References

- (1) For leading references and reviews see: (a) J. Yamaguchi, A. D. Yamaguchi and K. Itami, *Angew. Chem. Int. Ed.*, **2012**, *51*, 8960 (b) W. R. Gutekunst and P. S. Baran, *Chem. Soc. Rev.*, **2011**, *40*, 1976 (c) F. Collet, C. Lescot and P. Dauban, *Chem. Soc. Rev.*, **2011**, *40*, 1926 (d) H. M. L. Davies and D. Morton, *Chem. Soc. Rev.*, **2011**, *40*, 1857 (e) C.-M. Che, V. K.-Y. Lo, C.-Y. Zhou and J.-S. Huang, *Chem. Soc. Rev.*, **2011**, *40*, 1950 (f) T. W. Lyons and M. S. Sanford, *Chem. Rev.*, **2010**, *110*, 1147 (g) C-H Activation, ed. J.-Q. Yu and Z. Shi, Springer-Verlag, Berlin, 2010.
- (2) Davies, H. M.; Manning, J. R. *Nature* **2008**, *451*, 417.
- (3) Doyle, M. P.; Duffy, R.; Ratnikov, M.; Zhou, L. *Chem. Rev.* **2010**, *110*, 704.
- (4) Du Bois, J. *Org. Proc. Res. Dev.* **2011**, *15*, 758.
- (5) Davies, H. M. L.; Beckwith, R. E. J. *Chem. Rev.* **2003**, *103*, 2861.
- (6) Roizen, J. L.; Harvey, M. E.; Du Bois, J. *Acc. Chem. Res.* **2012**, *45*, 911.
- (7) Hansen, J.; Autschbach, J.; Davies, H. M. L. *J. Org. Chem.* **2009**, *74*, 6555.
- (8) Davies, H. M. L.; Hansen, T.; Churchill, M. R. *J. Am. Chem. Soc.* **2000**, *122*, 3063.
- (9) Davies, H. M. L.; Beckwith, R. E. J.; Antoulinakis, E. G.; Jin, Q. *J. Org. Chem.* **2003**, *68*, 6126.
- (10) Fiori, K. W.; Espino, C. G.; Brodsky, B. H.; Du Bois, J. *Tetrahedron* **2009**, *65*, 3042.

- (11) Davies, H. M. L.; Venkataramani, C. *Angew. Chem. Int. Ed.* **2002**, *41*, 2197.
- (12) Hinman, A.; Du Bois, J. *J. Am. Chem. Soc.* **2003**, *125*, 11510.
- (13) Doyle, M. P. M., M.; Ye, T. *Modern Catalytic Methods for Organic Synthesis with Diazo Compounds: From Cyclopropanes to Ylides*; Wiley: New York, 1998.
- (14) Doyle, M. P.; Forbes, D. C. *Chem. Rev.* **1998**, *98*, 911.
- (15) Doyle, M. P.; Forbes, D. C.; Xavier, K. R. *Russ. Chem.* **1998**, *47*, 932.
- (16) Doyle, M. P.; Protopopova, M. N. *Tetrahedron* **1998**, *54*, 7919.
- (17) Dorwald, F. Z. *Metal Carbenes in Organic Synthesis*; Wiley-VCH: Weinheim, Germany, 1999.
- (18) Davies, H. M. L. *Organic Reactions* **2001**, *1*.
- (19) Regitz, M. M., G. *Aliphatic Diazo Compounds - Properties and Synthesis*; Academic Press: New York, 1986.
- (20) Ye, T.; Mckerverey, M. A. *Chem. Rev.* **1994**, *94*, 1091.
- (21) Davies, H. M. L.; Morton, D. *Chem. Soc. Rev.* **2011**, *40*, 1857.
- (22) Hansen, J.; Davies, H. M. L. *Coord. Chem. Rev.* **2008**, *252*, 545.
- (23) Davies, H. M. L.; Lian, Y. *Acc. Chem. Res.* **2012**, *45*, 923.
- (24) Hansen, J. H.; Gregg, T. M.; Ovalles, S. R.; Lian, Y.; Autschbach, J.; Davies, H. M. L. *J. Am. Chem. Soc.* **2011**, *133*, 5076.
- (25) Wang, H.; Li, G.; Engle, K. M.; Yu, J.-Q.; Davies, H. M. L. *J. Am. Chem. Soc.* **2013**, *135*, 6774.

- (26) Abd-Elazem, I. S.; Chen, H. S.; Bates, R. B.; Huang, R. C. C. *Antiviral Res.* **2002**, *55*, 91.
- (27) Diaz-Requejo, M. M.; Pérez, P. J. *Chem. Rev.* **2008**, *108*, 3379.
- (28) Müller, P.; Tohill, S. *Tetrahedron* **2000**, *56*, 1725.
- (29) Caballero, A.; Díaz-Requejo, M. M.; Belderraín, T. R.; Nicasio, M. C.; Trofimenko, S.; Pérez, P. J. *Organometallics* **2003**, *22*, 4145.
- (30) Díaz-Requejo, M. M.; Belderraín, T. R.; Nicasio, M. C.; Trofimenko, S.; Pérez, P. J. *J. Am. Chem. Soc.* **2002**, *124*, 896.
- (31) Fructos, M. R.; de Frémont, P.; Nolan, S. P.; Díaz-Requejo, M. M.; Pérez, P. J. *Organometallics* **2006**, *25*, 2237.
- (32) Caballero, A.; Díaz-Requejo, M. M.; Belderraín, T. R.; Nicasio, M. C.; Trofimenko, S.; Pérez, P. J. *J. Am. Chem. Soc.* **2003**, *125*, 1446.
- (33) Urbano, J.; Belderraín, T. R.; Nicasio, M. C.; Trofimenko, S.; Díaz-Requejo, M. M.; Pérez, P. J. *Organometallics* **2005**, *24*, 1528.
- (34) Dias, H. V. R.; Browning, R. G.; Richey, S. A.; Lovely, C. J. *Organometallics* **2004**, *23*, 1200.
- (35) Díaz-Requejo, M. M.; Caballero, A.; Fructos, M.; Pérez, P. In *Alkane C-H Activation by Single-Site Metal Catalysis*; Pérez, P. J., Ed.; Springer Netherlands: 2012; Vol. 38, p 229.
- (36) Díaz-Requejo, M. M.; Belderraín, T. R.; Trofimenko, S.; Pérez, P. J. *J. Am. Chem. Soc.* **2001**, *123*, 3167.

- (37) Trofimenko, S. *Scorpionates, The Coordination Chemistry of Polypyrazolylborate Ligands*; Imperial College Press: River Edge, NJ, 1999.
- (38) Chiral non-racemic ruthenium, manganese, and rhenium heteroscorpionate (N,N,O) complexes are known. See references 39 and 40.
- (39) Peters, L.; Hübner, E.; Haas, T.; Heinemann, F. W.; Burzlaff, N. *J Organomet. Chem.* **2009**, *694*, 2319.
- (40) Peters, L.; Burzlaff, N. *Polyhedron* **2004**, *23*, 245.
- (41) Doyle, M. P.; Phillips, I. M. *Tetrahedron Lett.* **2001**, *42*, 3155.
- (42) Doyle, M. P.; Hu, W. *Chirality* **2002**, *14*, 169.
- (43) Lu, H.; Zhang, X. P. *Chem. Soc. Rev.* **2011**, *40*, 1899.
- (44) Collet, F.; Lescot, C.; Dauban, P. *Chem. Soc. Rev.* **2011**, *40*, 1926.
- (45) Collet, F.; Dodd, R. H.; Dauban, P. *Chem. Commun.* **2009**, 5061.
- (46) Badiei, Y. M.; Dinescu, A.; Dai, X.; Palomino, R. M.; Heinemann, F. W.; Cundari, T. R.; Warren, T. H. *Angew. Chem. Int. Ed.* **2008**, *47*, 9961.
- (47) Müller, P.; Fruit, C. *Chem. Rev.* **2003**, *103*, 2905.
- (48) Stokes, B. J.; Liu, S.; Driver, T. G. *J. Am. Chem. Soc.* **2011**, *133*, 4702.
- (49) Sun, K.; Liu, S.; Bec, P. M.; Driver, T. G. *Angew. Chem. Int. Ed.* **2011**, *50*, 1702.
- (50) Shen, M.; Leslie, B. E.; Driver, T. G. *Angew. Chem. Int. Ed.* **2008**, *120*, 5134.
- (51) Rigoli, J. W.; Boralsky, L. A.; Hershberger, J. C.; Marston, D.; Meis, A. R.; Guzei, I. A.; Schomaker, J. M. *J. Org. Chem.* **2012**, *77*, 2446.

- (52) Weatherly, C. D.; Rigoli, J. W.; Schomaker, J. M. *Org. Lett.* **2012**, *14*, 1704.
- (53) Adams, C. S.; Boralsky, L. A.; Guzei, I. A.; Schomaker, J. M. *J. Am. Chem. Soc.* **2012**, *134*, 10807.
- (54) Boralsky, L. A.; Marston, D.; Grigg, R. D.; Hershberger, J. C.; Schomaker, J. M. *Org. Lett.* **2011**, *13*, 1924.
- (55) Abramovitch, R. A.; Bailey, T. D.; Takaya, T.; Uma, V. *J. Org. Chem.* **1974**, *39*, 340.
- (56) Yamada, Y.; Yamamoto, T.; Okawara, M. *Chem. Lett.* **1975**, *4*, 361.
- (57) Breslow, R.; Gellman, S. H. *J. Am. Chem. Soc.* **1983**, *105*, 6728.
- (58) Nägeli, I.; Baud, C.; Bernardinelli, G.; Jacquier, Y.; Moraon, M.; Müller, P. *Helv. Chim. Acta* **1997**, *80*, 1087.
- (59) Muller, P. *Transition Metal-catalyzed Nitrene Transfer: Aziridination and Insertion*; JAI Press: Greenwich, 1997; Vol. 2.
- (60) Wehn, P. M.; Du Bois, J. *Angew. Chem. Int. Ed. Engl.* **2009**, *48*, 3802.
- (61) Andresen, B. M.; Du Bois, J. *J. Am. Chem. Soc.* **2009**, *131*, 12524.
- (62) Che, C.-M.; Huang, J.-S. *Chem. Commun.* **2009**, 3996.
- (63) Zhang, J.-L.; Huang, J.-S.; Che, C.-M. *Chem. Eur. J.* **2006**, *12*, 3020.
- (64) Fantauzzi, S.; Caselli, A.; Gallo, E. *Dalton Trans.* **2009**, 5434.
- (65) Yu, X.-Q.; Huang, J.-S.; Zhou, X.-G.; Che, C.-M. *Org. Lett.* **2000**, *2*, 2233.

- (66) Espino, C. G.; Wehn, P. M.; Chow, J.; Du Bois, J. *J. Am. Chem. Soc.* **2001**, *123*, 6935.
- (67) Espino, C. G.; Fiori, K. W.; Kim, M.; Du Bois, J. *J. Am. Chem. Soc.* **2004**, *126*, 15378.
- (68) Lebel, H.; Huard, K.; Lectard, S. *J. Am. Chem. Soc.* **2005**, *127*, 14198.
- (69) Driver, T. G. *Org. Biomol. Chem.* **2010**, *8*, 3831.
- (70) Lu, H.; Tao, J.; Jones, J. E.; Wojtas, L.; Zhang, X. P. *Org. Lett.* **2010**, *12*, 1248.
- (71) Ruppel, J. V.; Kamble, R. M.; Zhang, X. P. *Org. Lett.* **2007**, *9*, 4889.
- (72) Kong, C.; Jana, N.; Driver, T. G. *Org. Lett.* **2013**, *15*, 824.
- (73) Nguyen, Q.; Sun, K.; Driver, T. G. *J. Am. Chem. Soc.* **2012**, *134*, 7262.
- (74) Nguyen, Q.; Nguyen, T.; Driver, T. G. *J. Am. Chem. Soc.* **2012**, *135*, 620.
- (75) Hennessy, E. T.; Betley, T. A. *Science* **2013**, *340*, 591.
- (76) Liang, J. L.; Yuan, S. X.; Huang, J. S.; Che, C. M. *J. Org. Chem.* **2004**, *69*, 3610.
- (77) Liang, J. L.; Yuan, S. X.; Huang, J. S.; Yu, W. Y.; Che, C. M. *Angew. Chem. Int. Ed. Engl.* **2002**, *41*, 3465.
- (78) Milczek, E.; Boudet, N.; Blakey, S. *Angew. Chem. Int. Ed.* **2008**, *47*, 6825.
- (79) Zalatan, D. N.; Du Bois, J. *J. Am. Chem. Soc.* **2008**, *130*, 9220.
- (80) Che, C.-M.; Lo, V. K.-Y.; Zhou, C.-Y.; Huang, J.-S. *Chem. Soc. Rev.* **2011**, *40*, 1950.
- (81) Fiori, K. W.; Du Bois, J. *J. Am. Chem. Soc.* **2007**, *129*, 562.

- (82) Yamawaki, M.; Tsutsui, H.; Kitagaki, S.; Anada, M.; Hashimoto, S. *Tetrahedron Lett.* **2002**, *43*, 9561.
- (83) Reddy, R. P.; Davies, H. M. *Org. Lett.* **2006**, *8*, 5013.
- (84) Lu, H.; Subbarayan, V.; Tao, J.; Zhang, X. P. *Organometallics* **2009**, *29*, 389.
- (85) Kawabata, H.; Omura, K.; Uchida, T.; Katsuki, T. *Chem. Asian. J.* **2007**, *2*, 248.
- (86) Nishioka, Y.; Uchida, T.; Katsuki, T. *Angew. Chem. Int. Ed.* **2013**, *52*, 1739.
- (87) Janowicz, A. H.; Bergman, R. G. *J. Am. Chem. Soc.* **1982**, *104*, 352.
- (88) Shilov, A. E.; Shulpin, G. B. *Chem. Rev.* **1997**, *97*, 2879.
- (89) Arndtsen, B. A.; Bergman, R. G.; Mobley, T. A.; Peterson, T. H. *Acc. Chem. Res.* **1995**, *28*, 154.
- (90) Hashiguchi, B. G.; Bischof, S. M.; Konnick, M. M.; Periana, R. A. *Acc. Chem. Res.* **2012**, *45*, 885.
- (91) Choi, J.; Goldman, A. S. In *Iridium Catalysis*; Andersson, P. G., Ed.; Springer Berlin Heidelberg: 2011; Vol. 34, p 139.
- (92) Niimi, T.; Uchida, T.; Irie, R.; Katsuki, T. *Adv. Synth. Catal.* **2001**, *343*, 79.
- (93) Kanchiku, S.; Suematsu, H.; Matsumoto, K.; Uchida, T.; Katsuki, T. *Angew. Chem. Int. Ed.* **2007**, *46*, 3889.

- (94) Suematsu, H.; Kanchiku, S.; Uchida, T.; Katsuki, T. *J. Am. Chem. Soc.* **2008**, *130*, 10327.
- (95) Ichinose, M.; Suematsu, H.; Katsuki, T. *Angew. Chem. Int. Ed.* **2009**, *48*, 3121.
- (96) Bykowski, D.; Wu, K.-H.; Doyle, M. P. *J. Am. Chem. Soc.* **2006**, *128*, 16038.
- (97) Uehara, M.; Suematsu, H.; Yasutomi, Y.; Katsuki, T. *J. Am. Chem. Soc.* **2010**, *132*, 170.
- (98) Cobalt porphyrin catalysts have since been shown to perform enantioselective acceptor-acceptor cyclopropenation. See: Cui, X.; Xu, X.; Lu, H.; Zhu, S.; Wojtas, L.; Zhang, X. P. *J. Am. Chem. Soc.* 2011, *133*, 3304.
- (99) Davies, H. M. L.; Lee, G. H. *Org. Lett.* **2004**, *6*, 1233.
- (100) Briones, J. F.; Hansen, J.; Hardcastle, K. I.; Autschbach, J.; Davies, H. M. L. *J. Am. Chem. Soc.* **2010**, *132*, 17211.
- (101) Briones, J. F.; Davies, H. M. L. *J. Am. Chem. Soc.* **2012**, *134*, 11916.
- (102) Suematsu, H.; Katsuki, T. *J. Am. Chem. Soc.* **2009**, *131*, 14218.
- (103) DeAngelis, A.; Dmitrenko, O.; Fox, J. M. *J. Am. Chem. Soc.* **2012**, *134*, 11035.
- (104) Boruta, D. T.; Dmitrenko, O.; Yap, G. P. A.; Fox, J. M. *Chem. Sci.* **2012**, *3*, 1589.
- (105) DeAngelis, A.; Dmitrenko, O.; Yap, G. P. A.; Fox, J. M. *J. Am. Chem. Soc.* **2009**, *131*, 7230.

- (106) Panne, P.; DeAngelis, A.; Fox, J. M. *Org. Lett.* **2008**, *10*, 2987.
- (107) Panish, R.; Chintala, S. R.; Boruta, D. T.; Fang, Y.; Taylor, M. T.; Fox, J. M. *J. Am. Chem. Soc.* **2013**, *135*, 9283.
- (108) Panne, P.; Fox, J. M. *J. Am. Chem. Soc.* **2007**, *129*, 22.
- (109) DeAngelis, A.; Taylor, M. T.; Fox, J. M. *J. Am. Chem. Soc.* **2009**, *131*, 1101.
- (110) DeAngelis, A.; Panne, P.; Yap, G. P. A.; Fox, J. M. *J. Org. Chem.* **2008**, *73*, 1435.
- (111) DeAngelis, A.; Shurtleff, V. W.; Dmitrenko, O.; Fox, J. M. *J. Am. Chem. Soc.* **2011**, *133*, 1650.
- (112) Hashimoto has also reported C-H functionalization of indoles using alkyl diazoesters. See: Goto, T.; Natori, Y.; Takeda, K.; Nambu, H.; Hashimoto, S. *Tetrahedron: Asymmetry* 2011, *22*, 907.
- (113) Yasutomi, Y.; Suematsu, H.; Katsuki, T. *J. Am. Chem. Soc.* **2010**, *132*, 4510.
- (114) Adler, A. D.; Longo, F. R.; Finarelli, J. D.; Goldmacher, J.; Assour, J.; Korsakoff, L. *J. Org. Chem.* **1967**, *32*, 476.
- (115) Ogoshi, H.; Setsune, J.-I.; Yoshida, Z.-I. *J. Organomet. Chem.* **1978**, *159*, 317.
- (116) Maxwell, J.; Brown, K.; Bartley, D.; Kodadek, T. *Science*, 1992, 256, 1544.
- (117) Brown, K. C.; Kodadek, T. *J. Am. Chem. Soc.* 1992, *114*, 8336.

- (118) Anding, B. J.; Brgoch, J.; Miller, G. J.; Woo, L. K. *Organometallics* **2012**, *31*, 5586.
- (119) Davies, H. M. L.; Jin, Q.; Ren, P.; Kovalevsky, A. Y. *J. Org. Chem.* **2002**, *67*, 4165.
- (120) Runge, E.; Gross, E. K. *U. Phys. Rev. Lett.* **1984**, *52*, 997.
- (121) Wang, J. C.; Xu, Z. J.; Guo, Z.; Deng, Q. H.; Zhou, C. Y.; Wan, X. L.; Che, C. M. *Chem. Commun.* **2012**, *48*, 4299.
- (122) Housecroft, C. E.; Sharpe, A. G. *Inorganic Chemistry*; 3rd ed.; Prentice Hall, 2008.
- (123) Anding, B. J.; Woo, L. K. *Organometallics* **2013**, *32*, 2599.
- (124) Thu, H.-Y.; Tong, G. S.-M.; Huang, J.-S.; Chan, S. L.-F.; Deng, Q.-H.; Che, C.-M. *Angew. Chem. Int. Ed.* **2008**, *47*, 9747.
- (125) Halterman, R. L.; Jan, S. T. *J. Org. Chem.* **1991**, *56*, 5253.
- (126) Wang, J.-C.; Zhang, Y.; Xu, Z.-J.; Lo, V. K.-Y.; Che, C.-M. *ACS Catal.* **2013**, *3*, 1144.
- (127) Iridium(I) catalyzed intramolecular C-H insertion has also been reported. See Lopez-Sanchez, C.; Alvarez, Corral, M.; Munoz-Dorado, M.; Rodriguez-Garcia, I. *Synlett* **2012**, *23*, 2469.
- (128) Mangion, I. K.; Nwamba, I. K.; Shevlin, M.; Huffman, M. A. *Org. Lett.* **2009**, *11*, 3566
- (129) Mangion, I. K.; Ruck, R. T.; Rivera, N.; Huffman, M. A.; Shevlin, M. *Org. Lett.* **2011**, *13*, 5480.

- (130) Ichinose, M.; Suematsu, H.; Yasutomi, Y.; Nishioka, Y.; Uchida, T.; Katsuki, T. *Angewandte Chemie International Edition* **2011**, *50*, 9884.
- (131) Nishioka, Y.; Uchida, T.; Katsuki, T. *Angew. Chem. Int. Ed.* **2013**, *52*, 1739.
- (132) Ryu, J.; Kwak, J.; Shin, K.; Lee, D.; Chang, S. *J. Am. Chem. Soc.* **2013**, *135*, 12861.
- (133) Scriven, E. F. V.; Turnbull, K. *Chem. Rev.* **1988**, *88*, 297.
- (134) Lee, D.; Kim, Y.; Chang, S. *J. Org. Chem.* **2013**, *78*, 11102.
- (135) Johnson, E. D.; Basolo, F. *Inorg. Chem.* **1977**, *16*, 554.
- (136) Basolo, F.; Lane, B. C.; McDonald John, W.; Myers, V. G.; Pearson, R. G. *J. Am. Chem. Soc.* **1971**, *93*, 4934.
- (137) Sun, K.; Sachwani, R.; Richert, K. J.; Driver, T. G. *Org. Lett.* **2009**, *11*, 3598.
- (138) Huheey, J. E.; Keiter, E. A.; Keiter, R. L. *Inorganic chemistry : principles of structure and reactivity*; 4th ed.; HarperCollins College Publishers: New York, NY, 1993.
- (139) Desimoni, G.; Faita, G.; Quadrelli, P. *Chem. Rev.* **2003**, *103*, 3119.
- (140) Nishiyama, H.; Itoh, Y.; Matsumoto, H.; Park, S.-B.; Itoh, K. *J. Am. Chem. Soc.* **1994**, *116*, 2223.
- (141) Nishiyama, H.; Ito, J.-i. *Chem. Commun.* **2010**, *46*, 203.
- (142) Nishiyama, H. *Chem. Soc. Rev.* **2007**, *36*, 1133.

- (143) Denmark, S. E.; Stavenger, R. A.; Faucher, A.-M.; Edwards, J. P. *J. Org. Chem.* **1997**, *62*, 3375.
- (144) Stark, M. A.; Richards, C. J. *Tetrahedron Lett.* **1997**, *38*, 5881.
- (145) Ito, J.-i.; Nishiyama, H. *Synlett* **2012**, *2012*, 509.
- (146) Motoyama, Y.; Okano, M.; Narusawa, H.; Makihara, N.; Aoki, K.; Nishiyama, H. *Organometallics* **2001**, *20*, 1580.
- (147) Kanazawa, Y.; Tsuchiya, Y.; Kobayashi, K.; Shiomi, T.; Itoh, J.-i.; Kikuchi, M.; Yamamoto, Y.; Nishiyama, H. *Chem. Eur. J.* **2006**, *12*, 63.
- (148) Motoyama, Y.; Koga, Y.; Nishiyama, H. *Tetrahedron* **2001**, *57*, 853.
- (149) Ito, J.-i.; Miyakawa, T.; Nishiyama, H. *Organometallics* **2008**, *27*, 3312.
- (150) Ito, J.; Nishiyama, H. *Eur. J. Inorg. Chem.* **2007**, 1114.
- (151) Inoue, H.; Ito, J.-i.; Kikuchi, M.; Nishiyama, H. *Chem. Asian J.* **2008**, *3*, 1284.
- (152) Ito, J.-i.; Kitase, M.; Nishiyama, H. *Organometallics* **2007**, *26*, 6412.
- (153) Ito, J.-i.; Miyakawa, T.; Nishiyama, H. *Organometallics* **2006**, *25*, 5216.
- (154) Motoyama, Y.; Shimozono, K.; Aoki, K.; Nishiyama, H. *Organometallics* **2002**, *21*, 1684.
- (155) Motoyama, Y.; Koga, Y.; Kobayashi, K.; Aoki, K.; Nishiyama, H. *Chem. Eur. J.* **2002**, *8*, 2968.
- (156) Tsuchiya, Y.; Uchimura, H.; Kobayashi, K.; Nishiyama, H. *Synlett* **2004**, 2099.
- (157) Ito, J. I.; Shiomi, T.; Nishiyama, H. *Adv. Synth. Catal.* **2006**, *348*, 1235.

- (158) Tsuchiya, Y.; Kanazawa, Y.; Shiomi, T.; Kobayashi, K.; Nishiyama, H. *Synlett* **2004**, 2493.
- (159) Kanazawa, Y.; Nishiyama, H. *Synlett* **2006**, 3343.
- (160) Nishiyama, H.; Shiomi, T.; Tsuchiya, Y.; Matsuda, I. *J. Am. Chem. Soc.* **2005**, *127*, 6972.
- (161) Zhao, C. X.; Duffey, M. O.; Taylor, S. J.; Morken, J. P. *Org. Lett.* **2001**, *3*, 1829.
- (162) Shiomi, T.; Adachi, T.; Ito, J.; Nishiyama, H. *Org. Lett.* **2009**, *11*, 1011.
- (163) Shiomi, T.; Nishiyama, H. *Org. Lett.* **2007**, *9*, 1651.
- (164) Hashimoto, T.; Ito, J.-i.; Nishiyama, H. *Tetrahedron* **2008**, *64*, 9408.
- (165) Trost, B. M.; Brindle, C. S. *Chem. Soc. Rev.* **2010**, *39*, 1600.
- (166) Inoue, H.; Kikuchi, M.; Ito, J.; Nishiyama, H. *Tetrahedron* **2008**, *64*, 493.
- (167) Nishiyama, H.; Ishikawa, J.; Shiomi, T. *Tetrahedron Lett.* **2007**, *48*, 7841.
- (168) Shiomi, T.; Adachi, T.; Toribatake, K.; Zhou, L.; Nishiyama, H. *Chem. Commun.* **2009**, 5987.
- (169) Toribatake, K.; Nishiyama, H. *Angew. Chem. Int. Ed.* **2013**, *52*, 11011.
- (170) Wang, T.; Hao, X.-Q.; Huang, J.-J.; Niu, J.-L.; Gong, J.-F.; Song, M.-P. *J. Org. Chem.* **2013**, *78*, 8712.
- (171) Ito, J.-i.; Ujiiie, S.; Nishiyama, H. *Chem. Eur. J.* **2010**, *16*, 4986.
- (172) Fossey, J. S.; Richards, C. J. *Organometallics* **2004**, *23*, 367.
- (173) Fossey, J. S.; Richards, C. J. *Organometallics* **2002**, *21*, 5259.
- (174) Ito, J.-i.; Kaneda, T.; Nishiyama, H. *Organometallics* **2012**, *31*, 4442.

- (175) Hartwig, J. F. *Chem. Rev.* **2011**, *40*, 1992.
- (176) Mkhaliid, I. A. I.; Barnard, J. H.; Marder, T. B.; Murphy, J. M.; Hartwig, J. F. *Chem. Rev.* **2010**, *110*, 890.
- (177) Allen, K. E.; Heinekey, D. M.; Goldman, A. S.; Goldberg, K. I. *Organometallics* **2013**, *32*, 1579.
- (178) Morales-Morales, D.; Lee, D. W.; Wang, Z.; Jensen, C. M. *Organometallics* **2001**, *20*, 1144.
- (179) Liu, F.; Pak, E. B.; Singh, B.; Jensen, C. M.; Goldman, A. S. *J. Am. Chem. Soc.* **1999**, *121*, 4086.
- (180) Owens, C. P.; Varela-Alvarez, A.; Boyarskikh, V.; Musaev, D. G.; Davies, H. M. L.; Blakey, S. B. *Chem. Sci.* **2013**, *4*, 2590.
- (181) Kishida, T.; Ieda, N.; Yamauchi, T.; Komura, K.; Sugi, Y. *Ind. & Eng. Chem. Res.* **2009**, *48*, 5566.
- (182) Schroder, A.; Karbach, D.; Guthier, R.; Vogtle, F. *Chem. Ber.* **1992**, *125*, 1881.
- (183) Davies, H. M. L.; Stafford, D. G.; Hansen, T. *Org. Lett.* **1999**, *1*, 233.
- (184) Bugarin, A.; Connell, B. T. *Organometallics* **2008**, *27*, 4357.
- (185) Tamura, H.; Yamazaki, H.; Sato, H.; Sakaki, S. *J. Am. Chem. Soc.* **2003**, *125*, 16114.
- (186) Collaborations ongoing with Dr. John Berry, University of Wisconsin, as of December, 2013.
- (187) Camps, P.; Giménez, S. *Tetrahedron: Asymmetry* **1996**, *7*, 1227.

- (188) Camps, P.; Giménez, S.; Font-Bardia, M.; Solans, X. *Tetrahedron: Asymmetry* **1995**, *6*, 985.
- (189) Barlow, R. B.; Franks, F. M.; Pearson, J. D. M. *J. Med. Chem.* **1973**, *16*, 439.
- (190) Peng, C.; Zhang, W.; Yan, G.; Wang, J. *Org. Lett.* **2009**, *11*, 1667.
- (191) Dai, X.; Strotman, N. A.; Fu, G. C. *J. Am. Chem. Soc.* **2008**, *130*, 3302.
- (192) Raghavan, S.; Subba Rao, G. S. R. *Tetrahedron*, **1994**, *50*, 2599
- (193) Davies, H. M. L.; Stafford, D. G.; Hansen, T.; Churchill, M. R.; Keil, K. *M. Tetrahedron Lett.* **2000**, *41*, 2035.
- (194) The absolute stereochemistry was assigned by analogy to the literature value, see: Davies, H. M. L.; Hansen, T.; Churchill, M. R. *J. Am. Chem. Soc.* **2000**, *122*, 3063.
- (195) Reddy, R. P.; Lee, G. H.; Davies, H. M. L. *Org. Lett.* **2006**, *8*, 3437.
- (196) Denton, J. R.; Cheng, K.; L. Davies, H. M. *Chem. Commun.* **2008**, 1238.
- (197) Denton, J. R.; Sukumaran, D.; Davies, H. M. L. *Org. Lett.* **2007**, *9*, 2625.
- (198) Density Functional Theory (DFT) calculations were based on the local functional M06L [Y. Zhao and D. G. Truhlar, *J. Chem. Phys.* 2006, *125*, 194101]. Pople's 6-31G** (C, H, O and N atoms) and 6-31+G* (Cl atoms) basis sets [W. J. Hehre, L. Radom, P. v. R. Schleyer and J. A. Pople, *Ab initio Molecular Orbital Theory*, John Wiley & Sons, New York, 1986] and LANL2DZ (for Ir atoms) basis set and ECP were employed [P. J. Hay and W. R. Wadt, *J. Chem. Phys.*, 1985, *82*, 299]. The combination of the used basis sets is denoted as BS1, in this paper. Solvent effects were incorporated

by means of the Conductor-like Polarizable Continuum Model (CPCM) and all the structures were optimized including the solvent effects [J. Tomasi, B. Menucci and R. Cammi, *Chem. Rev.*, 2005, 105, 2999]. Dichloromethane has been employed as solvent. ($\epsilon = 8.93$). We call this level of theory CPCM-M06L/BS1. All calculations were carried out using Gaussian 09 suite of programs [Gaussian 09, Revision A.02, M. J. Frisch, et al., Gaussian, Inc., Wallingford CT, 2009, for full reference see the experimental section.

(199) Park, S.-B.; Sakata, N.; Nishiyama, H. *Chem. Eur. J.* **1996**, 2, 303.

(200) Cornejo, A.; Fraile, J. M.; García, J. I.; Gil, M. J.; Martínez-Merino, V.; Mayoral, J. A.; Salvatella, L. *Organometallics* **2005**, 24, 3448.

(201) Lebel, H.; Marcoux, J.-F.; Molinaro, C.; Charette, A. B. *Chem. Rev.* **2003**, 103, 977.

(202) Fraile, J. M.; García, J. I.; Mayoral, J. A.; Roldán, M. *Org. Lett.* **2007**, 9, 731.

(203) Fraile, J. M.; Mayoral, J. A.; Ravasio, N.; Roldán, M.; Sordelli, L.; Zaccheria, F. *Journal of Catalysis* **2011**, 281, 273.

(204) Jiménez-Osés, G.; Vispe, E.; Roldán, M.; Rodríguez-Rodríguez, S.; López-Ram-de-Viu, P.; Salvatella, L.; Mayoral, J. A.; Fraile, J. M. *J. Org. Chem.* **2013**, 78, 5851.

(205) Cadierno, V.; Gamasa, M. P.; Gimeno, J.; Iglesias, L.; García-Granda, S. *Inorg. Chem.* **1999**, 38, 2874.

- (206) Kornecki, K. P.; Briones, J. F.; Boyarskikh, V.; Fullilove, F.; Autschbach, J.; Schrote, K. E.; Lancaster, K. M.; Davies, H. M. L.; Berry, J. F. *Science* **2013**, *342*, 351.
- (207) Campos, J.; Peloso, R.; Brookhart, M.; Carmona, E. *Organometallics* **2013**, *32*, 3423.
- (208) Morilla, M. E.; Molina, M. J.; Díaz-Requejo, M. M.; Belderráin, T. R.; Nicasio, M. C.; Trofimenko, S.; Pérez, P. J. *Organometallics* **2003**, *22*, 2914.
- (209) Maas, G. *Angew. Chem. Int. Ed.* **2009**, *48*, 8186.
- (210) Clark, J. D.; Heise, J. D.; Shah, A. S.; Peterson, J. C.; Chou, S. K.; Levine, J.; Karakas, A. M.; Ma, Y.; Ng, K.-Y.; Patelis, L.; Springer, J. R.; Stano, D. R.; Wettach, R. H.; Dutra, G. A. *Org. Proc. Res. Dev.* **2004**, *8*, 176.
- (211) Anthes, R.; Bello, O.; Benoit, S.; Chen, C.-K.; Corbett, E.; Corbett, R. M.; DelMonte, A. J.; Gingras, S.; Livingston, R.; Sausker, J.; Soumeillant, M. *Org. Proc. Res. Dev.* **2008**, *12*, 168.
- (212) Clark, J. D.; Shah, A. S.; Peterson, J. C.; Patelis, L.; Kersten, R. J. A.; Heemskerk, A. H. *Thermochimica Acta* **2002**, *386*, 73.
- (213) Clark, J. D.; Shah, A. S.; Peterson, J. C. *Thermochimica Acta* **2002**, *392–393*, 177.
- (214) TenBrink, R. E.; Bergh, C. L.; Duncan, J. N.; Harris, D. W.; Huff, R. M.; Lahti, R. A.; Lawson, C. F.; Lutzke, B. S.; Martin, I. J.; Rees, S. A.; Schlachter, S. K.; Sih, J. C.; Smith, M. W. *J. Med. Chem.* **1996**, *39*, 2435.

- (215) Lorente, A.; Lamariano-Merketegi, J.; Albericio, F.; Álvarez, M. *Chem. Rev.* **2013**, *113*, 4567.
- (216) The racemic sample for HPLC analysis was obtained by slow addition (12 hours) of ethyl diazoacetate in THF to a stirring mixture of THF and Rh₂(OAc)₄. This method was especially low yielding and needed to be performed on a significant scale (> 200mg) to obtain the racemic insertion product in adequate yield.
- (217) Nicewicz, D. A.; Breteche, G.; Johnson, J. S. *Org. Synth.* Vol. 85, **2008**, 278.
- (218) Doyle, M. P.; Kalinin, A. V. *J. Org. Chem.* **1996**, *61*, 2179.
- (219) Chanthamath, S.; Phomkeona, K.; Shibatomi, K.; Iwasa, S. *Chem. Commun.* **2012**, *48*, 7750.
- (220) Ruppel, J. V.; Gauthier, T. J.; Snyder, N. L.; Perman, J. A.; Zhang, X. P. *Org. Lett.* **2009**, *11*, 2273.
- (221) Ouhia, A.; Rene, L.; Guilhem, J.; Pascard, C.; Badet, B. *J. Org. Chem.* **1993**, *58*, 1641.
- (222) Evans, D. A.; Peterson, G. S.; Johnson, J. S.; Barnes, D. M.; Campos, K. R.; Woerpel, K. A. *J. Org. Chem.* **1998**, *63*, 4541.
- (223) Banka, A.; Catalano, J. G.; Chong, P. Y.; Fang, J.; Garrido, D. M.; Maynard, A.; Miller, J.; Patterson, D.; Peat, A. J.; Powers, J.; Price, D. J.; Roberts, C.; Tai, V.; Youngman, M.; GlaxoSmithKline LLC: 2011; Vol. WO Patent 2,011,050,284.
- (224) Rotstein, D. M.; Melville, C. R.; Roche Palo Alto LLC: 2008; Vol. US Patent 2008/0249087 A1.

- (225) Anslyn, E. V.; Dougherty, D. A. *Modern Physical Organic Chemistry*; University Science Books: Sausalito, 2006.
- (226) Sulikowski, G. A.; Lee, S. *Tetrahedron Lett.* **1999**, *40*, 8035.
- (227) Carey, F. A.; Sundberg, R. J. *Advanced Organic Chemistry*; 5th ed.; Springer: New York, 2007.
- (228) Dias, L. C.; Meira, P. R. R. *J. Org. Chem.* **2005**, *70*, 4762.
- (229) Davies, H. M. L.; Antoulinakis, E. G.; Hansen, T. *Org. Lett.* **1999**, *1*, 383.
- (230) Roseblade, S. J.; Pfaltz, A. *Acc. Chem. Res.* **2007**, *40*, 1402.
- (231) Anding, B. J.; Ellern, A.; Woo, L. K. *Organometallics* **2012**, *31*, 3628.
- (232) Unpublished results.
- (233) For dirhodium tetracarboxylate catalyzed C-H insertion of donor/acceptor carbenes into cyclopentane and 1,4 cyclohexadiene, the potential energy barriers were calculated to be much higher at 17.4 kcal·mol⁻¹ and 6.2 kcal·mol⁻¹, respectively. See Hansen, J.; Autschbach, J.; Davies, H. M. L. *J. Org. Chem.* **2009**, *74*, 6555.
- (234) Mulliken, R. S. *J. Chem. Phys.* **1955**, *23*, 1833.
- (235) (a) Menges, F.; Neuburger, M. Pfaltz, A. *Org. Lett.* **2002**, *4*, 4713. (b) Dupont, J.; Ebeling, G.; Delgado, M. R.; Consorti, C. S.; Burrow, R.; Farrar, D. H.; Lough, A.J. *Inorg. Chem. Commun.* **2001**, *4*, 471. (c) Davinport, A. J.; Davies, D. L.; Fawcett, J.; Russel, D. R. *J. Chem. Soc. Perkin Trans. 1* **2001**, 1500. (d) Ma, K.; You, J. *Chem. Eur. J.* **2007**, *13*, 1863.
- (236) Yang, M.-J.; Liu, Y.-J.; Gong, J.-F.; Song, M.-P. *Organometallics* **2011**, *30*, 3793.

- (237) Wu, L.-Y.; Hao, X.-Q.; Xu, Y.-X.; Jia, M.-Q.; Wang, Y.-N.; Gong, J.-F.; Song, M.-P. *Organometallics* **2009**, *28*, 3369.
- (238) Hao, X.-Q.; Xu, Y.-X.; Yang, M.-J.; Wang, L.; Niu, J.-L.; Gong, J.-F.; Song, M.-P. *Organometallics* **2012**, *31*, 835.
- (239) Hao, X.-Q.; Gong, J.-F.; Du, C.-X.; Wu, L.-Y.; Wu, Y.-J.; Song, M.-P. *Tetrahedron Lett.* **2006**, *47*, 5033.
- (240) Shao, D.-D.; Niu, J.-L.; Hao, X.-Q.; Gong, J.-F.; Song, M.-P. *Dalton Trans.* **2011**, *40*, 9012.
- (241) Wang, T.; Niu, J.-L.; Liu, S.-L.; Huang, J.-J.; Gong, J.-F.; Song, M.-P. *Adv. Synth. Catal.* **2013**, *355*, 927.
- (242) Akiyama, T.; Saito, K.; Shibata, Y.; Yamanaka, M. *J. Am. Chem. Soc.* **2013**, *135*, 11740
- (243) Fernandez-Torres, P.; Gotor, V.; Gotor-Fernandez, V. *Tetrahedron: Asymmetry* **2006**, *17*, 2558
- (244) Hou, X. L.; Zheng, B. H. *Org. Lett.* **2009**, *11*, 1789
- (245) Santangelo, E. M.; Unelius, C. R.; Mudalige, A.; Santangelo, E. M.; Liblikas, I.; Toernroos, K. W.; Norrby, P.-O.; Unelius, C. R. *Eur. J. Org. Chem.* **2008**, 5915
- (246) Bräse, S.; Gil, C.; Knepper, K.; Zimmermann, V. *Angew. Chem. Int. Ed.* **2005**, *44*, 5188.

